50272-101

REPORT DOCUMENTATION PAGE	1. REPORT NO. NCEER-93-0014	2.	3. PB94-142767

4. Title and Subtitle: An Energy Approach to Seismic Analysis and Design of Secondary Systems	5. Report Date: August 6, 1993 6.
7. Author(s): G. Chen and T.T. Soong	8. Performing Organization Rept. No.
9. Performing Organization Name and Address: State University of New York at Buffalo, Department of Civil Engineering, Buffalo, New York 14260	10. Project/Task/Work Unit No. 11. Contract(C) or Grant(G) No. (C) BCS 90-25010 (G) NEC-91029
12. Sponsoring Organization Name and Address: National Center for Earthquake Engineering Research, State University of New York at Buffalo, Red Jacket Quadrangle, Buffalo, New York 14261	13. Type of Report & Period Covered: Technical Report 14.

15. Supplementary Notes

This research was conducted at the State University of New York at Buffalo and was partially supported by the National Science Foundation under Grant No. BCS 90-25010 and the New York State Science and Technology Foundation under Grant No. NEC-91029.

16. Abstract (Limit: 200 words)

In this report, statistical energy analysis is systematically introduced to simplify the analysis and design procedures of secondary systems. This investigation starts out with the identification of special problems and assumption verification associated with this effort. The relation between power flow transmitted from one system to another and energies stored in two systems coupled by a conservative element is naturally extended to non-conservatively coupled systems. The concept of dissipative and penetrating power flow is developed to characterize the dissipating and transmitting properties of the coupling element. The relationship developed in a generic system is then applied to a simple primary-secondary system to investigate the general behavior of power flow and energy quantities. Their equivalence to the conventional response variables such as relative displacement and absolute acceleration is demonstrated analytically as well as through numerical examples. The power flow and energy analyses are further extended to a class of complex primary-secondary systems. Finally, decoupling criterion for the dynamic response of secondary systems is systematically established.

17. Document Analysis a. Descriptors

b. Identifiers/Open-Ended Terms

Earthquake engineering. Secondary systems. Primary secondary system interaction.
Input energy. Power flow. Statistical energy analysis.
Vibration modes. Modal energy. Dynamic response analysis.
Decoupling.

c. COSATI Field/Group

18. Availability Statement	19. Security Class (This Report)	21. No. of Pages
Release Unlimited	Unclassified	252
	20. Security Class (This Page) Unclassified	22. Price

NATIONAL CENTER FOR EARTHQUAKE
ENGINEERING RESEARCH
State University of New York at Buffalo

An Energy Approach to Seismic Analysis and Design of Secondary Systems

by

G. Chen and T.T. Soong
State University of New York at Buffalo
Department of Civil Engineering
Buffalo, New York 14260

Technical Report NCEER-93-0014

August 6, 1993

This research was conducted at the State University of New York at Buffalo and was partially supported by the National Science Foundation under Grant No. BCS 90-25010 and the New York State Science and Technology Foundation under Grant No. NEC-91029.

NOTICE

An Energy Approach to Seismic Analysis and Design of Secondary Systems

by

G. Chen[1] and T.T. Soong[2]

August 6, 1993

Technical Report NCEER-93-0014

NCEER Project Numbers 91-5221 and 92-3201B

NSF Master Contract Number BCS 90-25010
and
NYSSTF Grant Number NEC-91029

1 Structural Engineer, Steinman, Parsons Transportation Group, New York, formerly Research Assistant, Department of Civil Engineering, State University of New York at Buffalo
2 Samuel P. Capen Professor, Department of Civil Engineering, State University of New York at Buffalo

NATIONAL CENTER FOR EARTHQUAKE ENGINEERING RESEARCH
State University of New York at Buffalo
Red Jacket Quadrangle, Buffalo, NY 14261

PREFACE

The National Center for Earthquake Engineering Research (NCEER) was established to expand and disseminate knowledge about earthquakes, improve earthquake-resistant design, and implement seismic hazard mitigation procedures to minimize loss of lives and property. The emphasis is on structures in the eastern and central United States and lifelines throughout the country that are found in zones of low, moderate, and high seismicity.

NCEER's research and implementation plan in years six through ten (1991-1996) comprises four interlocked elements, as shown in the figure below. Element I, Basic Research, is carried out to support projects in the Applied Research area. Element II, Applied Research, is the major focus of work for years six through ten. Element III, Demonstration Projects, have been planned to support Applied Research projects, and will be either case studies or regional studies. Element IV, Implementation, will result from activity in the four Applied Research projects, and from Demonstration Projects.

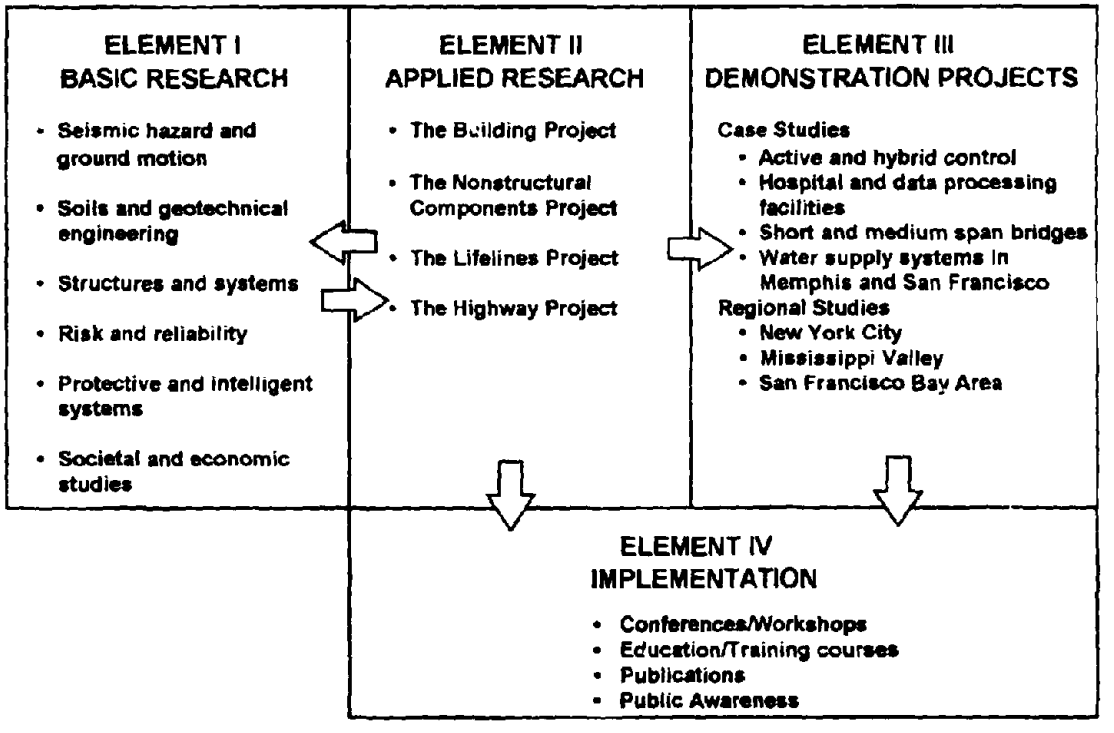

Research tasks in the **Nonstructural Components Project** focus on analytical and experimental investigations of seismic behavior of secondary systems, investigating hazard mitigation through optimization and protection, and developing rational criteria and procedures for seismic design and performance evaluation. Specifically, tasks are being performed to: (1) provide a risk analysis of a selected group of nonstructural elements; (2) improve simplified analysis so that research results can be readily used by practicing engineers; (3) protect sensitive equipment and critical subsystems using passive, active or hybrid systems; and (4) develop design and performance evaluation guidelines.

The end product of the **Nonstructural Components Project** will be a set of simple guidelines for design, performance evaluation, support design, and protection and mitigation measures in the form of handbooks or computer codes, and software and hardware associated with innovative protection technology.

The **protective and intelligent systems program** constitutes one of the important areas of research in the **Nonstructural Components Project**. Current tasks include the following:

1. Evaluate the performance of full-scale active bracing and active mass dampers already in place in terms of performance, power requirements, maintenance, reliability and cost.
2. Compare passive and active control strategies in terms of structural type, degree of effectiveness, cost and long-term reliability.
3. Perform fundamental studies of hybrid control.
4. Develop and test hybrid control systems.

The work presented in this report is aimed at developing a simple yet accurate procedure for seismic analysis and design of secondary systems. Considerable gaps exist between the state-of-the-research and the state-of-the-practice in this area and the attempt here is to incorporate recent research results into the development of practical design and performance evaluation procedures for secondary systems. An energy-based approach is developed for this purpose. It is shown that this approach facilitates the examination of basic dynamic characteristics of primary-secondary systems of engineering interest, thus leading to a simple procedure for the analysis and design of secondary systems under seismic loads.

ABSTRACT

The dynamic analysis and design of secondary systems have been extensively studied over the last two decades, resulting in a better understanding of their general dynamic characteristics. One of the current challenges for researchers is to develop simple yet accurate procedures incorporating these research results and transfer them into the development of practical design and performance evaluation procedures. This is the basic thrust of this report.

Statistical energy analysis has been proven to be a powerful tool in the dynamic analysis of complex systems involving interaction effect between acoustic field and structure. In this report, such a tool is systematically introduced to simplify the analysis and design procedures of secondary systems. This investigation starts out with the identification of special problems and assumption verification associated with the extension of its application. The relation between power flow transmitted from one system to another and energies stored in two systems coupled by a conservative element is naturally extended to non-conservatively coupled systems which are commonly encountered in civil engineering. The concept of dissipative and penetrating power flow is developed to characterize the dissipating and transmitting properties of the coupling element. The relationship developed in a generic system is then applied to a simple primary-secondary system to investigate the general behavior of power flow and energy quantities. Their equivalence to the conventional response variables such as relative displacement and absolute acceleration is demonstrated analytically as well as through numerical examples.

For a general complex system in which many high-frequency modes are excited by the external excitation, a simple procedure in statistical energy analysis is directly applicable. For intermediate cases commonly encountered in civil engineering where a few low-frequency modes in primary-secondary system are excited by external forces, a mean-square condensation method is developed to condense the number of degrees of freedom step-by-step through energy equivalence

before and after condensation. Closed-form formulations used in the condensation process are derived so that response calculations can be expedited.

The power flow and energy analyses are further extended to a class of complex primary-secondary systems for which the interaction effect between different branches of the secondary system is thoroughly studied; optimum damping of the secondary system is recognized as in the simple primary-secondary system and the dynamic characteristics of multi-tuned primary-secondary systems are investigated. The exact solution for this class of complex systems can also serve to assess many types of approximated schemes proposed in the past.

A decoupling criterion for the dynamic response of secondary systems is systematically established. The question about which response characteristics (primary or secondary) are more sensitive to the decoupling action is first raised and studied. The conservative domains in which non-interaction analyses give rise to overestimated results for different systems are investigated and compared under different conditions. Sufficient conditions for dynamic decoupling of secondary systems are also developed in this report.

ACKNOWLEDGEMENTS

Financial support from the National Center for Earthquake Engineering Research under Grant Nos. NCEER 91-5221 and NCEER-92-3201B is gratefully acknowledged.

TABLE OF CONTENTS

TABLE OF CONTENTS (continued)

TABLE OF CONTENTS (continued)

TABLE OF CONTENTS (continued)

TABLE OF CONTENTS (continued)

LIST OF FIGURES

LIST OF FIGURES (continued)

LIST OF FIGURES (continued)

LIST OF FIGURES (continued)

LIST OF TABLES

SECTION 1

GENERAL INTRODUCTION

The dynamic behavior of complex structural systems such as one or more light secondary systems (S-system) attached to a heavier primary system (P-system) in a seismic environment has been an active research topic during the last twenty years. As a result, a better understanding of their general dynamic characteristics has been reached. On the other hand, practical regulations and design codes in this area are still at a crude stage where the static-equivalent lateral force methodology is still being used to design an S-system and the amplification factor due to flexibility of the S-system has not been properly taken into account. Therefore, one of the challenges for researchers is to simplify the abundant research results obtained in the past and transfer the new technology to practical design levels [87].

For a preliminary design, only preliminary data on S-systems are available at the time when a design engineer seeks a reasonable or even optimal design of anchorages linking the S- with P-systems and attachment configurations. These limited information prevent the engineer from doing a detailed analysis for a specific response quantity of interest. A comprehensive dynamic analysis of combined primary-secondary systems (P-S system) is thus not only uneconomical but also impossible. Consequently, the conventional floor response spectrum approach as well as its various modification by including interaction and non-classical damping effects has found extensive applications.

The procedure to calculate maximum response quantities of S-systems using floor response spectrum is basically deterministic although random vibration analysis is often involved in the interim to establish the relation between floor response spectrum and ground response spectrum. It may be reasonable to interpret the floor response spectrum as an average maximum response within certain design period and earthquake randomness has therefore been implied. On the other

hand, uncertainties associated with structural parameter variations and those of the foundation (if the soil-structure interaction is of concern) can not be incorporated into the deterministic analysis. These uncertainties will have a significant influence on the behavior of P-S systems, especially in the tuned case. The situation becomes even worse when higher modes in a complex system are not negligible in the response calculation. Under these circumstances, classical modal analysis is incapable of incorporating uncertainties arising from seismic input and structural parameters. Based on these observations, statistical analysis can be considered as a good alternative.

Statistical energy analysis (SEA), developed in the early 1960s, has its extensive applications in the sound-structure interaction environment. Its application was extended to structure-structure interactions among which electronic package vibration was initially studied. This powerful tool was introduced in [45] to the analysis of P-S systems excited by white noise. Further research on the application of this basic principle incorporating the characteristics of both earthquake inputs and P-S systems is clearly warranted.

For the purpose of this study, both P- and S-systems are defined as viscously and proportionally damped, linearly elastic systems. All parameters of an S-system such as mass, stiffness and damping are considered to be much smaller than the corresponding parameters of the P-system. The S-system is supported by the P-system in an arbitrary manner which is in turn anchored to a rigid base subjected to random excitations. These excitations are considered throughout this report as broad-band stochastic processes with unity power spectral density except for specified cases.

1.1 Objectives

The major motivation in this study is to apply statistical energy analysis to the dynamic analysis of P-S systems. Special problems (assumptions) associated with the application in this particular field are identified and evaluated in detail. It appears that SEA can be directly applied to the dynamic analysis of a stiff S-system attached to a structure when excitations have rich high frequency components so that the dynamic responses of high frequency modes are appreciable. Since these conditions are not satisfied in most civil engineering problems, an approximate method derived from SEA is motivated. Consequently, a whole framework of energy based analysis of

P-S combined systems is developed to cover all the cases encountered in civil engineering.

There is no doubt that the ultimate impact of the energy principles mentioned in the preceding paragraph rests with their applicability in practical engineering. Relationship between energy and power flow on the one hand and relative displacement and absolute acceleration on the other is first established for a simple P-S system. This is then extended to one class of complex systems for which interaction effects between different branches of the S-system, multiply tuned and non-classical damping effects, are precisely evaluated. For general P-S systems, a simple yet accurate approach referred to as mean-square condensation is developed and errors associated with these formulations are qualitatively evaluated through illustrative examples as well as the decoupling analysis presented in a separate section.

1.2 Organization

The investigation presented here is composed of nine sections whose interrelationships can be best described by Fig. 1-1.

In Section 2, extensive literature surveys both for the dynamic analysis of P-S systems and for the development of SEA are presented. Emphasis for the P-S system analysis is placed on the decoupling criteria and combination rules which are directly related to the research presented herein, as well as the key papers to help us better understand the fundamental dynamic characteristics involved in P-S complex systems. For the second part, attention is paid to the fundamental development of SEA for the convenience of civil engineers.

Section 3 deals with the issues related to the applicability of SEA in earthquake engineering. In particular, energy equipartition assumption between modes are verified under the excitation of ground displacement and acceleration.

Decoupling criteria (sufficient conditions) of coupled P-S systems for different response quantities under various excitations are studied in Section 4. Comparisons between various decoupling criteria are made to demonstrate the ultimate behavior of sufficient conditions proposed here and detailed analysis of conservatism involved in the non-interaction analysis is presented in an interactive graph between the mass ratio and the frequency ratio. This study provides a basis

for the assessment of different approximate approaches used for evaluating the S-system response.

In Section 5, a fundamental relation between power flow transmitted from one oscillator to another and energies stored in two individual oscillators is established, which is central to the development of SEA. The definition of power flow between conservatively-coupled systems is extended in a consistent way to non-conservatively coupled systems commonly encountered in civil engineering. The power flow is divided into penetrating and dissipative parts on physical ground; the first part corresponds to the power flow between conservatively-coupled oscillators whereas the second represents the dissipated power in the connection. Its direct application to simple P-S systems is followed in Section 6 to examine the basic dynamic characteristics of P-S systems of engineering interest from the viewpoint of power flow and energy representations.

In Section 7, further applications of the fundamental relation developed in Section 5 to a class of multi-degree-of-freedom (MDOF) P-S systems are examined to determine the exact solution of dynamic response of both P- and S-systems. These exact results are obtained by transforming the MDOF P-S system into a series of subsystems with a small number of degree-of-freedom (DOF), for example, 2-DOF systems for which the fundamental relation is valid.

Section 8 deals with the most commonly-encountered cases in civil engineering, in which a few low modes of the P-S system play an essential part in the dynamic response of P- and S-systems. Due to relative low sensitivity of these modal properties to a small variation in structural parameters, the power flow and energy defined in Section 5 are adopted here through individual members instead of their population. It is on this basis that the mean-square condensation approach is developed.

In Section 9, the basic procedure and characteristic of previously developed approaches are summarized and future research directions are indicated.

SECTION 2

LITERATURE SURVEY

2.1 Dynamic Analysis and Design of S-System

A large amount of effort has been devoted over the last two decades to the development of methods for seismic analysis and design of S-systems which are anchored or attached to heavier P-systems. These efforts were motivated mainly by increasing utilization of critical S-systems such as mechanical and electrical assemblages as well as piping systems in nuclear power plants and industrial facilities. In many situations, these systems are valuable themselves and play a vital role in safeguarding the supporting structural integrity.

2.1.1 Classification of S-Systems

A variety of S-systems, forming a part of and/or supported by a structure, are categorized in [63] into three groups based on their involvement in the structure, i.e., structural elements, nonstructural components (architectural components), and equipment.

Structural elements are defined as portions of a structure having a structural function. Included are structural walls, diaphragms, and penthouses.

Nonstrutural components are portions of a structure not having a structural function. Nonstructural exterior or interior walls and partitions, ornaments and building appendages, suspended ceilings, etc., are in this category.

Equipment consisting of mechanical, plumbing, and electrical assemblies include but are not limited to: (a) chimney, stacks and towers; (b) machinery; (c) boilers, pressure vessels, tanks, pumps, motors, cooling towers, control panels, and standby power equipment; (d) piping, conduit and ducts.

From the connection property point of view, they can be divided into the following two groups:

Rigid Attachment. In this group, an S-system is rigidly connected to its supporting P-system. The effect of the S-system on the P-system is only an increase of vibrational period and

the small S-system can be designed separately to withstand the equivalent static force generated from earthquakes.

Flexible Attachment. An S-system is often designed in such a way that it is attached to the P-system through some flexible elements which are supposed to isolate the vibrational energy from the P-system. Due to dynamic characteristics of the S-system, the dynamic response of the S-system is most often interrelated with the frequency characteristics of the supporting system.

Most practical codes such as [96] employ the equivalent static force design with discrimination under distinct attachments described above.

2.1.2 Damage Pattern of S-Systems in Building

Damage in S-systems has generally been caused by earthquake-induced motions with excessive deformation and stresses. From post-earthquake investigations in the field, it can be observed that any particular component of the S-system undergoes either one or both of two different types of actions, namely, (a) change of shape forced by the overall deformation of its supporting building (P-system) as a whole, such as the wall set within the structural frame; (b) vibrational response of the component excited by the structural motions, such as mechanical and electrical equipment [56]. Corresponding to these actions damage in S-systems during earthquakes can be distinguished into two different effects – relative displacement effects and vibration effects.

Relative Displacement Effects. The relative displacement effects on the S-system behavior can be qualitatively described in terms of overstress and impact actions. An S-system whose movement is subjected to the restraint of the P-system will experience crushing and cracking during strong earthquakes and generate overstress. In many cases, any gap existing between adjacent elements (S-systems) will be widened or narrowed repeatedly, leading to impacting effect (pounding effect) between the S-systems.

Vibrational Effects. A structure subjected to seismic loads will experience a severe motion which in turn excites the S-system attached to the structure. The damage due to the vibration can be any combination of overstresses, excessive deflections, impact of adjacent elements and instability.

Based on the observation of possible patterns that an S-system will experience during moderate or strong earthquakes, there is no doubt that it is desirable to consider potential damage reduction in any structural or even architectural detailing design for the S-system. Beyond that, however, dynamic or equivalent static design of individual element is necessary, which is the scope of this report.

2.1.3 Current Practice in Response Calculation and Design

As reviewed in [14], floor response spectrum and combined P-S system analysis are the two basic approaches currently used in practical design to analyze the dynamic response of S-systems.

2.1.3.1 Floor Response Spectrum Approach

Design of an S-system by floor response spectrum (FRS), as many design codes recommend [5,100], is consistent with P-system design by ground response spectrum and is thus easy to be accepted by professional communitiers. In this method, the dynamic response of the P-system at the support point of an S-system is determined first with the absence of the S-system and then adopted as an input to calculate the maximum response of a fictitious single-degree-of-freedom (SDOF) oscillator with varying period and damping ratio, namely, FRS. In multiple supported cases, the envelop of floor response spectra at all supporting locations is considered as the design response spectrum for the S-system. As one can see, this code-specified approach allows the dynamic analyses of P- and S-systems to be performed separately, which is usually referred to as an uncoupled analysis.

Accounting for uncertainties in structural parameters as well as earthquake input and its propagating media properties [2], a design FRS is obtained by broadening spectrum peaks of the calculated FRS. A suggested method for a quantitative determination of peak broadening associated with the structural frequencies is proposed in [98], in which variations of structural frequencies with each significant uncertain parameter such as soil modulus or material density are first calculated and then combined together to obtain the total frequency variation by the commonly-used square-root-of-the-sum-of-squares (SRSS) rule.

Since FRS method provides a simple procedure for response calculations of S-systems, it has been widely used by engineering practitioners and applied in their professional participations. However, the method may produce serious inaccuracies when frequency of the S-system is tuned to one or more frequencies of the P-system. In these tuned cases, design code for nuclear power plant allows a combined analysis of P-S systems in the time domain to incorporate the interaction effect between the P- and S-system.

2.1.3.2 Combined P-S System Approach

In this approach, an S-system is considered as an integral part of a P-S structural system. Both modal analysis and direct integration method in the conventional sense are thus quite straightforward. A few deficiencies associated with this approach include: (a) large number of degrees of freedom that will make the combined analysis uneconomical or even impossible; (b) numerical inaccuracy due to the fact that P- and S-systems have quite dissimilar orders of structural parameters; (c) incapability of capturing the construction process of the P- and S-system, i.e., P-system is always designed prior to the S-system. At the time of designing the P-system, only tentative information on the S-system is available, which is in favor of describing P- and S-systems by their individual frequency characteristics in nature; and (d) re-analysis of the whole P-S system subjected to any modification in the S-system alone.

2.1.3.3 Dynamic Decoupling Criteria

As seen from the preceding paragraphs, the FRS method is obviously more attractive than the combined P-S system approach. Therefore, it has always been given first priority in engineering designs. The limitation of this approach is often described as the dynamic decoupling criterion of S-system. A simple design criterion was employed in [98] to decide whether the FRS approach is acceptable or not as shown in Fig. 2-1, in which R_m and R_ω are defined as mass ratio and frequency ratio between the S- and P-system. They are often considered as indices of interaction and tuning degree between P- and S-systems, respectively.

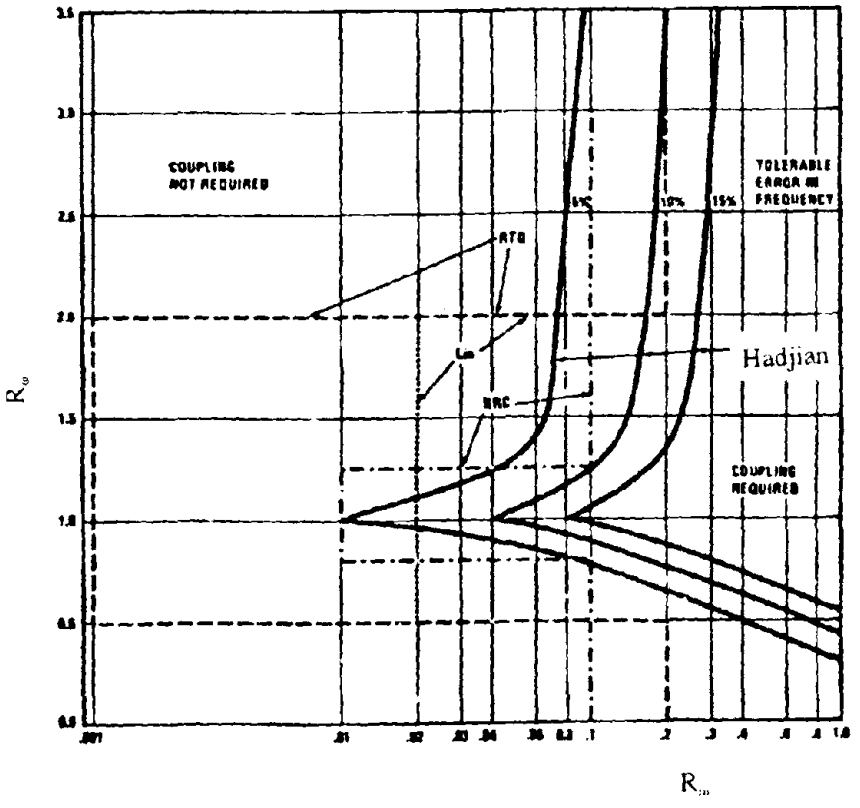

Fig. 2-1 Schematic Representation of Decoupling Criterion
(Taken from [29])

2.1.4 Recent Development

2.1.4.1 General Characteristics of P-S System

Although there are a variety of different forms and characteristics, some of the basic dynamic characteristics of P-S systems are common. These general characteristics, which constitute the topics of intensive studies in the past, are summarized in the followings.

1. *General Attachment Configuration.* An S-system can be supported by a P-system at any arbitral locations or even at the base of the P-S system directly.

2. *General Resonance Characteristics.* Any number of frequencies of the S-system may be in any manner tuned or nearly tuned with the P-system.

3. *Dynamic Interaction.* In general, P- and S- systems interact with each other, especially when the modal masses of the S-system are not negligible and its frequencies are tuned with the P-system.

4. *Dynamic Correlations.* Both modal correlation and correlation between multiple support excitations can not be ignored in the dynamic analysis of the S-system under certain conditions. The correlation between pseudo-static and dynamic components of the S-system response, the division complying with conventional code-specified method [5], can not be neglected, either.

5. *Non-Classical Damping.* Even though each subsystem has proportional damping characteristics, their combined P-S system may have non-proportional damping. The effect of this damping characteristic on the behavior of the S-system becomes significant when the damping difference between the P- and S- systems increases, particularly if two subsystems are tuned.

All of the above five characteristics are generally interrelated in their effect on the dynamic response of an S-system. However, the dynamic interaction between P- and S-systems may be the most important characteristic, the neglect of which will substantially facilitate the analysis and design of the S-system and yet involve potentially the greatest amount of error in the S-system analysis.

2.1.4.2 Decoupling Criteria

As shown in Fig. 2-1, the decoupling criteria in [48,67,98] are characterized by abrupt discontinuities, which lack sufficient justification. A much more rational approach was investigated in [29] to develop the relationship between R_ω and R_m. To extend this approach to MDOF P-S systems, a subjective expression was proposed to evaluate the modal mass, which led to arguments of [26]. While this criterion is usually considered to be a necessary condition for allowable response error of a coupled system, this has been found not to be sufficient. Based on the above two points, an analysis of response error due to decoupling by the response spectrum approach was conducted and a new expression for modal mass was thus introduced in [26,27]. The dynamic characteristics of 2-DOF equipment-structure systems was also studied in [34] to arrive at a decoupling criterion by perturbation approach

$$R_m < \epsilon \left(4 + \frac{\beta^2}{\xi_a^2}\right) \xi_p \xi_s \tag{2.1}$$

in which $\xi_a = (\xi_p + \xi_s)/2$, ξ_p and ξ_s are damping ratios of the P- and S-system, respectively; ϵ is a tolerable error for mean-square displacement of the S-system and $\beta = 2(1 - R_\omega)/(1 + R_\omega)$ is a tuning parameter. This criterion has been further applied to evaluate the error due to the neglect of interaction effect in the response calculation of general MDOF P-S systems [37].

2.1.4.3 Dynamic Response Calculation of Singly-Attached S-System

Analysis Without Interaction. The FRS approach is a powerful tool to calculate the dynamic response of S-systems in non-interaction analysis. Among earlier research works in this realm, direct generation procedures for FRS were developed in [8,39] based on the concept that the maximum acceleration of an S-system may be approximated as an amplification of either (a) the ground response spectrum or (b) the peak acceleration of the floor at which the S-system is supported. When the first mode representation of a structural system is acceptable, the first approximation is more accurate for small R_ω while the second more accurate for large R_ω. For MDOF P-systems, the conventional SRSS combination rule has been incorporated, which appears to be much more conservative than those of time history approach. Thus, this approach has

not been widely applied in the industry. An alternate approach based on Fourier transform was developed in [11,71]. Random vibration theory was also employed to establish the relationship between FRS and ground response spectrum [74,75,103].

All of these methods have been shown to give reasonable accuracy for SDOF systems with relatively small mass and frequency that is not tuned into any frequency of the P-system. Otherwise, the error generated by neglecting the interaction effect will consistently make the methods unacceptable. A quantitative evaluation of these errors was performed in [16,39,75]. Since the inherent tuning characteristics in the P-S system will make many formulations derived in the above yield infinite results, the perfectly tuned system was treated separately in [62, 76]. However, these results continue to ignore interaction and are inaccurate for nearly tuned systems. The error involved in the analysis without interaction increases rapidly as mass ratio R_m increases and frequency ratio R_ω approaches unity as shown in Fig. 2-1.

Analysis With Interaction. Under this category, extensive research to generate FRS with interaction effect have been conducted during the past decades. A simple 2-DOF system is employed in [16] to compute the exact root-mean-square (RMS) response to a stationary excitation. For MDOF P-systems, analytical methods were presented in [90] for the calculation of exact eigenproperties of combined P-S systems by solving a nonlinear algebraic equation. These methods can be effectively applied to both light and heavy equipment.

In other studies, approximations are made to simplify the analysis of the combined system. An MDOF P- and S-system was reduced to a series of 2-DOF subsystems and their responses were calculated in terms of 2-DOF response spectra [61]. A notion of effective mass ratio to obtain approximate mode shapes and frequencies of the P-S system was used in [58,60]. Although these methods have sound theoretical basis, a certain level of accuracy has to be satisfied to obtain good approximations for the combined system response in the formulations of modal properties and combination rule of modal response quantities [105].

Most of the research in this category have been carried out using the perturbation method

The small parameters (perturbed parameters) are the mass, stiffness, and damping terms of the S-system [69]. With the knowledge of the relative orders of different small parameters, a tuned 2-DOF system was accurately analyzed and closed-form expressions for the frequency characteristics were obtained. Other research using the modal approach to the analysis of P-S systems includes those of [17,68,70,105]. In this method, the frequency characteristics of a combined P-S system are first obtained and then adopted to calculate the modal responses of the S-system which are further combined with certain rules to come up with the total response of the S-system. More thorough analyses using perturbation theory were conducted to obtain the modal frequency parameters of complex P-S systems, including all the inherent problems [34,36]. A more formal and systematic perturbation scheme has also been developed in [76].

Modal Combination Rule. A statistically-based SRSS rule has extensively been applied in the dynamic analysis of traditional structures with well-spaced natural frequencies [15]. For a complex P-S system, however, this rule basically fails to give an accurate prediction of the S-system response from the modal responses including the interaction effect. The effect of cross-correlation between closely-spaced modes of the combined P-S system has been studied in [108]. They proposed a more rational combination rule in certain cases, namely, complete quadratic combination (CQC). These two rules were further mixed in the response analysis of P-S systems in [85], using CQC to combine all the modal correlation effect in each direction and using SRSS to combine the directional correlation for multi-directional earthquake excitations. In order to account for the so-called "missing mass" effect [64], an alternative SRSS rule was suggested to calculate the seismic design response [77]. They utilized a mode acceleration method instead of mode displacement method to reduce the "missing mass" error due to truncation of the higher frequency modes in the response calculation [78]. The seismic input in such a case, however, has to be described by relative acceleration and velocity response spectrum instead of the conventional pseudo-acceleration spectrum.

A great improvement about the combination rule has been achieved in [25,29-31]. They divided the response of any mode into a damped periodic and rigid parts which are combined by

SRSS and algebraic sum rules, respectively. The idea behind this approach is that, beyond a certain "rigid" frequency, all the modal responses are perfectly correlated and should be combined by algebraic sums while, for modes with intermediate frequencies, the correlation between the damped response and the rigid response varies from zero to one. This correlation factor (α_{rc}), defined as *rigid response coefficient*, is approximately calculated by

$$\alpha_{rrc} = \begin{cases} 0, & \omega < \omega^{(1)} \\ \dfrac{\log(\omega/\omega^{(1)})}{\log(\omega^{(2)}/\omega^{(1)})}, & \omega^{(1)} \le \omega < \omega^{(2)} \\ 1, & \omega^{(2)} \le \omega \end{cases} \tag{2.2}$$

where the frequencies $\omega^{(1)}$ and $\omega^{(2)}$ are related to the spectral response characteristics; they are expressed as

$$\omega^{(1)} = \frac{S_{a,max}}{S_{v,max}} \tag{2.3}$$

$$\omega^{(2)} = \frac{\omega^{(1)} + \omega^{(r)}}{3} \tag{2.4}$$

in which $S_{a,max}$ and $S_{v,max}$ are the maximum spectral acceleration and velocity; $\omega^{(r)}$ is the "rigid" frequency. To avoid the involvement of multiple spectra consideration, a full zero period acceleration was applied to globally compute the rigid part response [23].

For a multiply-supported S-system such as a piping system, the required combination rule is much more complex. It usually involves the modal and multiple-support correlations [3].

Non-Classical Damping Effects. A general P-S system is non-classically damped in nature due to differences that exist between the damping characteristics in the P- and S- systems. Hence, the damping matrix of the combined system can not be diagonalized by normal modes of the undamped system. The neglect of off-diagonal terms of the resulting damping matrix in the modal space will induce significant errors in response computations in some situations. Errors in response calculation of 2-DOF non-classically damped structures by neglecting the off-diagonal damping terms were analyzed in [107]. It was indicated that the resulting errors are significant

only when $1/R_c$ (c_p/c_s : c_p and c_s are damping coefficients of the P- and S-systems, respectively) is less than 10^{-3} in this case. A criterion for neglecting the non-classical damping effect in the tuned case was developed in [34] as

$$\delta^2 \leq \epsilon(4\xi_a^2 + R_m) \tag{2.5}$$

in which δ is a non-classical damping parameter which is defined as

$$\delta = \left(\xi_p - \frac{\xi_s}{R_w}\right)\frac{1}{R_w} \tag{2.6}$$

In nearly tuned cases, there is no simple criterion yet under which non-classical damping is negligible. A more comprehensive parametric study of an SDOF equipment attached to a classically damped MDOF structure has been made in [110]. Other works approximately accounting for non-classical damping effect in the response calculation of S-systems have also been done [28,33,87].

2.1.4.4 Dynamic Response Calculation of Multiple-Supported S-System

The uncoupled analysis of a multiple-supported S-system is more complicated in computation than that of singly-attached S-system when time history analysis is adopted. However, analysis with FRS will generate additional problems in this case, namely, (a) conventional FRS can not carry the phase information between different supports to which an S-system is connected; (b) one more level of combination of maximum responses due to different support excitations is required, resulting in a more complex combination rule as mentioned before.

The response analysis of S-systems with FRS in terms of its individual support motions with heuristic procedures for combination have been performed in [1,73,104]. This subjective nature of combination can not properly account for important effects such as cross-correlations between modal responses as well s support excitations, which will lead to erroneous prediction of the total response as demonstrated in [106]. A random vibration approach was also developed to analyze multiple-supported S-systems, including the cross-correlation effect [9,10,47,80]. Following the

standard practice in industry [5], an analytical formulation for seismic analysis of these complex systems has been developed by decomposing the response of an S-system into "inertial" or "dynamic" effects and effects due to "relative seismic support displacements" or "pseudo-static motion". The seismic input in this approach is defined in terms of auto and cross pseudo-acceleration and relative velocity FRS.

Regarding the application of perturbation theory, the same methodology can be used and the same procedures can be followed in this general cases as in singly-attached systems to obtain the frequency characteristics of the combined P-S system. These frequency characteristics in the case of two separate SDOF S-systems have been employed to develop cross-oscillator cross-floor response spectrum (CCFS), an extension of the conventional FRS that takes into account correlations between support excitations and between modal responses as well as other general dynamic characteristics identified in Section 2.1.4.1. As in the conventional FRS analysis, the CCFS method consists of two main steps: (a) evaluation of CCFS in terms of ground response spectrum; and (b) evaluation of S-system response by modal combination in terms of CCFS.

2.1.5 Further Research Needs

As pointed out in [14,83], several areas deserve more research attentions:

Effect of Inelastic Behavior of P-system. Engineering structures may behave inelastically under the action of severe earthquakes. The effect of yielding in the P-system on the input to the S-system was first studied in [50]. Recently, linear and nonlinear response of structures and equipment subjected to California and Eastern United States earthquakes have been investigated in [94]. The response characteristics of inelastic 2-DOF P-S system was also studied in [38]. However, this scarce information is not sufficient to provide a good understanding of the seismic characteristics of multiply-supported piping systems attached to nonlinear structures.

Optimization and Protection. One direct way to mitigate the potential seismic damage to S-systems is to enhance their dynamic performance through optimization in their placement within a P-system or in their support design as demonstrated in [46].

A variety of passive control devices can be incorporated into a P-system to dissipate

supplemental energy and thus reduce its dynamic response, which isolates the input energy from the S-system. Viscoelastic damper is one of such devices that has been demonstrated by numerical analyses as well as by experiments to be effective in upgrading the structural performance [114]. The seismic input to an S-system can also be reduced by isolating either the P-system or the S-systems directly. Such isolation can be installed at the base of the P-system or under a floor [41,95].

Codes and Standards. A better understanding of the dynamic behavior of S-systems has been gained with significant progress over the last few years. A major thrust now has been to develop a framework which captures the important findings or dynamic characteristics of P-S systems but can be readily applied to improve simple design procedures in practice [87]. The first step toward this goal has been achieved in [88].

2.2 Development of Statistical Energy Analysis (SEA)

In general, conventional vibration analyses of mechanical and structural systems subjected to various environmental loads such as earthquakes are conducted for a few lower modes as these modes receive almost all the energy generated by external loads. However, a complex system such as a P-S combined assemblage often possesses multiply tuned modes between the P- and S-system as listed in Section 2.1.4.1. Moreover, frequencies of these resonant modes are sometimes over the higher range due to the designers' prior knowledge about detuning the low frequency modes between the P- and the S- system as well as their truncation of higher modes in synthesizing the total response. The existence of closely-spaced modes in the individual P- or S-systems further adds complexity to these types of problems. Modal parameters of higher modes are characterized by uncertainties and so are the dynamic response attributed to these modes. The resonance frequencies and mode shapes of these modes show great sensitivity to details of geometry and construction. This means that the system can realistically be represented only by a statistical model.

If there is a reason for statistical approach stemming from the nature of the dynamic problems, there is equal motivation from the viewpoint of application. As indicated in Section

2.1.3.2, only tentative design information is available about S-systems when structural engineers are faced with making response estimations at a given stage of preliminary design. These estimations are required to qualify the S-system and to design appropriate attachements, the amount of damping, and attachment configurations. Highly detailed analyses with specific knowledge of geometric configuration, construction and loading environment are impossible. At this stage, simpler statistical estimations of response to external loads that preserve a rough parameter dependence are appropriate to the designer's needs.

It is relevant to mention here that some of the dynamic characteristics associated with a P-S system are actually beneficial from a statistical point of view. The very large number of degrees of freedom, for example, tends to smooth out the fluctuations in response prediction. The tuning effect and closely-spaced mode effect can also reduce the variation of predicted response because, in these cases, modal energies will concentrate in a narrow frequency band. These properties assure that a statistical vibrational analysis would be attractive in this particular field under certain circumstances.

2.2.1 A Brief Historical Survey

Statistical energy analysis was originally developed by Lyon and Smith in the 1960s. Lyon calculated the power flow between two lightly and linearly coupled resonators subjected to independent white noise sources in the first part of [53]. It was found that the power flow between two conservatively-coupled oscillators is proportional to the difference of average modal energies of the two oscillators, which formed a fundamental relationship in the further development of SEA framework.

Smith [86] independently calculated the response of a resonator excited by a diffuse, broad band sound field, and discovered that the system response reached a limit when radiation damping of the resonator exceeded its internal damping. Moreover, this limit due to the reaction of the sound field was independent of the precise value of the radiation damping.

In the second part of [53], they studied the power flow between two multi-modal systems

and explained that the Smith's limiting vibration amounted to an equality of energy between the resonator and the average modal energy of the sound field.

Lyon's work for two weakly coupling resonators was extended to general coupling conditions [72,97]. They defined the uncoupled systems as the blocked ones, meaning that the other system was held fixed while the system being considered was allowed to vibrate. The two-system theory was also extended in [20] to develop predictions from energy distribution for three systems coupled in tandem. The vibrational energy transmission in three-element structures was further investigated in [54].

SEA theory originally applied in the acoustic field, specifically the sound-structure interaction problem, was utilized to predict the energy transmission between structure-structure systems [52]. Involved in the SEA formulation are modal density and coupling loss factor. Their evaluation under various interacting connections between systems is the key to the application of SEA. The plate-edge admittance related to the structural coupling loss factor was calculated in [21]. Modal density prediction is not as difficult as the calculation of coupling loss factors as demonstrated in [32].

SEA is developed to grasp the gross features of a complex system with little information available in a preliminary design. The question of uncertainty quantification will therefore be raised by practical engineers. The variance of dynamic responses of a system with structure-structure interaction was evaluated in [52], where relatively few modes participate in the energy sharing process.

Attempts to better understand the theoretical basis for SEA and the limiting effect with its assumptions on the range of applications have been made by many investigators. Among them, the most notable efforts to elucidate implications of the SEA model in terms of classical vibration analysis were made in [111-113]. The power flow prediction by SEA was compared with an "exact" calculation within a high frequency range in [66] and a good agreement has been obtained between them. Rayleigh's classical approach was applied in [106] to the study of vibration of systems with a finite number of degrees of freedom to probe the regions of applicability of SEA.

The research objective is twofold: one is to show how the classical approach can yield the exact results of [52] as well as an interesting extension; the other is to see wider conditions under which the necessary assumptions associated with SEA are approximately satisfied. The connection between classical modal analysis and SEA was also investigated in [19,43]. It was shown that results of SEA can be obtained by studying the asymptotic behavior of classical modal analysis for a general structural system.

While the SEA model for conservatively-coupled subsystems is well developed, it has been recently extended to include non-conservative coupling between subsystems by incorporating effects of coupling element in the loss factor terms. The power flow between two non-conservatively coupled oscillators subjected to broad-band stochastic forces was first derived in [91] and was shown to be not only proportional to the energy difference of the two oscillators, but also dependent on the energy absolute values. Due to dissipative effect in the connection element, the absolute values of power flows in each direction are generally not identical. A different definition or power flow between two non-conservatively coupled oscillators has been introduced in [22]. With the advent of theoretical research on this issue, the experimental measurement for loss factors attributed to the non-conservatively coupled elements have recently been made [42,91,93]. For instance, the coupling damping of non-conservatively-coupled cylindrical shells was estimated.

All the previous work are mainly focused on the steady state power flow relationship between linearly-coupled subsystems. The energy flow relation in the transient state has been studied in [44] and its theoretical prediction was in good agreement with the measured result for the case of two plates coupled through a force transducer. The steady-state power balance equations of SEA was also extended in [65] to include unsteady excitations and responses. The resulting first-order linear differential equations are analogous to those encountered in unsteady heat conduction. The assumption of linear coupling has been eliminated in the work of [40,59]. For certain classes of nonlinear systems, the same formulas of input power as in the linear system hold.

2.2.2 Framework of Statistical Energy Analysis

It is supposed here that readers in civil engineering are not quite familiar with SEA. A general procedure is presented in this section for their convenience. For further detailed information, readers are referred to the most authoritative book in this area [55].

2.2.2.1 Fundamental Formulation of SEA

The basic relation of SEA is established by studying the power flow from one oscillator to another which are coupled together by a conservative element as shown in Fig. 2-2. The two oscillators are subjected to independent broad-band stochastic forces. Power flow is defined as the rate of energy flow between two oscillators which is probably best described as a radiation energy from the viewpoint of one oscillator. The power flow is found to be proportional to the difference of energies stored in each oscillator [55], i.e.,

$$P_{12} = \alpha (E_1 - E_2) \tag{2.7}$$

in which P_{12}, E_1 and E_2 are the time-averages of the power flow from oscillator 1 to 2, total energies stored in oscillators 1 and 2, respectively. The proportionality constant α is positive definite and symmetric in system parameters.

Equation (2.7) plays an essential role in the SEA development. It links the power flow between two oscillators to the measurable variable, energy, through a constant coefficient independent of environmental vibration sources. By comparing Eq. (2.7) with the equation governing the heat conduction problem, one can find that the power flow relation is analogous to the heat conduction problem in which the thermal energy flows from the higher to the lower temperature level.

2.2.2.2 Power Flow Between Two Multi-Modal Subsystems

When two subsystems consist of multi-modal oscillators, relations similar to Eq. (2.7) can be derived. For a complex system with N_1 modes for subsystem 1 and N_2 modes for subsystem 2 over a finite range of frequency $\Delta\omega$, the modal interaction between these modes of the two subsystems can be described by Fig.2-3. In order to develop a simple power flow relation for this complex

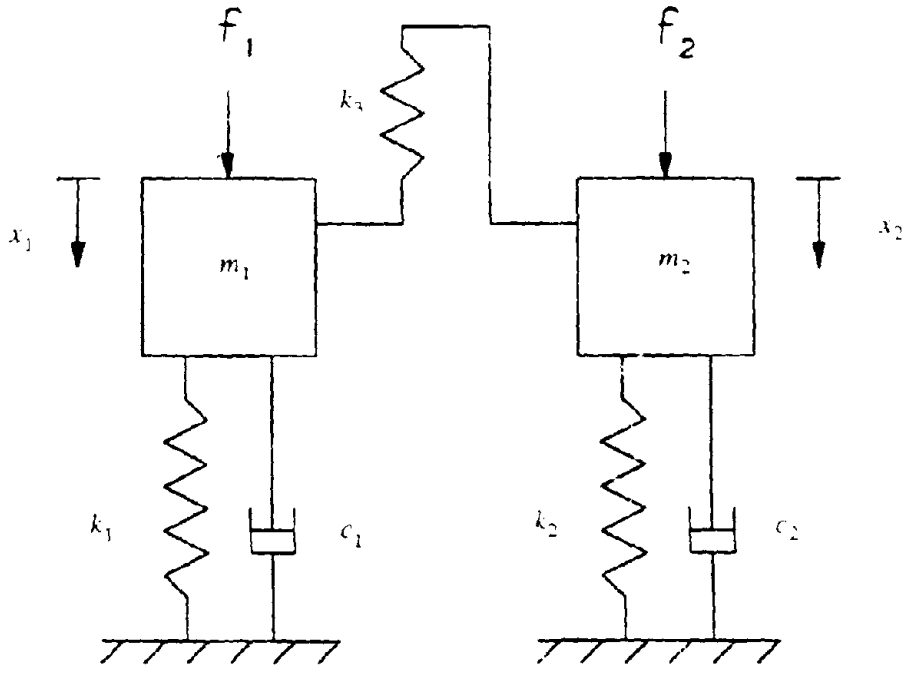

Fig. 2-2 Two Oscillators Coupled Through a Spring

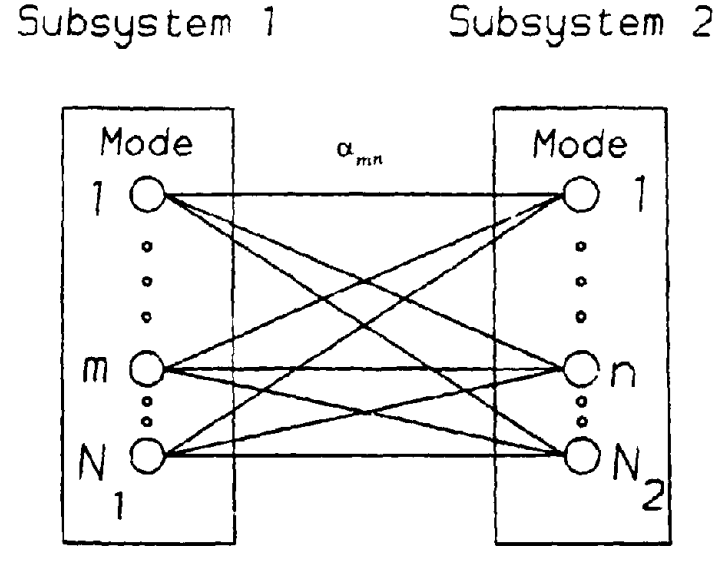

Fig. 2-3 Modal Interaction Between Two Subsystems

system, several assumptions have to be made, namely, (a) The natural frequency of each mode is assumed to be uniformly distributed over the frequency range $\Delta\omega$. This implies that each subsystem is a member of a population of systems that are physically similar; (b) All modes in a subsystem are equally energetic and their amplitudes are incoherent.

Under these assumptions, the power flow between mode m of subsystem 1 and mode n of subsystem 2 can be expressed as

$$P_{mn} = \alpha_{mn}(E_{1,m} - E_{2,n}) \tag{2.8}$$

where α_{mn} is the proportionality factor α; and $E_{1,m}$ and $E_{2,n}$ are the modal energies of subsystems 1 and 2. They can be represented by E_1/N_1 and E_2/N_2, respectively.

The total average power flow from subsystem 1 to 2 then becomes

$$\bar{P}_{12} = \bar{\alpha} N_1 N_2 \left(\frac{E_1}{N_1} - \frac{E_2}{N_2}\right)$$

$$= \omega_c(\eta_{12}E_1 - \eta_{21}E_2) \tag{2.9}$$

in which E_1 and E_2 are the total energies stored in subsystem 1 and subsystem 2 and $\bar{\alpha}$ is the average proportionality constant of α_{mn} over the frequency range $\Delta\omega$. If only a spring coupling is applied between the two subsystems, its expression can be written as

$$\bar{\alpha} = \frac{\pi}{2}\frac{\kappa^2/\omega_c^2}{\Delta\omega} \tag{2.10}$$

and thus

$$\bar{P}_{12} = \frac{\pi}{2}\Delta\omega\frac{\kappa^2/\omega_c^2}{(\Delta\omega/N_1)(\Delta\omega/N_2)}\left(\frac{E_1}{N_1} - \frac{E_2}{N_2}\right) \tag{2.11}$$

in which ω_c is the central frequency over frequency band $\Delta\omega$; κ^2/ω_c^2 represents the frequency shift of the combined system from individual subsystems produced by stiffness coupling alone. The quantity $(\kappa^2/\omega_c^2)/[(\Delta\omega/N_1)(\Delta\omega/N_2)]$ is a measure of the strength of power flow. The coupling loss factors η_{12} and η_{21} for subsystems 1 and 2 can be expressed by

$$\eta_{12} = \bar{\alpha}N_2/\omega_c \tag{2.12}$$

$$\eta_{21} = \bar{\alpha}N_1/\omega_c \tag{2.13}$$

Obviously, we have a basic relation

$$n_1\eta_{12} = n_2\eta_{21} \tag{2.14}$$

in which $n_i=\Delta\omega/N_i$ $(i=1,2)$ is the modal density of subsystem i.

2.2.2.3 Power Balance Equations

After evaluating the power flow between two subsystems in Eq. (2.11), we can formulate the power balance equation as follows

$$P_1^{(in)} = P_1^{(diss)} + \bar{P}_{12} \tag{2.15}$$

$$P_2^{(in)} = P_2^{(diss)} + \bar{P}_{21} \tag{2.16}$$

in which the dissipated power $P_i^{(diss)}$ of subsystem i can be written as a function of kinetic energy:

$$P_i^{(diss)} = 2\omega_c\eta_i E_i^{(k)} \tag{2.17}$$

For a weak-coupling case, the kinetic energy of subsystem i is approximately equal to the potential energy, i.e.,

$$P_i^{(diss)} = \omega_c\eta_i E_i \tag{2.18}$$

Upon substituting Eqs. (2.10) and (2.18) into (2.15) and (2.16), two algebraic equations governing energy parameters can be implemented. They are

$$P_1^{(in)} = (\eta_1+\eta_{12})\,\omega_c E_1 - \eta_{21}\omega_c E_2 \tag{2.19}$$

$$P_2^{(in)} = -\eta_{12}\omega_c E_1 + (\eta_2+\eta_{21})\,\omega_c E_2 \tag{2.20}$$

Solving the above equations for E_1 and E_2 simultaneously gives rise to the final solutions of interest.

SECTION 3

MODAL ENERGY DISTRIBUTION UNDER EARTHQUAKE LOAD

3.1 Introduction

As discussed in Section 2.2.2.2, one of the two assumptions involved in SEA is energy equipartition among all modes within a certain frequency interval, which has been justified in the application to sound-structure interaction problems. It is the major objective of this section to investigate whether this assumption is still true in the case of structural systems under the excitation of earthquake loads.

3.2 Modal Energy Distribution Under Ground Acceleration Input

3.2.1 Equation of Motion of Continuous Shear-Beam

For simplicity, a laterally loaded multi-story building in Fig. 3-1(a) with uniform story height, stiffness and weight is treated as a continuous shear beam as shown in Fig. 3-1(b). The governing equation of motion for this beam can be formulated by following the procedure of [15].

$$\frac{\partial^2}{\partial t^2}x(s,t) - \omega_0^2 h^2 \frac{\partial^2}{\partial s^2}x(s,t) = -\ddot{x}_g(t) \tag{3.1}$$

in which x(s,t) is the relative displacement at position s with respect to the base; $\omega_0=(12EI/mh^3)^{1/2}$ $=(12EI/\bar{m}h^4)^{1/2}$ is a frequency constant of shear beam; $\bar{m}$ is a pseudo-mass density along the height; and EI and h are story rigidity and story height, respectively, as shown in Fig. 3-1(a).

3.2.2 Free Vibration

The base input $\ddot{x}_g(t)$ in Eq. (3.1) is set to zero for the analysis of free vibration. The natural frequency and mode function of the shear beam can be expressed as [15]

$$\omega_k = \frac{\pi(2k-1)}{2N}\omega_0 \tag{3.2}$$

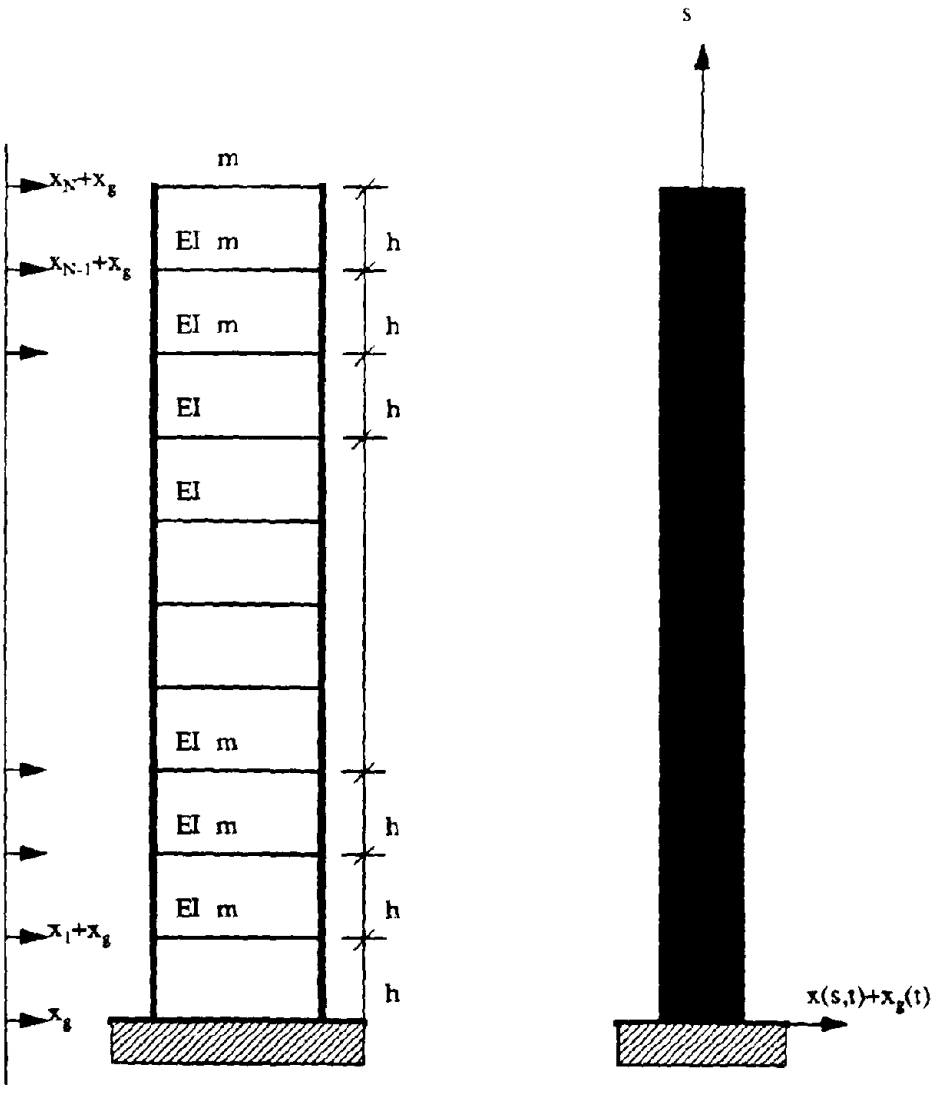

(a) Discrete Model (b) Continuous Model

Fig. 3-1 Shear-Beam Model of Multistory Building

$$X_k(s) = \sin\left[\frac{\pi(2k-1)}{2}\frac{s}{Nh}\right] \tag{3.3}$$

(k=1,2,3, ..., N)

in which N represents the number of story.

3.2.3 Forced Vibration

Displacement x(s,t) can be expanded as a summation of mode functions:

$$x(s,t) = \sum_{i=1}^{N} X_i(s)\, q_i(t) \tag{3.4}$$

Upon substituting Eq. (3.4) into Eq. (3.1) and multiplying both sides of the resulting equation by $X_k(s)$ and then integrating over the total height of the shear beam, the following simple equation can be obtained:

$$\ddot{q}_k(t) + 2\xi_k\omega_k\dot{q}_k(t) + \omega_k^2 q_k(t) = -\Gamma_k\ddot{x}_g(t) \tag{3.5}$$

$$\Gamma_k = \frac{\int_0^{Nh} X_k(s)\,ds}{\int_0^{Nh} X_k^2(s)\,ds} = \frac{4}{\pi(2k-1)} \tag{3.6}$$

In Eq. (3.5), the proportional damping term $2\xi_k\omega_k\dot{q}_k(t)$ has been introduced to represent energy dissipation in the shear beam.

3.2.4 Modal Energy Evaluation of Continuous Shear-Beam

The average kinetic energy of the *k-th* mode due to a white noise input $\ddot{x}_g(t)$ with power spectral density $S_{\ddot{x}_g}$ can be expressed as

$$E_k^{(k)} = \int_0^{Nh} \frac{1}{2}\bar{m}X_k^2(s)\langle\dot{q}_k^2\rangle\, ds = \frac{\bar{m}Nh}{4}\cdot\frac{\pi S_{\ddot{x}_g}\Gamma_k^2}{2\xi_k\omega_k} \tag{3.7}$$

Here, superscript *k* in brackets denotes the kinetic energy.

Consequently, the ratio of kinetic energies between the *k-th* mode and the first mode can be expressed as

$$\frac{E_k^{(k)}}{E_1^{(k)}} = \frac{\Gamma_k^2 \xi_1 \omega_1}{\Gamma_1^2 \xi_k \omega_k} \tag{3.8}$$

which can be further simplified by introducing Eqs. (3.2) and (3.6) and assuming ξ_k=constant, i.e.,

$$\frac{E_k^{(k)}}{E_1^{(k)}} = \frac{1}{(2k-1)^3} \tag{3.9}$$

Equation (3.9) means that kinetic energy of a lower mode is always larger than that stored in a higher mode, a result that agrees with our intuition. However, the rate of energy ratio reduces substantially when the mode order increases as demonstrated in Table 3-1. Also observed in this table is that the energy ratio will be larger than 0.9 when the mode order is beyond thirty, indicating that at least 10% error in the energy ratio for two neighboring modes is involved in the assumption of equal modal energy when a thirty or lower multi-story building is considered. In contrast, when energy differences between r number of consecutive modes are limited to less than 10%, the number of stories must be greater than k_0 which can be obtained by solving

$$\left(\frac{2k_0 - 1}{2(k_0 + r - 1) - 1}\right)^3 = 0.9 \tag{3.10}$$

or

$$k_0 = Int\{27.98r - 27.48\} \tag{3.11}$$

in which Int{x} represents the minimum integer greater than x. When r=5, k_0=113, meaning that a 113-story building or lower can not generate any five consecutive modes whose differences in kinetic energy remain less than 10%.

Up to this point, a conclusion can be drawn that the equal modal energy assumption is generally not acceptable for structures under the action of ground acceleration. In other words, individual mode actions are significant, especially for a few lower frequency modes. However, the modal energy ratio shown in Eq. (3.9) is a function of only mode order or is independent of structural parameters. This implies that group treatment of modal energies can still be effective when the exact energy relation between different modes has been incorporated. Nevertheless, this

TABLE 3-1: Variation of Kinetic Energy Ratio Under Ground Acceleration Input

(1)	(2)	(3)	(4)	(5)	(6)	(7)	(8)	(9)	(10)	(11)
mode No.(k)	2	3	4	5	10	15	20	30	40	50
$E_1^{(k)}/E_1^{(k)}$	0.0370	0.0080	0.0029	0.0014	0.0010					
$E_{k+1}^{(k)}/E_k^{(k)}$	0.2160	0.3644	0.4705	0.5477	0.7406	0.8187	0.8607	0.9048	0.9277	0.9418

analysis is based on an idealized continuous shear-beam model and extension of this result into discrete multi-story buildings requires further justification. In what follows, conditions under which this extension is successful are investigated.

3.2.5 Natural Frequency Characteristics of Discrete Shear-Beam

Recalling the discrete model of the N-story building in Fig. 3-1(a), the equation of motion can be written in matrix form

$$\underline{M}\ddot{\underline{X}}(t) + \underline{C}\dot{\underline{X}}(t) + \underline{K}\underline{X}(t) = -\underline{M}\underline{e}_a\ddot{x}_g(t) \tag{3.12}$$

in which

$$\underline{M} = \begin{bmatrix} m & & & & \\ & m & & & \\ & & \bullet & & \\ & & & \bullet & \\ & & & & m \\ & & & & & m \end{bmatrix}, \quad \underline{K} = \begin{bmatrix} 2k & -k & & & \\ -k & 2k & -k & & \\ & & \bullet & & \\ & & & \bullet & -k \\ & & & -k & 2k & -k \\ & & & & -k & k \end{bmatrix}$$

$$\underline{X} = \{x_1, x_2, \ldots, x_N\}^T$$

and damping matrix $\underline{C}$ is assumed to be proportional to the mass and stiffness matrices; $\underline{e}_a$ is an earthquake input index vector and is taken to be $\{1, 1, \ldots, 1\}^T$ in this case. $k(=12EI/h^3)$ in the above is the interval stiffness of one story.

For the purpose of evaluating frequency characteristics, the damping and force terms in Eq.(3.12) are neglected and the displacement vector $\underline{X}(t)$ is substituted by

$$\underline{X}(t) = \underline{\phi}\sin\omega t \tag{3.13}$$

which gives rise to the characteristic equation

$$(\underline{K} - \omega^2\underline{M})\underline{\phi} = \underline{o} \tag{3.14}$$

Subsequently, natural frequencies of the shear-beam can be determined by solving the equation

$$|\underline{K} - \omega^2 \underline{M}| = 0 \tag{3.15}$$

or

$$I_N = \begin{vmatrix} 2-\lambda & -1 & & & & \\ -1 & 2-\lambda & -1 & & & \\ & -1 & \bullet & & & \\ & & & \bullet & -1 & \\ & & & -1 & 2-\lambda & -1 \\ & & & & -1 & 1-\lambda \end{vmatrix}_{N\times N} = 0 \tag{3.16}$$

in which $\lambda=\omega^2/\omega_0^2$

A simple determinant operation on Eq. (3.16) leads to

$$I_N = (1-\lambda)\tilde{I}_{N-1} - \tilde{I}_{N-2} \tag{3.17}$$

$$\tilde{I}_N = \begin{vmatrix} 2-\lambda & -1 & & & & \\ -1 & 2-\lambda & -1 & & & \\ & -1 & \bullet & -1 & & \\ & & -1 & 2-\lambda & -1 & \\ & & & -1 & 2-\lambda & \end{vmatrix}_{N\times N}$$

From any standard mathematical manual or table, one can find the solution of the banded determinant $\tilde{I}_N$ which can be expressed as

$$\tilde{I}_N = \begin{cases} (N+1)\left(\dfrac{2-\lambda}{2}\right)^N, & \lambda=0 \text{ or } \lambda=4 \\ \dfrac{a^{N+1}-b^{N+1}}{a-b}, & \text{otherwise} \end{cases} \tag{3.18}$$

in which

$$a = \frac{1}{2}\left(2-\lambda+\sqrt{(2-\lambda)^2-4}\right) \tag{3.19}$$

$$b = \frac{1}{2}\left(2-\lambda-\sqrt{(2-\lambda)^2-4}\right) \tag{3.20}$$

It is easy to check that $\lambda=0$ and $\lambda=4$ are not solutions of Eq. (3.16). Consequently, Eq. (3.17) can be rewritten as

$$I_N = \frac{1}{a-b}\left[(1-\lambda)(a^N - b^N) - (a^{N-1} - b^{N-1})\right]$$

and Eq. (3.16) becomes

$$(1-\lambda)(a^N - b^N) - (a^{N-1} - b^{N-1}) = 0 \tag{3.21}$$

Let $2-\lambda=2\cos\theta$, a and b in Eqs. (3.19) and (3.20) can be expressed as

$$a = e^{j\theta}$$
$$b = e^{-j\theta}$$

and Eq. (3.21) is then changed to

$$2j\left[(2\cos\theta - 1)\sin(N\theta) - \sin(N-1)\theta\right] = 0$$

or

$$\sin\frac{\theta}{2}\cos\frac{2N+1}{2}\theta = 0 \tag{3.22}$$

In the above, $j=(-1)^{1/2}$ is a complex unit and $\sin(\theta/2)$ can not be equal to zero. Eq. (3.22) is thus equivalent to

$$\cos\frac{2N+1}{2}\theta = 0$$

with the solution of

$$\theta_k = \frac{2k-1}{2N+1}\pi \tag{3.23}$$

$$(k = 1, 2, \ldots, N)$$

Therefore, eigenvalue (λ_k) can be expressed as

$$\lambda_k = \frac{\omega_k^2}{\omega_0^2} = 4\sin^2\frac{\theta_k}{2} \tag{3.24}$$

The modal vector $\underline{\phi}_k$ can be obtained from Eq. (3.14) with ω_k in place of ω, i.e.,

$$\phi_k(N) = 1$$

$$\phi_k(N-1) = 1-\lambda_k \tag{3.25}$$

$$\phi_k(i) = (2-\lambda_k)\phi_k(i+1) - \phi_k(i+2)$$

$$(i = 1, 2, \ldots, N-2)$$

3.2.6 Modal Energy Evaluation of Discrete Shear-Beam

Modal energy of the *k-th* mode corresponding to Eq. (3.7) can be formulated as

$$E_k^{(k)} = \frac{1}{2}\underset{\sim}{\phi}_k^T M \underset{\sim}{\phi}_k \frac{\pi S_{\ddot{x}_g} \Gamma_k^2}{2\xi_k \omega_k} = \frac{m}{2}\underset{\sim}{\phi}_k^T \underset{\sim}{\phi}_k \frac{\pi S_{\ddot{x}_g} \Gamma_k^2}{2\xi_k \omega_k} \tag{3.26}$$

in which

$$\Gamma_k = \frac{\underset{\sim}{\phi}_k^T \underset{\sim}{e}_a}{\underset{\sim}{\phi}_k^T \underset{\sim}{\phi}_k} \tag{3.27}$$

The modal energy ratio of interest can be finally expressed as

$$\frac{E_k^{(k)}}{E_1^{(k)}} = \frac{\underset{\sim}{\phi}_k^T \underset{\sim}{\phi}_k}{\underset{\sim}{\phi}_1^T \underset{\sim}{\phi}_1} \cdot \frac{\Gamma_k^2}{\Gamma_1^2} \cdot \frac{\xi_1 \omega_1}{\xi_k \omega_k} \tag{3.28}$$

Comparing Eq.(3.28) with Eq. (3.8), one can see that the only difference between them lies in the additional factor in the former equation.

Modal energy ratios of discrete and continuous models are compared in Fig. 3-2, indicating that, for the *N*-story building, the first *N*/2 number of modal energies can be approximated by those of structure-free model (continuous model). Together with the observation that modal energy ratio is always less than unity, especially for lower order of modes, this approximation can greatly facilitate the calculation of total energy stored in the structure.

3.3. Modal Energy Distribution Under Ground Displacement Input

3.3.1 Modal Energy Evaluation of Continuous Shear-Beam

The equation of motion of the continuous shear beam in this case is exactly the same as Eq. (3.1) except that the right-hand force is changed to $\omega_0^2 x_g(t)\delta(s-h)$ and the absolute displacement representation of $x(s,t)$ is employed. All the frequency characteristics obtained in the previous section are therefore applicable. Participation factor (Γ_k), however, is altered to

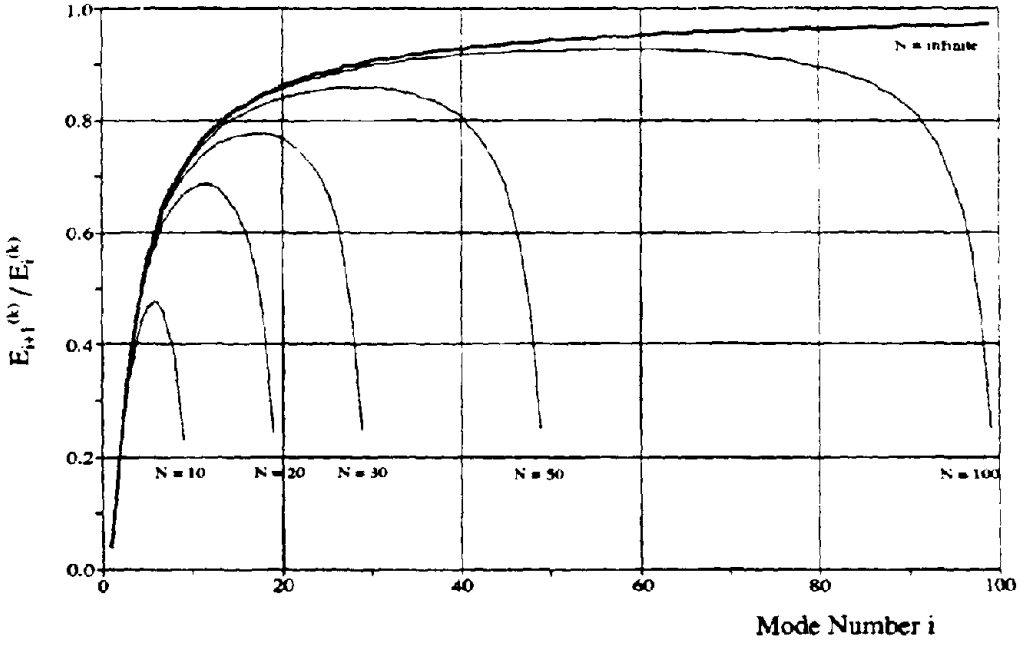

Fig. 3-2 Comparison of Energy Ratios Between Discrete and Continuous Models Under the Excitation of Acceleration

$$\Gamma_k = \frac{\int_0^{Nh} X_k(s)\,\delta(s-h)\,ds}{\int_0^{Nh} X_k^2(s)\,ds} = \frac{2}{Nh} X_k(h) \tag{3.29}$$

and Eq. (3.5) becomes

$$\ddot{q}_k(t) + 2\xi_k\omega_k\dot{q}_k(t) + \omega_k^2 q_k(t) = \Gamma_k\omega_0^2 x_g(t) \tag{3.30}$$

The ratio of modal energies can then be expressed as

$$\frac{E_k^{(k)}}{E_1^{(k)}} = \frac{\Gamma_k^2}{\Gamma_1^2}\cdot\frac{\xi_1\omega_1}{\xi_k\omega_k} = \frac{X_k^2(h)}{X_1^2(h)}\cdot\frac{1}{2k-1} \tag{3.31}$$

for constant modal damping ratio. It is noted that the energy ratio in this case is a function of both the number of stories of the building and mode order, but remains independent of structural parameters.

3.3.2 Modal Energy Evaluation of Discrete Shear-Beam

The right-hand side of Eq. (3.12) in this case becomes $\underline{e}_d m\omega_0^2 x_g(t)$ in which $\underline{e}_d=\{1, 0, 0, \ldots, 0\}^T$. The participation factor is therefore changed to

$$\Gamma_k = \frac{\phi_k(1)}{\underline{\phi}_k^T\underline{\phi}_k} \tag{3.32}$$

and modal energy ratio can be calculated from Eq. (3.28).

The modal energy ratios of the discrete model agree very well with those of the continuous model as shown in Fig. 3-3. This means that modal energy relation of the N-story building under the action of base displacement can be accurately calculated by Eq. (3.31). Further observation on Fig. 3-3 shows that the modal energy ratio is approximately equal to unity for a great number of modes which justifies the energy equipartition assumption.

3.4 Acceleration Input vs. Displacement Input

Figs. 3-2 and 3-3 show comparisons of modal energy ratio between discrete and continuous

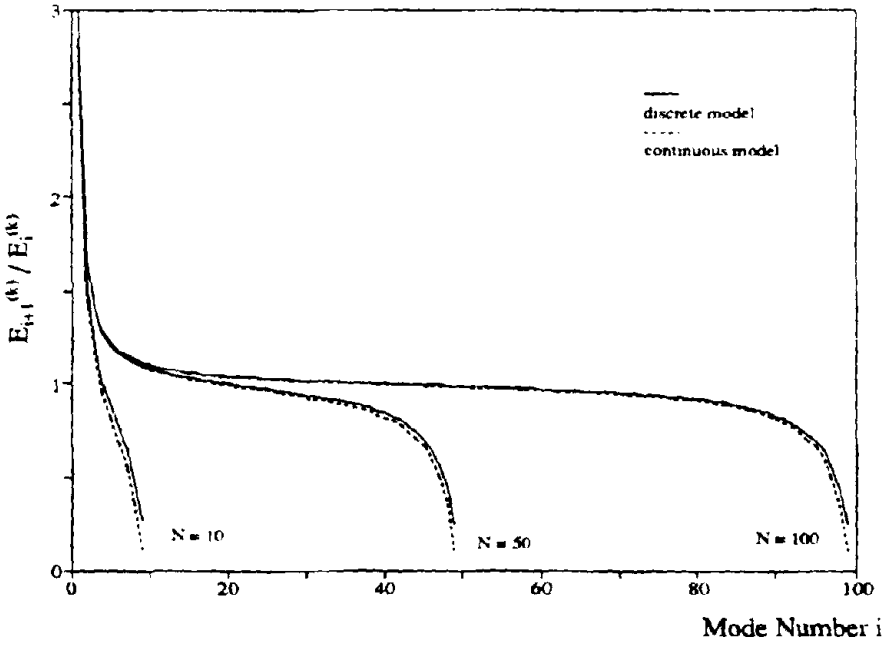

Fig. 3-3 Comparison of Energy Ratios Between Discrete and Continuous Models Under the Excitation of Displacement

models under acceleration and displacement inputs, respectively. Both their variation patterns and their comparisons with corresponding models are quite different. These can be interpreted as follows:

(1). Under acceleration input, participation factor decreases as the mode order increases. This, together with frequency effect, results in a consistent reduction of modal energy as the order of mode goes up. On the other hand, participation factor of first $(N+1)/2$ modes increases with the mode order under the action of displacement input, whose effect on modal energy is offset by the modal frequency. The combination of these effects leads to a much wider platform on the plot of modal energy ratio vs. mode order and a possibility that more energy in higher modes could be generated than that in lower modes as illustrated in Fig. 3-3.

(2). Effective seismic force distributions on a structure subjected to ground acceleration are different for discrete and continuous models as shown in Fig. 3-4(a). The larger the number of stories of the structure, the more uniform the seismic force distribution on the structure which asymptotically approaches the continuous model. The increasing accuracy of energy calculation in a building with larger number of stories can be clearly seen in Fig. 3-2 while a large discrepancy of energy in higher modes between discrete and continuous models still exists due to different distributions and probably the so-called "wave-contaminated" effect when a wave propagates along a series of discrete meshes. In contrast, the effective seismic forces on both discrete and continuous models of the structure due to ground displacement are exactly the same. Energy ratio of the continuous model depends on number of stories as shown in Eq. (3.31), which is attributed to the variation of acting position of the forces with respect to the total height of the structure.

3.5 Conclusions

It can be observed from the preceding sections that the modal energy relation between lower modes of a structure excited by ground acceleration can be modelled approximately by a structure-free relation in Eq. (3.9). However, the assumption of equal modal energy basically fails.

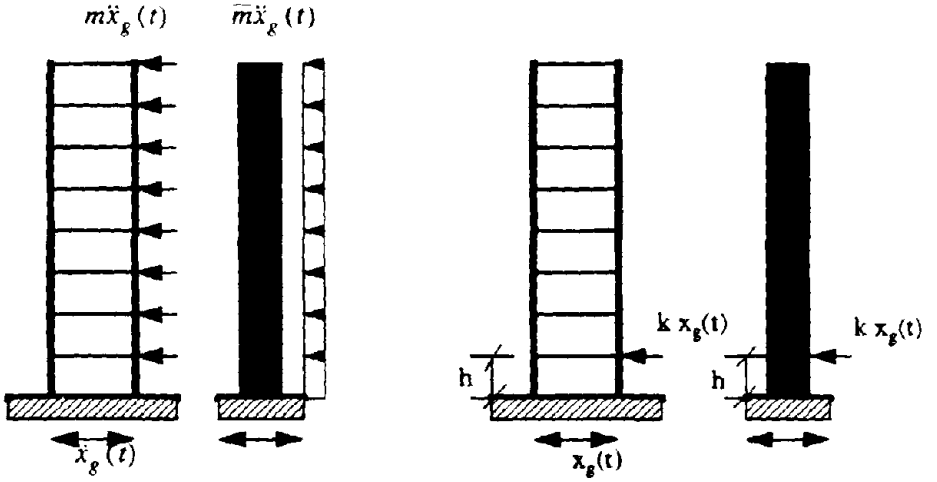

(a) Ground Acceleration Input (b) Ground Displacement Input

Fig. 3-4 Comparison of Forces Exerting on Discrete and Continuous Models

Modal energies of a structure subjected to ground displacement can accurately be substituted by those of corresponding continuous model. In addition, the equipartition assumption of modal energy, which is of major concern here, still holds for a great number of modes with intermediate frequencies. The ground displacement input is therefore preferable in the application of SEA discussed in Section 2.2. This can also circumvent the difficulties encountered due to correlated inertia forces exerting on P- and S- systems when ground acceleration input is employed.

It is worthwhile to mention that, in principle, the relative displacement representation of motion of a structure subjected to ground acceleration and absolute displacement representation for the same structure subjected to ground displacement are interchangeable. A large discrepancy happens due to the incompatibility between input acceleration and input displacement. In the previous examples, both ground acceleration and displacement are assumed to be white noise which is obviously not compatible. To look at this from a different angle, one may conclude that what really matters about the assumption of energy equipartition is the frequency content in the vibrational source since the absolute displacement representation for a structure under white noise is nothing but the relative displacement representation for the same structure under ground acceleration described by a stationary stochastic process with a power spectral density proportional to the fourth power of frequency. For example, results in the study of [24] showed that the response varies little with structural frequency.

SECTION 4

DECOUPLING OF S-SYSTEM FOR DYNAMIC ANALYSIS

4.1 Introduction

A decoupled analysis is always preferred in the dynamic analysis of P-S systems due to many reasons. Not only does a coupled analysis likely involve intensive computational effort, it also can be numerically difficult to solve due to dissimilarities in structural parameters of the P- and S- systems. In practice, design of a P-system often precedes the design of an S-system and they may be undertaken by different designers. Decoupling in the analysis of P-S systems thus requires minimum communication between different design teams and avoid many of the intervening problems.

A decoupling criterion for S-system analysis can be justified if the interaction effect is negligible between the P- and S- systems whose parameters are covered by the criterion. A small variation of frequency calculation of the P-system is often considered to be a necessary condition for this insignificant interaction effect on responses, which has also been taken to be a sufficient condition in practice. However, it was indicated in [26] that a small change in frequency does not assure response error from an uncoupled analysis to be within the same tolerance and is therefore not sufficient. In fact, careful re-examination on results of [26,29] will lead to the conclusion that the frequency decoupling criterion is not necessarily covered by response decoupling criterion, either. That is to say, an exact displacement response of the P-system can be obtained by an uncoupled analysis even though the frequency change due to interaction effect is significant. Nevertheless, considering the frequency decoupling criterion as a necessary condition is on the conservative side in the sense that the permissible domain in the R_m — R_w plane for decoupling is reduced.

Past investigations on this issue mainly focused on the decoupling effect on the frequency characteristics or response of the P-system. The influence of so-obtained criterion on the response

of the S-system has seldom been studied. The only preliminary investigation on the S-system behavior due to decoupling was conducted in [34]. However, the perturbation theory for obtaining the decoupling criterion in Eq. (2.1) limits its application to light S-systems. In this section, a sufficient condition for uncoupled analysis of S-systems is defined as one that limits the error involved in the determination of the maximum displacement under harmonic loads. This condition is then compared to decoupling criteria for various response quantities of interest under different inputs. While emphasis is placed on the decoupling effect on the S-system response, the decoupling criterion for the P-system response is also presented for comparison. The issue related to response calculation of which system (S or P) is more sensitive to the decoupling action is first investigated.

It is also relevant to S-system design since the developed criterion will help us better understand approximations involved in the derivation of computational schemes for the response calculation of S-systems.

4.2 Dynamic Decoupling Based on Maximum Response

4.2.1 Equations of Motion

Consider a 2-DOF P-S system as shown in Fig. 4-1. The equations of motion of the system can be formulated as follows:

$$m_s\ddot{x}_s + c_s(\dot{x}_s - \dot{x}_p) + k_s(x_s - x_p) = 0 \tag{4.1}$$

$$m_p\ddot{x}_p + c_s(\dot{x}_p - \dot{x}_s) + c_p(\dot{x}_p - \dot{x}_g) + k_s(x_p - x_s) + k_p(x_p - x_g) = 0 \tag{4.2}$$

in which m_i, c_i, k_i are the mass, damping coefficient and stiffness of subsystem i (i=p, s), respectively, and x_s, x_p and x_g represent absolute displacement of the S-system, the P-system and base. When the relative displacements of the P- and S- system with respect to their supports are introduced, i.e., z_s=x_s-x_p and y_p=x_p-x_g, Eqs. (4.1) and (4.2) become

$$m_s\ddot{z}_s + c_s\dot{z}_s + k_s z_s + m_s\ddot{y}_p = -m_s\ddot{x}_g \tag{4.3}$$

$$m_p\ddot{y}_p + c_p\dot{y}_p + k_p y_p - c_s\dot{z}_s - k_s z_s = -m_p\ddot{x}_g \tag{4.4}$$

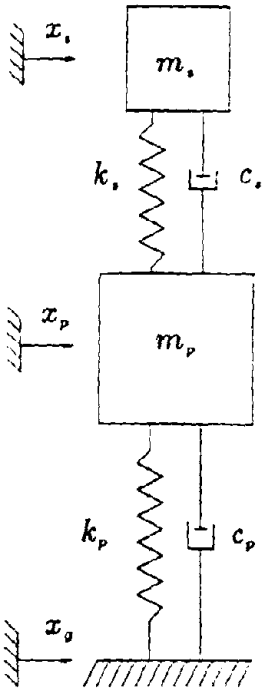

Fig. 4-1 2-DOF Idealized Model for P-S System

or

$$\ddot{z}_s + 2\xi_s\omega_s\dot{z}_s + \omega_s^2 z_s + \ddot{y}_p = -\ddot{x}_g \tag{4.5}$$

$$\ddot{y}_p + 2\xi_p\omega_p\dot{y}_p + \omega_p^2 y_p - R_m(2\xi_s\omega_s\dot{z}_s + \omega_s^2 z_s) = -\ddot{x}_g \tag{4.6}$$

in which a number of new parameters are introduced. ξ_i and ω_i are the damping ratio and frequency of subsystem *i* (*i*=*p*, *s*); R_m is the mass ratio. They are defined as

$$\omega_s = \sqrt{\frac{k_s}{m_s}}, \qquad \omega_p = \sqrt{\frac{k_p}{m_p}} \tag{4.7}$$

$$\xi_s = \frac{c_s}{2m_s\omega_s}, \qquad \xi_p = \frac{c_p}{2m_p\omega_p} \tag{4.8}$$

$$R_m = \frac{m_s}{m_p} \tag{4.9}$$

4.2.2 Harmonic Solution

When $\ddot{x}_g = e^{j\omega t}$, displacements of the S- and P-systems can be respectively expressed as $z_s = Z_s e^{j\omega t}$ and $y_p = Y_p e^{j\omega t}$. By substituting these into Eqs. (4.5) and (4.6), the displacement amplitudes Z_s and Y_p can be obtained and written as

$$Z_s = -\frac{1}{D}\left(\frac{1}{H_p} + \omega^2\right) \tag{4.10}$$

$$Y_p = -\frac{1}{D}\left[\frac{1}{H_s} + R_m(j\omega 2\xi_s\omega_s + \omega_s^2)\right] \tag{4.11}$$

in which D can be expressed as

$$D = \frac{1}{H_p H_s} - R_m\omega^2(j\omega 2\xi_s\omega_s + \omega_s^2) \tag{4.12}$$

When R_m is equal to zero, Eqs. (4.10) and (4.11) degenerate into

$$Z_{s0} = -\frac{1}{D_0}\left(\frac{1}{H_p} + \omega^2\right) \tag{4.13}$$

$$Y_{p0} = -\frac{1}{D_0}\frac{1}{H_s} \tag{4.14}$$

and Eq. (4.12) becomes

$$D_0 = \frac{1}{H_s H_p} \tag{4.15}$$

Here, H_i is the transfer function of subsystem i alone, which can be written as

$$H_i = \frac{1}{\omega_i^2 - \omega^2 + j\omega 2\xi_i\omega_i} \tag{4.16}$$

(i=p, s)

The ratios of displacement amplitudes of the S- as well as the P-system with and without interaction can be formulated as follows:

$$\frac{Z_s}{Z_{s0}} = \frac{D_0}{D} \tag{4.17}$$

$$\frac{Y_p}{Y_{p0}} = \frac{D_0}{D}\left[1 + R_m\left(j\omega 2\xi_s\omega_s + \omega_s^2\right)H_s\right] \tag{4.18}$$

4.2.3 Sufficient Conditions

The sufficient conditions for dynamic decoupling are defined as

$$\max_{\omega}\left|\left|\frac{Z_s}{Z_{s0}}\right| - 1\right| = e \tag{4.19}$$

for the response calculation of the S-system and

$$\max_{\omega}\left|\left|\frac{Y_p}{Y_{p0}}\right| - 1\right| = e \tag{4.20}$$

for the response calculation of the P-system, where e is the tolerance error.

It is noted that multiple solutions of Eqs. (4.19) and (4.20) for Z_s and Y_p may exist as demonstrated in the plots of maximum magnitudes of $|Z_s/Z_{s0}|$-1 and $|Y_p/Y_{p0}|$-1 vs. R_ω in Figs. 4-2 (a, b), $R_\omega(=\omega_s/\omega_p)$ being frequency ratio between the S- and the P-system. For a specified mass ratio

R_m, required here are the frequency ratios whose differences from unity are the minimum or maximum. For example, when e=0.2, R_m=0.005, ξ_s=0.05 and ξ_p=0.01, frequency ratios R_1 and R_2 in Fig. 4-2(a) are required frequency ratios.

The sufficient conditions calculated from Eqs. (4.19) and (4.20) for different damping combinations of the P-S system and different tolerance errors are presented in Figs. 4-3(a-c) and Figs. 4-4(a-c), respectively. It can be observed that the total damping ($\xi_s+\xi_p$) has a significant influence on the sufficient conditions. The larger the total damping, the looser the restrictions to the selection of R_m and R_ω. When the total damping is kept constant, the effect of individual damping (ξ_s or ξ_p) on the conditions for the S-system response calculation is insignificant whereas its effect on the conditions for the P-system is different. The larger the damping of the P-system (S-system), the looser the restriction for a stiff S-system (P-system). The effect of the stiff S-system on the behavior of the P-system is basically one of adding a small mass to the P-system so that the frequency of the P-system is slightly modified. Consequently, larger damping (ξ_p) relieves the sensitivity of resonant amplitude to the small frequency modification and alleviates the restriction for an uncoupled analysis. The effect of a relatively soft S-system on the dynamic response of the P-system is to slightly modify the force exerting on the P-system as expressed in Eq.(4.6). A larger damping (ξ_s) reduces the relative movement between the S- and P-systems so that modification to the exciting force is suppressed.

Regarding to the issue of which system (S or P) is more sensitive to the decoupling effect, frequency variations of both systems are reviewed first. The characteristic equation can be implemented by setting D in Eq. (4.12) equal to zero and neglecting damping terms, giving

$$R_F^4 - \left(1 + R_m + \frac{1}{R_\omega^2}\right)R_F^2 + \frac{1}{R_\omega^2} = 0 \qquad (4.21)$$

in which $R_F = \Omega/\omega_s$.

Two positive values of R_F can be obtained from the above equation, which are corresponding to the frequencies (Ω) of the combined P-S system. If decoupling is required, one of the frequencies has to be close to ω_s, or R_F^2 can be written as $1+\varepsilon$, where ε is a small quantity. By

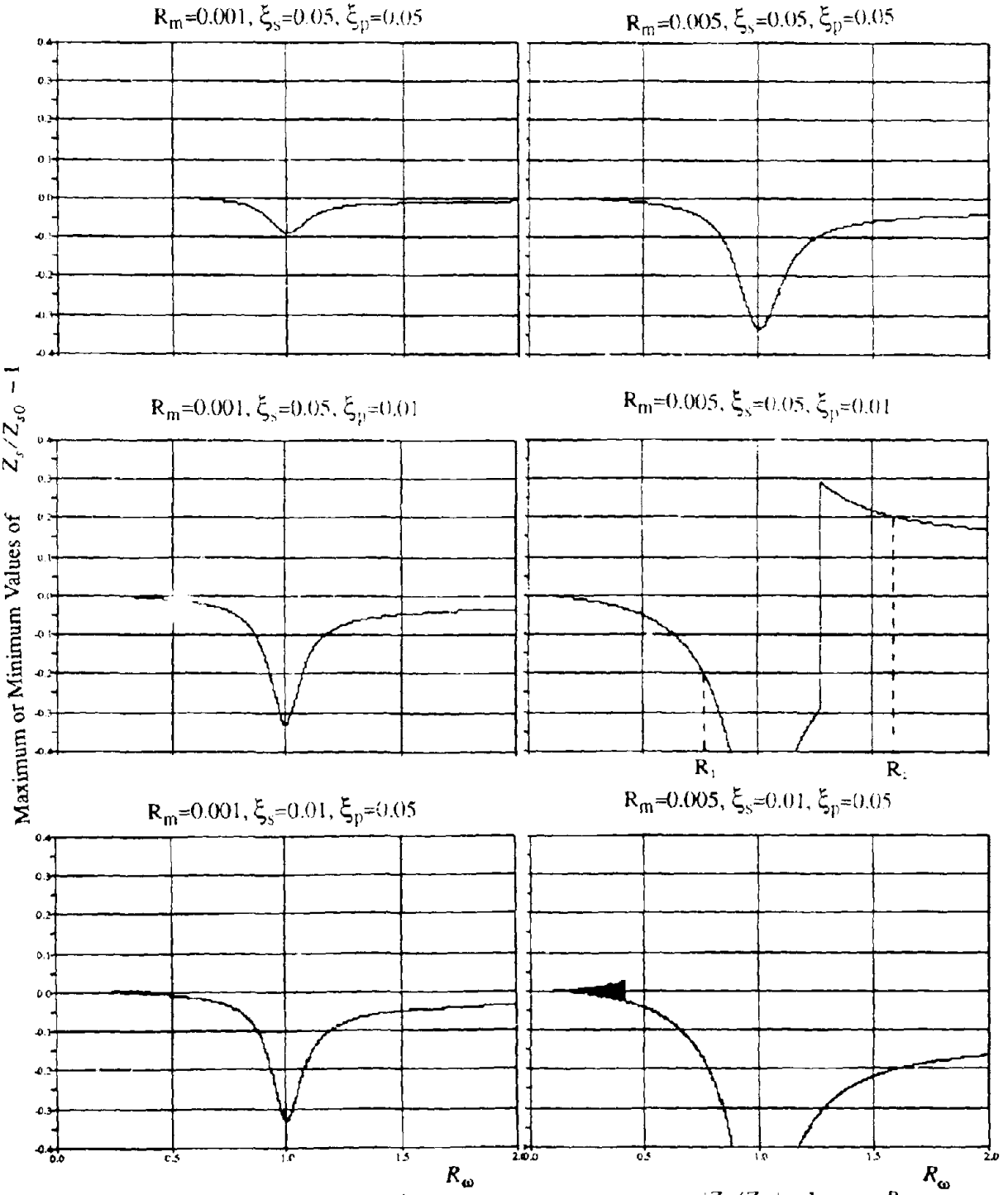

Fig. 4-2(a) Maximum or Minimum Values of $|Z_s/Z_{s0}| - 1$ vs. R_ω

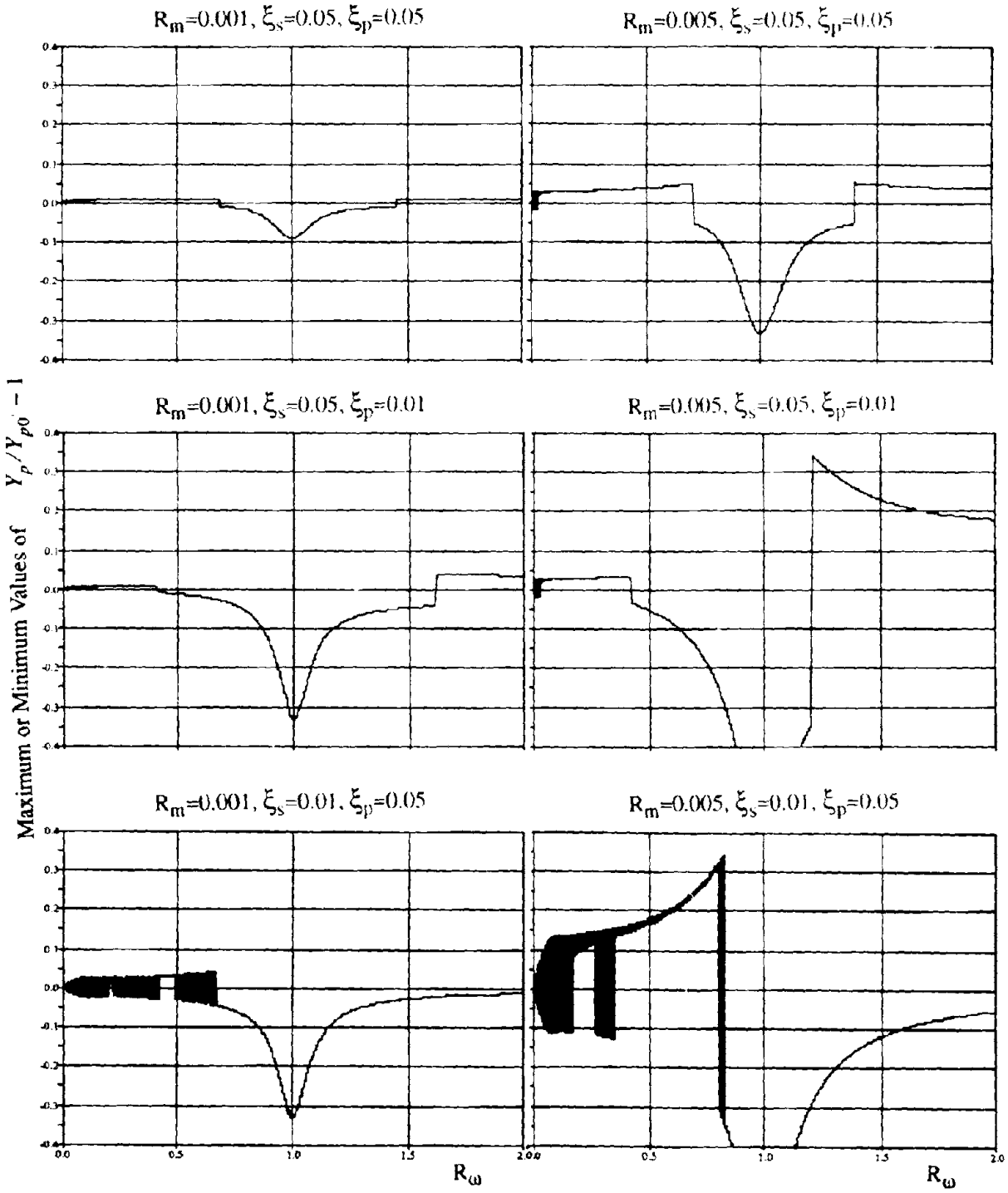

Fig. 4-2(b) Maximum or Minimum Values of $|Y_p / Y_{p0}| - 1$ vs. R_ω

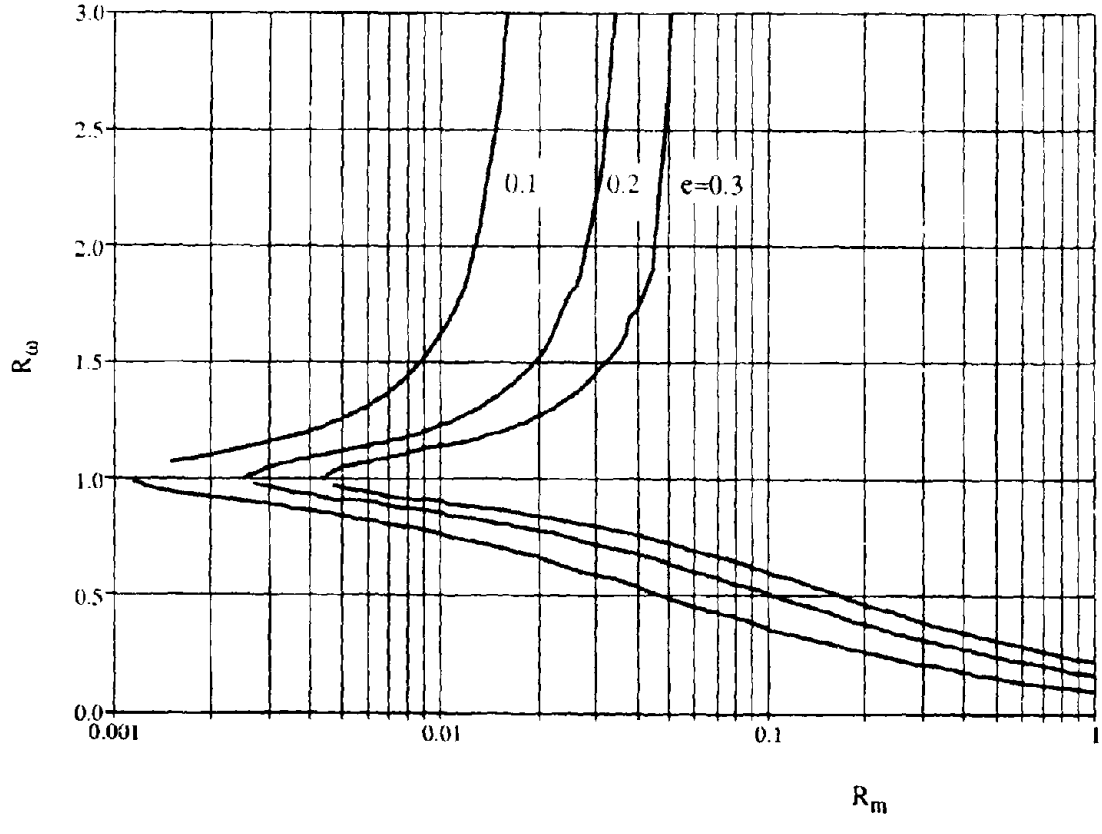

Fig. 4-3(a) Sufficient Conditions for Decoupling on S-System Response

$\xi_s = 0.05, \xi_p = 0.05$

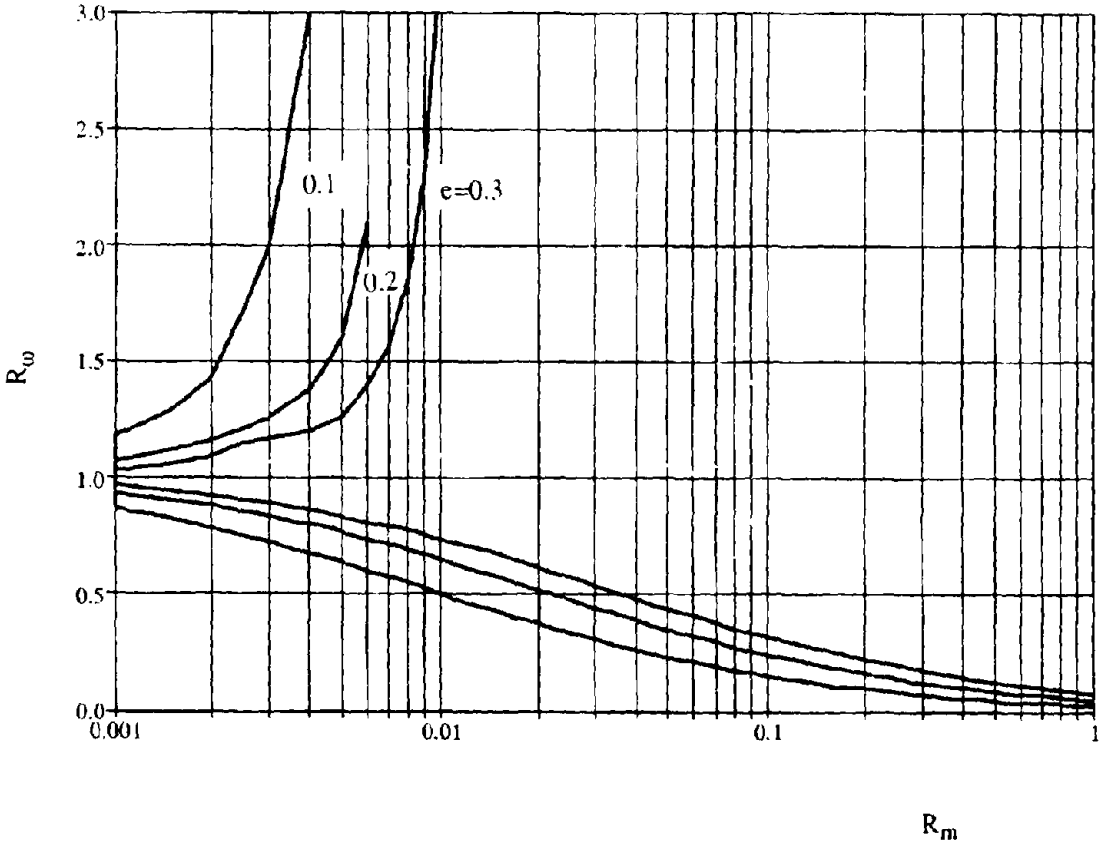

Fig. 4-3(b) Sufficient Conditions for Decoupling on S-System Response

$\xi_s = 0.05, \xi_p = 0.01$

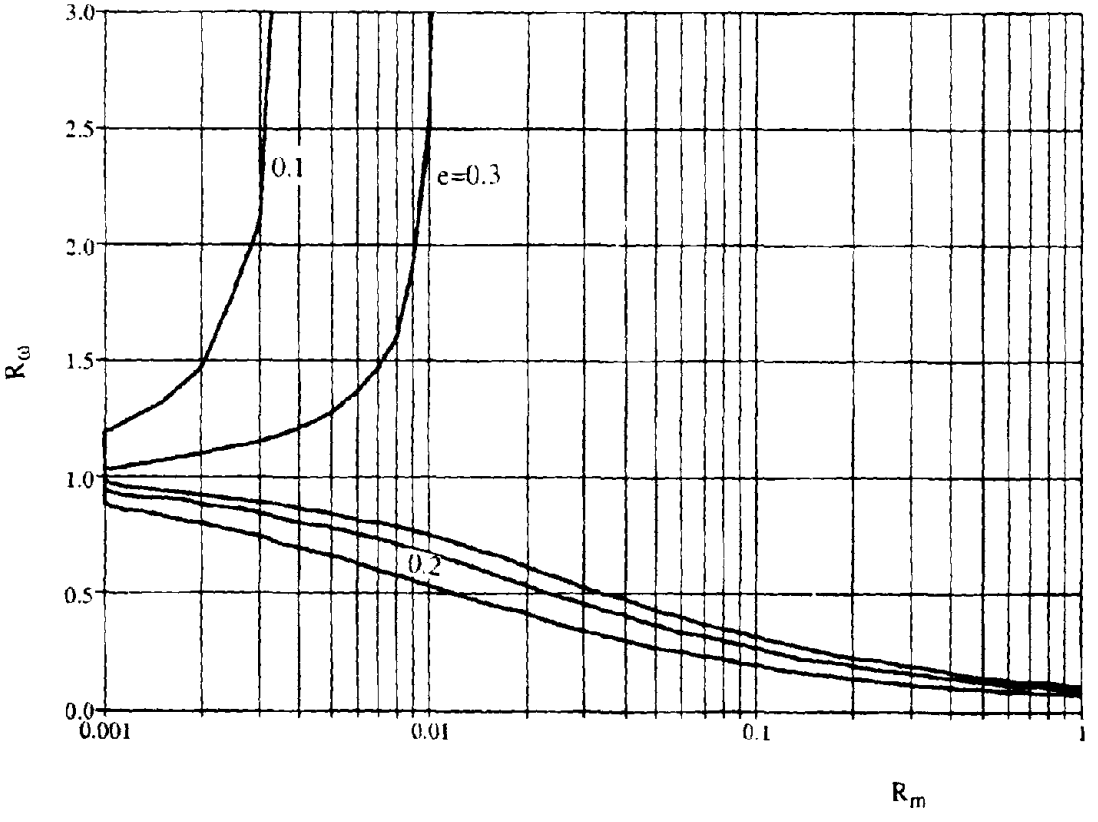

Fig. 4-3(c) Sufficient Conditions for Decoupling on S-System Response

$\xi_s = 0.01, \xi_p = 0.05$

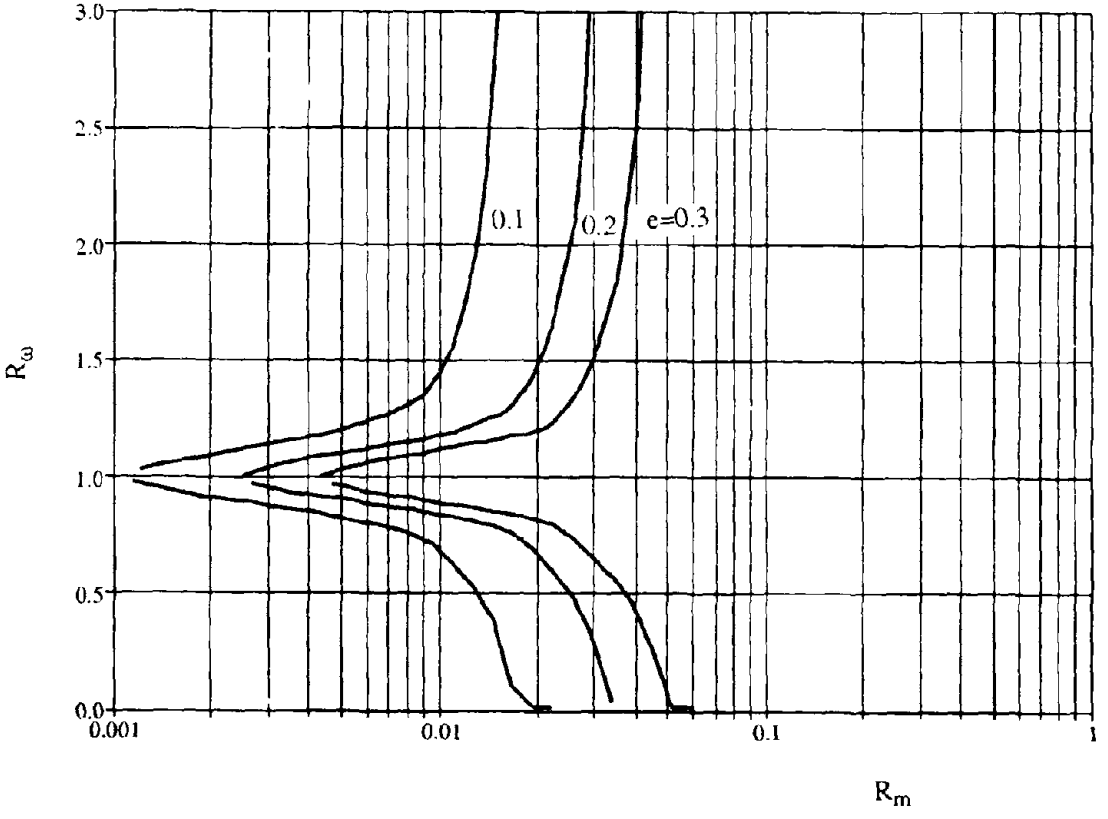

Fig. 4-4(a) Sufficient Conditions for Decoupling on P-System Response

$\xi_s = 0.05, \xi_p = 0.05$

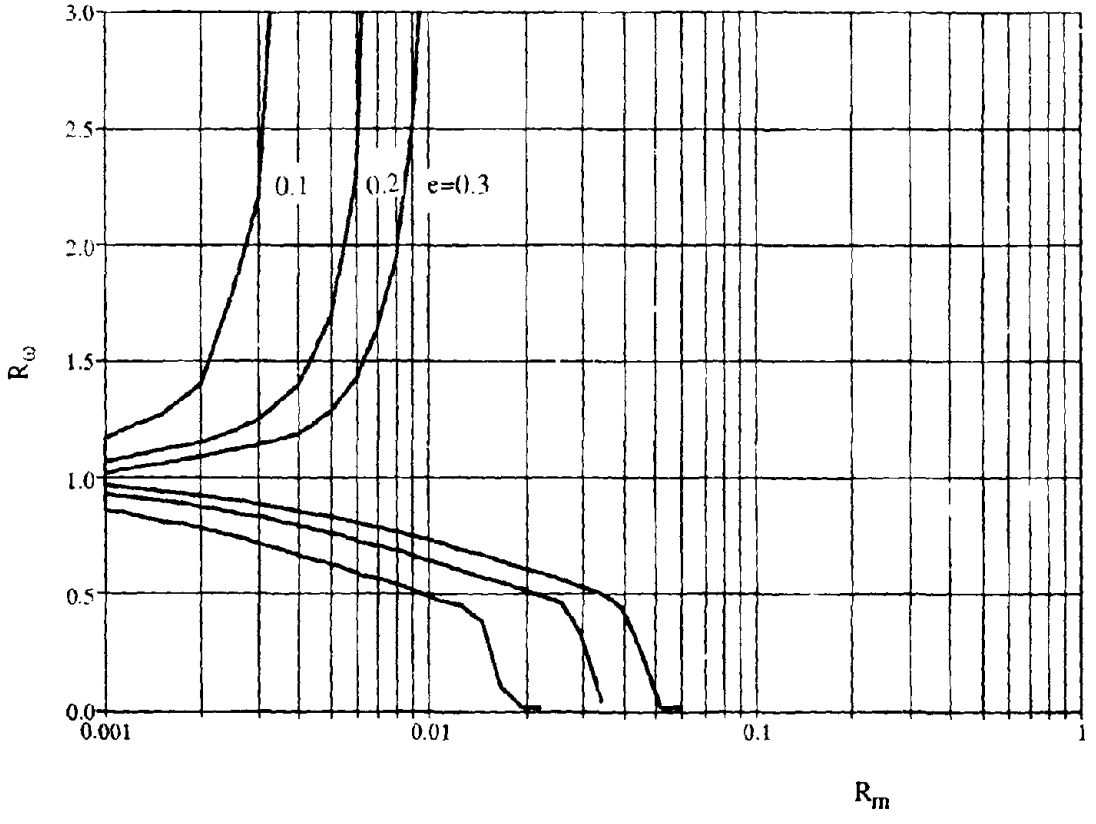

Fig. 4-4(b) Sufficient Conditions for Decoupling on P-System Response

$\xi_s = 0.05, \xi_p = 0.01$

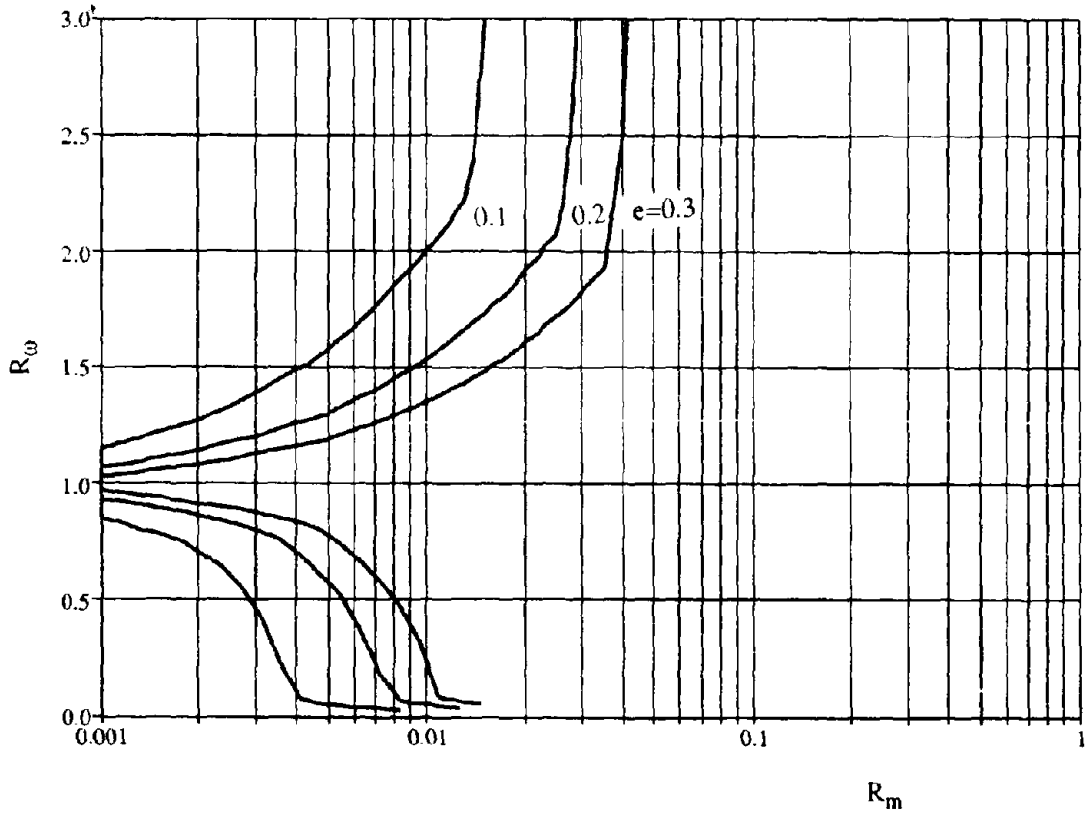

Fig. 4-4(c) Sufficient Conditions for Decoupling on P-System Response

$\xi_s = 0.01, \xi_p = 0.05$

substituting $(1+\varepsilon)$ for R_f^2 in Eq. (4.21), the following interactive equation between R_m and R_ω can be obtained:

$$R_\omega^2 = \frac{\varepsilon}{(1+\varepsilon)(\varepsilon - R_m)} \tag{4.22}$$

A similar formula has been reported in [26] for small variations of frequency Ω with respect to ω_p which is rewritten as follows:

$$R_\omega^2 = \frac{\varepsilon(1+\varepsilon)}{\varepsilon + (1+\varepsilon)R_m} \tag{4.23}$$

For a 10% variation in frequency, $R_f^2=(1\pm0.1)^2=1.21, 0.81$. Then, the small quantity ε is taken to be 0.21 or -0.19. The variations of R_ω with mass ratio (R_m) for both the P- and S-systems are plotted in Fig. 4-5. It can be seen that the natural frequency variation of the S-system controls decoupling of a stiff S-system whereas the variation of P-system controls decoupling of a flexible S-system.

Back to the question about sensitivity of responses to decoupling effect, a conclusion can be drawn based on the comparison between Fig. 4-3 and Fig. 4-4 that the response of a stiff S-system attached to a relatively flexible P-system is more sensitive to the decoupling action especially when damping ratio (ξ_s) decreases as demonstrated in the comparison of Fig. 4-3(b) and Fig. 4-4(b). Otherwise, the response of a P-system supporting a relatively flexible S-system is more vulnerable to the variation of interaction effect. These results are consistent with the frequency variation of the S- and P-systems due to decoupling action.

It is instructive to compare the above analysis with the previous work of [26]. The present analysis takes into account all the dynamic characteristics such as tuning effect, non-classical damping, etc. involved in a P-S system as listed in Section 2.1.4.1. In contrast, one mode approximation has been taken in the response calculation of [26] and the spectral displacement was assumed to not change significantly at the frequencies of the uncoupled P-system and the coupled P-S system. The one mode representation for a 2-DOF system will lead to an erroneous result when frequencies of the S- and P-systems are tuned, cases that initiated intensive research

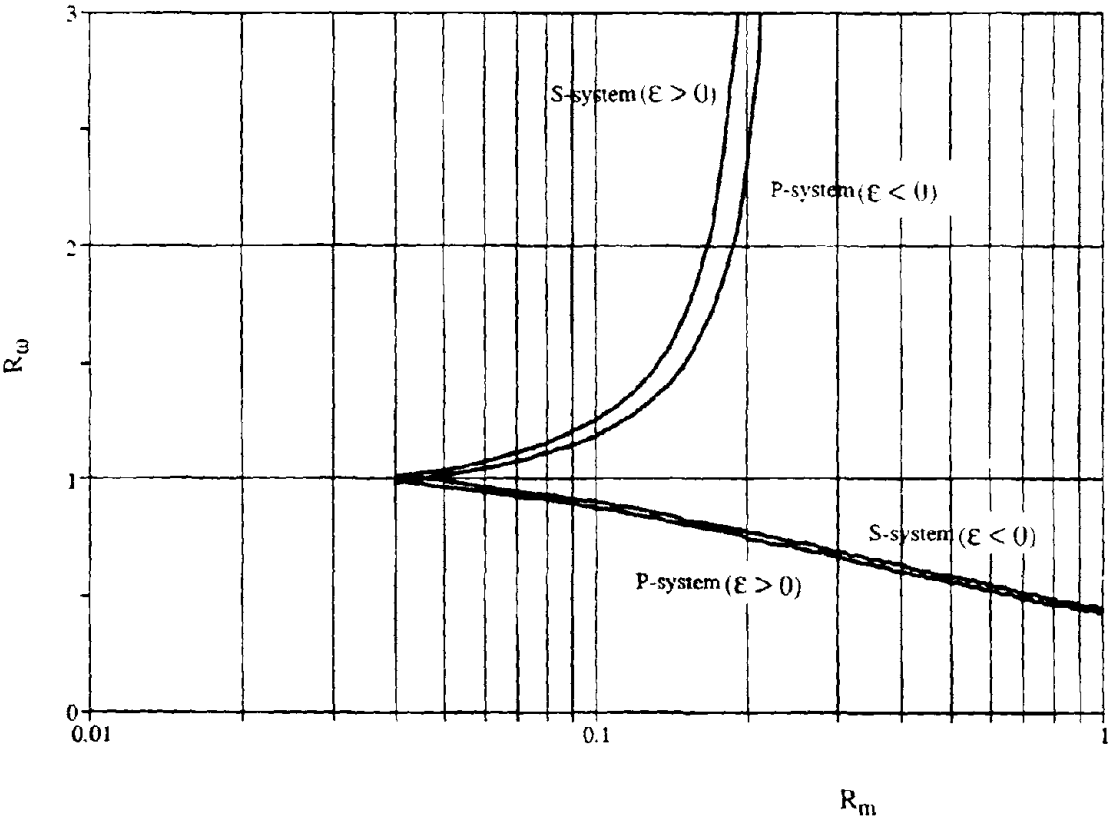

Fig. 4-5 Frequency Variation Due to Decoupling

activities in the past. In addition, the assumption of invariant spectral displacement took for granted that the damping characteristics of the combined P-S system remain proportional and modal damping ratio is independent of decoupling action which contradicts the results of [34].

4.3 Dynamic Decoupling Based on Energy Parameters

Response quantities such as energy (or its mean-square value) are of major concern in this report and therefore the decoupling effect on such parameters is of interest.

4.3.1 Decoupling Effect on Root-Mean-Square (RMS) Displacement

The mean-square displacements of the S- and P-systems under the excitation of white noise can be formulated as

$$\sigma_s^2 = S_{\ddot{x}_g} \int_{-\infty}^{\infty} |Z_s(\omega)|^2 d\omega \tag{4.24}$$

$$\sigma_p^2 = S_{\ddot{x}_g} \int_{-\infty}^{\infty} |Y_p(\omega)|^2 d\omega \tag{4.25}$$

and their corresponding mean-square values without interaction take the forms

$$\sigma_{s0}^2 = S_{\ddot{x}_g} \int_{-\infty}^{\infty} |Z_{s0}(\omega)|^2 d\omega \tag{4.26}$$

$$\sigma_{p0}^2 = S_{\ddot{x}_g} \int_{-\infty}^{\infty} |Y_{p0}(\omega)|^2 d\omega \tag{4.27}$$

Then, the dynamic decoupling criterion with tolerable error e can be defined as

$$\left| \frac{\sigma_s}{\sigma_{s0}} - 1 \right| = e \tag{4.28}$$

for the response calculation of the S-system and

$$\left| \frac{\sigma_p}{\sigma_{p0}} - 1 \right| = e \tag{4.29}$$

for the response calculation of the P-system.

Plots of R_m—R_ω obtained from Eq. (4.28) for different sets of damping ratios are presented in Figs. 4-6(a-c). It can be observed that influences of damping in the S- and P-systems on the response error due to neglect of interaction are qualitatively the same as the cases discussed in Section 4.2. This is particularly evident for small mass ratios. The larger the total damping, the smaller the error involved in non-interaction calculation of response of the S-system. Except for very flexible S-systems, the results computed from uncoupled procedures are generally on the conservative side.

The decoupling criteria for the calculation of the P-system response are shown in Figs. 4-7(a-c). Unlike maximum response of the P-system excited by harmonic loads, mean-square responses under the action of broad-band acceleration appear to be peculiar. The larger total damping does not necessarily mean a small amount of error involved in the response calculation. In contrast, the damping ratio of the P-system itself seems to have a predominant effect on the response. In comparison with Fig. 4-7(a), Fig. 4-7(c) demonstrates that an S-system with smaller damping attached to the same P-system will alleviate the interaction effect. This may be in part because the power flow (will be discussed in next section) contributed by the interaction action becomes smaller for a lightly damped S-system.

4.3.2 Decoupling Effect on Root-Mean-Square Acceleration

Acceleration response may be of great concern in practice when high precision instruments are installed or occupant comfort in high-rise buildings is a major factor in design considerations. The decoupling influence on this quantity is then of practical significance itself. The comparison of decoupling effect on displacement and acceleration will shed more light on the sensitivity of low and high frequency responses to the interaction.

The acceleration amplitudes of S- and P-systems subjected to harmonic load can be formulated from Eqs. (4.5) and (4.6) as

$$-\omega^2 (Z_s + Y_p) + 1 = \frac{1}{D} (j\omega 2\xi_s \omega_s + \omega_s^2) (\frac{1}{H_p} + \omega^2) \qquad (4.30)$$

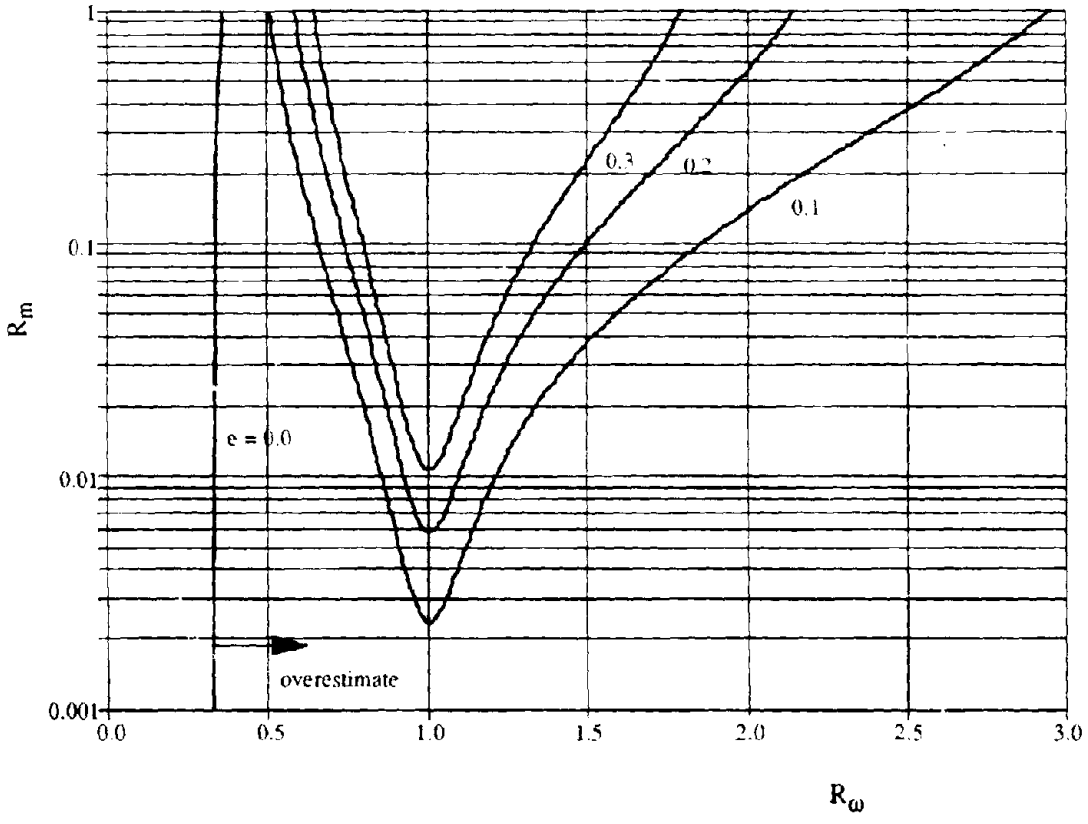

Fig. 4-6(a) Decoupling Conditions for RMS Displacement of S-System

$\xi_s = 0.05, \xi_p = 0.05$

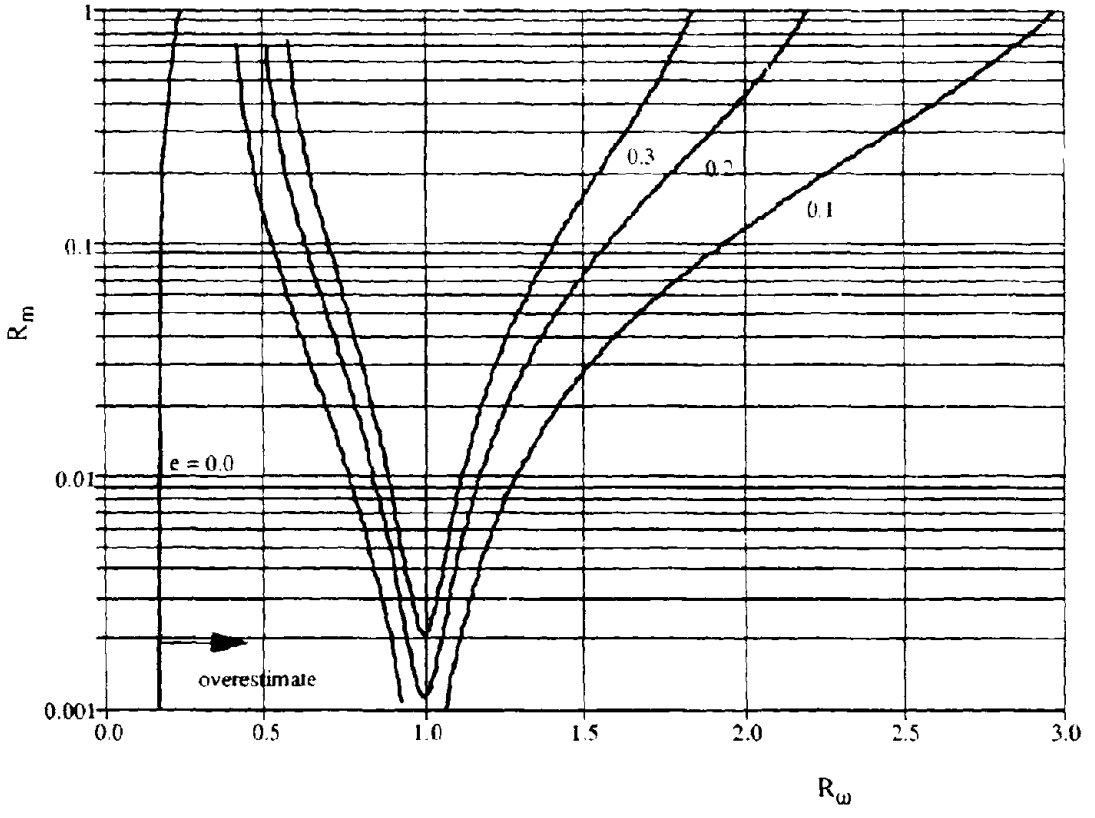

Fig. 4-6(b) Decoupling Conditions for RMS Displacement of S-System

$\xi_s = 0.05, \xi_p = 0.01$

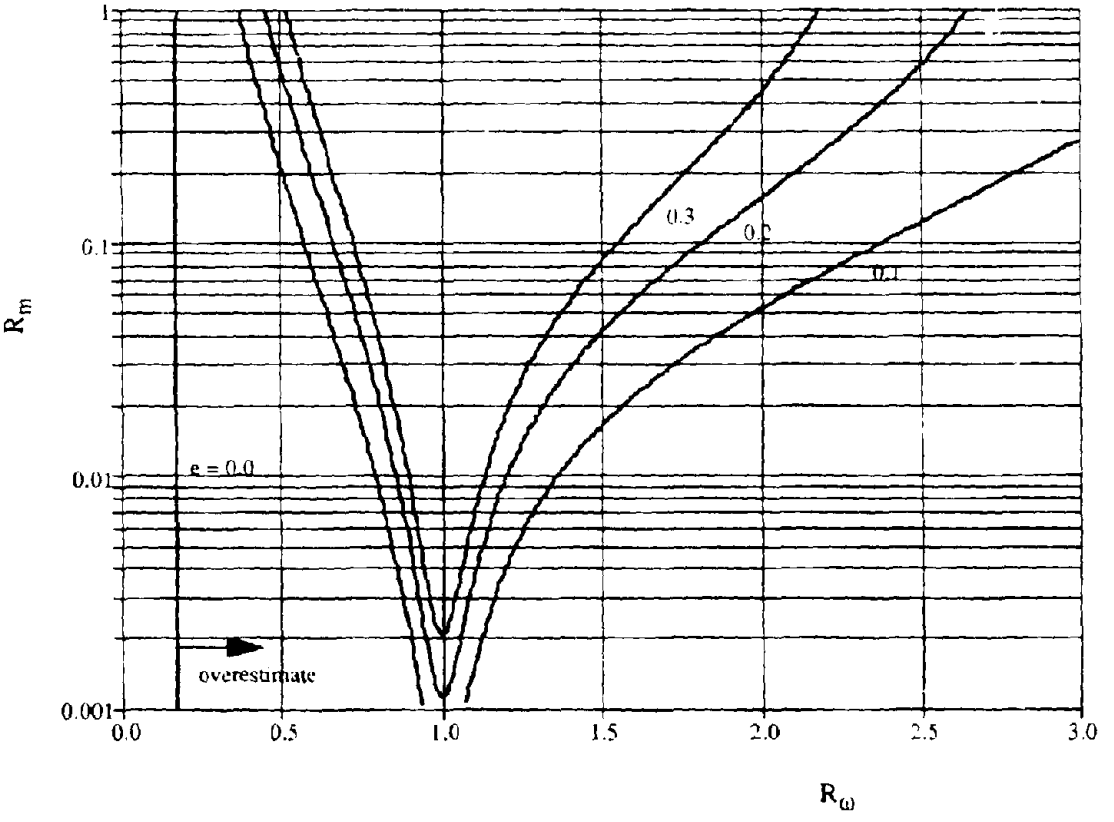

Fig. 4-6(c) Decoupling Conditions for RMS Displacement of S-System

$\xi_s = 0.01, \xi_p = 0.05$

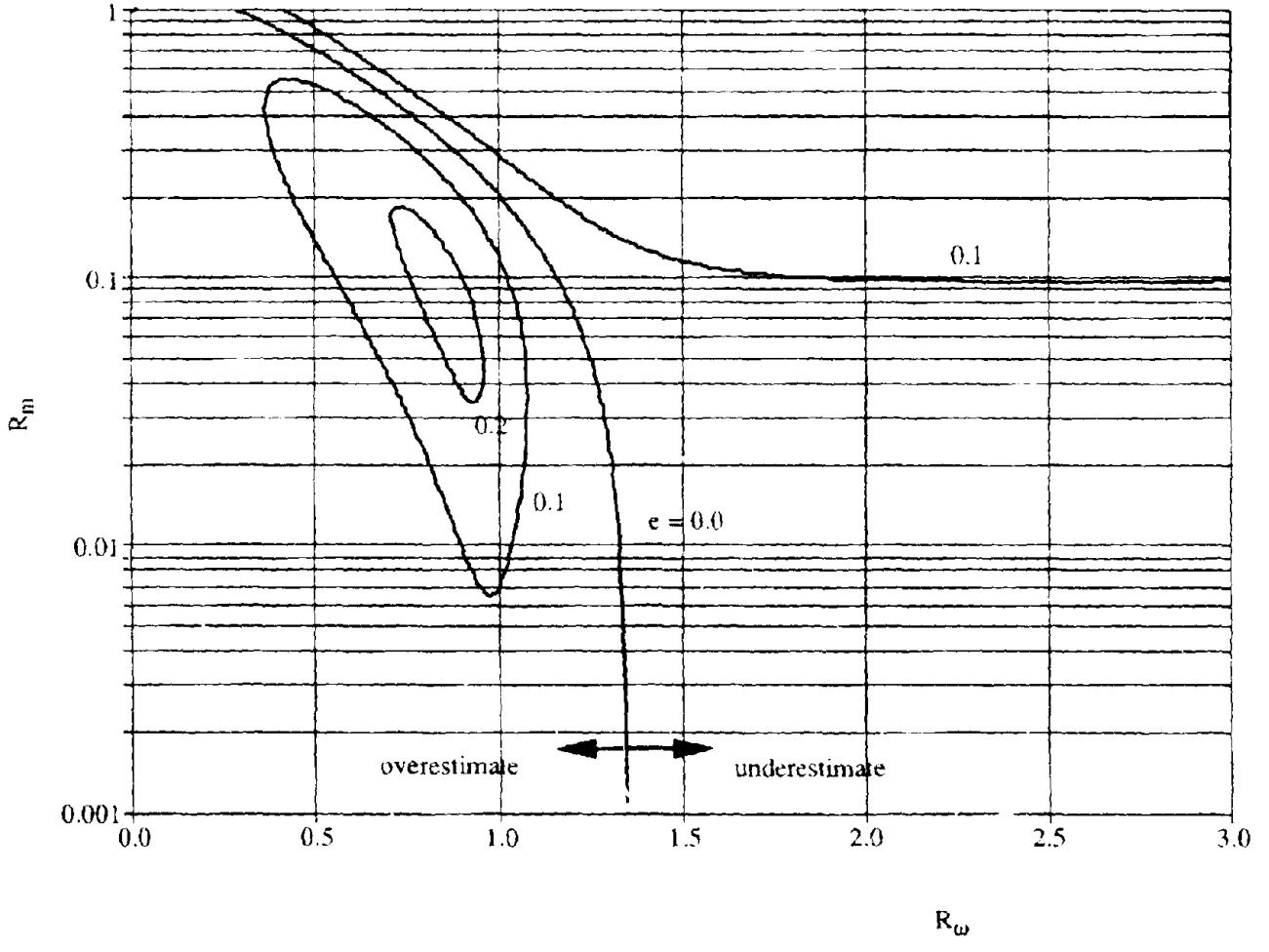

Fig. 4-7(a) Decoupling Conditions for RMS Displacement of P-System

$\xi_s = 0.05, \xi_p = 0.05$

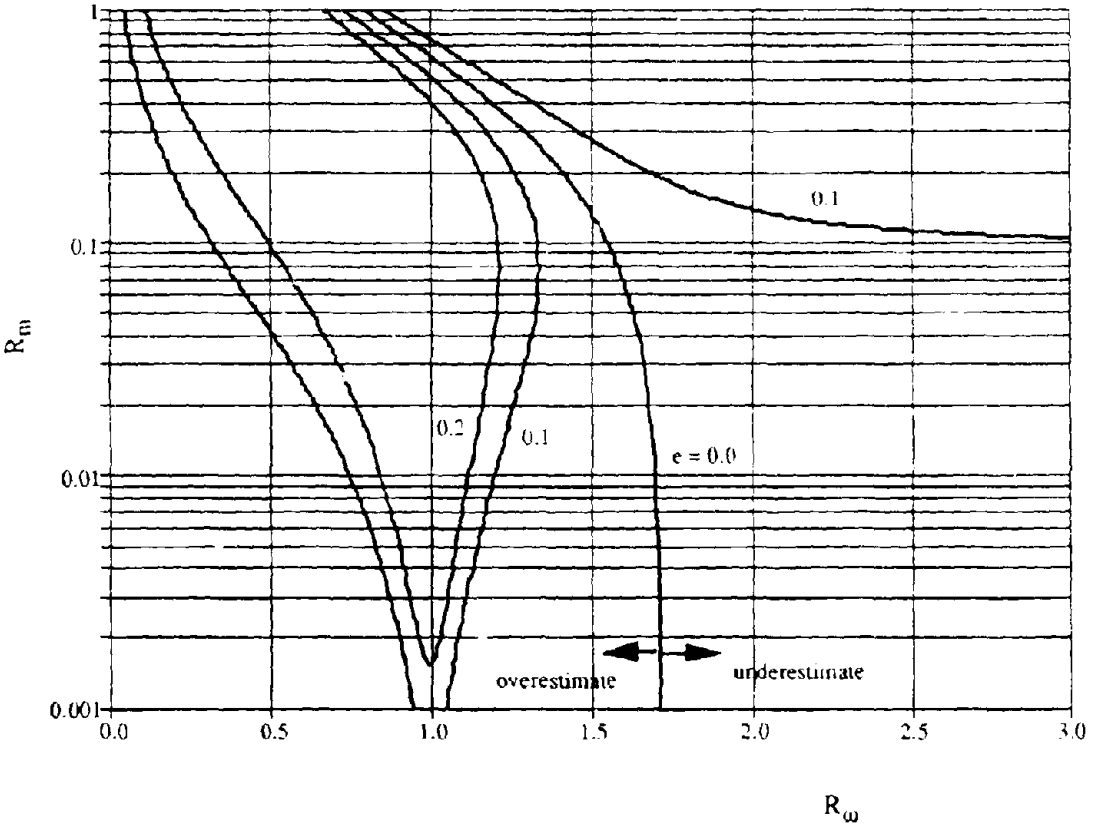

Fig. 4-7(b) Decoupling Conditions for RMS Displacement of P-System

$\xi_s = 0.05, \xi_p = 0.01$

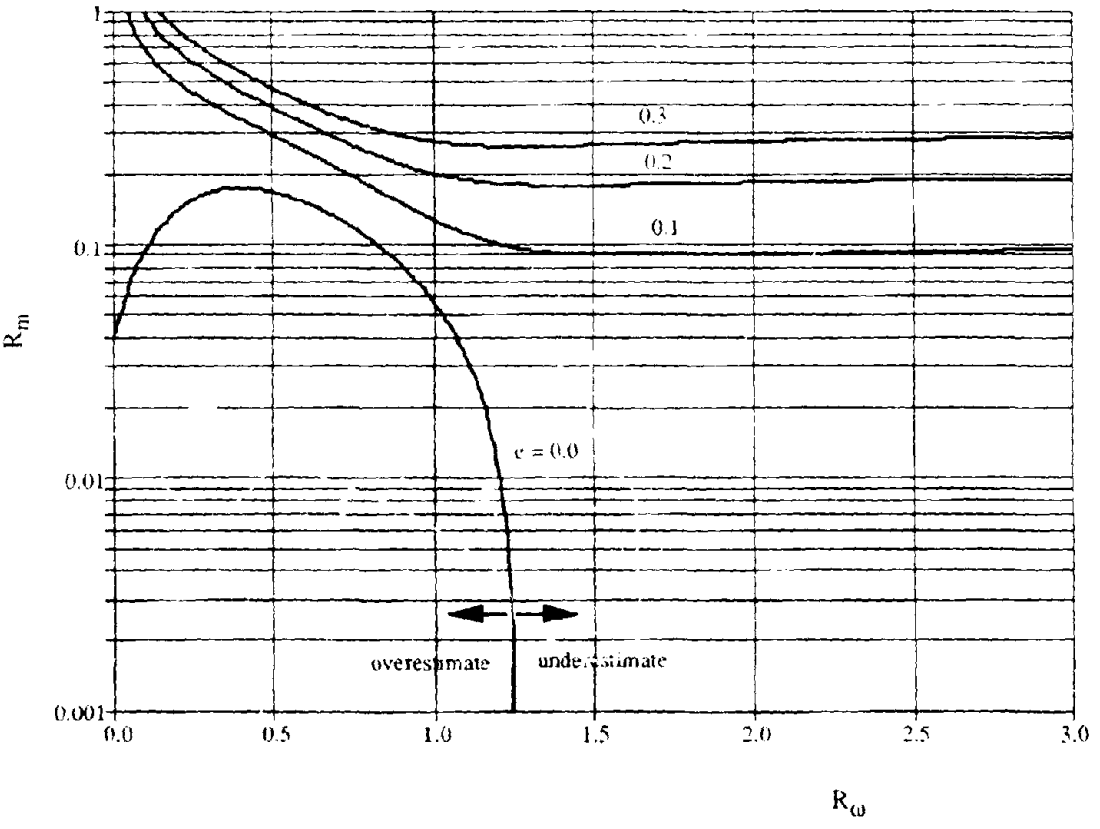

Fig. 4-7(c) Decoupling Conditions for RMS Displacement of P-System

$\xi_s = 0.01, \xi_p = 0.05$

$$-\omega^2 Y_p + 1 = \frac{1}{D}\frac{1}{H_s}\left(\frac{1}{H_p} + \omega^2\right) \tag{4.31}$$

By following the same procedure from Eq. (4.24) to Eq. (4.27), formulas similar to Eqs. (4.28) and (4.29) can be found in place of acceleration for displacement quantities. The effect of interaction on mean-square acceleration response of the S-system is approximately the same as the displacement result described by Eq. (4.28) due to light damping. The prevailing role that damping ratio ξ_p plays in the displacement response of the P-system remains unchanged in the acceleration response as shown in Figs. 4-8(a-c). However, acceleration variations due to interaction action for different dampings are consistently demonstrated to be not as sensitive as the displacement variations, implying that feedback from the S- to the P-system is more vulnerable to low frequency than high frequency components. Furthermore, non-interaction solution for acceleration of the P-system is always on the conservative side in the practical range or R_m and R_ω, a characteristic that is different from displacement response of the P-system but quite similar to that of the S-system. From the mathematical point of view, these relative relations among displacement response of the S-system, acceleration response of the P-system, and displacement response of the P-system reflect the fact that the numerators of total transfer functions of the S-system displacement and the P-system acceleration to ground acceleration are independent of the mass ratio whereas the numerator of the P-system displacement transfer function is a function of the mass ratio as shown in Eqs. (4.10), (4.11), and (4.31). For this reason, the absolute acceleration ratio of the P-system subjected to a harmonic load with and without interaction is exactly the same as displacement ratio of the S-system as given in Eq. (4.17) and so is its sufficient condition of decoupling as discussed in Section 4.2.3.

4.3.3 Dynamic Decoupling for MDOF P-S System

The results obtained in the preceding sections can be extended to MDOF P- and MDOF S-systems by following the procedure of [26,27]. In what follows, only dynamic decoupling of an

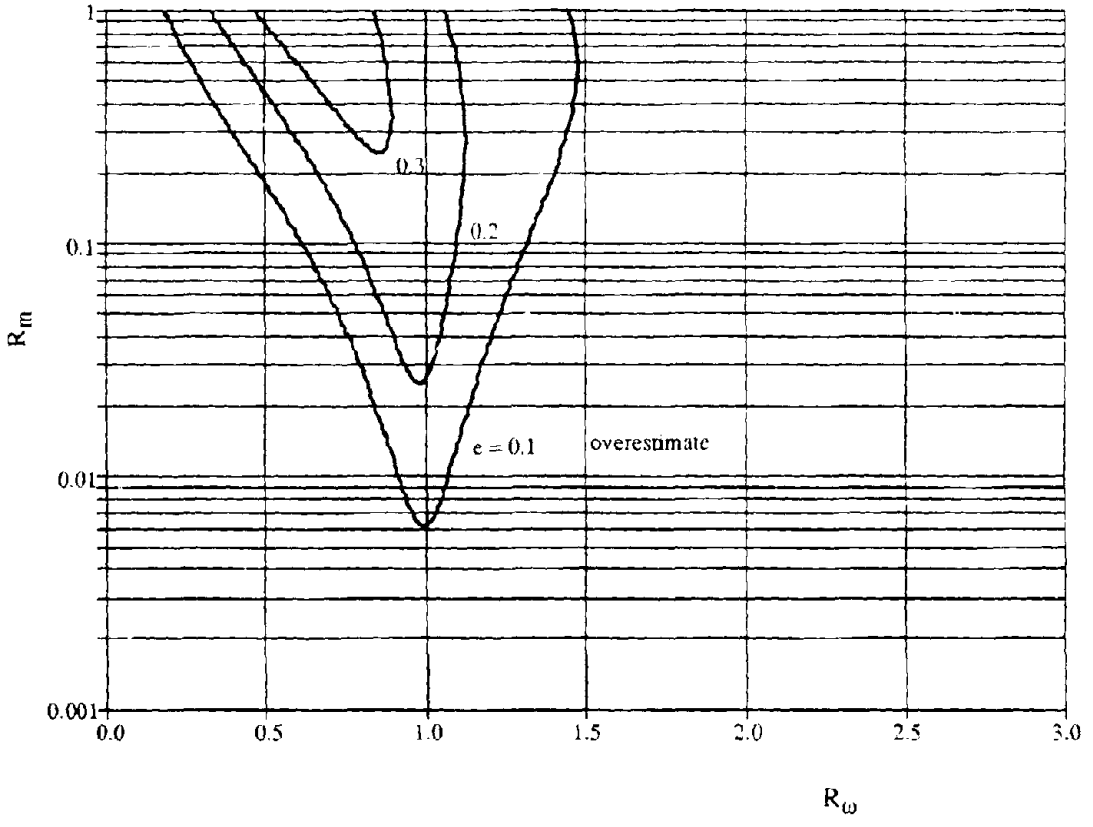

Fig. 4-8 (a) Decoupling Conditions for RMS Acceleration of P-System

$\xi_s = 0.05, \xi_p = 0.05$

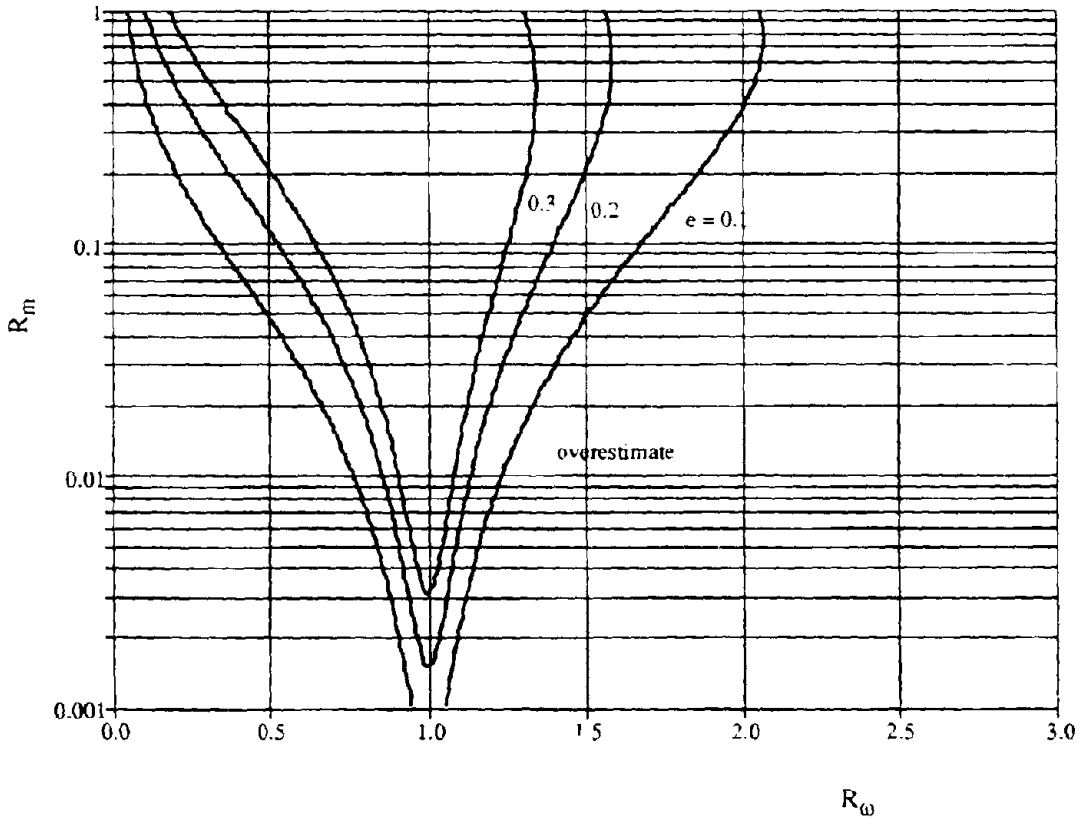

Fig. 4-8(b) Decoupling Conditions for RMS Acceleration of P-System

$\xi_s = 0.05, \xi_p = 0.01$

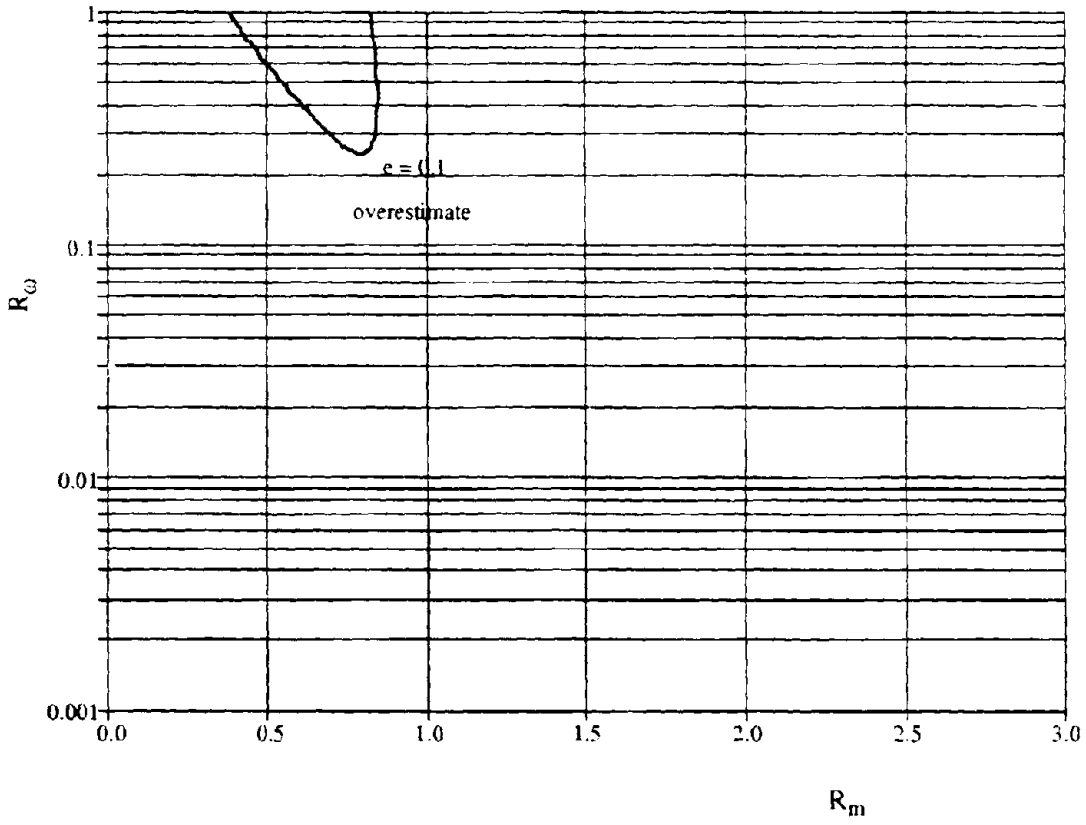

Fig. 4-8(c) Decoupling Conditions for RMS Acceleration of P-System

$\xi_s = 0.01, \xi_p = 0.05$

SDOF S- and one mode representation of an MDOF P-system is discussed as an indication of the application to SDOF S- and MDOF P-systems.

Consider an SDOF S-system attached to the top of the same multi-story building (P-system) as discussed in Section 3. The equations of motion for the SDOF S-system and first mode representation of the P-system are exactly the same as Eqs. (4.5) and (4.6) except that the right-hand side of the second equation includes a participation factor due to load distribution on the multi-story building. This factor is taken here from Eq. (3.6) for simplicity, i.e., $\Gamma_1 = 4/\pi$. The decoupling criterion for such a system is plotted in Fig. 4-9. The comparison between this figure and Fig. 4-7(a) assures the applicability of decoupling criterion generated from a simple P-S system.

4.4 Conclusions

From the preceding discussions, some conclusions can be drawn about the decoupling issue of S-systems. Sufficient conditions for decoupling under different damping combinations of the P-S system have been proposed to assure that any selection of R_ω and R_m on the left-hand side of the sufficient condition will have the error induced by interaction less than the value designated in the sufficient condition. Total damping of S- and P-systems plays an important role in reducing the error brought about from interaction for both systems. For a constant total damping, an increase in P-system damping can not significantly change the error in the calculation of the S-system response but can reduce the error in the response of the P-system supporting a relatively stiff S-system. The displacement response of an S-system (P-system) is generally more sensitive to the interaction effect than that of a relatively flexible P-system (S-system).

The conservative ranges in the $R_m - R_\omega$ plane for the S- and P-systems, within which uncoupled calculation of the mean-square displacement is overestimated, are on different sides of their own exact solutions ($e = 0.0$) but may overlap in a certain range. This suggests that any selection of R_ω and R_m, which assures the design of the P-system by uncoupled analysis on the conservative side, may underestimate the response of the S-system. This point should be noted in practical design.

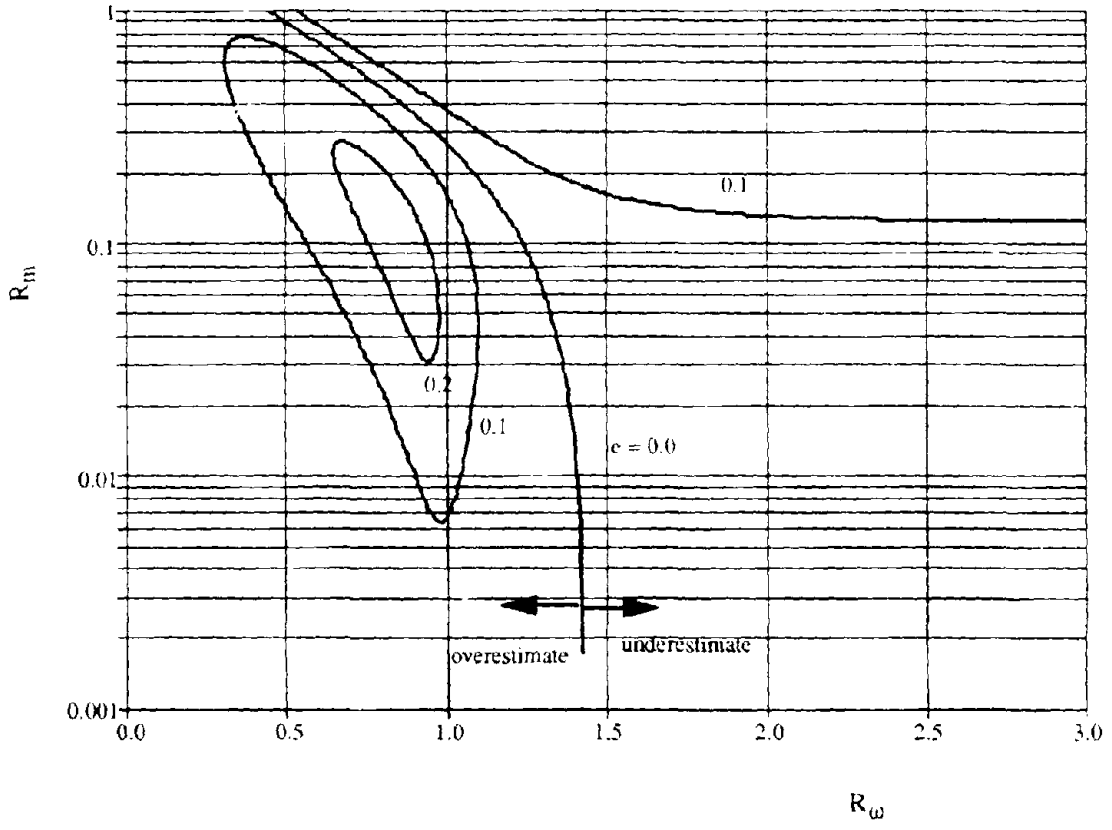

Fig. 4-9 Decoupling Conditions for RMS Displacement of SDOF Representation

$\xi_s = 0.05, \xi_p = 0.05$

For a certain tolerable error, uncoupled calculation of mean-square displacement of the P-system under broad-band input should be limited to a small domain in the $R_m - R_\omega$ plane, whereas those of the S-system displacement and P-system acceleration could be much more flexible.

SECTION 5

POWER FLOW AND ENERGY BALANCE BETWEEN NON-CONSERVATIVELY COUPLED OSCILLATORS

5.1 Introduction

As indicated in Section 2.2.2.1, the concept of power flow is the foundation of SEA. For conservatively coupled oscillators, SEA has given two fundamental relationships [55]: (1) Without energy dissipation in the joint element between two subsystems, the total average power flow from subsystem 1 to the coupling element is equal to the average power flow from subsystem 1 to subsystem 2 and the power flows in two opposite directions have the same absolute value; (2) The average power flow from oscillator 1 to oscillator 2 is directly proportional to the difference of the average vibrational energies as shown in Eq. (2.7).

In practice, however, mechanical and structural systems composed of many subsystems with spring and damping connections are usually dealt with, in which non-conservative couplings are involved. Therefore, the conventional SEA technique cannot be directly applied and further studies on the extension of SEA to non-conservatively coupled cases are needed.

The power flow between non-conservatively coupled oscillators has been investigated in [22,91] who gave different definitions for it. In [91], power flow is defined as $P_{12} = Re\{F_{12}V_2^*\}$, in which V_2^* is the complex conjugate of the velocity of oscillator 2 in the frequency domain and F_{12} denotes the force that acts on oscillator 2 due to the motion of oscillator 1. There exist two inconsistencies in this definition: (1) In expressing the interaction force F_{12}, oscillator 2 is considered to be fixed so that interaction between the two oscillators is neglected; and (2) The velocity of oscillator 2 is involved. This appears to be contrary to conventional power flow definition. These two deficiencies result in a contradiction in the derivation of the power balance equations and some of the numerical results are not reasonable on physical ground.

In [22], the expression for the interaction force has been improved, but the definition of power flow is basically the same as in [91]. Therefore, the contradiction in power balance equations continues to exist and inconsistencies remain.

Additionally, both references [22,91] assume that the potential energy stored in each oscillator is approximately equal to its kinetic energy. This may not be true when the coupling spring stiffness is greater than the two spring stiffnesses of the oscillators, which will be verified by numerical results in this section. Moreover, it has been pointed out that the power flow is not only proportional to the difference between the average energies of oscillators but also to the vibrational energies themselves, i.e.,

$$P_{12} = \alpha(E_1 - E_2) + \beta E_1 + \gamma E_2$$

This relationship is formed with arbitrariness in [22,91] because the two independent inputs cannot be uniquely expressed by the three arguments $(E_1, E_2, E_1 - E_2)$. This may in part explain the reason why the coefficient α behaves quite differently in relation to the coupling element c_3 from these two references.

In this section, an auxiliary system with a variable coupling spring K between the two oscillators is designed so that the concept of power flow between two conservatively coupled oscillators can be directly extended to the non-conservative case. As K approaches infinity in the limit, the auxiliary system approaches the non-conservatively coupled case and a consistent expression for power flow from oscillator 1 can be formulated. The system considered here is generic in order to reach a general relation between power flow and energy which can be served as a fundamental formulation in the SEA framework for non-conservatively coupled systems and a starting point in the application to complex P-S systems.

5.2 Equations of Motion and Power Flow

In order to follow the formulation associated with conservatively coupled oscillators, a spring element with spring constant K is inserted between one of the masses and the non-conservative coupling elements as shown in Fig. 5-1(a) or 5-1(b). In the limiting case when $K \to \infty$, the configuration of the two non-conservatively coupled oscillators results as shown in Fig. 5-1(c).

The configuration shown in Fig. 5-1(a) is used for the derivation of power balance equation

for oscillator 1. As one sees, one more degree of freedom is introduced due to the presence of K and the equations of motion are

$$m_1\ddot{x}_1 + c_1\dot{x}_1 + (k_1 + K)x_1 - Kx_3 = f_1 \tag{5.1}$$

$$m_2\ddot{x}_2 + (c_2 + c_3)\dot{x}_2 + (k_2 + k_3)x_2 - c_3\dot{x}_3 - k_3x_3 = f_2 \tag{5.2}$$

$$c_3\dot{x}_3 + (k_3 + K)x_3 - c_3\dot{x}_2 - Kx_1 - k_3x_2 = 0 \tag{5.3}$$

where m_1 and m_2 are, respectively, the masses of oscillators 1 and 2 with associated spring constants k_1 and k_2 and damping coefficients c_1 and c_2. The coupling elements are represented by k_3 and c_3. The excitations f_1 and f_2 acting on, respectively, m_1 and m_2 are assumed to be uncorrelated wide-band stationary processes. In Eqs. (5.1)-(5.3), x_1 and x_2 represent the displacements of the two oscillators while x_3 denotes the displacement at the interface between K and (k_3, c_3).

Upon multiplying Eqs. (5.1)-(5.3) by $\dot{x}_1$, $\dot{x}_2$ and $\dot{x}_3$, respectively, and taking statistical average of both sides of the resulting equations, the above equations become

$$m_1\langle\ddot{x}_1\dot{x}_1\rangle + c_1\langle\dot{x}_1^2\rangle + (k_1 + K)\langle x_1\dot{x}_1\rangle - K\langle x_3\dot{x}_1\rangle = \langle f\dot{x}_1\rangle \tag{5.4}$$

$$m_2\langle\ddot{x}_2\dot{x}_2\rangle + (c_2 + c_3)\langle\dot{x}_2^2\rangle + (k_2 + k_3)\langle x_2\dot{x}_2\rangle - c_3\langle\dot{x}_3\dot{x}_2\rangle - k_3\langle x_3\dot{x}_2\rangle = \langle f_2\dot{x}_2\rangle \tag{5.5}$$

$$c_3\langle\dot{x}_3^2\rangle + (k_3 + K)\langle x_3\dot{x}_3\rangle - c_3\langle\dot{x}_2\dot{x}_3\rangle - K\langle x_1\dot{x}_3\rangle - k_3\langle x_2\dot{x}_3\rangle = 0 \tag{5.6}$$

where the symbol < . > denotes mathematical expectation.

It is well known that, for steady-state response to a stationary input,

$$\langle x_i\dot{x}_i\rangle = 0 \qquad and \qquad \langle\dot{x}_i\ddot{x}_i\rangle = 0, \qquad (i = 1, 2, 3)$$

$$\frac{d\langle x_1x_3\rangle}{dt} = 0$$

Equations (5.4)-(5.6) thus reduce to

$$c_1\langle\dot{x}_1^2\rangle - K\langle x_3\dot{x}_1\rangle = \langle f_1\dot{x}_1\rangle \tag{5.7}$$

$$(c_2 + c_3)\langle\dot{x}_2^2\rangle - c_3\langle\dot{x}_3\dot{x}_2\rangle - k_3\langle x_3\dot{x}_2\rangle = \langle f_2\dot{x}_2\rangle \tag{5.8}$$

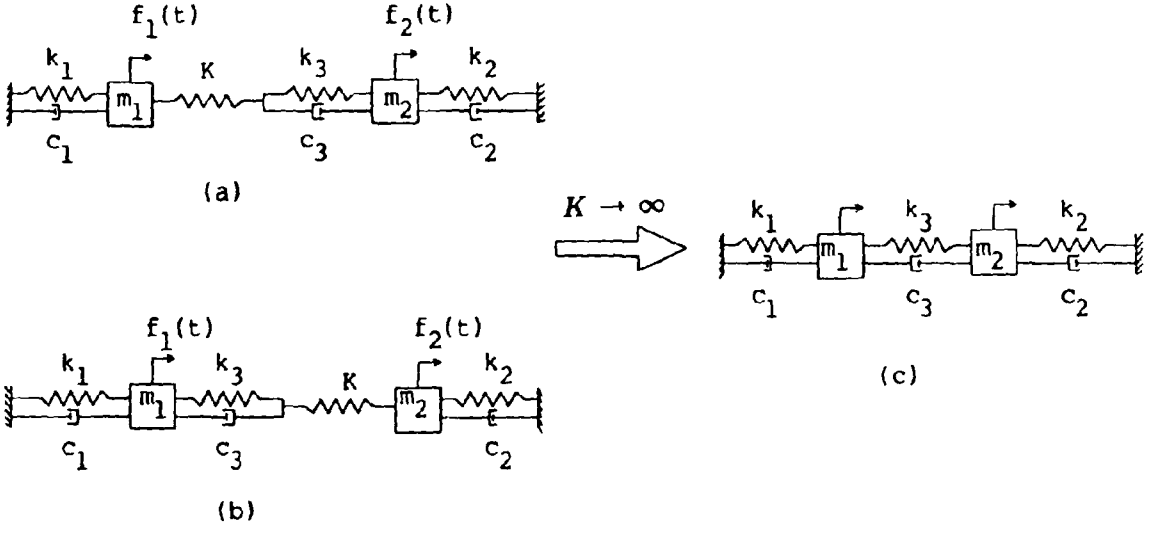

Fig. 5-1 Configurations of Auxiliary and Original System

$$c_3\langle \dot{x}_3^2\rangle - c_3\langle \dot{x}_2\dot{x}_3\rangle - K\langle x_1\dot{x}_3\rangle - k_3\langle x_2\dot{x}_3\rangle = 0 \tag{5.9}$$

By summing Eqs. (5.7)-(5.9), the total power balance equation for the system has the form

$$c_1\langle \dot{x}_1^2\rangle + c_2\langle \dot{x}_2^2\rangle + c_3\langle (\dot{x}_2 - \dot{x}_3)^2\rangle = \langle f_1\dot{x}_1\rangle + \langle f_2\dot{x}_2\rangle \tag{5.10}$$

Equation (5.7) is the power balance equation for oscillator 1; but, for oscillator 2 with element (k_3, c_3), the power balance equation is

$$c_2\langle \dot{x}_2^2\rangle + c_3\langle (\dot{x}_2 - \dot{x}_3)^2\rangle - K\langle x_1\dot{x}_3\rangle = \langle f_2\dot{x}_2\rangle \tag{5.11}$$

The power flow from oscillator 1 is then

$$P_{12} = -\lim_{K\to\infty} K\langle x_3\dot{x}_1\rangle = \lim_{K\to\infty} K\langle x_1\dot{x}_3\rangle \tag{5.12}$$

5.3 Formulation of Power Flow P_{12}

Upon substituting $x_i = X_i e^{j\omega t}$ and $f_i = F_i e^{j\omega t}$ into Eqs. (5.1)-(5.3), the equations of motion in the frequency domain take the forms

$$[-m_1\omega^2 + j\omega c_1 + (k_1 + K)]X_1 - KX_3 = F_1 \tag{5.13}$$

$$[-m_2\omega^2 + j\omega(c_2 + c_3) + (k_2 + k_3)]X_2 - (k_3 + j\omega c_3)X_3 = F_2 \tag{5.14}$$

$$j\omega c_3 X_3 + (k_3 + K)X_3 - KX_1 - (k_3 + j\omega c_3)X_2 = 0 \tag{5.15}$$

whose solution can be represented by

$$X_1 = H_{11}(\omega)F_1 + H_{12}(\omega)F_2 \tag{5.16}$$

$$X_2 = H_{21}(\omega)F_1 + H_{22}(\omega)F_2 \tag{5.17}$$

$$X_3 = H_{31}(\omega)F_1 + H_{32}(\omega)F_2 \tag{5.18}$$

where

$$H_{11}(\omega) = \frac{1}{D}\left\{(\omega_2^2 - \omega^2 + j\omega\Delta_2)\left[\frac{K}{m_1} + \lambda_{21}(\nu + j\omega\mu)\right] - (\nu + j\omega\mu)^2\right\}$$

$$H_{12}(\omega) = H_{21}(\omega) = \frac{1}{D}\frac{K}{m_2}\lambda_{21}(\nu + j\omega\mu)$$

$$H_{22}(\omega) = \frac{1}{D}\left\{(\omega_1^2 - \omega^2 + j\omega\Delta_1)\left[\frac{K}{m_2} + \lambda_{12}(\nu + j\omega\mu)\right] - (\nu + j\omega\mu)^2\right\}$$

$$H_{31}(\omega) = \frac{1}{D}\frac{K}{m_1}(\omega_2^2 - \omega^2 + j\omega\Delta_2)$$

$$H_{32}(\omega) = \frac{1}{D}\lambda_{12}(\nu + j\omega\mu)\left[\omega_1^2 - \omega^2 + j\omega\Delta_1 - \lambda_{21}(\nu + j\omega\mu) + \frac{K}{m_1}\right]$$

$$D = K[(\omega_1^2 - \omega^2 + j\omega\Delta_1)(\omega_2^2 - \omega^2 + j\omega\Delta_2) - (\nu + j\omega\mu)^2]$$
$$+ \sqrt{m_1 m_2}(\nu + j\omega\mu)[\omega_1^2 - \omega^2 + j\omega\Delta_1 - \lambda_{21}(\nu + j\omega\mu)][\omega_2^2 - \omega^2 + j\omega\Delta_2 - \lambda_{12}(\nu + j\omega\mu)]$$

In the above, a number of new parameters are introduced and they are defined by

$\Delta_1 = \frac{c_1 + c_3}{m_1}$, $\Delta_2 = \frac{c_2 + c_3}{m_2}$: *blocked* damping parameters of oscillator 1 and 2;

$\omega_1 = \sqrt{\frac{k_1 + k_3}{m_1}}$, $\omega_2 = \sqrt{\frac{k_2 + k_3}{m_2}}$: *blocked* frequency of oscillator 1 and 2;

$\mu = \frac{c_3}{\sqrt{m_1 m_2}}$: coupling damping parameter;

$\nu = \frac{k_3}{\sqrt{m_1 m_2}}$: coupling spring stiffness parameter;

$\lambda = \sqrt{\frac{m_i}{m_j}}$ $(i, j = 1, 2)$: mass ratio.

The power flow P_{12} as defined by Eq. (5.12) can now be found by performing the contour integration

$$P_{12} = \lim_{K \to \infty} \int_{-\infty}^{\infty} j\omega K [H_{31}(\omega) H_{11}^*(\omega) S_1 + H_{32}(\omega) H_{12}^*(\omega) S_2] d\omega \qquad (5.19)$$

in which $H^*_{ij}(\omega)$ is the complex conjugate of $H_{ij}(\omega)$ (i=1,2) and S_1 and S_2 are the power spectra of excitations $f_1(t)$ and $f_2(t)$, respectively. The integral in Eq. (5.19) can be carried out and P_{12} can be explicitly written as

$$P_{12} = \lambda_{21}\mu E_{1b} - \left(1 - \frac{\lambda_{21}\mu}{\Delta_1}\right)[(\gamma_{12} - \alpha)E_{1b} + (\alpha + \beta)E_{2b}] \tag{5.20}$$

in which

$$\alpha = \frac{\Delta_1\Delta_2}{Q}\nu^2(\Delta_1 + \Delta_2), \quad \beta = \frac{\Delta_1\Delta_2}{Q}\mu^2(\Delta_1\omega_2^2 + \Delta_2\omega_1^2 - 2\mu\nu)$$

$$\gamma_{ij} = \frac{\Delta_i\Delta_j}{Q}\mu^2(\Delta_i\omega_j^2 + \Delta_j\omega_i^2 - 2\mu\nu) + 2\mu\nu(\omega_j^2 - \omega_i^2) + \frac{4\mu^2\nu^2}{\Delta_j}$$

$$(i, j = 1, 2)$$

$$Q = \Delta_1\Delta_2[(\omega_1^2 - \omega_2^2)^2 + (\Delta_1 + \Delta_2)(\Delta_1\omega_2^2 + \Delta_2\omega_1^2 - 2\mu\nu)] + \nu^2(\Delta_1 + \Delta_2)^2$$
$$- \mu^2(\Delta_1 + \Delta_2)(\Delta_1\omega_2^2 + \Delta_2\omega_1^2 - 2\mu\nu) + 2\mu\nu[(\Delta_1\omega_2^2 + \Delta_2\omega_1^2 - 2\mu\nu) - (\Delta_1\omega_1^2 + \Delta_2\omega_2^2)]$$

where $E_{1b}=\pi S_1/m_1\Delta_1$ and $E_{2b}=\pi S_2/m_2\Delta_2$ are the average total energies of the corresponding *blocked* oscillators.

In the same fashion, Fig. 5-1(b) can be used to derive the power flow from oscillator 2, which can be written as

$$P_{21} = \lambda_{12}\mu E_{2b} - \left(1 - \frac{\lambda_{12}\mu}{\Delta_2}\right)[(\gamma_{21} - \alpha)E_{2b} + (\alpha + \beta)E_{1b}] \tag{5.21}$$

5.4 Input Power and Total Stored Energy

Other quantities of interest such as input power to each oscillator and the total energy stored in each oscillator can be similarly expressed explicitly. The input powers to oscillators 1 and 2 are, respectively,

$$P_I = \lim_{K\to\infty}\langle f_1\dot{x}_1\rangle = \Delta_1 E_{1l} \tag{5.22}$$

$$P_{II} = \lim_{K\to\infty}\langle f_2\dot{x}_2\rangle = \Delta_2 E_{2b} \tag{5.23}$$

The potential energies of the oscillators are

$$E_{1p} = \frac{1}{2}(k_1 + k_3)\lim_{K\to\infty}\langle x_1^2\rangle = \frac{1}{2}C_{12}E_{1b} + \frac{1}{2}D_{21}E_{2b} \tag{5.24}$$

$$E_{2p} = \frac{1}{2}(k_2 + k_3) \lim_{K \to \infty} \langle x_2^2 \rangle = \frac{1}{2} C_{21} E_{2b} + \frac{1}{2} D_{12} E_{1b} \tag{5.25}$$

and their kinetic energies are

$$E_{1t} = \frac{1}{2} m_1 \lim_{K \to \infty} \langle \dot{x}_1^2 \rangle = \frac{1}{2} A_{12} E_{1b} + \frac{1}{2} B_{21} E_{2b} \tag{5.26}$$

$$E_{2t} = \frac{1}{2} m_2 \lim_{K \to \infty} \langle \dot{x}_2^2 \rangle = \frac{1}{2} A_{21} E_{2b} + \frac{1}{2} B_{12} E_{1b} \tag{5.27}$$

Here,

$$C_{ij} = \frac{\omega_i^2 \Delta_i}{Q} \{ (\Delta_i + \Delta_j)(-2\omega_j^2 + \Delta_j^2) + (\Delta_i \omega_j^2 + \Delta_j \omega_i^2 - 2\mu\nu) + \frac{\omega_j^4 [\Delta_i \omega_i^2 + \Delta_j \omega_j^2 + 2\mu\nu + (\Delta_i + \Delta_j)(\Delta_i \Delta_j - \mu^2)]}{\omega_i^2 \omega_j^2 - \nu^2} \}$$

$$D_{ij} = \frac{\omega_j^2 \Delta_i}{Q} \{ \mu^2 (\Delta_i + \Delta_j) + \frac{\nu^2 [\Delta_i \omega_i^2 + \Delta_j \omega_j^2 + 2\mu\nu + (\Delta_i + \Delta_j)(\Delta_i \Delta_j - \mu^2)]}{\omega_i^2 \omega_j^2 - \nu^2} \}$$

$$A_{ij} = \frac{\Delta_i \Delta_j}{Q} [(\omega_i^2 - \omega_j^2)^2 + (\Delta_i + \Delta_j)(\Delta_i \omega_j^2 + \Delta_j \omega_i^2)]$$

$$- \frac{\Delta_i}{Q} \{ \mu^2 (\Delta_i \omega_j^2 + \Delta_j \omega_i^2 - 2\mu\nu) - \nu^2 (\Delta_i + \Delta_j) + 2\mu\nu [\omega_i^2 - \omega_j^2 + \Delta_j (\Delta_i + \Delta_j)] \}$$

$$B_{ij} = \frac{\Delta_i}{Q} [\nu^2 (\Delta_i + \Delta_j) + \mu^2 (\Delta_i \omega_j^2 + \Delta_j \omega_i^2 - 2\mu\nu)]$$

$$(i, j = 1, 2)$$

The average total energies of the oscillators are

$$E_1 = E_{1t} + E_{1p} = A'_{12} E_{1b} + B'_{21} E_{2b} \tag{5.28}$$

$$E_2 = E_{2t} + E_{2p} = A'_{21} E_{2b} + B'_{12} E_{1b} \tag{5.29}$$

in which

$$A'_{ij} = \frac{1}{2}(A_{ij} + C_{ij}), \qquad B'_{ij} = \frac{1}{2}(B_{ij} + D_{ij})$$

By solving Eqs. (5.28) and (5.29) simultaneously, the average total energies of the blocked oscillators can be expressed as functions of average total energies of the two coupled oscillators as

$$E_{1b} = \frac{A'_{21}E_1 - B'_{21}E_2}{A'_{12}A'_{21} - B'_{12}B'_{21}} \tag{5.30}$$

$$E_{2b} = \frac{A'_{12}E_2 - B'_{12}E_1}{A'_{12}A'_{21} - B'_{12}B'_{21}} \tag{5.31}$$

Similarly, power flows P_{12} and P_{21} can also be determined from E_1 and E_2 as

$$P_{12} = \alpha_{11}E_1 - \alpha_{12}E_2 \tag{5.32}$$

$$P_{21} = \alpha_{22}E_2 - \alpha_{21}E_1 \tag{5.33}$$

where

$$\alpha_{ii} = \zeta_i \frac{(\alpha - \gamma'_{ii})A'_{ji} + (\alpha + \beta)B'_{ij}}{A'_{ij}A'_{ji} - B'_{ij}B'_{ji}}$$

$$\alpha_{ij} = \zeta_i \frac{(\alpha - \gamma'_{ij})B'_{ji} + (\alpha + \beta)A'_{ij}}{A'_{ij}A'_{ji} - B'_{ij}B'_{ji}}$$

$$\zeta_i = 1 - \frac{\lambda_{ji}\mu}{\Delta_i} \tag{5.34}$$

$$\gamma'_{ij} = \gamma_{ij} - \frac{\lambda_{ji}\mu}{1 - \lambda_{ji}\mu/\Delta_i}$$

$$(i, j = 1, 2, \qquad j \neq i)$$

Finally, the actual dissipative power due to damping element c_3 can be expressed by

$$P_3^{(c)} = \lim_{K \to \infty} c_3 \langle (\dot{x}_2 - \dot{x}_3)^2 \rangle = \lim_{K \to \infty} c_3 \langle (\dot{x}_1 - \dot{x}_2)^2 \rangle$$

$$= G_1E_{1b} + G_2E_{2b} = G'_1E_1 + G'_2E_2 \tag{5.35}$$

where

$$G_i = \frac{\Delta_i + \gamma_{ij} - \alpha}{\lambda_{ij}\Delta_i/\mu} + \frac{\alpha + \beta}{\lambda_{ji}\Delta_j/\mu} - (\gamma_{ij} + \beta)$$

$$G'_i = \frac{G_iA'_{ji} - G_jB'_{ij}}{A'_{ij}A'_{ji} - B'_{ij}B'_{ji}}$$

$$(i, j = 1, 2, \qquad j \neq i)$$

5.5 Special Cases

It is instructive to consider two special cases and point out the important differences that exist between the results following this approach and those of [22,91].

Case 1. When $c_3 = \sqrt{m_1 m_2}\ \mu = 0$, the system reduces to one involving conservatively coupled oscillators. One obtains

$$\alpha = \frac{\Delta_1 \Delta_2}{Q} \nu^2 (\Delta_1 + \Delta_2), \quad \beta = 0, \quad \gamma'_{12} = 0, \quad \gamma'_{21} = 0, \quad \zeta_1 = \zeta_2 = 1.0$$

and P_{12} and P_{21} as given by Eqs.(5.20) and (5.21) reduce to

$$P_{12} = \frac{\nu^2 (\Delta_1 + \Delta_2)}{(\omega_1^2 - \omega_2^2)^2 + (\Delta_1 + \Delta_2)(\Delta_1 \omega_2^2 + \Delta_2 \omega_1^2)} (E_1 - E_2) \tag{5.36}$$

and

$$P_{21} = -P_{12} \tag{5.37}$$

These are consistent with the conventional results obtained for conservatively coupled oscillators.

Case 2. Consider the case in which $c_1=c_2=0$ and $k_3=0$. Thus,

$$\nu = 0, \quad \Delta_1 = \lambda_{21}\mu, \quad \Delta_2 = \lambda_{12}\mu, \quad Q = \mu^2 (\omega_1^2 - \omega_2^2)^2$$

and

$$P_{12} = P_I = \Delta_1 E_{1b} \tag{5.38}$$

$$P_{21} = P_{II} = \Delta_2 E_{2b} \tag{5.39}$$

On the other hand, the formulations of [22,91] would lead to, in this case,

$$P_{12} = \frac{\Delta_1 \Delta_2}{Q} \mu^2 (\Delta_1 \omega_2^2 + \Delta_2 \omega_1^2)(E_{1b} + E_{2b}) \tag{5.40}$$

$$P_{21} = P_{12} \tag{5.41}$$

and

$$P_{12} = -P_{II} = -\Delta_2 E_{2b} \tag{5.42}$$

$$P_{21} = -P_I = -\Delta_1 E_{1b} \tag{5.43}$$

In comparison with Eqs. (5.40)-(5.43), Eqs. (5.38) and (5.39) are more straightforward and

physically reasonable in the sense that (a) the coupling connection c_3 is the only element dissipating energy from input forces so that both P_{12} and P_{21} should be positive in this particular case, and (b) power flows P_{12} and P_{21} cannot be equal unless the input powers from the two oscillators are equal. This is true even for the case of two identical oscillators.

5.6 Dissipative Power and Penetrating Power Flow

Equation (5.35) shows that power dissipation takes place at the non-conservative coupling connection. Hence, it becomes an important issue when power flow is considered in the case of non-conservatively coupled oscillators. In what follows, dissipating power and penetrating power flow are defined and these will become important concepts in the development of power balance equations.

The dissipative power due to coupling element c_3, $P_3^{(c)}$, is defined in Eq. (5.35), which can be found from the power flow equation

$$P_{12} - P_3^{(c)} = -P_{21} \tag{5.44}$$

or

$$P_3^{(c)} = P_{12} + P_{21} = G'_1 E_1 + G'_2 E_2 \tag{5.45}$$

On the other hand, the amount of power penetrating the coupling connection and flowing form oscillator 1 to oscillator 2 is

$$P_{12}^{(k)} = \frac{1}{2}(P_{12} - P_{21}) \tag{5.46}$$

Clearly,

$$P_{21}^{(k)} = -P_{12}^{(k)} \tag{5.47}$$

which indicates the behavior of power flow through a conservative connection.

When $c_3=0$, $P_3^{(c)}=0$ and Eq. (5.44) gives

$$P_{12} = -P_{21}$$

which is **Case 1** in Section 5.5. When $k_3=0$, however, $P_{12}^{(k)}$ and $P_{21}^{(k)}$ do not vanish, as seen from **Case 2**,

$$P_{12}^{(k)} = -P_{21}^{(k)} = \frac{1}{2}(P_{12} - P_{21}) = \frac{1}{2}(P_I - P_{II})$$

The penetrating power is equal to zero only when input powers to the two oscillators are equal.

5.7 Power Balance Equations

For the system shown in Fig. 5-1(a), it follows from Eqs. (5.7) and (5.11) that the input powers to the oscillators are given by

$$P_I = 2\eta_1\omega_1 E_{1t} + P_{12} \tag{5.48}$$

$$P_{II} = 2\eta_2\omega_2 E_{2t} + P_3^{(c)} - P_{12} \tag{5.49}$$

where the internal loss factors η_1 and η_2 are

$$\eta_1 = \frac{c_1}{\omega_1 m_1}, \qquad \eta_2 = \frac{c_2}{\omega_2 m_2}$$

Similarly, for the system shown in Fig. 5-1(b), the corresponding equations are

$$P_I = 2\eta_2\omega_2 E_{2t} + P_{21} \tag{5.50}$$

$$P_{II} = 2\eta_1\omega_1 E_{1t} + P_3^{(c)} - P_{21} \tag{5.51}$$

Since Eqs. (5.48)-(5.49) and Eqs. (5.50)-(5.51) represent the power balance of the same system as $K\to\infty$, only two of these equations are independent. Eqs. (5.48) and (5.50) are chosen for their simplicity. Furthermore, when k_3 is small as compared with k_1 and k_2, $E_1\cong 2E_{1t}$ and $E_2\cong 2E_{2t}$ which will be verified in the numerical examples. Hence, the power balance equations can be written as

$$P_I = \eta_1\omega_1 E_1 + P_{12} \tag{5.52}$$

$$P_{II} = \eta_2\omega_2 E_2 + P_{21} \tag{5.53}$$

which have exactly the same forms as those for the conservatively coupled system. Furthermore, the introduction of penetrating power flow and dissipative power leads to

$$P_I = (\eta_1 + \eta_{12})\,\omega_1 E_1 + \eta_{21}\omega_2 E_2 + P_{12}^{(k)} \tag{5.54}$$

$$P_{II} = (\eta_2 + \eta_{21})\,\omega_2 E_2 + \eta_{12}\omega_1 E_1 + P_{21}^{(k)} \tag{5.55}$$

where the dissipative factors, η_{12} and η_{21}, due to the coupling damping element are

$$\eta_{12} = \frac{G_1}{2\omega_1}, \qquad \eta_{21} = \frac{G_2}{2\omega_2}$$

with $$P_{12}^{(k)} = -P_{21}^{(k)} = \frac{1}{2}(\alpha_{11} + \alpha_{21})E_1 - \frac{1}{2}(\alpha_{12} + \alpha_{22})E_2$$

It is noted that the dissipative factors defined here are different from the coupling loss factors given for conservatively coupled systems.

5.8 Numerical Examples and Discussions

In this section, the properties of power flow between non-conservatively coupled oscillators are presented and discussed through numerical examples. They also help to verify the rationale behind the power flow formulation developed in the preceding sections. In what follows, four cases are discussed with their defining parameters given in Table 5-1.

Case 1. As k_2 varies, the ratios of power flows P_{12} and P_{21} to the total input power $P(=P_1+P_{II})$ are functions of ω_1/ω_2, as shown in Figs. 5-2 and 5-3. It is observed that these power flows are sensitive to ω_1/ω_2 when it approaches one. This is especially noticeable when the bandwidths of the oscillators become small.

In comparison with the results of [22], more straightforward and convincing results are obtained in this section. As c_3 increases, the energy dissipated in the connecting element plays a more and more important role in energy distribution and more of the energy will flow into the connection and this will lead to the positive and progressive power flows for P_{12} and P_{21}, which is clearly demonstrated in Figs. 5-2 and 5-3. The rate of power flow increment, however, gradually becomes smaller as c_3 becomes larger. At the same time, c_3 modulates the peak magnitudes of both P_{12} and P_{21} within a small range around $\omega_1/\omega_2=1$.

Case 2. Consider the case in which only one of the two strongly-coupled oscillators with large bandwidths is excited. The ratios associated with power flow, P_{12}/P, and with the penetrating power flow, $P_{12}^{(k)}/P$, are respectively presented in Figs. 5-4 and 5-5 with the corresponding energy

TABLE 5-1: Parameter Values Used in Numerical Examples

case	m_1	m_2	k_1	k_2	k_3	c_1	c_2	c_3	S_1	S_2
(1)	(2)	(3)	(4)	(5)	(6)	(7)	(8)	(9)	(10)	(11)
1	0.2	0.1	50000	v	1000	0.5	1.0	v	1.0	1.0
2	0.1	0.6	10006	v	30018	v	v	v	2.0	0.0
3	1.0	2.0	v	v	25000	0.5	0.8	v	2.0	0.0
4	1.0	2.0	25000	50000	v	0.5	0.8	v	2.0	0.0

Note: v means variable

ratio E_1/E_2 shown in Fig. 5-6. Figures 5-4 and 5-5 confirm the insensitivity of P_{12}/P and $P_{12}^{(\lambda)}/P$ to ω_1/ω_2 in systems with strong connection elements. This becomes more obvious when coupling damping c_3 increases. Except for the range with frequency ratios less than one, Fig. 5-6 shows that an increase in damping c_3 will reduce the ratio of vibrational energies of two oscillators. This suggests the possibility that energy propagates through coupling damping element into oscillator 2, indicating that the damping element not only dissipates energy but also affects power flow between the two oscillators. Furthermore, the combination of E_1/E_2 and P_{12}/P presents an important feature, which is quite different from results observed in conservatively coupled systems, namely, a positive power flow P_{12} does not automatically lead to the conclusion that E_1 is greater than E_2 and *vice versa*. In order to explain this phenomenon more effectively, the energy dissipation percentage $G[= G_1'E_1/(G_1'E_1 + G_2'E_2)]$ is calculated and is shown in Fig. 5-7. As shown in this figure, G will become greater than one when ω_1/ω_2 goes from values smaller to those greater than one. This suggests that the damping element dissipates a part of the vibrational energy transmitted from oscillator 1 while propagates the rest into oscillator 2. A conclusion can then be drawn that a damped joint element may transmit energy from the excitation-driven oscillator to the other while it dissipates energy and that the "cause and effect" relation between P_{12} and E_1/E_2 no longer holds because the dissipative energy in the coupling element is a function of the frequency ratio. The higher the value ω_1/ω_2 takes, the more energy the coupling element absorbs from oscillator 1. This will lead to the situation where E_1 is smaller than E_2.

Case 3. Figure 5-8 is produced when c_3 varies between 0.125 and 1.0 with a set of fixed frequency ratios. This diagram shows a completely different feature from that of [22] in that P_{12} changes in direct proportion to c_3. This further confirms the conclusion drawn from **case 2** and this difference results from the different definitions used for power flow in this section in [22].

Case 4. This special case consists of a variable spring connection and is designed to examine the accuracy in approximating the energy (E) stored in the oscillators by twice the kinetic energy ($2E_t$). The relation between kinetic energy percentage in oscillator 2 (E_{2t}/E) and connecting spring stiffness (k_3) is shown in Fig. 5-9. It is observed that the kinetic energy percentage approaches 0.5

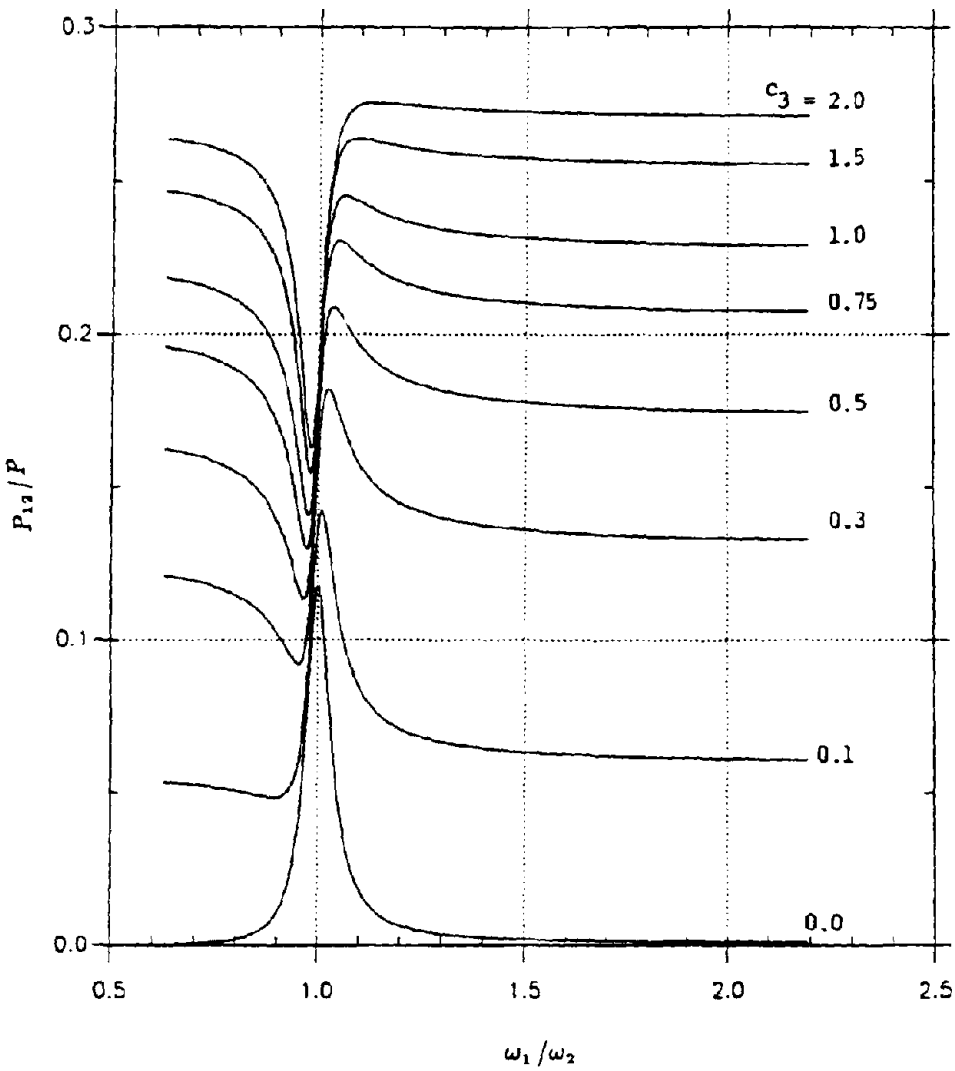

Fig. 5-2 Power Flow P_{12}/P vs. Frequency Ratio ω_1/ω_2 (case 1)

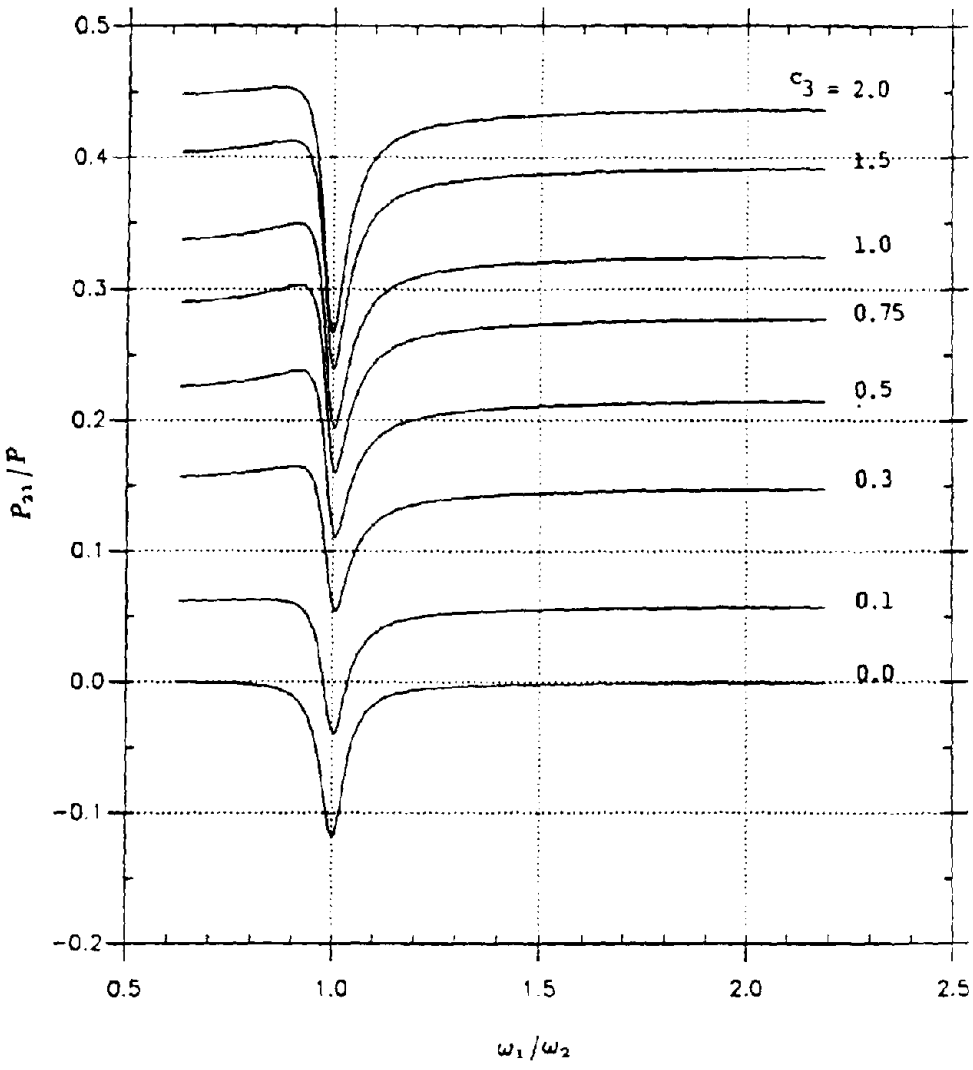

Fig. 5-3 Power Flow P_{21}/P vs. Frequency Ratio ω_1/ω_2 (case 1)

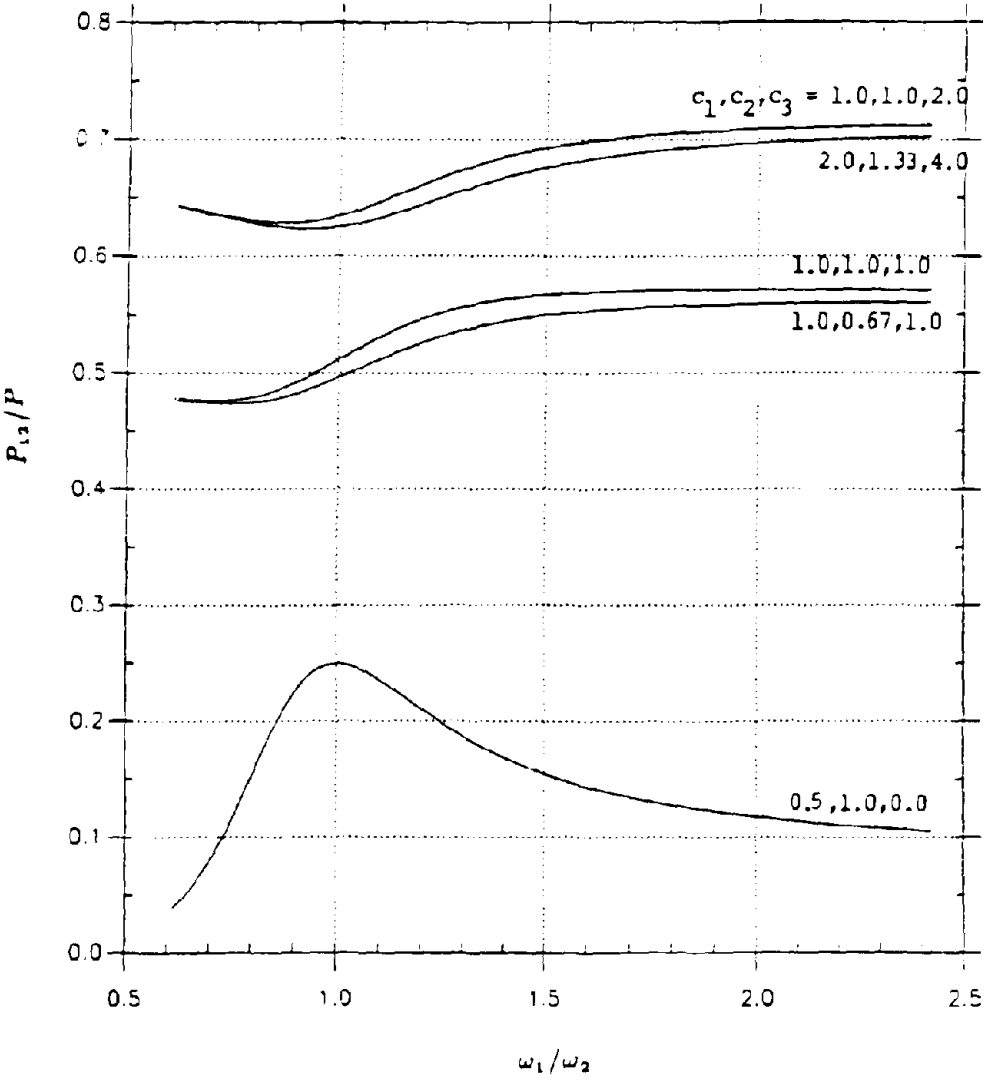

Fig. 5-4 Power Flow P_{12}/P vs. Frequency Ratio ω_1/ω_2 (case 2)

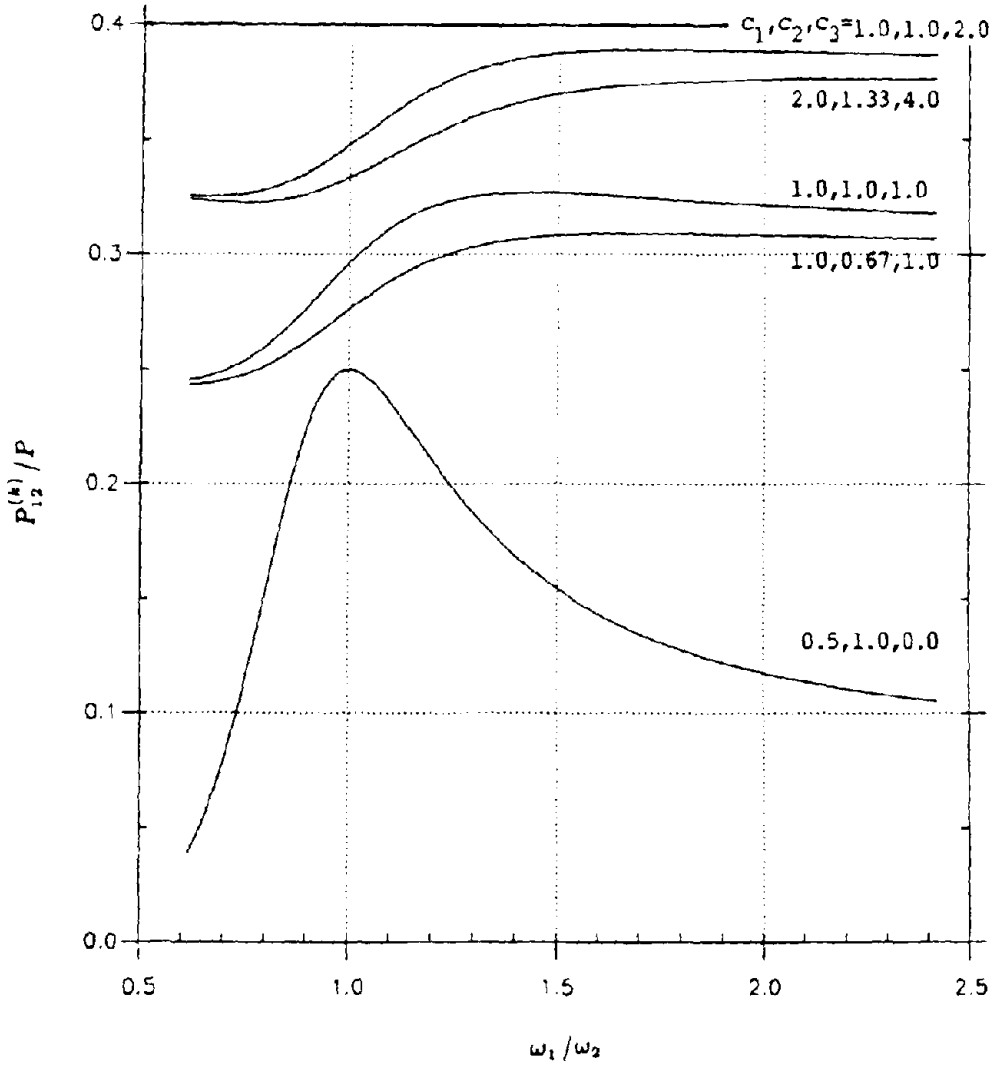

Fig. 5-5 Power Flow $P_{12}^{(k)}/P$ vs. Frequency Ratio ω_1/ω_2 (case 2)

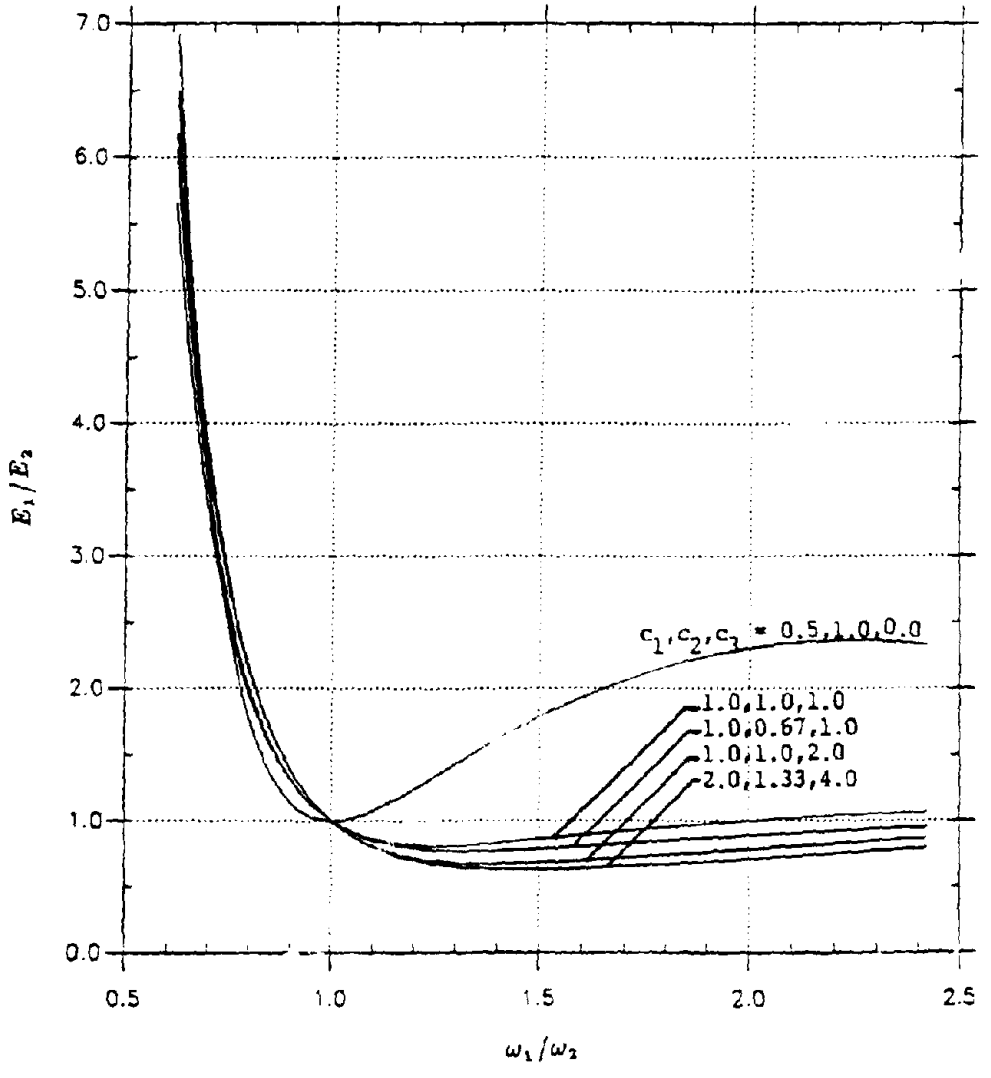

Fig. 5-6 Energy Ratio E_1/E_2 vs. Frequency Ratio ω_1/ω_2 (case 2)

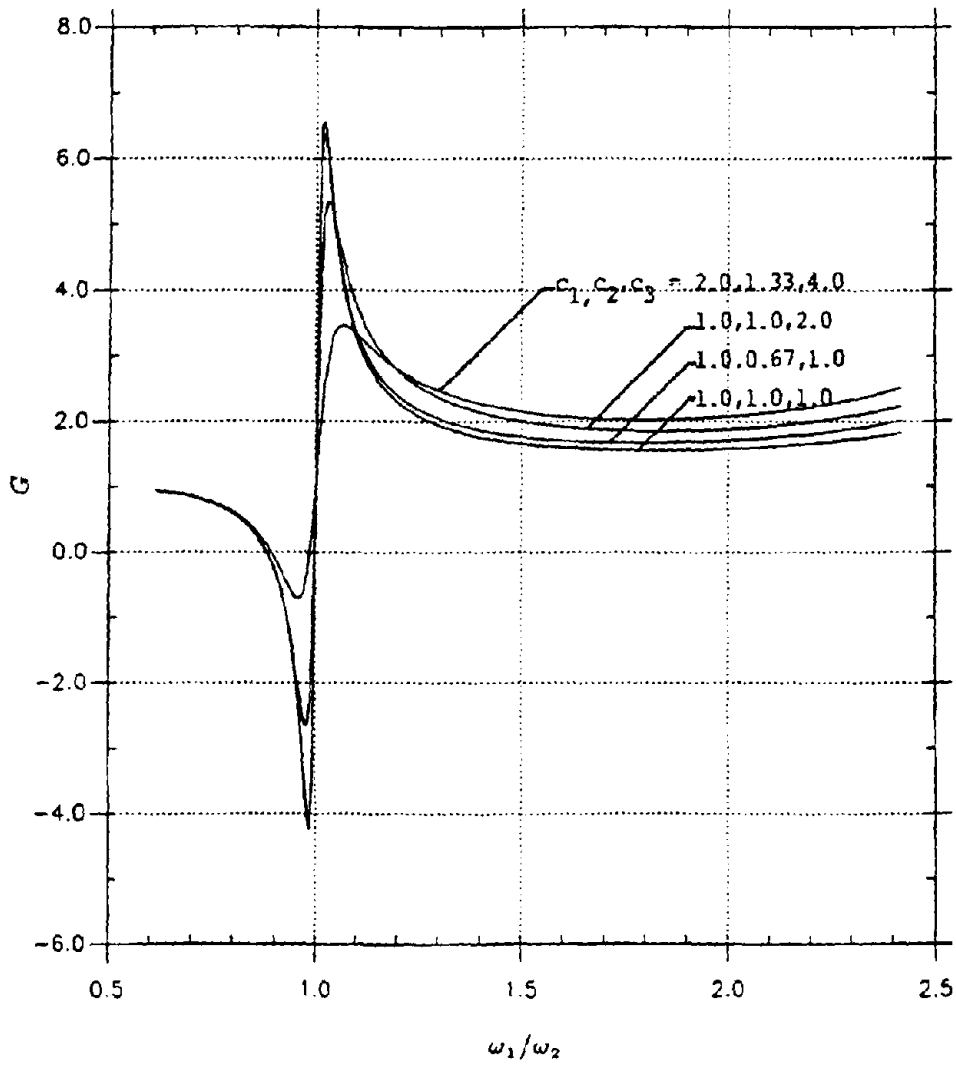

Fig. 5-7 Energy Dissipation Percentage G vs. Frequency Ratio ω_1/ω_2 (case 2)

as k_3 decreases, indicating that twice the kinetic energy is a good approximation of the vibrational energy in the oscillators in this case. However, the stiffness of the connecting spring should be limited to the smaller of the two spring stiffnesses. Furthermore, the larger the connecting damping (c_3), the worse the accuracy of this approximation.

5.9 Concluding Remarks

Power flow relations for non-conservatively coupled oscillators have been established by considering the system as a limiting case of two conservatively coupled oscillators. As the derivations and numerical examples show, this approach provides a physically consistent formulation of power flow and eliminates the need for any subjective choice of a definition of power flow through a damaged connecting element. Furthermore, the introduction of penetrating power flow and dissipative power gives more insight into the physical problem. Although the absolute values of power flows in the two directions are not the same in general, the penetrating power flows developed in this section are always identical.

It is seen that systems with non-conservatively coupled oscillators are not reversible in general. The absolute values of power flows in the two directions are therefore not identical even when the two oscillators are tuned. The direction in which power flows varies with the relative magnitude of P_{12} and $P_3^{(c)}$. When only one of the two oscillators is excited, the increase in coupling damping may attract more energy from the directly driven oscillator and transfer energy to the other when ω_1/ω_2 exceeds unity For this reason, the properties of the indirectly driven oscillator define an upper limit of the vibrational energy which changes with c_3.

Since the development presented herein is consistent with the power flow formulation of conservatively coupled systems, extensions to multi-modal non-conservatively coupled oscillators can be made when the knowledge of mode distributions is provided [93].

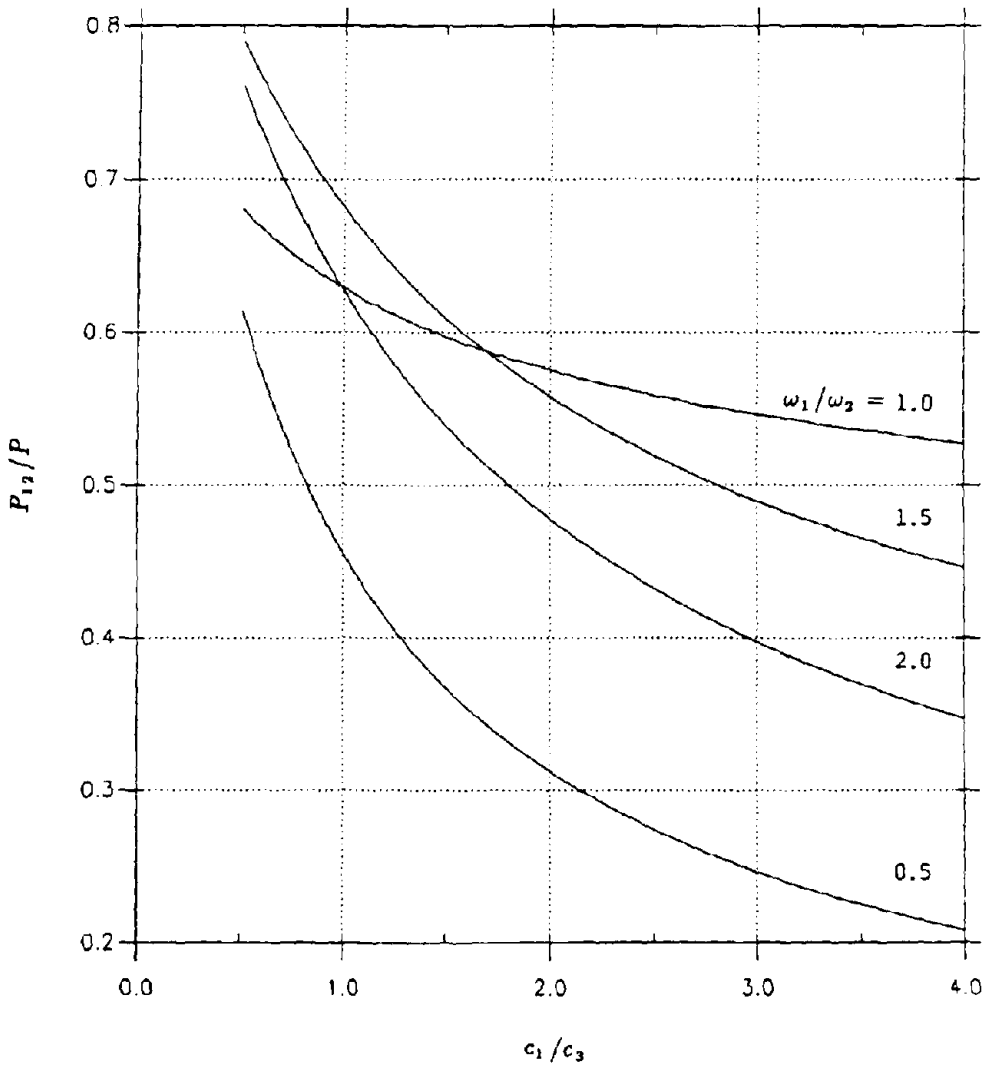

Fig. 5-8 Power Flow P_{12} vs. Coupling Damping c_3 (case 3)

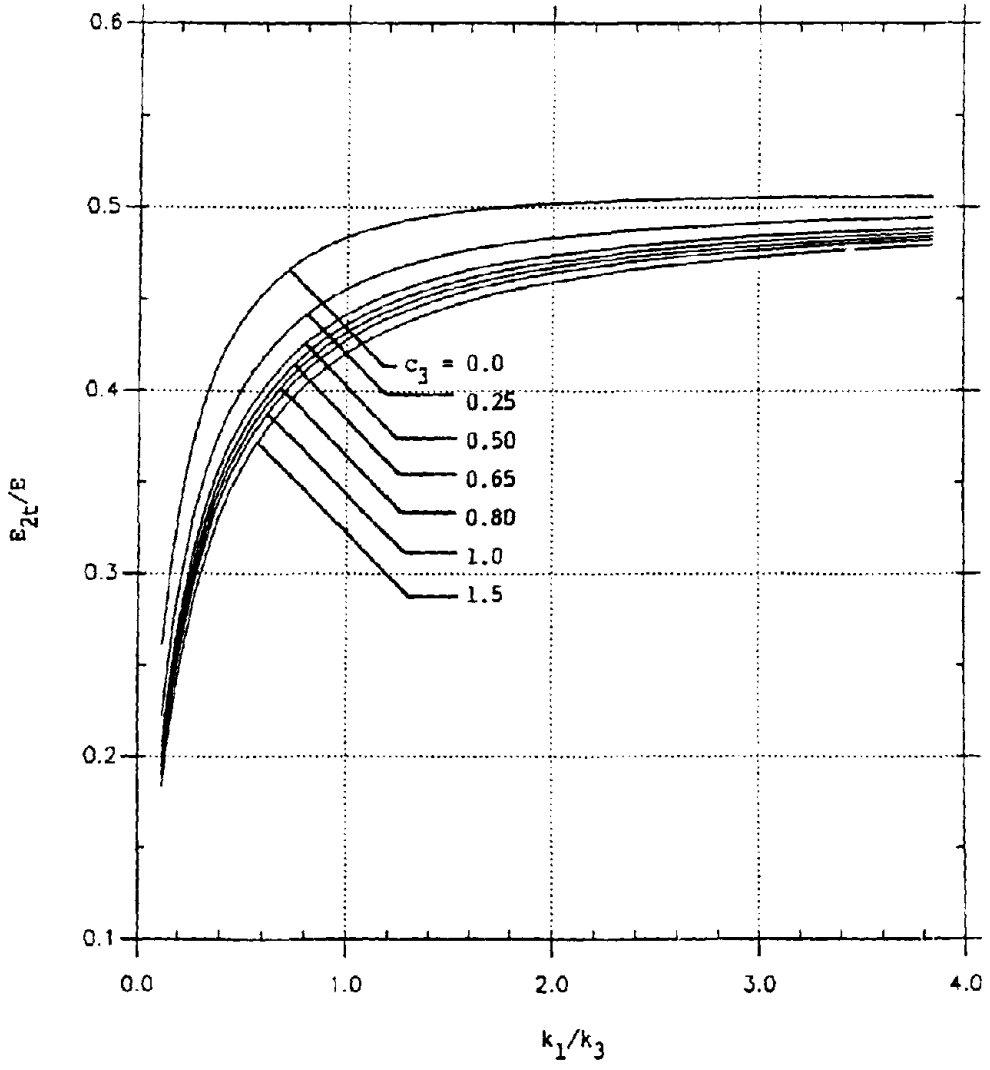

Fig. 5-9 Kinetic Energy Percentage E_{2t}/E_2 vs. Coupling Spring k_3 (case 4)

SECTION 6

POWER FLOW AND ENERGY IN P-S SYSTEMS WITH NON-CONSERVATIVE COUPLING

6.1 Introduction

With the exception of the nuclear industry, static lateral force requirements remain to govern performance evaluation and design guidelines for P-S systems [87]. The S-system in this situation is assumed to respond to the excitation independent of the P-system. Therefore, dynamic characteristics of P-S systems such as tuning, attachment configuration and non-classical damping can not be taken into account. Attempts to incorporate P-S system interaction into the analysis have pointed to the need to develop simple and yet accurate procedures [82]. It is the purpose of this section to demonstrate that the concept of power flow and energy can lead to simple procedures for the analysis and design of S-systems.

In Section 5, relationship between power flow and energy of a generic 2-DOF system has been formulated. Although this could be a realistic model for a piping system with subsystem interaction [49], the most commonly encountered case in civil engineering is the one with an S-system attached to a P-system as shown in Fig. 4-1. In this section, this system is considered and it serves as a simplest application of power flow and energy concept to the dynamic analysis of P-S coupled systems.

6.2 Formulation of Power Flow and Energy

The equation of motion of simple system shown in Fig. 4-1 has been formulated in Eqs.(4.1) and (4.2) and rewritten here for convenience

$$m_s\ddot{x}_s + c_s\dot{x}_s + k_s x_s - c_s\dot{x}_p - k_s x_p = 0 \tag{6.1}$$

$$m_p\ddot{x}_p + (c_p + c_s)\dot{x}_p + (k_p + k_s)x_p - c_s\dot{x}_s - k_s x_s = f_p = c_p\dot{x}_g + k_p x_g \tag{6.2}$$

It is noted that Fig.4-1 described by the above equations is a special case of Fig. 5-1(c), when both c_2 and k_2 as well as $f_2(t)$ are set to zero. All the formulations developed in Section 5 for power flow,

input power, and kinetic energy are therefore applicable in this simple case. They can be written as follows when proper substitutions of structural parameters have been made.

Power flow transmitted from P- to S- system:

$$P_{ps} = (2\xi_p \omega_p R_m R_\omega R_\xi - \alpha) E_{pb} \tag{6.3}$$

Input power to the P-system:

$$P_p^{(in)} = 2\xi_p \omega_p (1 + R_m R_\omega R_\xi) E_{pb} \tag{6.4}$$

Here,

$$\alpha = \frac{8\xi_p^3 \omega_p^7 R_m R_\omega^4 R_\xi}{Q} \{R_\omega (R_\omega R_\xi - 1) + 2R_\xi [2\xi_p^2 R_\xi (R_\xi + R_\omega) - 1] + R_m R_\omega^2 R_\xi\} \tag{6.5}$$

$$Q = 4\xi_p^2 \omega_p^6 R_\omega \{ R_\xi [(1 - R_\omega^2)^2 + 4\xi_p^2 (1 + R_\xi R_\omega)(R_\xi + R_\omega)^2] + R_m R_\omega [(R_\xi + R_\omega)^2 + 4\xi_p^2 R_\xi^2 R_\omega (R_\xi + R_\omega) + 2R_\xi R_\omega (R_\omega^2 - 1)] + R_m^2 R_\omega^4 R_\xi \} \tag{6.6}$$

in which $R_\xi = \xi_s / \xi_p$ and $E_{pb} = \pi S_0 / [m_p 2\xi_p \omega_p (1 + R_m R_\omega R_\xi)]$ are, respectively, the ratio of damping ratios of S- and P- system and the average total energy of the corresponding *blocked* P-system subjected to a broad-band stochastic process with power spectral density S_0, i.e., the P-system with $x_s = 0$ and $\dot{x}_s = 0$.

For the P-S system under investigation, the ratio of kinetic to potential energy does not converge to 0.5 as discussed in Section 5. Hence, instead of the total energy, the kinetic energy is chosen here to describe the dynamic behavior of the P-S system, which takes the form

$$E_{pt} = \frac{1}{2} A E_{pb} \tag{6.7}$$

$$E_{st} = \frac{1}{2} B E_{pb} \tag{6.8}$$

for the P-system and the S-system, respectively. Here,

$$A = \frac{4\xi_p^2 \omega_p^6 R_\omega}{Q} \{R_\xi (R_\omega^2 - 1)^2 + 4\xi_p^2 R_\xi R_\omega (1 + R_\xi R_\omega)(R_\xi + R_\omega) + R_m [R_\xi^2 R_\omega (R_\omega^2 - 1)^2$$

$$+ R_\omega^3 (1 + R_\xi R_\omega) + 4\xi_p^2 R_\xi^2 R_\omega^2 (1 + R_\xi R_\omega)(R_\xi + R_\omega)] + R_m^2 R_\xi R_\omega^4 (1 + R_\xi R_\omega) \} \quad (6.9)$$

$$B = \frac{4\xi_p^2 \omega_p^6 R_m R_\omega^3}{Q} [R_\omega (1 + R_\xi R_\omega) + 4\xi_p^2 R_\xi^2 (R_\xi + R_\omega) + R_m R_\xi R_\omega^2] \quad (6.10)$$

Degenerated from Eq. (5.49), the dissipative power defined in Eq. (5.35) can be calculated by

$$P_{ps} = c_s \langle (\dot{x}_s - \dot{x}_p)^2 \rangle \quad (6.11)$$

6.3 Power Flow as a Response Variable

The dynamic performance of an S-system is commonly characterized by its relative displacement with respect to the P-system and by its absolute acceleration. In this section, the relationship between power flow and these two response variables is established, showing that power flow can be used as an appropriate response variable.

Recalling from Eq. (6.1), the absolute acceleration of the S-system can be expressed as

$$\ddot{x}_s = \omega_s^2 (x_p - x_s) + 2\xi_s \omega_s (\dot{x}_p - \dot{x}_s) \quad (6.12)$$

For the steady-state response corresponding to the Gaussian stationary input $f_p(t)$, cross correlation $\langle (x_p - x_s)(\dot{x}_p - \dot{x}_s) \rangle$ vanishes. Hence, the mean-square absolute acceleration is

$$\langle \ddot{x}_s^2 \rangle = \omega_s^4 \langle (x_p - x_s)^2 \rangle + 4\xi_s^2 \omega_s^2 \langle (\dot{x}_p - \dot{x}_s)^2 \rangle \quad (6.13)$$

However, from Eq. (6.11),

$$\langle (\dot{x}_p - \dot{x}_s)^2 \rangle = \frac{P_{ps}}{c_s} = \frac{P_{ps}}{2\xi_s \omega_s m_s} \quad (6.14)$$

Therefore,

$$\langle \ddot{x}_s^2 \rangle = \omega_s^4 \langle (x_p - x_s)^2 \rangle + \frac{2\xi_s \omega_s}{m_s} P_{ps} \quad (6.15)$$

which is the relation between power flow and absolute acceleration $\ddot{x}_s$ and relative displacement $(x_p - x_s)$.

6.4 Illustrative Examples and Discussions

In this section, the properties of power flow transmitted from the P- to the S- system as well as the energy of each system are presented and discussed through numerical examples. They also help to verify the similarity between power flow and energy on the one hand and absolute acceleration and relative displacement on the other in the sense that both sets of parameters can be used to describe dynamic properties of the P-S system. In what follows, two cases are discussed with their defining parameters given in Table 6-1.

Case 1. The power flow transmitted from the P-system is shown in Fig. 6-1 and energies of the P- and S- systems are shown in Figs. 6-2(a) and 6-2(b). From these plots, one can easily see the tuning effect, an inherent behavior of P-S systems, which is also reflected by the absolute acceleration and relative displacement shown in Figs. 6-3 and 6-4. As frequency ratio R_ω approaches zero, the P-S system will converge to the P-system and, therefore, the kinetic energies of the P- and S- systems are $0.5\pi S_f/c_p$ and zero, respectively. On the other hand, when R_ω approaches infinity, the coupling connection becomes rigid and, therefore, the kinetic energies of the P- and S-system will approach $0.5\pi S_f/c_p(1+R_m)$ and $0.5\pi S_f R_m/c_p(1+R_m)$, respectively. For example, when R_m=0.01, their asymptotic values are 0.155 and 0.00155, respectively, which can be observed from Figs. 6-2(a) and 6-2(b). In addition, when R_m increases, power flow from the P-system will likewise increase as demonstrated in Fig. 6-1. Consequently, the kinetic energies of the P- and S- systems decrease and increase, respectively.

One of the features to be observed is that the power flow and the kinetic energies of the P- and S-system are almost symmetrical about the tuning point within a certain bandwidth and the tuning effect is always located at R_ω=1, which can not be found from the absolute acceleration and the relative displacement shown in Figs. 6-3 and 6-4. This may be attributed to the unbiased frequency characteristic of kinetic energy quantities whereas acceleration and displacement are in favor of high and low frequency components, respectively.

TABLE 6-1: Parameter Values Used in Numerical Examples

case	m_p	k_p	c_p	S_p	R_m	R_k	R_c
	Ns^2/m	N/m	Ns/m	m^2/s^3			
(1)	(2)	(3)	(4)	(5)	(6)	(7)	(8)
1	4	2500	10	1.0	v	0.4	v
2	4	2500	2	1.0	v	v	0.5

Note: v means variable

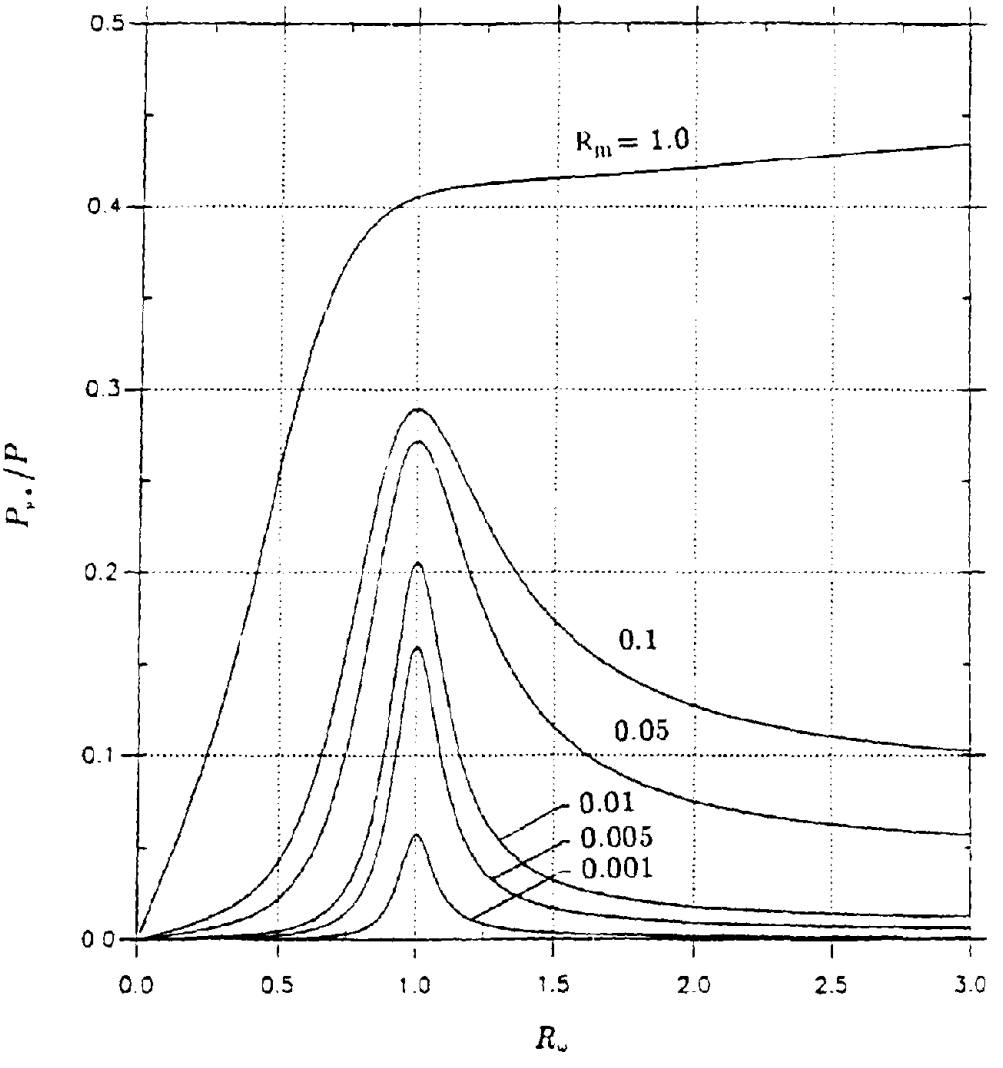

Fig. 6-1 Power Flow Transmitted From P-System vs. R_w

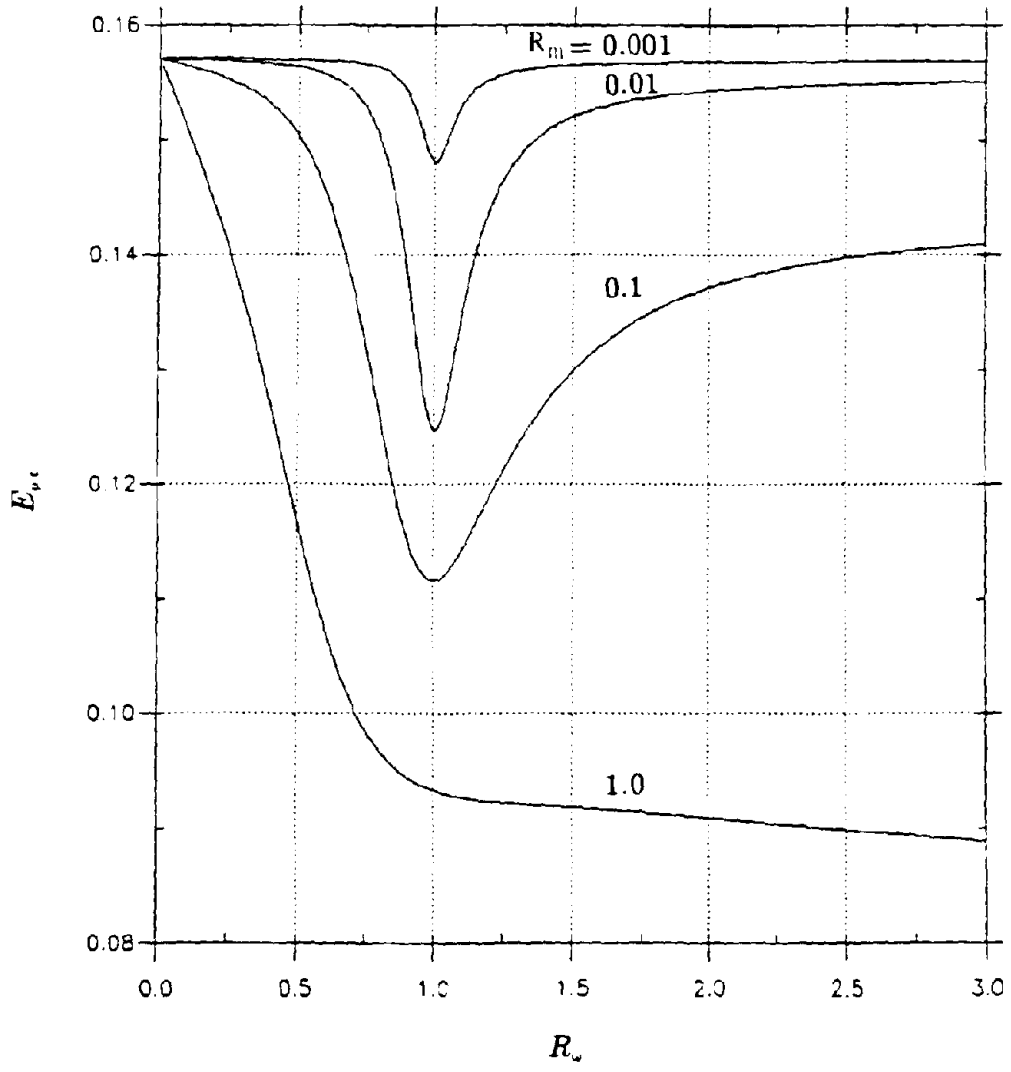

Fig. 6-2(a) Kinetic Energy vs. R_m: P-System

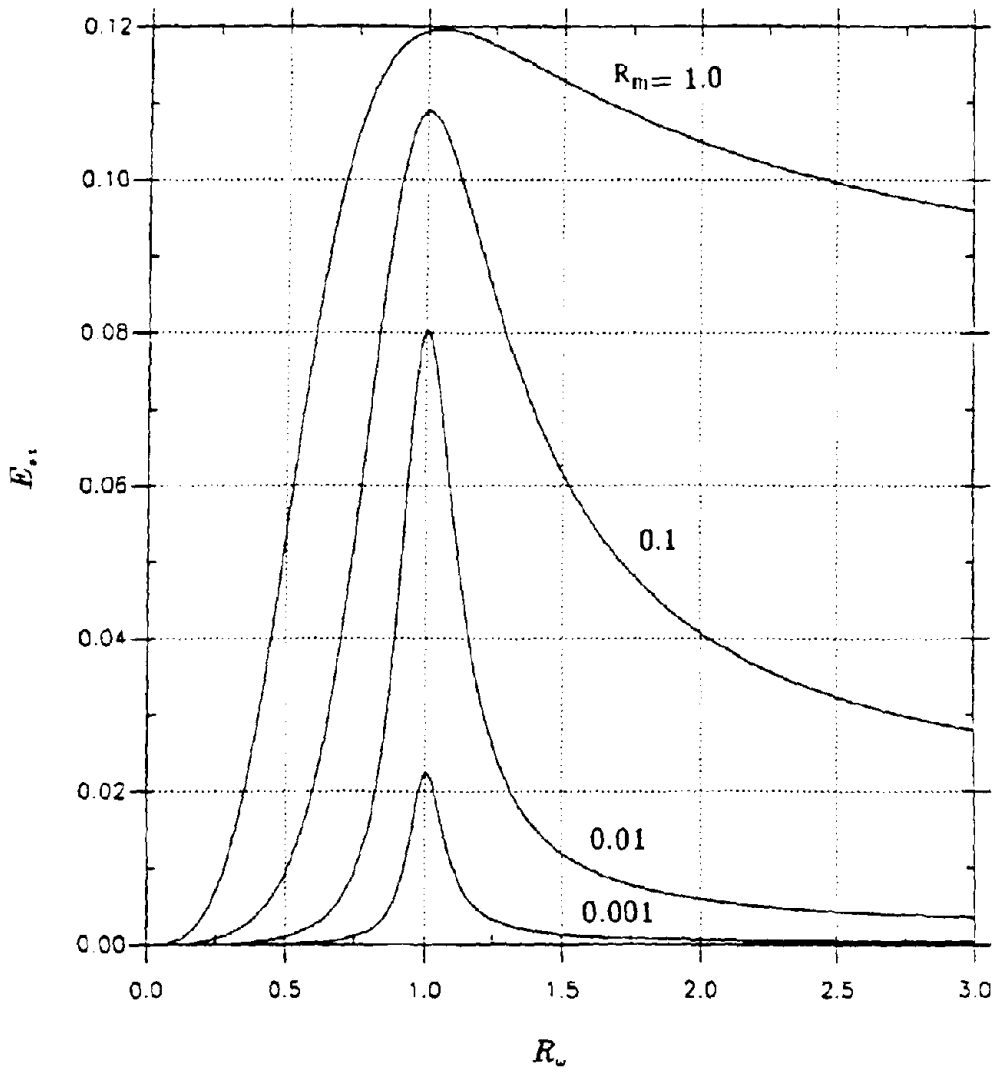

Fig. 6-2(b) Kinetic Energy vs. R_ω: S-System

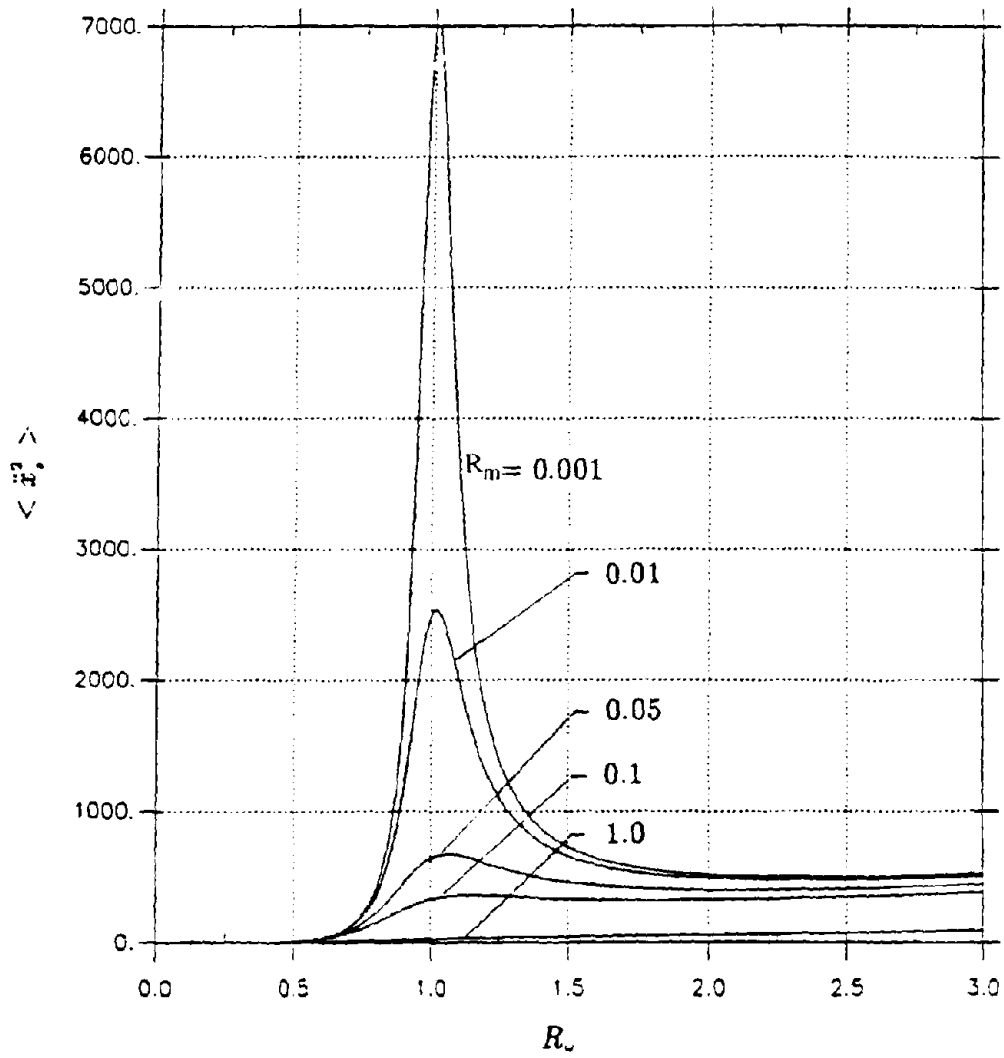

Fig. 6-3 Absolute Acceleration of S-System vs. R_m

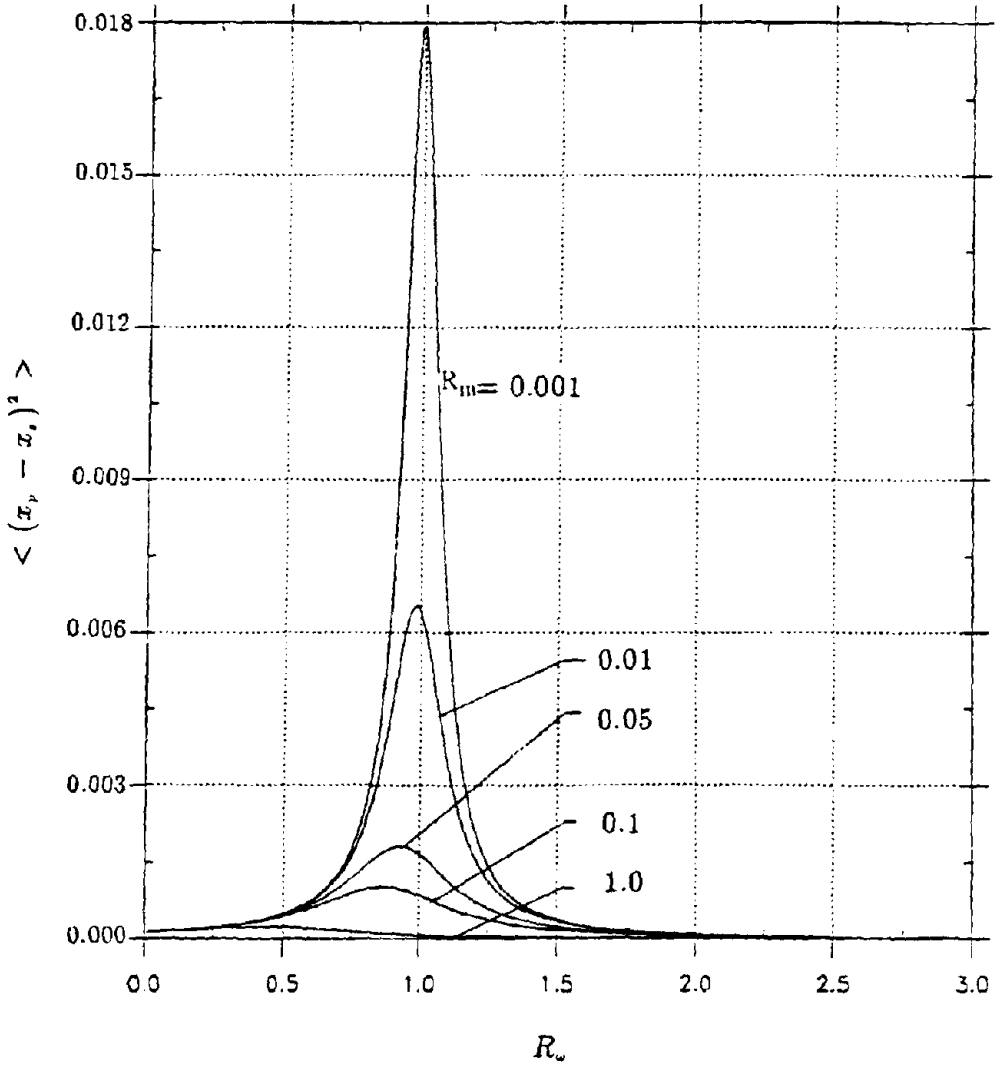

Fig. 6-4 Relative Displacement Between P- and S-System vs. R_ω

Case 2. The power flow and energies of the P- and S-system are shown in Figs. 6-5, 6-6(a) and 6-6(b) while the absolute acceleration and relative displacement are shown in Figs. 6-7 and 6-8. As one can observe from Fig. 6-5, power flow transmitted from the P-system increases with the damping ratio of the S-system at first and then becomes less sensitive to it for this case. Accordingly, the kinetic energy of the P-system decreases and then almost maintains a constant. However, the kinetic energy of the S-system has a minimum as the damping ratio ξ_s varies. This property is useful for design purposes since it provides an optimum solution for ξ_s which has been demonstrated earlier in [46,51,57]. This phenomenon can also be observed from the behavior of the absolute acceleration.

As ξ_s increases, the phase angle of the relative displacement between the P- and S-systems becomes larger and, therefore, its mean-square value always decreases as shown in Fig. 6-8. This, however, is not so for the absolute acceleration of the S-system due to its relation with the relative displacement and relative velocity between the P- and S-system as shown in Eq. (6.12). This behavior can also be proved from Eq. (6.15), in which $< (x_p - x_s)^2 >$ decreases monotonically while power flow P_{ps} increases with ξ_s.

6.5 Power Flow and Energy of the Simple P-S System Under Ground Acceleration Input

It is customary to assume a simple P-S system in Fig. 4-1 subjected to ground acceleration. The equations of motion of such a system for relative displacement representation $z_s(t)$ and $y_p(t)$ of the S- and P-system have been established in Eqs. (4.3) and (4.4). It is immediately recognized that inertia forces due to ground acceleration on two subsystems are perfectly correlated, a property that prohibits the direct application of formulations developed in Section 5. However, Eqs. (4.3) and (4.4) can be transformed into the generic form for the system delineated by Fig. 5-1(c) under certain conditions as follows.

Multiplying Eq. (4.4) by m_s and Eq. (4.3) by m_p and then subtracting the first equation from the second, we obtain

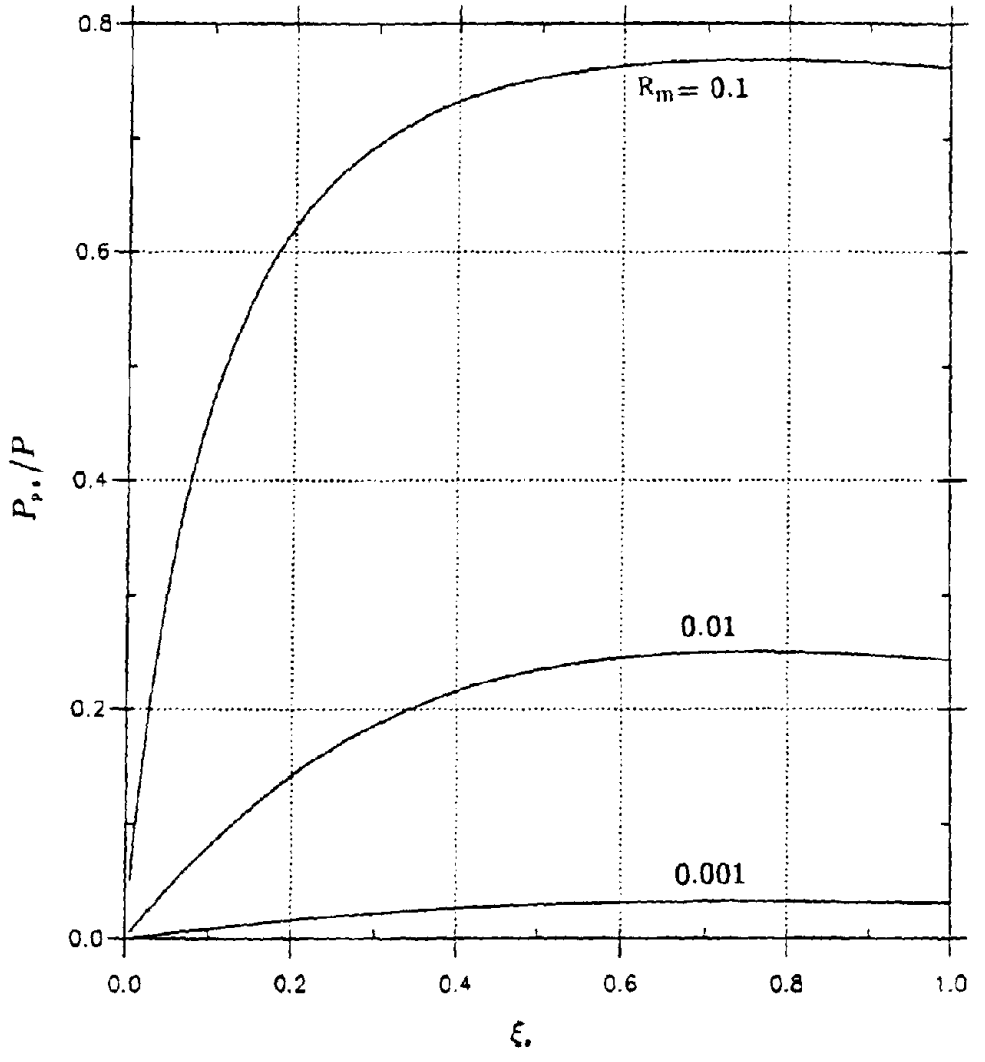

Fig. 6-5 Power Flow Transmitted From P-System vs. ξ_1

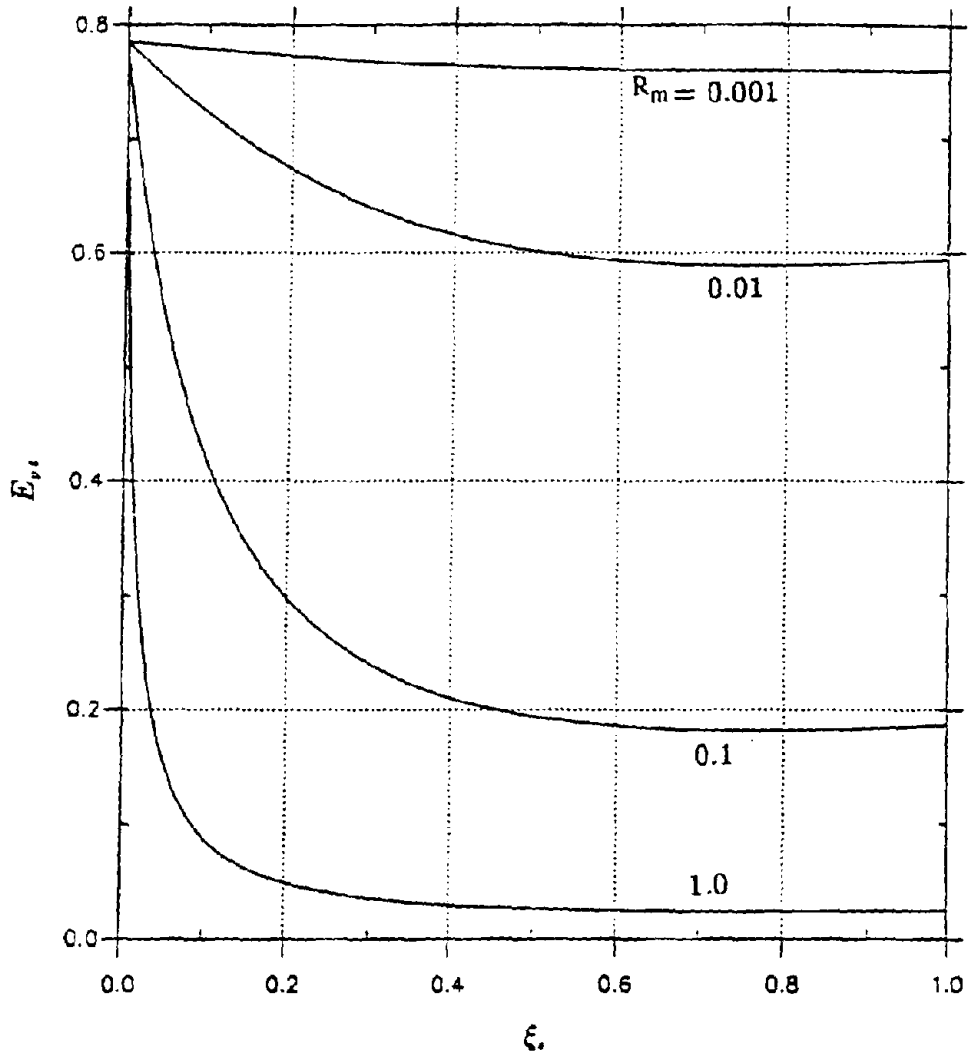

Fig. 6-6(a) Kinetic Energy vs. ξ_s: P-System

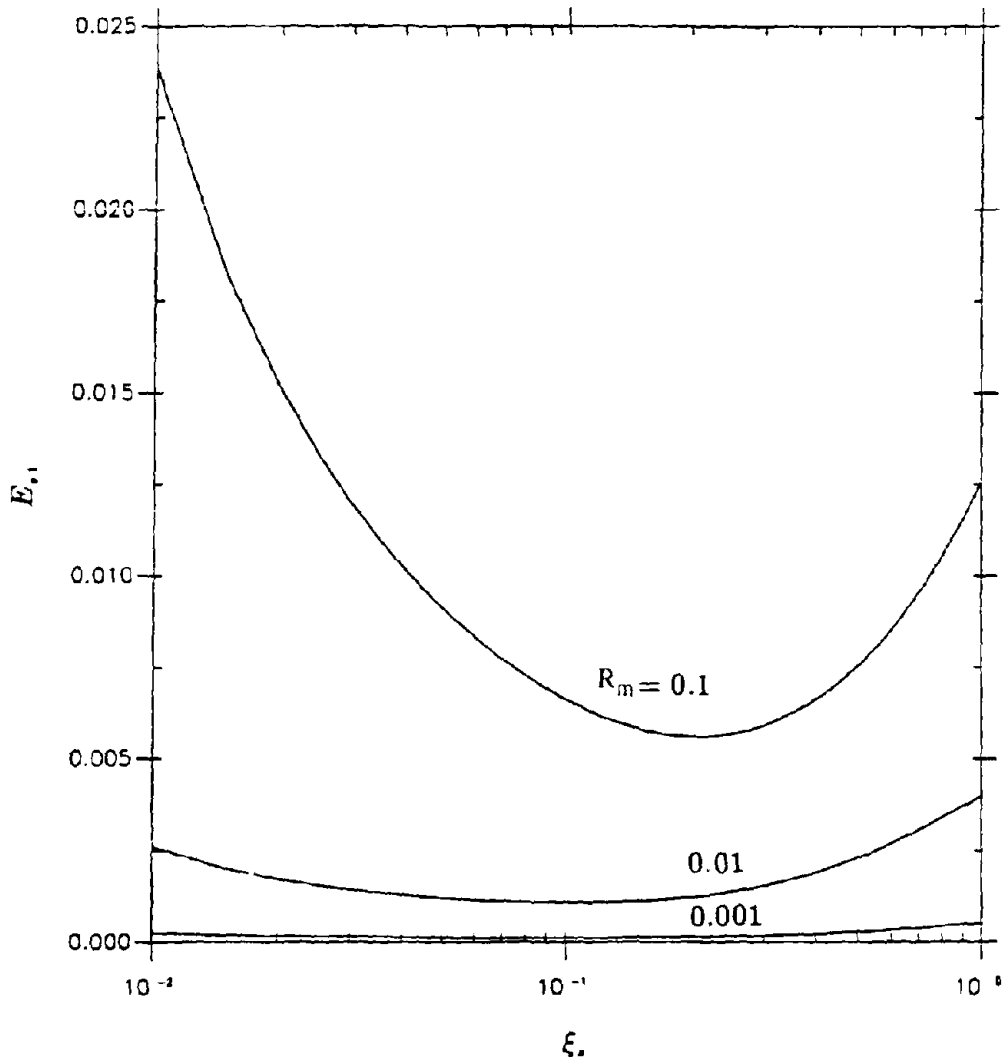

Fig. 6-6(b) Kinetic Energy vs. $\xi_{,}$: S-System

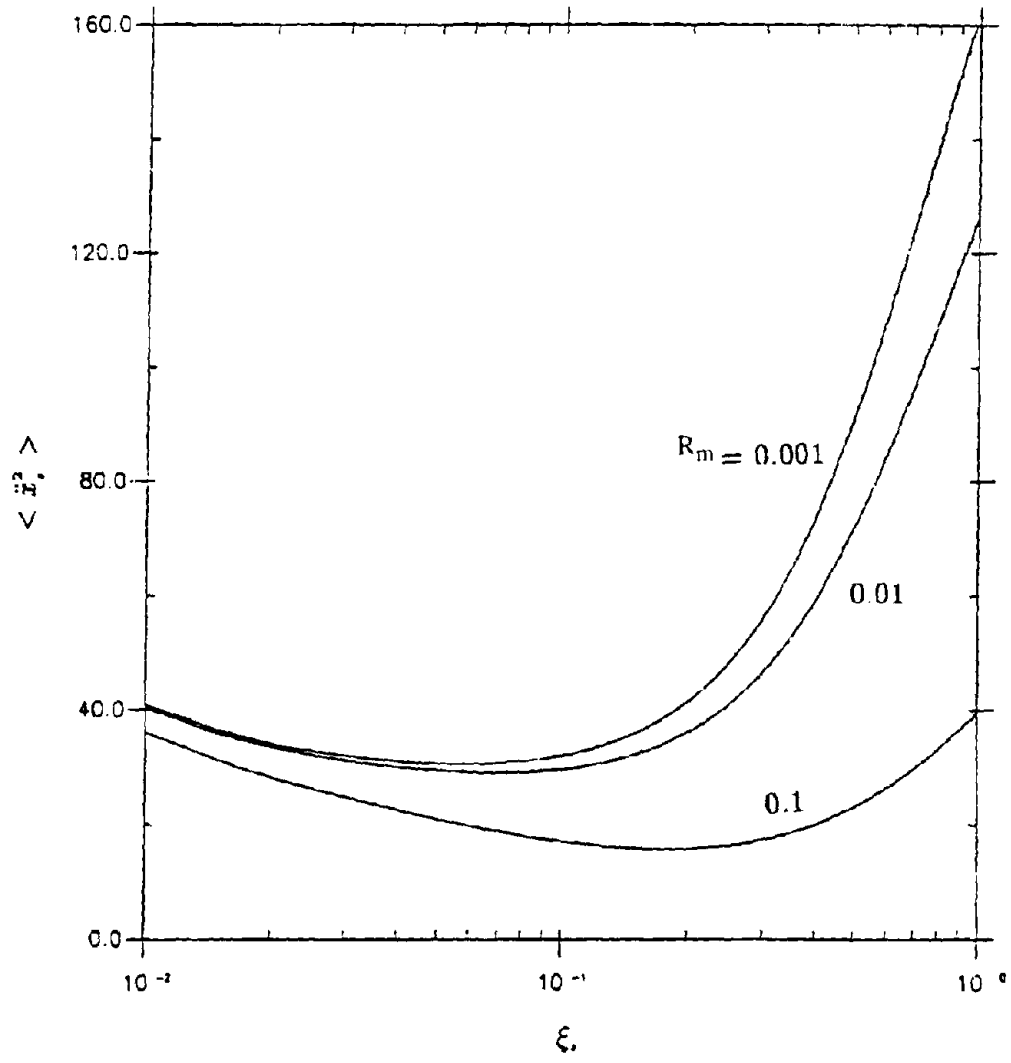

Fig. 6-7 Absolute Acceleration of S-System vs ξ.

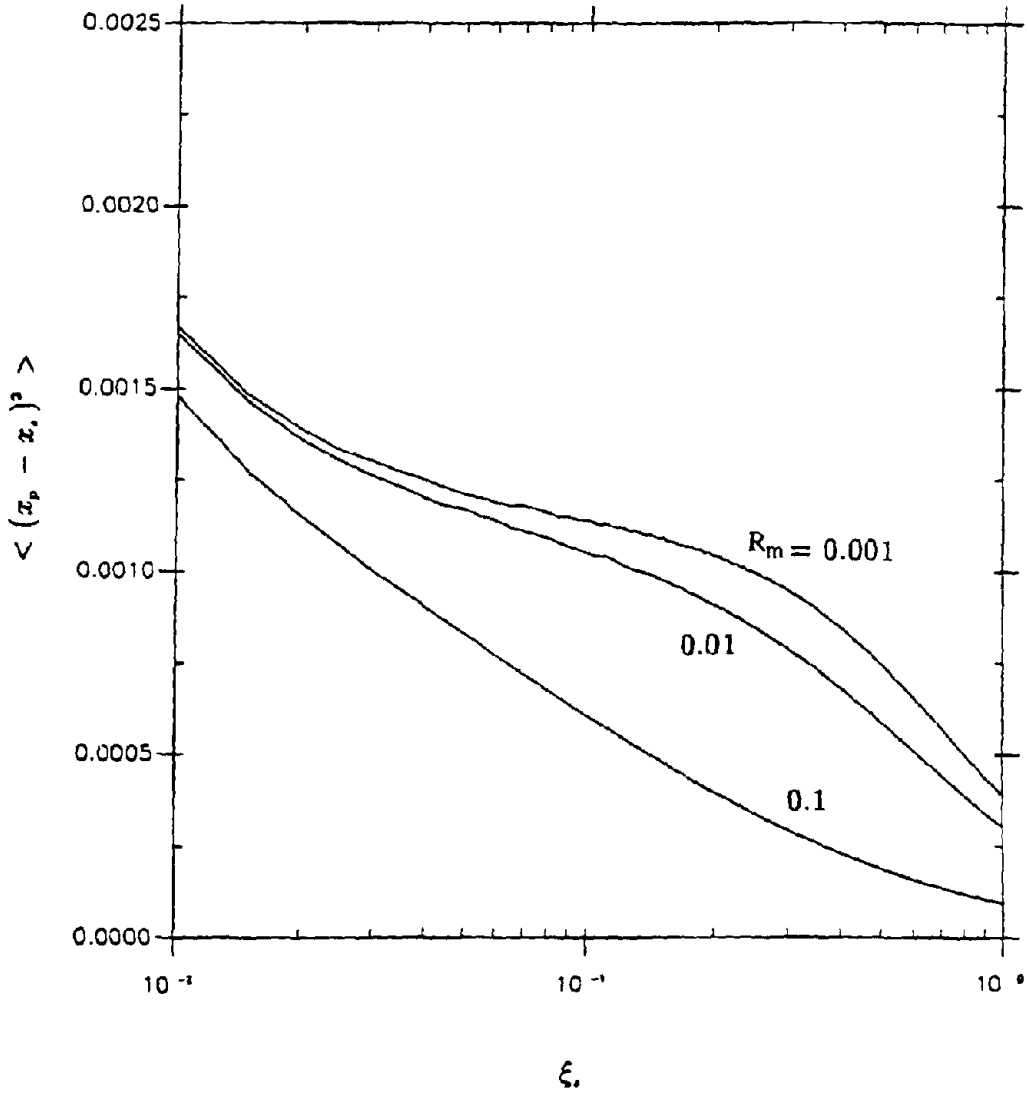

Fig. 6-8 Relative Displacement Between P- and S-System vs. ξ_s

$$m_s\ddot{z}_s + \frac{m_s + m_p}{m_p}c_s\dot{z}_s + \frac{m_s + m_p}{m_p}k_s z_s - \frac{m_s}{m_p}c_p\dot{y}_p - \frac{m_s}{m_p}k_p y_p = 0 \tag{6.16}$$

Assuming $R_\xi = R_\omega$ and $z_s = z_{s1}/R_\omega$ Eq. (4.4) and (6.16) become

$$m_s\ddot{z}_{s1} + (1 + R_m)c_s\dot{z}_{s1} + (1 + R_m)k_s z_{s1} - \frac{1}{R_\omega}(c_s\dot{y}_p + k_s y_p) = 0 \tag{6.17}$$

$$m_p\ddot{y}_p + c_p\dot{y}_p + k_p y_p - \frac{1}{R_\omega}(c_s\dot{z}_{s1} + k_s z_{s1}) = -m_p\ddot{x}_g \tag{6.18}$$

The above equations can be used to represent the generic system in Fig. 5-1(c) when the following system parameters are defined:

$$k_1 = (1 - R_m R_\omega)k_p, \qquad k_2 = \left(1 + R_m - \frac{1}{R_\omega}\right)k_s, \qquad k_3 = \frac{1}{R_\omega}k_s$$

$$c_1 = (1 - R_m R_\omega)c_p, \qquad c_2 = \left(1 + R_m - \frac{1}{R_\omega}\right)c_s, \qquad c_3 = \frac{1}{R_\omega}c_s$$

$$m_1 = m_p, \qquad m_2 = m_s$$

and the following condition is satisfied:

$$R_m \le \frac{1}{R_\omega} \le 1 + R_m \tag{6.19}$$

Power flow and energy can thus be calculated from Eqs. (5.32) and (5.33) as well as power balance equations in Eqs. (5.54) and (5.55).

6.6 Design Considerations of P-S Systems

In design practice, coupling spring and coupling damping coefficient are of interest. The main design objective for the P-S system is to minimize the kinetic energies of the P- and S-system under the action of external loads. To reach these goals, trade-offs between them should be conducted since tuning may produce minimum kinetic energy of the P-system but maximum kinetic energy of the S-system. Detuning is often necessary to limit the response of the P- and S-systems within allowable levels. Damping, however, can be taken at its optimum value for the S-system design

because the kinetic energy of the P-system is not very sensitive to it as explained in the preceding section.

6.7 Discussions

It has been shown that the concept of power flow and energy can be conveniently utilized in the analysis and design of simple P-S systems through the establishment of a fundamental relation between the power flow and energies of the P- and S-system with damping-coupled connection. Analysis has shown that power flow is closely related to the absolute acceleration of the S-system and the relative displacement between the P- and S-system. Numerical examples also demonstrate the equivalence between them in representing the dynamics of P-S systems and the optimum solution of the damping connection. Furthermore, considerations based on information on the kinetic energies of P- and S-systems provide another useful approach to the design of P-S systems.

SECTION 7

AN EXACT SOLUTION FOR A CLASS OF MDOF P-S SYSTEMS

7.1 Introduction

In Section 6, the concept of power flow and energy developed in Section 5 was applied to the study of a simple P-S system. However, more complex systems are often involved in practice and thus it is of practical interest to consider its application to more complex systems. Sections 7 and 8 are devoted to this topic. This section is designed to aim at an exact evaluation of frequency characteristics and response of a certain type of complex systems, namely, MDOF P-system with an S-system consisting of many branches with identical structure but different weight. This analysis can also help to evaluate the accuracy involved in various approximate schemes, to better understand the dynamic characteristics of multi-tuned P-S systems and to study the interaction effects among equipment installed in a building which has not been explored in the past. The mass of the S-system in this procedure does not have to be small as usually assumed in the development of a variety of schemes.

7.2 Equations of Motion of MDOF P-S System

Consider an n_p-story building with each floor supporting a branch of the S-system as shown in Fig. 7-1(a). The n_p number of branches are of identical frequency characteristics with different total weights, each having n_s-DOF as shown in Fig. 7-1(b).

The equations of motion of the system in Fig. 7-1 can be expressed as

$$\begin{bmatrix} M_p & \\ & M_s \end{bmatrix} \begin{bmatrix} \ddot{X}_p \\ \ddot{X}_s \end{bmatrix} + \begin{bmatrix} C_{pp} & C_{ps} \\ C_{sp} & C_{ss} \end{bmatrix} \begin{bmatrix} \dot{X}_p \\ \dot{X}_s \end{bmatrix} + \begin{bmatrix} K_{pp} & K_{ps} \\ K_{sp} & K_{ss} \end{bmatrix} \begin{bmatrix} X_p \\ X_s \end{bmatrix} = \begin{bmatrix} F_p \\ F_s \end{bmatrix} \tag{7.1}$$

in which the subscripts p and s are associated with the DOF of the P- and S- systems. The displacement vectors X_p and X_s denote, respectively, the absolute displacements of the P- and S-systems. The vector X_p is of dimension n_p and X_s is of dimension $n_p \times n_s$, n_p being the number of

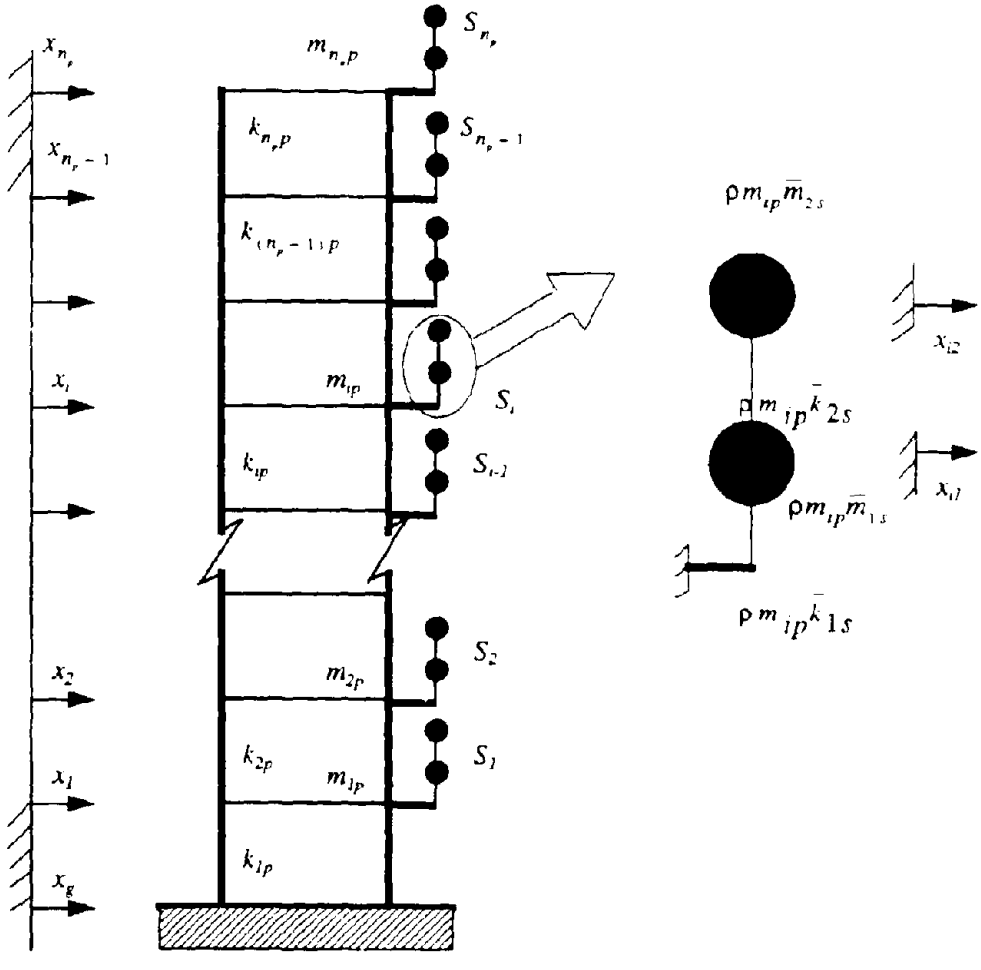

Fig. 7-1 Model of a Class of MDOF P-S System

branches of the S-system with n_s-DOF in each branch. Submatrices $\underline{K}_{pp}$ and $\underline{C}_{pp}$ can be decomposed into

$$\underline{K}_{pp} = \underline{K}_{pp}^{(0)} + \underline{K}_{pp}^{(s)} \tag{7.2}$$

$$\underline{C}_{pp} = \underline{C}_{pp}^{(0)} + \underline{C}_{pp}^{(s)} \tag{7.3}$$

In the above, $\underline{K}_{pp}^{(0)}$ and $\underline{C}_{pp}^{(0)}$ are stiffness and damping matrices of the P-system alone; $\underline{K}_{pp}^{(s)}$ and $\underline{C}_{pp}^{(s)}$ are the extra stiffness and damping of the P-system contributed by the S-system. For the system under consideration, they can be expressed as functions of mass matrix $\underline{M}_p$ of the P-system alone as

$$\underline{K}_{pp}^{(s)} = \rho \bar{k}_{1s} \underline{M}_p \tag{7.4}$$

$$\underline{C}_{pp}^{(s)} = \rho \bar{c}_{1s} \underline{M}_p \tag{7.5}$$

in which ρ represents the ratio of the S-system mass directly attached to the building floor to the floor mass. This is assumed to be constant over the height of the building in this section.

For clarification purposes, all the remaining matrices are explicitly written out in the following:

$$\underline{K}_{ss} = \begin{bmatrix} \underline{K}_{ss}^{(1)} & & & \\ & \underline{K}_{ss}^{(2)} & & \\ & & \ddots & \\ & & & \underline{K}_{ss}^{(n_p)} \end{bmatrix}, \quad \underline{M}_s = \begin{bmatrix} \underline{M}_s^{(1)} & & & \\ & \underline{M}_s^{(2)} & & \\ & & \ddots & \\ & & & \underline{M}_s^{(n_p)} \end{bmatrix}$$

in which the stiffness and mass matrices of each branch of the S-system alone can be further expressed as

$$\underline{K}_{ss}^{(i)} = \rho m_{ip} \bar{\underline{K}}_{ss}, \qquad \underline{M}_s^{(i)} = \rho m_{ip} \bar{\underline{M}}_s$$

The cross stiffness submatrix between P- and S- system can be described as

$$\underline{K}_{ps} = -\rho \bar{k}_{1s} \{ m_{1p} \underline{l}^{(1)} \quad m_{2p} \underline{l}^{(2)} \quad \cdots \quad m_{n_p p} \underline{l}^{(n_p)} \}$$

and

$$\underline{K}_{sp} = \underline{K}_{ps}^{T}$$

in which

$$\underline{I}^{(i)} = \begin{bmatrix} 0 & 0 & \cdots & 0 \\ \vdots & \vdots & & \vdots \\ 1 & 0 & \cdots & 0 \\ \vdots & \vdots & & \vdots \\ 0 & 0 & 0 & 0 \end{bmatrix}_{n_s \times n_p} \leftarrow i^{th} \text{ row} \qquad (i = 1, 2, \ldots, n_p)$$

For the P-system alone:

$$\underline{M}_p = \begin{bmatrix} m_{1p} & & & \\ & m_{2p} & & \\ & & \ddots & \\ & & & m_{n_p p} \end{bmatrix}, \quad \underline{K}_{pp}^{(0)} = \begin{bmatrix} k_{1p}+k_{2p} & -k_{2p} & & \\ -k_{2p} & k_{2p}+k_{3p} & -k_{3p} & \\ & -k_{3p} & \ddots & -k_{n_p p} \\ & & -k_{n_p p} & k_{n_p p} \end{bmatrix}$$

For each branch of the S-system:

$$\underline{\bar{M}}_s = \begin{bmatrix} \bar{m}_{1s} & & & \\ & \bar{m}_{2s} & & \\ & & \ddots & \\ & & & \bar{m}_{n_s s} \end{bmatrix}, \quad \underline{\bar{K}}_{ss} = \begin{bmatrix} \bar{k}_{1s}+\bar{k}_{2s} & -\bar{k}_{2s} & & \\ -\bar{k}_{2s} & \bar{k}_{2s}+\bar{k}_{3s} & -\bar{k}_{3s} & \\ & -\bar{k}_{3s} & \ddots & -\bar{k}_{n_s s} \\ & & -\bar{k}_{n_s s} & \bar{k}_{n_s s} \end{bmatrix}$$

In this formulation, $\bar{m}_{1s}$ is set to be one without loss of generality. The damping matrices $\underline{C}_{pp}^{(0)}$ and $\underline{C}_{ss}$ have exactly the same structure as stiffness matrices $\underline{K}_{pp}^{(0)}$ and $\underline{K}_{ss}$, respectively.

7.3 Frequency Characteristics of Individual Systems

The frequency characteristic equation for each branch of the S-system on the fixed base can be formulated as follows:

$$(\underline{K}_{ss} - \omega^2 \underline{\bar{M}}_s)\underline{\Phi}_s = \underline{O} \tag{7.6}$$

The solution of the above equation gives n_s number of frequencies ω_s and mode vector $\underline{\phi}_{is}$ which constitute the stiffness matrix in the modal space. They can be presented by

$$\underline{\Omega}_s^2 = \begin{bmatrix} \omega_{1s}^2 & & & \\ & \omega_{2s}^2 & & \\ & & \ddots & \\ & & & \omega_{n_s s}^2 \end{bmatrix} \tag{7.7}$$

$$\underline{\Psi}_s = \{\underline{\phi}_{1s} \ \underline{\phi}_{2s} \ \cdots \ \underline{\phi}_{n_s s}\} \tag{7.8}$$

The mode matrix $\underline{\Psi}_s$ is orthogonal with respect to the mass matrix, i.e.,

$$\underline{\Psi}_s^T \underline{\bar{M}}_s \underline{\Psi}_s = \underline{I}_s \tag{7.9}$$

in which $\underline{I}_s$ is the unit matrix of dimension $n_s \times n_s$.

The total stiffness matrix in the modal space and the mode matrix for the integrated S-system can be written as

$$\underline{\Lambda}_s = \begin{bmatrix} \underline{\Omega}_s^2 & & & \\ & \underline{\Omega}_s^2 & & \\ & & \ddots & \\ & & & \underline{\Omega}_s^2 \end{bmatrix} \tag{7.10}$$

$$\underline{\Phi}_s = \begin{bmatrix} \underline{\Psi}_s / \sqrt{\rho m_{1p}} & & & \\ & \underline{\Psi}_s / \sqrt{\rho m_{2p}} & & \\ & & \ddots & \\ & & & \underline{\Psi}_s / \sqrt{\rho m_{n_p p}} \end{bmatrix} \tag{7.11}$$

In this section, the total response of the S-system is partitioned into the pseudo-static and dynamic components as in [9,10,47], which is also consistent with the design philosophy suggested by ASME Boiler and Pressure Vessel Code [5]. That is

$$\underline{X}_s = \underline{X}_s^{(p)} + \underline{X}_s^{(d)}$$

in which superscripts p and d denote "pseudo-static" and "dynamic" components of the displacement. The pseudo-static displacement results from the movement of the P-system, which can be easily obtained by setting the forces associated with the mass and damping matrices equal to zero in Eq. (7.1) and written in the form of

$$\begin{bmatrix} \underline{K}_{pp} & \underline{K}_{ps} \\ \underline{K}_{sp} & \underline{K}_{ss} \end{bmatrix} \begin{bmatrix} \underline{X}_p \\ \underline{X}_s^{(p)} \end{bmatrix} = \begin{bmatrix} \underline{F}_p \\ \underline{O} \end{bmatrix} \tag{7.12}$$

or

$$\underline{X}_s^{(p)} = \underline{T}_1 \underline{X}_p \tag{7.13}$$

$$\underline{T}_1 = -\underline{K}_{ss}^{-1} \underline{K}_{sp} \tag{7.14}$$

Here, $\underline{T}_1$ is a transformation matrix that transforms a unit displacement of the P-system into the static displacement of the S-system. This matrix can be expanded as

$$\underline{T}_1 = \begin{bmatrix} \underline{l} & & & \\ & \underline{l} & & \\ & & \ddots & \\ & & & \underline{l} \end{bmatrix}_{n_s \times n_p} \tag{7.15}$$

in which $\underline{l} = \{1, 1, \ldots, 1\}^T_{1 \times n_s}$

The masses of the S-system are lumped into the corresponding floors in the P-system to determine the frequency characteristics of the P-system. Consequently, its mass and stiffness matrices become

$$\overline{\underline{M}}_p = \begin{bmatrix} \underline{I} \\ \underline{T}_1 \end{bmatrix}^T \begin{bmatrix} \underline{M}_p & \\ & \underline{M}_s \end{bmatrix} \begin{bmatrix} \underline{I} \\ \underline{T}_1 \end{bmatrix} = \underline{M}_p + \underline{T}_1^T \underline{M}_s \underline{T}_1 \tag{7.16}$$

$$\overline{\underline{K}}_{pp} = \begin{bmatrix} \underline{I} \\ \underline{T}_1 \end{bmatrix}^T \begin{bmatrix} \underline{K}_{pp} & \underline{K}_{ps} \\ \underline{K}_{sp} & \underline{K}_{ss} \end{bmatrix} \begin{bmatrix} \underline{I} \\ \underline{T}_1 \end{bmatrix} = \underline{K}_{pp} + \underline{K}_{ps} \underline{T}_1 + \underline{T}_1^T \underline{K}_{sp} + \underline{T}_1^T \underline{K}_{ss} \underline{T}_1 \tag{7.17}$$

After introducing Eq. (7.15) and other matrices defined before, Eqs. (7.16) and (7.17) can be simplified to

$$\bar{\underline{M}}_p = \left(1 + \rho \sum_{i=1}^{n_s} \bar{m}_{is}\right) \underline{M}_p \tag{7.18}$$

$$\bar{\underline{K}}_{pp} = \underline{K}_{pp}^{(0)} \tag{7.19}$$

The frequency characteristic equation for the P-system can then be expressed as

$$(\bar{\underline{K}}_{pp} - \omega^2 \bar{\underline{M}}_p)\, \underline{\phi}_p = \underline{O} \tag{7.20}$$

whose solutions are n_p number of frequencies ω_{ip} and mode vector $\underline{\phi}_{ip}$ and the stiffness matrix in the modal space and mode matrix are given by

$$\underline{\Lambda}_p = \begin{bmatrix} \omega_{1p}^2 & & & \\ & \omega_{2p}^2 & & \\ & & \ddots & \\ & & & \omega_{n_p p}^2 \end{bmatrix} \tag{7.21}$$

$$\underline{\Phi}_p = \{\underline{\phi}_{1p}\ \underline{\phi}_{2p}\ \cdots\ \underline{\phi}_{n_p p}\} \tag{7.22}$$

where the modal matrix $\underline{\Phi}_p$ satisfies the orthogonal condition

$$\underline{\Phi}_p^T \bar{\underline{M}}_p \underline{\Phi}_p = \underline{I}_p \tag{7.23}$$

in which $\underline{I}_p$ is the unit matrix of dimension $n_p \times n_p$.

It is noted that, in the situation under investigation, damping matrix $\bar{\underline{C}}_{pp} = \underline{C}_{pp}^{(0)}$ as is the case for stiffness matrix $\bar{\underline{K}}_{pp}$. Furthermore, the structure of mass matrix $\bar{\underline{M}}_p$ is exactly the same as $\underline{M}_p$ so that participation of lumped masses from the S-system does not change the damping structure of the P-system, i.e., $\bar{\underline{C}}_{pp}$ is proportional to matrices $\bar{\underline{M}}_p$ and $\bar{\underline{K}}_{pp}$ if $\underline{C}_{pp}^{(0)}$ is proportional to matrices $\underline{M}_p$ and $K_{pp}^{(0)}$ of the P-system alone.

7.4 Group Analysis of P-S System in Modal Space

Let the displacement vector be expressed by

$$\begin{bmatrix} X_p \\ X_s \end{bmatrix} = \begin{bmatrix} \Phi_p & O \\ T_1\Phi_p & \Phi_s \end{bmatrix} \begin{bmatrix} q_p \\ q_s \end{bmatrix} = \Phi q \tag{7.24}$$

By substituting Eq. (7.24) into Eq. (7.1) and pre-multiplying both sides of the resulting equation by Φ^T, the following equations in the modal space are obtained after introducing the orthogonal conditions:

$$\begin{bmatrix} I_p & M_{sp}^T \\ M_{sp} & I_s \end{bmatrix} \begin{bmatrix} \ddot{q}_p \\ \ddot{q}_s \end{bmatrix} + \begin{bmatrix} \Delta_p & \\ & \Delta_s \end{bmatrix} \begin{bmatrix} \dot{q}_p \\ \dot{q}_s \end{bmatrix} + \begin{bmatrix} \Lambda_p & \\ & \Lambda_s \end{bmatrix} \begin{bmatrix} q_p \\ q_s \end{bmatrix} = \begin{bmatrix} F'_p \\ F'_s \end{bmatrix} \tag{7.25}$$

in which I_s is the unit matrix of dimension $n_p n_s \times n_p n_s$. Δ_p and Δ_s are damping matrices of the P- and S-systems in the modal space which are diagonal when the individual P- and S-systems alone are proportionally damped. The coupling mass matrix M_{sp} and force vectors F'_p and F'_s can be calculated by

$$M_{sp} = \Phi_s^T M_s T_1 \Phi_p = [\bar{m}_{ik}] \tag{7.26}$$

$$\bar{m}_{ik} = \sqrt{\rho m_{ip}}\,\phi_{kp}(i)\,\Psi_s^{-1}\,l \qquad (i,k = 1, 2, \ldots, n_p) \tag{7.27}$$

$$F'_p = \Phi_p^T (F_p + T_1^T F_s) \tag{7.28}$$

$$F'_s = \Phi_s^T F_s \tag{7.29}$$

In the above, the first and second indices in the coupling mass matrix denote the building floor and mode order of the building, respectively. It is noted here that $\bar{m}_{ik}$=0 when $\phi_{kp}(i) = 0$. This means that the *k-th* mode of the P-system has no contribution to the dynamic response of a branch of the S-system attached to the *i-th* floor.

For simplicity of derivation, Eq. (7.25) is expanded in the form of a mode of the P-system and a branch of the S-system. That is,

$$\ddot{q}_{kp} + \Delta_{kp}\dot{q}_{kp} + \omega_{kp}^2 q_{kp} + \sum_{l=1}^{n_s} \bar{m}_{lk}^T \ddot{q}_{ls} = F'_{kp} \tag{7.30}$$

$$\ddot{q}_{is} + \Delta_s \dot{q}_{is} + \Omega_s^2 q_{is} + \sum_{l=1}^{n_p} \bar{m}_{il} \ddot{q}_{lp} = F'_{is} \tag{7.31}$$

Before we go further to simplify above equations, the following matrix notations are introduced:

(1). A diagonal matrix expanded from a vector is denoted as

$$diag(\underline{V}) = [V^{(r)}]_{n \times n} \tag{7.32}$$

in which $V^{(r)}$ is the *r-th* element of vector $\underline{V}$ of dimension *n*.

(2). A positive definite and diagonal matrix to the *s-th* power is denoted as

$$[diag(\underline{V})]^s = [(V^{(r)})^s]_{n \times n} \tag{7.33}$$

in which $V^{(r)}$ is a positive real value and *s* is any real number.

Pre-multiplying diag($\bar{\underline{m}}_{ik}$) on both sides of Eq. (7.31) and summing up all the terms with index *i*, we obtain

$$\ddot{\bar{\underline{q}}}_{ks} + \underline{\Delta}_s \dot{\bar{\underline{q}}}_{ks} + \underline{\Omega}_s^2 \bar{\underline{q}}_{ks} + \sum_{l=1}^{n_p} \left(\sum_{i=1}^{n_p} diag(\bar{\underline{m}}_{ik}) \bar{\underline{m}}_{il} \right) \dot{q}_{lp} = \underline{F}''_{ks} \tag{7.34}$$

$$\bar{\underline{q}}_{ks} = \sum_{i=1}^{n_p} diag(\bar{\underline{m}}_{ik}) \underline{q}_{is} \tag{7.35}$$

$$\underline{F}''_{ks} = \sum_{i=1}^{n_p} diag(\bar{\underline{m}}_{ik}) \underline{F}''_{is}$$

Furthermore, the vector in the brackets of Eq. (7.34) can be simplified as

$$\sum_{i=1}^{n_p} diag(\bar{\underline{m}}_{ik}) \bar{\underline{m}}_{il} = \sum_{i=1}^{n_p} \rho m_{i_p} \phi_{kp}(i) \phi_{lp}(i) diag(\underline{\Psi}_s^{-1} \ \underline{1}) (\underline{\Psi}_s^{-1} \ \underline{1}) = \bar{\underline{\Psi}} \delta_{lk}$$

$$\bar{\underline{\Psi}} = \frac{\rho}{1 + \rho \sum_{l=1}^{n_p} \bar{m}_{ls}} diag(\underline{\Psi}_s^{-1} \ \underline{1}) (\underline{\Psi}_s^{-1} \ \underline{1}) \tag{7.36}$$

in which the orthogonal condition in Eq. (7.23) has been introduced and δ_{lk} is the Kronector delta function defined by

$$\delta_{lk} = \begin{cases} 0 & l \neq k \\ 1 & l = k \end{cases} \tag{7.37}$$

Consequently, Eqs. (7.30) and (7.34) become

$$\ddot{q}_{kp} + \Delta_{kp}\dot{q}_{kp} + \omega_{kp}^2 q_{kp} + \underline{l}^T \ddot{\underline{q}}_{ks} = F'_{kp} \tag{7.38}$$

$$\ddot{\underline{q}}_{ks} + \underline{\Delta}_s \dot{\underline{q}}_{ks} + \underline{\Omega}_s^2 \underline{q}_{ks} + \underline{\bar{\Psi}} \ddot{q}_{kp} = \underline{F}''_{ks} \tag{7.39}$$

Up to this point, the $n_p(n_s+1)$-DOF system in Fig. 7-1(a) has been grouped into n_p number of (n_s+1)-DOF subsystems, each representing one mode of the P-system. When n_s is not greater than three, the dynamic response of the subsystems subjected to white noise can be analytically evaluated by employing the integrations listed in Appendix A.

It is desirable to convert Eqs. (7.38) and (7.39) into ones that are symmetric in subsystem's parameters so that this subsystem in the modal space can be directly modelled by a new physical system. From the orthogonal condition in Eq. (7.9), we know that vector $\bar{\Psi}$ defined in Eq. (7.36) actually consists of the squares of the participation factors of any branch of the S-system in Fig. 7-1(b) subjected to ground acceleration and therefore its elements can not be zero in this case. Based on this observation, pre-multiplication of matrix $[diag(\bar{\Psi})]^{-1/2}$ to Eq. (7.39) will give an equivalent equation. That is,

$$[diag(\bar{\Psi})]^{-\frac{1}{2}} (\ddot{\underline{q}}_{ks} + \underline{\Delta}_s \dot{\underline{q}}_{ks} + \underline{\Omega}_s^2 \underline{q}_{ks} + \underline{\bar{\Psi}} \ddot{q}_{kp}) = [diag(\bar{\Psi})]^{-\frac{1}{2}} \underline{F}''_{ks}$$

Noting that $[diag(\bar{\Psi})]^{-1/2}$, $\underline{\Delta}_s$, and $\underline{\Omega}_s^2$ are all diagonal matrices and the multiplication of two diagonal matrices is commutable, the above equation can be written in the form of

$$\ddot{\underline{q}}_{ks} + \underline{\Delta}_s \dot{\underline{q}}_{ks} + \underline{\Omega}_s^2 \underline{\hat{q}}_{ks} + [diag(\bar{\Psi})]^{-\frac{1}{2}} \underline{\bar{\Psi}} \ddot{q}_{kp} = \underline{F}'''_{ks} \tag{7.40}$$

and Eq. (7.38) becomes

$$\ddot{q}_{kp} + \Delta_{kp}\dot{q}_{kp} + \omega_{kp}^2 q_{kp} + \underline{l}^T [diag(\bar{\Psi})]^{\frac{1}{2}} \ddot{\underline{\hat{q}}}_{ks} = F'_{kp} \tag{7.41}$$

in which

$$\hat{q}_{ks} = [diag(\bar{\Psi})]^{-\frac{1}{2}} \bar{q}_{ks} \tag{7.42}$$

$$F'''_{ks} = [diag(\bar{\Psi})]^{-\frac{1}{2}} F'''_{ks}$$

However,

$$[diag(\bar{\Psi})]^{-\frac{1}{2}} \bar{\Psi} = [diag(\bar{\Psi})]^{-\frac{1}{2}} [diag(\bar{\Psi})] I = [diag(\bar{\Psi})]^{\frac{1}{2}} I$$

The substitution of this result into Eq. (7.41) leads to the equation

$$\ddot{q}_{kp} + \Delta_{kp}\dot{q}_{kp} + \omega_{kp}^2 q_{kp} + \bar{\Psi}^T [diag(\bar{\Psi})]^{-\frac{1}{2}} \ddot{\hat{q}}_{ks} = F'_{kp} \tag{7.43}$$

Equations (7.40) and (7.43) are the final formulas that can be employed to calculate the modal dynamic response of the P-S system. The two levels of transformation from Eqs. (7.30) and (7.31) to Eqs. (7.40) and (7.43) are illustrated in Fig. 7-2 in the case of a 2-DOF P-system and a (2×2) -DOF S-system, which helps us better understand the preceding procedure.

In the physical space, dynamic displacement of the S-system $(X_s^{(d)})$ or relative displacement of any branch of the S-system with respect to its supporting floor in this particular case can be expressed as

$$X_s^{(d)} = \Phi_s q_s = \begin{bmatrix} \Psi_s q_{1s} / \sqrt{\rho m_{1p}} \\ \cdot \\ \cdot \\ \Psi_s q_{n_p s} / \sqrt{\rho m_{n_p p}} \end{bmatrix} \tag{7.44}$$

and its *i-th* subvector for a branch of the S-system attached to the *i-th* floor is

$$X_i^{(d)} = \frac{1}{\sqrt{\rho m_{ip}}} \Psi_s q_{is} \tag{7.45}$$

or

$$q_{is} = \sqrt{\rho m_{ip}}\ \Psi_s^{-1} X_i^{(d)} \tag{7.46}$$

Recalling Eqs. (7.35) and (7.42), we can express modal displacement vector $(\hat{q}_{ks})$ as

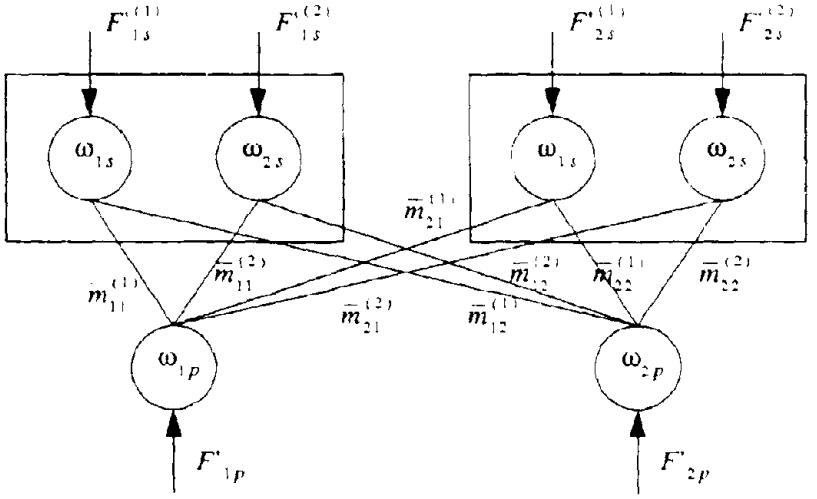

Eqs. (7.30) and (7.31)

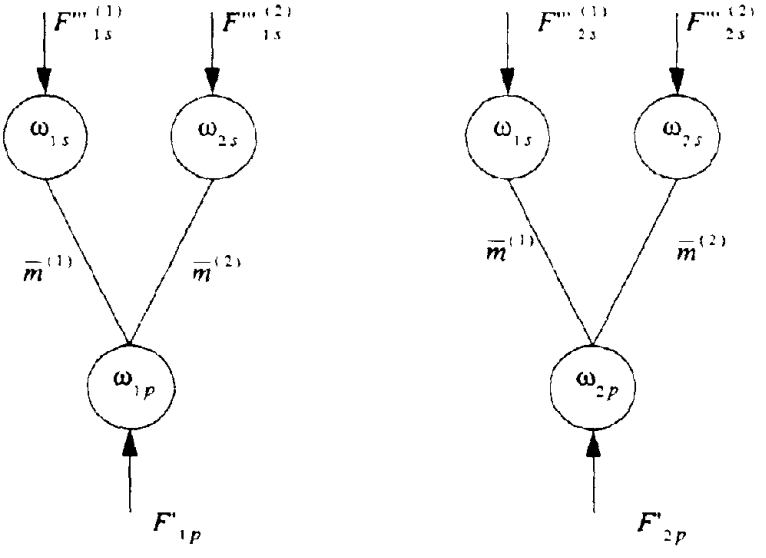

Eqs.(7.40) and (7.43)

Fig. 7-2 Illustration of Two- Level Transformation

$$\hat{\underline{q}}_{ks} = [diag(\bar{\Psi})]^{-\frac{1}{2}} \sum_{l=1}^{n_r} diag(\bar{m}_{lk})\, \underline{q}_{ls}$$

$$= \rho\, [diag(\bar{\Psi})]^{-\frac{1}{2}} diag(\Psi_s^{-1}\underline{l})\, \Psi_s^{-1} \sum_{l=1}^{n_r} m_{lp}\phi_{kp}(l)\, \underline{X}_l^{(d)} \tag{7.47}$$

In the above derivation, Eqs. (7.27) and (7.46) have been introduced. Expanding displacement vector $\underline{X}_l^{(d)}$ in a new way, i.e.,

$$\underline{X}_l^{(d)} = \sum_{i=1}^{n_r} \phi_{ip}(l)\, \bar{\underline{X}}_i^{(d)} \qquad (l = 1,\ 2,\ \ldots,\ n_p) \tag{7.48}$$

and substituting it into Eq. (7.47), we have

$$\hat{\underline{q}}_{ks} = \rho\, [diag(\bar{\Psi})]^{-\frac{1}{2}} diag(\Psi_s^{-1}\underline{l})\, \Psi_s^{-1} \sum_{l=1}^{n_r} m_{lp}\phi_{kp}(l) \sum_{i=1}^{n_r} \phi_{ip}(l)\, \bar{\underline{X}}_i^{(d)}$$

$$= \frac{\rho}{1 + \rho \sum_{l=1}^{n_r} \bar{m}_{ls}} [diag(\bar{\Psi})]^{-\frac{1}{2}} diag(\Psi_s^{-1}\underline{l})\, \Psi_s^{-1}\, \bar{\underline{X}}_k^{(d)} \tag{7.49}$$

or

$$\bar{\underline{X}}_k^{(d)} = \frac{1 + \rho \sum_{l=1}^{n_r} \bar{m}_{ls}}{\rho}\, \Psi_s\, [diag(\Psi_s^{-1}\underline{l})]^{-1}\, [diag(\bar{\Psi})]^{\frac{1}{2}}\, \hat{\underline{q}}_{ks} \tag{7.50}$$

In addition, substituting Eq. (7.36) for $\bar{\Psi}$ gives rise to

$$[diag(\Psi_s^{-1}\underline{l})]^{-1}\, [diag(\bar{\Psi})]^{\frac{1}{2}}$$

$$= \sqrt{\frac{\rho}{1 + \rho \sum_{l=1}^{n_r} \bar{m}_{ls}}}\, [diag(\Psi_s^{-1}\underline{l})]^{-1}\, [diag(diag(\Psi_s^{-1}\underline{l})\ (\Psi_s^{-1}\underline{l}))]^{\frac{1}{2}}$$

$$= \sqrt{\frac{\rho}{1 + \rho \sum_{l=1}^{n_r} \bar{m}_{ls}}}\, [diag(\Psi_s^{-1}\underline{l})]^{-1}\, [(diag(\Psi_s^{-1}\underline{l}))^2]^{\frac{1}{2}}$$

$$= \sqrt{\frac{\rho}{1+\rho\sum_{l=1}^{n_s}\bar{m}_{ls}}}\,\underline{I}_s \tag{7.51}$$

Eq. (7.50) then becomes

$$\bar{\underline{X}}_k^{(d)} = \sqrt{\frac{1+\rho\sum_{l=1}^{n_s}\bar{m}_{ls}}{\rho}}\,\underline{\Psi}_s\hat{\underline{q}}_{ks} \tag{7.52}$$

and the dynamic response of the *i-th* branch of the S-system can be calculated from Eq. (7.48).

In the derivation of Eq. (7.51), we take the sign of element of vector $\underline{\Psi}_s^{-1}\underline{I}$ for the square root value of $diag(\bar{\underline{\Psi}})$. This does not affect the frequency characteristics and dynamic response of the P-S system since the product of $[diag(\bar{\underline{\Psi}})]^{1/2}$ and $\hat{\underline{q}}_{ks}$ is independent of the sign convention.

7.5 Illustration of Two Transformations

To assure the appropriateness of the proposed procedure, the two transformations described in Eqs. (7.35) and (7.48) must guarantee that the equations before and after the transformations are equivalent, i.e., the transformations matrices must not be singular. This is demonstrated below.

Eqs. (7.35) and (7.48) can be rewritten in the matrix form of

$$\bar{\underline{q}}_s = \underline{T}_2^T\underline{q}_s \tag{7.53}$$

$$\underline{X}_s^{(d)} = \underline{T}_3\bar{\underline{X}}_s^{(d)} \tag{7.54}$$

in which

$$\underline{T}_2 = [diag(\bar{m}_{ik})] = [\sqrt{\rho m_{ip}}\ \phi_{kp}(i)\,diag(\underline{\Psi}_s^{-1}\underline{I})]$$

$$\underline{T}_3 = [\phi_{kp}(i)\,\underline{I}_s]$$

In what follows, we wish to illustrate that the determinants of $\underline{T}_2$ and $\underline{T}_3$ are not equal to zero. As a matter of fact, $\underline{T}_2$ and $\underline{T}_3$ have the same structure and therefore only $\underline{T}_3$ is demonstrated in the following.

The determinant $\underline{T}_3$ is defined by

$$\underline{T}_3 = \begin{vmatrix} \phi_{1p}(1)\underline{I}_s & \phi_{2p}(1)\underline{I}_s & \cdots & \phi_{n_r p}(1)\underline{I}_s \\ \phi_{1p}(2)\underline{I}_s & \phi_{2p}(2)\underline{I}_s & \cdots & \phi_{n_r p}(2)\underline{I}_s \\ \vdots & \vdots & & \vdots \\ \phi_{1p}(n_p)\underline{I}_s & \phi_{2p}(n_p)\underline{I}_s & \cdots & \phi_{n_r p}(n_p)\underline{I}_s \end{vmatrix}_{(n_p \times n_r)}$$

$$= [\phi_{1p}(1)]^{-n_r(n_r-2)} \begin{vmatrix} \phi_{1p}^{(1)}(1)\underline{I}_s & \cdots & \phi_{(n_r-1)p}^{(1)}(1)\underline{I}_s \\ \phi_{1p}^{(1)}(2)\underline{I}_s & \cdots & \phi_{(n_r-1)p}^{(1)}(2)\underline{I}_s \\ \vdots & & \vdots \\ \phi_{1p}^{(1)}(n_p-1)\underline{I}_s & \cdots & \phi_{(n_r-1)p}^{(1)}(n_p-1)\underline{I}_s \end{vmatrix}_{(n_r-1)\times(n_p-1)}$$

$$= (\phi_{1p}(1))^{-n_r(n_r-2)} (\phi_{1p}^{(1)}(1))^{-n_r(n_r-1)} \cdots (\phi_{1p}^{(n_r-2)}(1))^{0} (\phi_{1p}^{(n_r-1)}(1))^{n_r} \qquad (7.55)$$

Here, new coefficients $\phi_{kp}^{(l)}(i)$ can be expressed in the recursive form, i.e.,

$$\phi_{kp}^{(l)}(i) = \begin{vmatrix} \phi_{1p}^{(l-1)}(1) & \phi_{(k+1)p}^{(l-1)}(1) \\ \phi_{1p}^{(l-1)}(i+1) & \phi_{(k+1)p}^{(l-1)}(i+1) \end{vmatrix} \qquad (l = 1, 2, \ldots, n_p - 1) \qquad (7.56)$$

and $\phi_{kp}^{(0)}(i) = \phi_{kp}(i)$ represents the mode value of the *k-th* mode of the P-system at the *i-th* floor.

In order to assure nonzeroness of $\underline{T}_3$, all the factors in Eq. (7.55) must be finite and nonzero, i.e., $\phi_{1p}^{(l)}(1) \neq 0$ and $|\phi_{1p}^{(l)}(1)| < \infty$. After a series of tedious derivations, the following relations hold:

$$\phi_{1p}^{(1)}(1) = \begin{vmatrix} \phi_{1p}(1) & \phi_{2p}(1) \\ \phi_{1p}(2) & \phi_{2p}(2) \end{vmatrix} \qquad (7.57)$$

$$\phi_{1p}^{(2)}(1) = \Phi_{1p}(1) \begin{vmatrix} \Phi_{1p}(1) & \Phi_{2p}(1) & \Phi_{3p}(1) \\ \Phi_{1p}(2) & \Phi_{2p}(2) & \Phi_{3p}(2) \\ \Phi_{1p}(3) & \Phi_{2p}(3) & \Phi_{3p}(3) \end{vmatrix} \tag{7.58}$$

$$\phi_{1p}^{(3)}(1) = \phi_{1p}^{2}(1) \begin{vmatrix} \Phi_{1p}(1) & \Phi_{2p}(1) \\ \Phi_{1p}(2) & \Phi_{2p}(2) \end{vmatrix} \begin{vmatrix} \Phi_{1p}(1) & \Phi_{2p}(1) & \Phi_{3p}(1) & \Phi_{4p}(1) \\ \Phi_{1p}(2) & \Phi_{2p}(2) & \Phi_{3p}(2) & \Phi_{4p}(2) \\ \Phi_{1p}(3) & \Phi_{2p}(3) & \Phi_{3p}(3) & \Phi_{4p}(3) \\ \Phi_{2p}(4) & \Phi_{2p}(4) & \Phi_{3p}(4) & \Phi_{4p}(4) \end{vmatrix} \tag{7.59}$$

and so on. It can be observed that $\phi_{1p}^{(l)}(1)$ is a multiplication of all the determinants up to $(l+1)$ dimension of the "principal" submatrices in mode matrix Φ_p as shown in Eq. (7.59) and this is obviously finite but not equal to zero.

7.6 Dynamic Response of S-System

The dynamic responses of an S-system with each branch of dimension less than four can be analytically calculated from the integration formula in Appendix A. For the simplest case with n_s equal to one, Eq. (7.48) becomes

$$x_l^{(d)} = \sum_{i=1}^{n_p} \phi_{ip}(l)\bar{x}_i^{(d)} = \sqrt{\frac{1+\rho}{\rho}} \sum_{i=1}^{n_p} \phi_{ip}(l)\hat{q}_{is} \tag{7.60}$$

in which Eq. (7.52) has been introduced and $\Psi_s = 1$ has been recognized in this case.

The mean-square displacement and velocity can then be formulated as

$$\langle (x_l^{(d)})^2 \rangle = \frac{1+\rho}{\rho} \sum_{i=1}^{n_p} \sum_{k=1}^{n_p} \phi_{ip}(l)\phi_{kp}(l)\langle \hat{q}_{is}\hat{q}_{ks} \rangle \tag{7.61}$$

$$\langle (\dot{x}_l^{(d)})^2 \rangle = \frac{1+\rho}{\rho} \sum_{i=1}^{n_p} \sum_{k=1}^{n_p} \phi_{ip}(l)\phi_{kp}(l)\langle \dot{\hat{q}}_{is}\dot{\hat{q}}_{ks} \rangle \tag{7.62}$$

from which one can see that the mean-square values and covariances between modal responses are required. These can be obtained as follows.

In general, Eqs. (7.40) and (7.43) can be expressed for two modes of the P-system as follows:

$$\ddot{\hat{q}}_{ip} + \Delta_{ip}\dot{\hat{q}}_{ip} + \omega_{ip}^2 \hat{q}_{ip} + \bar{m}\ddot{\hat{q}}_{is} = \Gamma_{ip} f(t) \tag{7.63}$$

$$\ddot{\hat{q}}_{is} + \Delta_s \dot{\hat{q}}_{is} + \omega_s^2 \hat{q}_{is} + \bar{m}\ddot{\hat{q}}_{ip} = \Gamma_{is} f(t) \tag{7.64}$$

and

$$\ddot{\hat{q}}_{kp} + \Delta_{kp}\dot{\hat{q}}_{kp} + \omega_{kp}^2 \hat{q}_{kp} + \bar{m}\ddot{\hat{q}}_{ks} = \Gamma_{kp} f(t) \tag{7.65}$$

$$\ddot{\hat{q}}_{ks} + \Delta_s \dot{\hat{q}}_{ks} + \omega_s^2 \hat{q}_{ks} + \bar{m}\ddot{\hat{q}}_{kp} = \Gamma_{ks} f(t) \tag{7.66}$$

in which $\bar{m} = \dfrac{\rho}{\sqrt{1+\rho}}$.

When the base displacement input to the P-system is considered, $\Gamma_{ip}=\Gamma_{kp}=0$. Power flow transmitted from the P-system to the S-system through one mode and energies stored in the mode in this case can be calculated by referring to [53]. For more general systems with correlated inputs in Eqs. (7.65) and (7.66), same form of the power balance equation can be obtained as given in Eqs. (2.15) and (2.16). But, the expressions for input power and energies (mean-square values) take different forms. They are

$$P_{ks}^{(in)} = \Gamma_{ks}\langle f(t)\,\dot{\hat{q}}_{ks}(t)\rangle = \frac{\pi S_f \Gamma_{ks}(\Gamma_{ks} - \bar{m}\Gamma_{kp})}{1-\bar{m}^2} \tag{7.67}$$

$$\langle \hat{q}_{ks}^2 \rangle = \frac{\pi S_f}{\omega_s^2}\left(\frac{\bar{m}^2\Gamma_{kp}^2\Delta_s\omega_{kp}^2\omega_s^2 + \Delta_{kp}[\Gamma_{ks}(\omega_{kp}^2-\omega_s^2) + \bar{m}\Gamma_{kp}\omega_s^2]^2}{Q} \right.$$
$$\left. + \frac{\Gamma_{ks}^2(\Delta_{kp}\omega_s^2 + \Delta_s\omega_{kp}^2)[\Delta_{kp}(\Delta_s+\Delta_{kp}) + \bar{m}^2\omega_{kp}^2]}{Q} \right) \tag{7.68}$$

$$\langle \dot{\hat{q}}_{ks}^2 \rangle = \frac{\pi S_f(\Gamma_{ks} - \bar{m}\Gamma_{kp})^2}{(1-\bar{m}^2)(\Delta_s+\Delta_{kp})} + \frac{\pi S_f}{\Delta_s+\Delta_{kp}}\left(\frac{[\Gamma_{ks}\Delta_{kp}(\omega_{kp}^2-\omega_s^2) + \bar{m}\Gamma_{kp}(\Delta_s\omega_{kp}^2 + \Delta_{kp}\omega_s^2)]^2}{Q} \right.$$
$$\left. + \frac{\Gamma_{ks}^2\Delta_{kp}^2(\Delta_s+\Delta_{kp})(\Delta_s\omega_{kp}^2 + \Delta_{kp}\omega_s^2)}{Q} \right) \tag{7.69}$$

$$Q = \bar{m}^2(\Delta_{kp}\omega_s^2 + \Delta_s\omega_{kp}^2)^2 + \Delta_s\Delta_{kp}[(\omega_s^2-\omega_{kp}^2)^2 + (\Delta_s+\Delta_{kp})(\Delta_s\omega_{kp}^2 + \Delta_{kp}\omega_s^2)]$$

in which S_f is the power spectral density of broad-band stochastic process f(t).

For the calculation of covariance between any two modes, the transfer function approach as used in Section 5 is employed. After manipulating a series of mathematical derivations, the covariance between any two modes described by Eqs. (7.63)-(7.66) can be formulated as

$$\langle \hat{q}_{is} \hat{q}_{ks} \rangle = S_f \int_{-\infty}^{\infty} \frac{\left(\frac{\Gamma_{is}}{H_{ip}} + \bar{m}\omega^2 \Gamma_{ip} \right) \left(\frac{\Gamma_{ks}}{H_{kp}} + \bar{m}\omega^2 \Gamma_{kp} \right)}{\left(\frac{1}{H_s H_{ip}} - \bar{m}^2 \omega^4 \right) \left(\frac{1}{H_s H_{kp}} - \bar{m}^2 \omega^4 \right)} d\omega \tag{7.70}$$

in which

$$H_s = \frac{1}{\omega_s^2 - \omega^2 + j\omega\Delta_s}$$

$$H_{lp} = \frac{1}{\omega_{lp}^2 - \omega^2 + j\omega\Delta_{lp}} \qquad (l = i, k)$$

The integrand in Eq. (7.70) can be resolved into partial fractions as

$$\frac{\left(\frac{\Gamma_{is}}{H_{ip}} + \bar{m}\omega^2 \Gamma_{ip} \right) \left(\frac{\Gamma_{ks}}{H_{kp}} + \bar{m}\omega^2 \Gamma_{kp} \right)}{\left(\frac{1}{H_s H_{ip}} - \bar{m}^2 \omega^4 \right) \left(\frac{1}{H_s H_{kp}} - \bar{m}^2 \omega^4 \right)} = \frac{a_0 j\omega^3 + a_1 \omega^2 + a_2 j\omega + a_3}{\frac{1}{H_s H_{ip}} - \bar{m}^2 \omega^4} + \frac{-b_0 j\omega^3 + b_1 \omega^2 - b_2 j\omega + b_3}{\frac{1}{H_s H_{kp}} - \bar{m}^2 \omega^4}$$

where the coefficients of the partial fractions, $a_0, \ldots, a_3; b_0, \ldots, b_3$, are obtained from the solution of the simultaneous equations

$$\underline{W} \cdot \underline{U} = \underline{P} \tag{7.71}$$

where matrix $\underline{W}$, and vectors $\underline{U}$ and $\underline{P}$ are defined as

$$\underline{W} = \begin{bmatrix} d_0 & 0 & 0 & 0 & -d'_0 & 0 & 0 & 0 \\ -d_1 & d_0 & 0 & 0 & -d'_1 & d'_0 & 0 & 0 \\ d_2 & d_1 & d_0 & 0 & -d'_2 & -d'_1 & -d'_0 & 0 \\ -d_3 & d_2 & -d_1 & d_0 & -d'_3 & d'_2 & -d'_1 & d'_0 \\ d_4 & d_3 & d_2 & d_1 & -d'_4 & -d'_3 & -d'_2 & -d'_1 \\ 0 & d_4 & -d_3 & d_2 & 0 & d'_4 & -d'_3 & d'_2 \\ 0 & 0 & d_4 & d_3 & 0 & 0 & -d'_4 & -d'_3 \\ 0 & 0 & 0 & d_4 & 0 & 0 & 0 & d'_4 \end{bmatrix}$$

$$\underline{U} = \{a_0,\ a_1,\ a_2,\ a_3,\ b_0,\ b_1,\ b_2,\ b_3\}^T$$

$$\underline{P} = \{P_0,\ P_1,\ P_2,\ P_3,\ P_4,\ P_5,\ P_6,\ P_7\}^T$$

$$P_0 = 0, \qquad P_4 = \Gamma_{is}\Gamma_{ks}(\Delta_{kp} - \Delta_{ip}) + \bar{m}(\Gamma_{is}\Gamma_{kp}\Delta_{ip} - \Gamma_{ks}\Gamma_{ip}\Delta_{kp})$$

$$P_1 = 0, \qquad P_5 = \bar{m}(\Gamma_{ip}\Gamma_{ks}\omega_{kp}^2 + \Gamma_{kp}\Gamma_{is}\omega_{ip}^2) + \Gamma_{is}\Gamma_{ks}(\Delta_{ip}\Delta_{kp} - \omega_{ip}^2 - \omega_{kp}^2)$$

$$P_2 = 0, \qquad P_6 = \Gamma_{is}\Gamma_{ks}(\Delta_{ip}\omega_{kp}^2 - \Delta_{kp}\omega_{ip}^2)$$

$$P_3 = (\bar{m}\Gamma_{ip} - \Gamma_{is})(\bar{m}\Gamma_{kp} - \Gamma_{ks}), \qquad P_7 = \Gamma_{is}\Gamma_{ks}\omega_{ip}^2\omega_{kp}^2$$

and

$$d_0 = 1 - \bar{m}^2$$

$$d_1 = \Delta_s + \Delta_{kp}$$

$$d_2 = -(\omega_s^2 + \omega_{kp}^2 + \Delta_s\Delta_{kp}) \tag{7.72}$$

$$d_3 = -(\Delta_{kp}\omega_s^2 + \Delta_s\omega_{kp}^2)$$

$$d_4 = \omega_s^2\omega_{kp}^2$$

d'_l ($l = 0, 1, 2, 3, 4$) $= d_l$ in Eq. (7.72) when Δ_{kp} and ω_{kp} are, respectively, replaced by Δ_{ip} and ω_{ip}.

Equation (7.70) then becomes

$$\langle \hat{q}_{is}\dot{q}_{ks} \rangle = S_f \int_{-\infty}^{\infty} \left(\frac{B'_0\omega^6 + B'_1\omega^4 + B'_2\omega^2 + B'_3}{|d'_0\omega^4 + d'_1 j\omega^3 + d'_2\omega^2 + d'_3 j\omega + d'_4|^2} \right.$$

$$\left. + \frac{B_0\omega^6 + B_1\omega^4 + B_2\omega^2 + B_3}{|d_0\omega^4 + d_1 j\omega^3 + d_2\omega^2 + d_3 j\omega + d_4|^2} \right) d\omega$$

which can be analytically evaluated as shown in Eq. (A.2). Here, the coefficients $B_0, \ldots, B_3$ and $B'_0, \ldots, B'_3$ can be calculated by

$$B_0 = -b_0 d_1 + b_1 d_0, \qquad B'_0 = -a_0 d'_1 + a_1 d'_0$$

$$B_1 = -b_0 d_3 + b_1 d_2 - b_2 d_1 + b_3 d_0, \qquad B'_1 = -a_0 d'_3 + a_1 d'_2 - a_2 d'_1 + a_3 d'_0$$

$$B_2 = b_1 d_4 - b_2 d_3 + b_3 d_2, \qquad B'_2 = a_1 d'_4 - a_2 d'_3 + a_3 d'_2$$

$$B_3 = b_3 d_4, \qquad B'_3 = a_3 d'_4$$

For calculation of the velocity covariance between mode i and mode k of the P-system, the procedure is exactly the same except that vector $\underline{P}$ should be re-arranged into

$$\underline{P}' = \{P'_0, P'_1, P'_2, P'_3, P'_4, P'_5, P'_6, P'_7\}^T$$

$$P'_l = P_{l+1}, \qquad P'_7 = 0 \qquad (l = 0, 1, 2, 3, 4, 5, 6)$$

The absolute acceleration for this simple case can be expressed as

$$\ddot{x}_{la} = -\Delta_s \dot{x}_l^{(d_i)} - \omega_s^2 x_l^{(d_i)} \qquad (l = 1, 2, \ldots, n_p)$$

and its mean-square value takes the form

$$\langle \ddot{x}_{la}^2 \rangle = \Delta_s^2 \langle (\dot{x}_l^{(d_i)})^2 \rangle + \omega_s^4 \langle (x_l^{(d_i)})^2 \rangle \tag{7.73}$$

7.7 Illustrative Examples and Analyses

In this section, three examples are presented to illustrate the interaction effects between different branches of the S-system, the effect of the number of degree-of-freedom of each branch on the dynamic responses of the S-system, the existence of optimum damping in the S-system to minimize its dynamic responses such as absolute acceleration. Frequency characteristics of the coupled P-S system are also studied and employed to indicate the possibility of uncoupled analysis.

7.7.1 Example 1: Interaction Effects Between Different Branches of S-System

A uniform two-story building supporting two oscillators as shown in Fig. 7-3(a) is designated as example structure 1. The mass (m_p) and stiffness (k_p) of the building (P-system) are assumed to be 175078.9 kg and 350236220.5 kN/m, respectively, and the damping matrix is considered to be proportional to the stiffness matrix in this example. The ratio between mass of one oscillator to floor mass (m_p) is kept at 0.1 while damping ratios of the oscillator and the first mode of the P-system are assigned to be 0.05. The natural frequencies of the P-system considering a lumped S-system mass can be found to be 26.356 rad/sec and 69.000 rad/sec, respectively. Three types of loads which include the load on the S-system (either one of oscillators), displacement input and acceleration input are sketched in Fig. 7-3(b). All the external excitations in the three types of loading schemes are assumed to be broad-band stochastic

processes with unit power spectral density. Mean-square values of relative displacements of the S-system with respect to the P-system and displacement of the P-system are tabulated in Tables 7-1 - 7-3 when the frequency of the oscillator (ω_s) takes values 1.0, 26.356, and 69.000 rad/sec. Except for the displacement input, x_{ip} (i=1,2) represents the relative displacement with respect to the base. It can be observed from Tables 7-1 - 7-3 that $\langle (x_{2s} - x_{2p})^2 \rangle$ and $\langle x_{2p}^2 \rangle$ under the action of load on the S_1-system are exactly the same as $\langle (x_{1s} - x_{1p})^2 \rangle$ and $\langle x_{1p}^2 \rangle$ under the action of load on the S_2-system which agrees with our intuition. $\langle (x_{1s} - x_{1p})^2 \rangle$ and $\langle (x_{2s} - x_{2p})^2 \rangle$ under the excitation of load either on the S_1- or on the S_2- system are almost of the same order for tuned cases as presented in Tables 7-2 and 7-3 whereas those are quite different for the detuned case as given in Table 7-1. In fact, S_1-system (or S_2-system) almost remains still when S_2-system (or S_1-system) is subjected to a broad-band random force. This is because the vibration-propagating medium (P-system) is not excited appreciably for the detuned case. When the displacement and acceleration input through the base are considered, the mean-square displacements of the S_1- and S_2- systems are of the same order for both tuned and detuned cases. Moreover, the mean-square displacement under the acceleration input generally decreases with the increase of frequency of the S-system due to direct loading on the S-system.

7.7.2 Example 2: Optimum Damping of S-System

A six-story building to which six oscillators are attached is presented in Fig. 7-4, which is designated as example structure 2 in this section. Each story has the same mass (m_p) of 1.0 kip.s^2/in ($\cong 1.8\times10^5$ kg) and interval stiffness (k_p) of 5000 kips/in ($\cong 9\times10^8$ N/m). The six identical oscillators are characterized by mass ratio (ρ) between mass of one oscillator and floor mass, frequency (ω_s) and damping ratio (ξ_s). The frequencies and mode vectors of the P-system alone are given in Table 7-4.

Frequency Characteristics and Non-Classical Damping Effects. Although frequency characteristics of the coupled P-S system are not required to calculate the dynamic response of the S-system as demonstrated in Section 7.6, they can help us better understand general dynamics of the complex P-S system considered here. The frequency characteristic equation can be easily

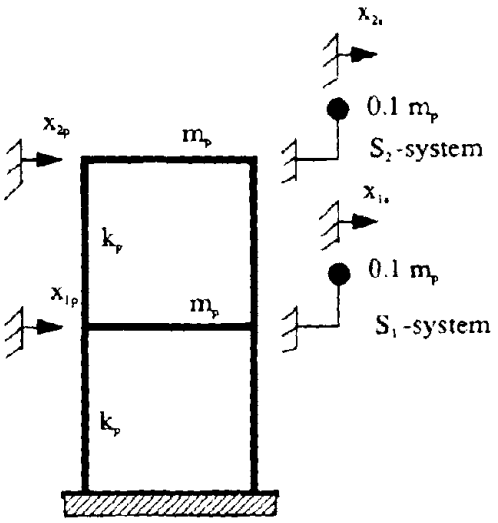

(a) P- and S-Systems

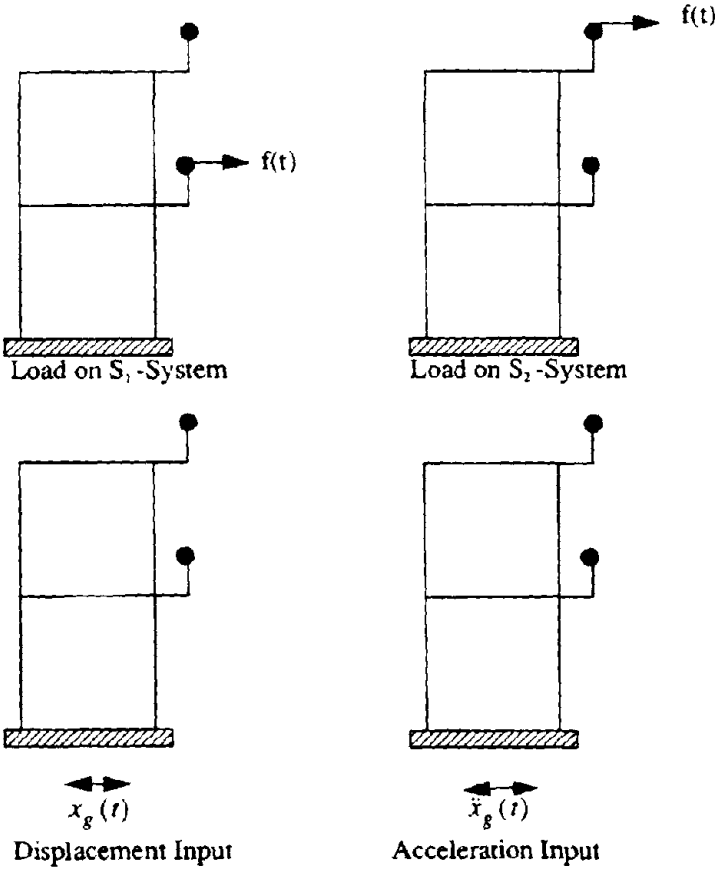

(b) Loading Schemes

Fig. 7-3 Structure Model of Example 1

TABLE 7-1: Mean-Square Displacements of Example 1 (ω_s=1.0 rad/sec)

	Load on S-system		Displacement input	Acceleration input
	S_1	S_2		
(1)	(2)	(3)	(4)	(5)
$<(x_{1s}-x_{1p})^2>$	1.0249×10^{-7}	1.2976×10^{-14}	4.0907×10^{-15}	31.4826
$<(x_{2s}-x_{2p})^2>$	1.2976×10^{-14}	1.0250×10^{-7}	9.6047×10^{-15}	31.5168
$<x^2_{1p}>$	2.5926×10^{-16}	2.5962×10^{-16}	4.1274×10^{-15}	7.4517×10^{-4}
$<x^2_{2p}>$	2.5962×10^{-16}	1.0377×10^{-15}	9.3266×10^{-15}	1.9356×10^{-3}

TABLE 7-2: Mean-Square Displacements of Example 1 (ω_s=ω_{1p}=26.356 rad/sec)

	Load on S-system		displacement input	Acceleration input
	S_1	S_2		
(1)	(2)	(3)	(4)	(5)
$<(x_{1s}-x_{1p})^2>$	3.8950×10^{-12}	1.0519×10^{-12}	1.9477×10^{-14}	5.5031×10^{-3}
$<(x_{2s}-x_{2p})^2>$	1.0519×10^{-12}	2.8807×10^{-12}	4.5654×10^{-14}	1.2632×10^{-2}
$<x^2_{1p}>$	2.647×10^{-14}	4.9689×10^{-14}	2.5474×10^{-15}	5.3935×10^{-4}
$<x^2_{2p}>$	4.9689×10^{-14}	1.3495×10^{-13}	5.1691×10^{-15}	1.3833×10^{-3}

TABLE 7-3: Mean-Square Displacements of Example 1 (ω_s=ω_{2p}=69.000 rad/sec)

	Load on S-system		Displacement input	Acceleration input
	S_1	S_2		
(1)	(2)	(3)	(4)	(5)
$<(x_{1s}-x_{1p})^2>$	1.3820×10^{-13}	3.0746×10^{-14}	3.9941×10^{-15}	4.8726×10^{-5}
$<(x_{2s}-x_{2p})^2>$	3.0746×10^{-14}	1.8053×10^{-13}	1.6360×10^{-15}	7.6269×10^{-5}
$<x^2_{1p}>$	8.7479×10^{-15}	1.3906×10^{-14}	3.9696×10^{-15}	9.0959×10^{-4}
$<x^2_{2p}>$	1.3906×10^{-14}	3.4303×10^{-14}	9.0857×10^{-15}	2.3645×10^{-3}

formulated from Eqs. (7.65) and (7.66) with the absence of damping and external force terms, i.e.,

$$\begin{bmatrix} \omega_{kp}^2 - \Omega^2 & -\bar{m}\Omega^2 \\ -\bar{m}\Omega^2 & \omega_s^2 - \Omega^2 \end{bmatrix} \begin{Bmatrix} \varphi_{kp} \\ \varphi_{ks} \end{Bmatrix} = \begin{Bmatrix} 0 \\ 0 \end{Bmatrix} \tag{7.74}$$

which gives the following natural frequencies and mode vectors:

$$\frac{\Omega_{1,2}^2}{\omega_{kp}^2} = \frac{1}{2(1-\bar{m}^2)} \left[\frac{\omega_s^2}{\omega_{kp}^2} + 1 \mp \sqrt{\left(\frac{\omega_s^2}{\omega_{kp}^2} + 1 \right)^2 - 4(1-\bar{m}^2) \frac{\omega_s^2}{\omega_{kp}^2}} \right] \tag{7.75}$$

$$\begin{Bmatrix} \varphi_{ks} \\ \varphi_{kp} \end{Bmatrix}_i = \begin{Bmatrix} 1 - \dfrac{\Omega_i^2}{\omega_{kp}^2} \\ \bar{m} - \dfrac{\Omega_i^2}{\omega_{kp}^2} \end{Bmatrix}^T \begin{Bmatrix} 1 \\ 0 \end{Bmatrix} \qquad (i = 1, 2) \tag{7.76}$$

The non-classical damping effect between the P- and the S- system under consideration can be described by an indicator defined as

$$c_{12} = \frac{\begin{Bmatrix} \varphi_{ks} \\ \varphi_{kp} \end{Bmatrix}_1^T \begin{bmatrix} \Delta_s & 0 \\ 0 & \Delta_{kp} \end{bmatrix} \begin{Bmatrix} \varphi_{ks} \\ \varphi_{kp} \end{Bmatrix}_2}{\sqrt{\left(\begin{Bmatrix} \varphi_{ks} \\ \varphi_{kp} \end{Bmatrix}_1^T \begin{bmatrix} \Delta_s & 0 \\ 0 & \Delta_{kp} \end{bmatrix} \begin{Bmatrix} \varphi_{ks} \\ \varphi_{kp} \end{Bmatrix}_1 \right) \left(\begin{Bmatrix} \varphi_{ks} \\ \varphi_{kp} \end{Bmatrix}_2^T \begin{bmatrix} \Delta_s & 0 \\ 0 & \Delta_{kp} \end{bmatrix} \begin{Bmatrix} \varphi_{ks} \\ \varphi_{kp} \end{Bmatrix}_2 \right)}} \tag{7.77}$$

which can serve as a generalization of indicators defined in [34,89]. This definition can be easily applied to measure the damping coupling strength between any two modes of a complex system. Moreover, the indicator is represented by a dimensionless number ranging from zero to one which may provide a natural scale to compare the degree of non-classical damping effect on the dynamic response of a complex system.

The frequency ratios calculated from Eq. (7.75) and non-classical damping indicator from Eq.(7.77) are presented in Figs. 7-5 and 7-6. It can be observed that frequencies (Ω) of the combined P-S system gradually deviate from their individual frequencies (ω_s and ω_{kp}) as mass

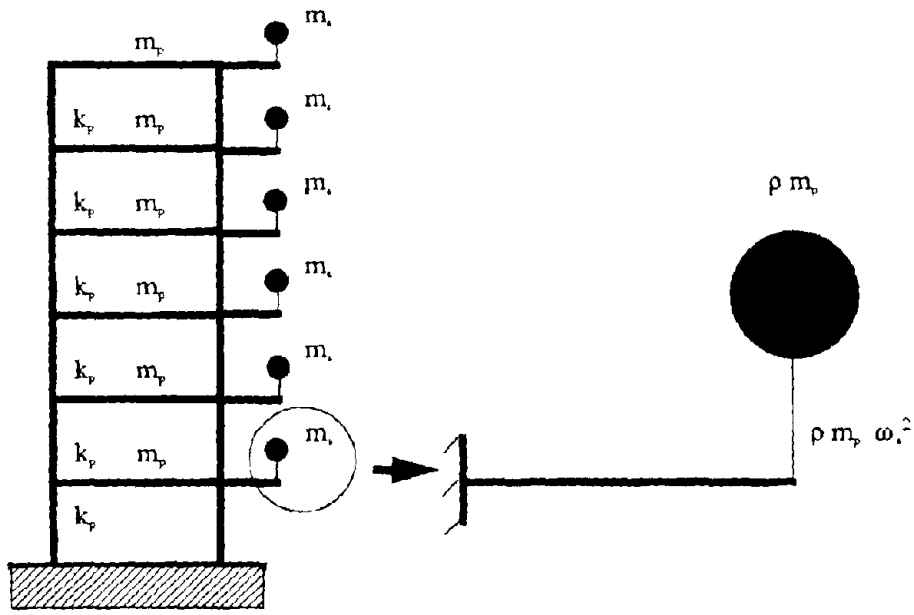

k_p = 5000 kips/in

m_p = 1.0 kips.sec^2/in

Fig. 7-4 Structure Model of Example 2

TABLE 7-4: Natural Frequencies and Mode Vectors of P-System

		1st mode	2nd mode	3rd mode	4th mode	5th mode	6th mode
(1)		(2)	(3)	(4)	(5)	(6)	(7)
frequency		17.046	50.140	80.362	105.872	125.224	137.350
vectors	1st floor	0.1327	+0.3678	-0.5187	+0.5507	-0.4565	+0.2578
	2nd floor	0.2578	+0.5507	-0.3678	-0.1327	+0.5187	-0.4565
	3rd floor	0.3678	+0.4565	+0.2578	-0.5187	-0.1327	+0.5507
	4th floor	0.4565	+0.1327	+0.5507	+0.2578	-0.3678	-0.5187
	5th floor	0.5187	-0.2578	+0.1327	+0.4565	+0.5507	+0.3678
	6th floor	0.5507	-0.5187	-0.4565	-0.3678	-0.2578	-0.1327

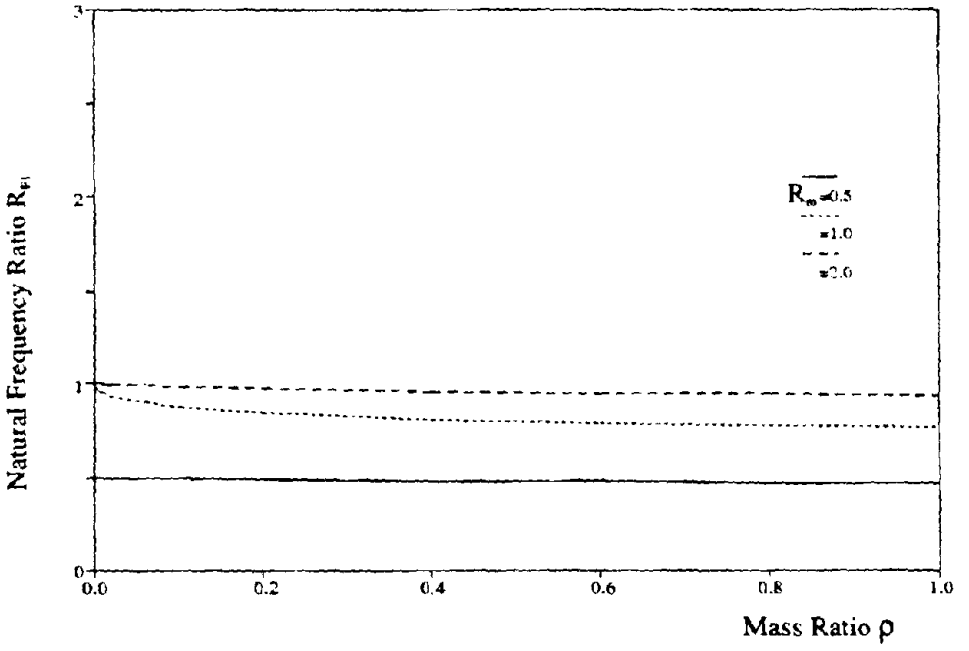

(a)

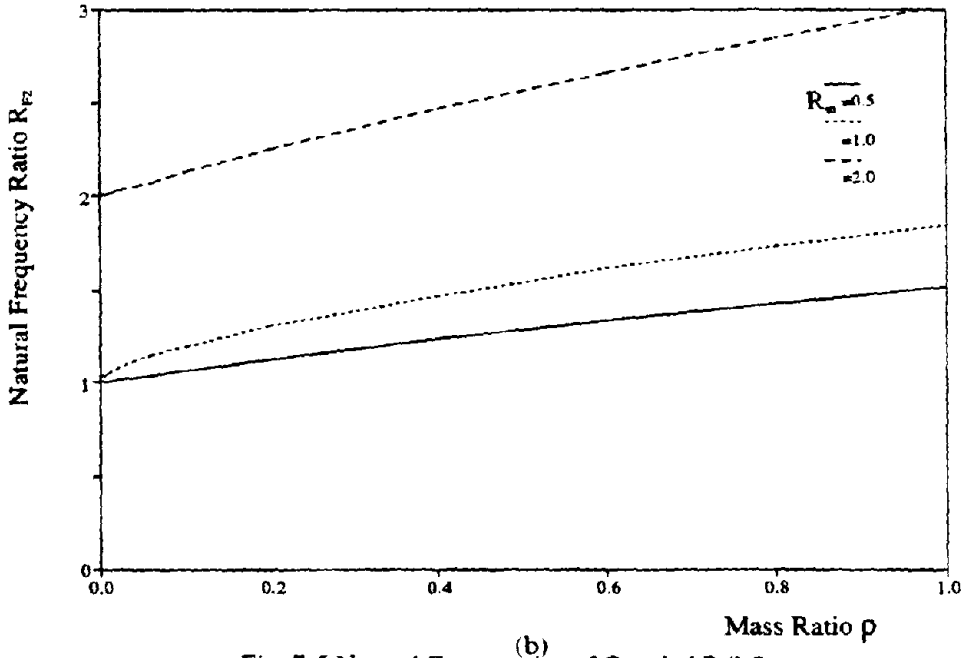

(b)

Fig. 7-5 Natural Frequencies of Coupled P-S System

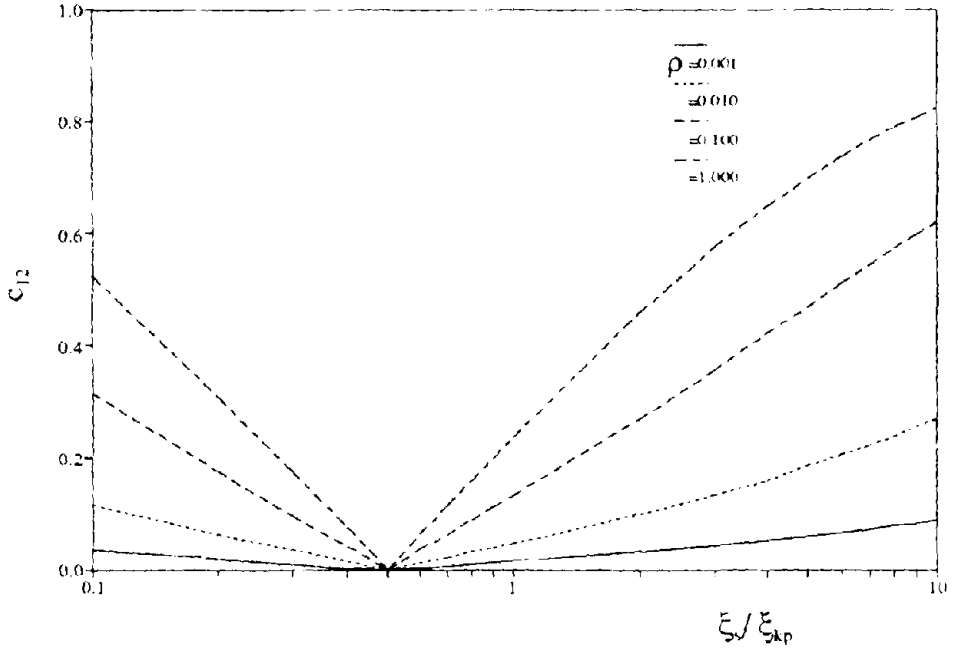

(a) $\omega_s / \omega_{kp} = 0.5$

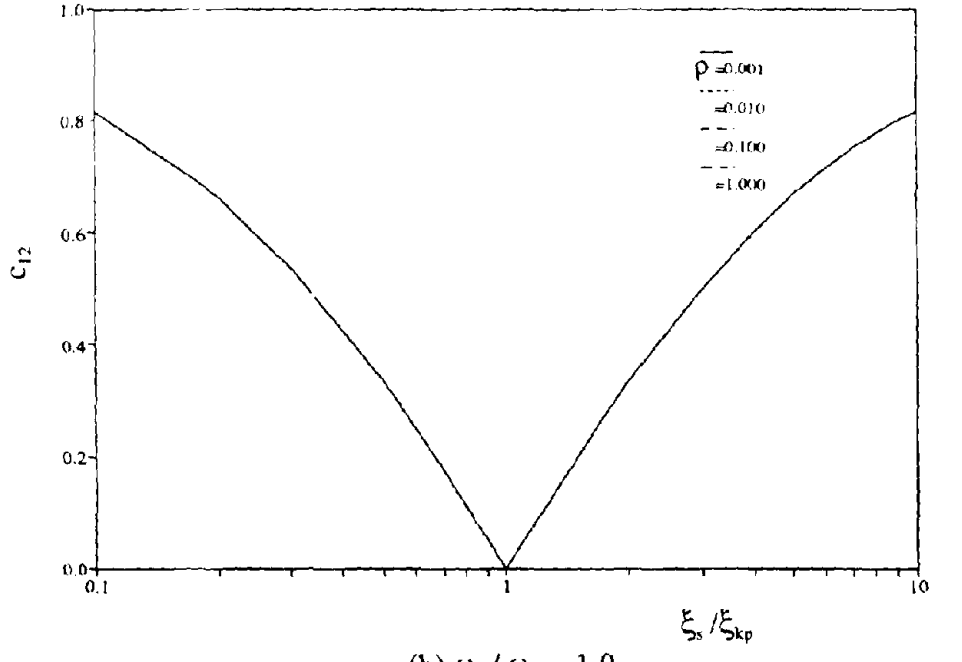

(b) $\omega_s / \omega_{kp} = 1.0$

Fig. 7-6 Non-Classical Damping Effect of P-S System

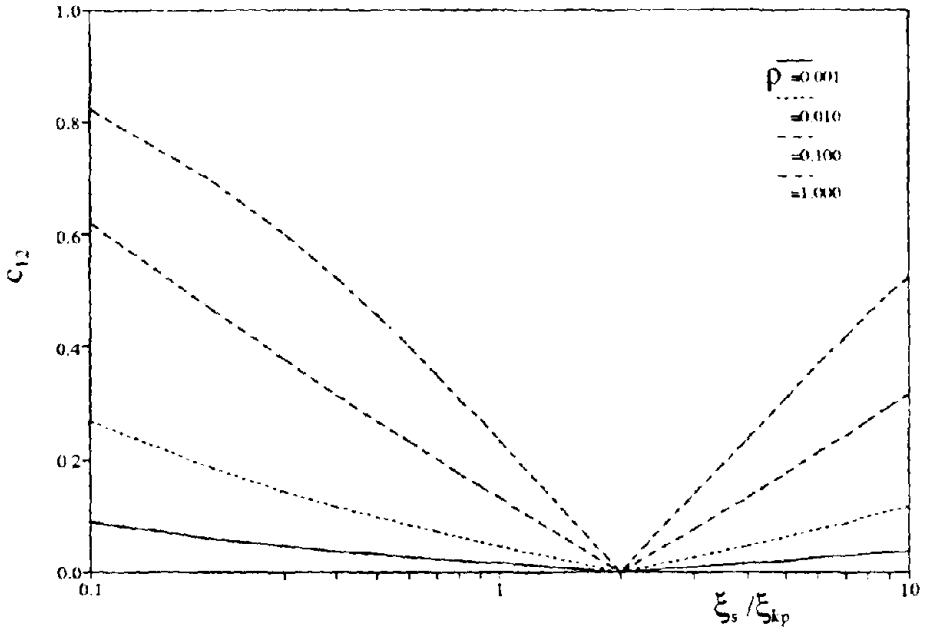

(c) ω_s / ω_{kp} =2.0

Fig. 7-6 Non-Classical Damping Effect of P-S System

ratio (ρ) increases, indicating increased interaction between two systems. This is especially evident in the tuned case. In addition, careful examination will show that frequency variation of the P-system (S-system) is more obvious than that of the relatively flexible S-system (P-system), a result which coincides with the decoupling criterion based on frequency change as shown in Fig. 4-5. This implies applicability of the decoupling criterion developed in Section 4 to a complex system.

It can be observed from Figs. 7-6(a-c) that the 2-DOF system under investigation is classically damped when frequency ratio (ω_s/ω_{sp}) is equal to the ratio of damping ratios (ξ_s/ξ_{sp}) which has been indicated in [34]. Furthermore, the non-classical damping indicator c_{12} defined in Eq.(7.77) increases with the parameter δ defined in Eq.(2.6). Unlike parameter δ, the indicator c_{12} is independent of mass ratio (ρ) only in the tuned case. The inclusion of mass ratio in the expression of c_{12} can make the indicator itself become a good criterion for evaluating non-classical damping effect. For a constant c_{12}, the smaller the mass ratio, the larger the parameter δ and therefore the error involved in the calculation of dynamic response without taking into account the non-classical damping effect. This result can be inferred from [34]. A comparison between Fig. 7-6(a) and Fig. 7-6(c) demonstrates the reversibility of indicator c_{12} about frequency ratio (ω_s/ω_{sp}) and ratio of damping ratios (ξ_s/ξ_{sp}). This can easily be explained by recalling the physical system that Eqs. (7.65) and (7.66) describe, i.e., for a constant $\overline{m}$, substitutions of ω_{sp}/ω_s and ξ_{sp}/ξ_s for ω_s/ω_{sp} and ξ_s/ξ_{sp} only exchange the structural parameters between these oscillators.

Mean-Square Response of S-System. When the example structure is subjected to an acceleration input, mean-square displacements of all branches of the S-system are shown in Figs. 7-7 and 7-8 for various frequencies (ω_s) and for various mass ratios (ρ), respectively. While the mean-square displacements generally decrease with the increase of ω_s, tuning effect around natural frequencies of the P-system alone can be clearly seen. Figure 7-8 shows that mean-square displacements of the S-system with a fixed frequency are rapidly reduced as mass ratio (ρ) increases.

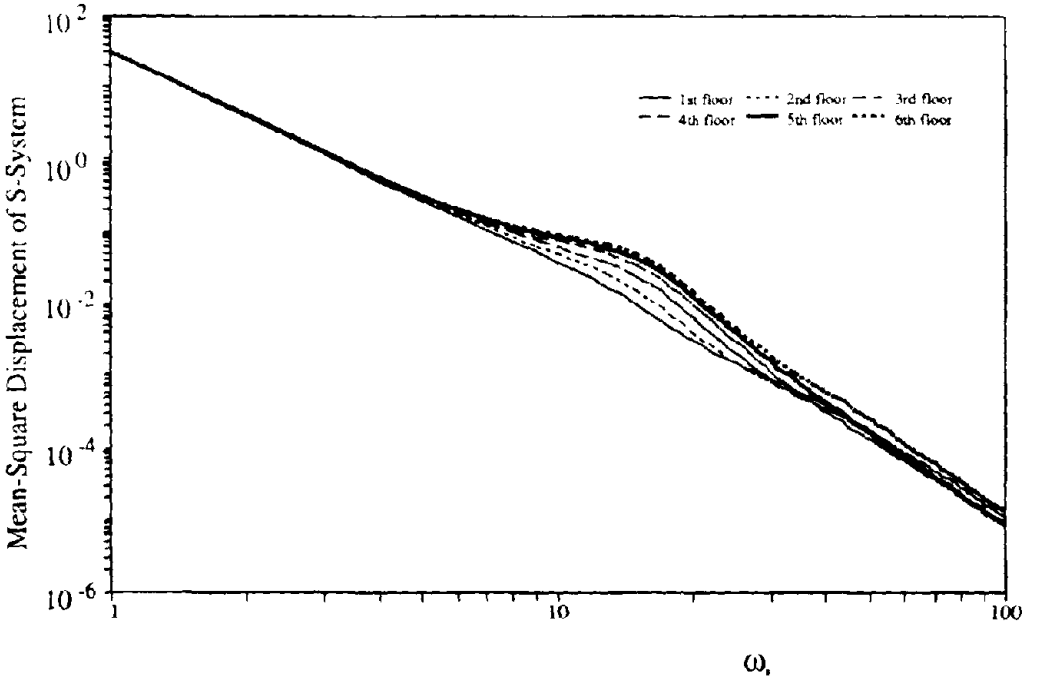

Fig. 7-7 Mean-Square Displacement vs. Frequency of S-System(ω_s) :

$\xi_p = \xi_s = 0.05, \rho = 0.2$

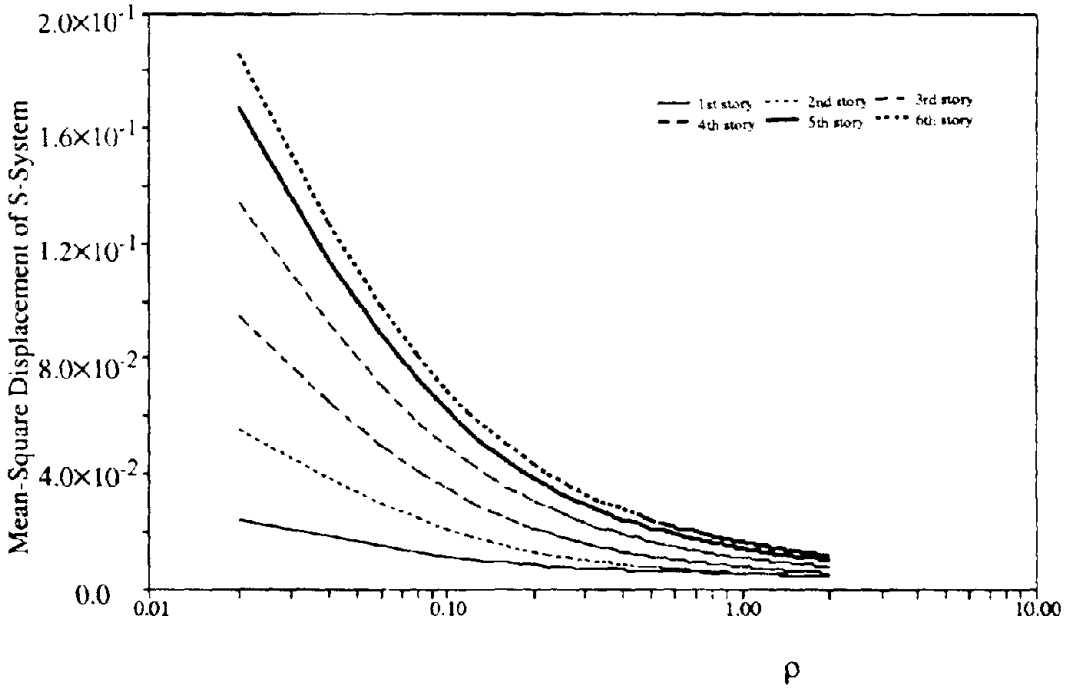

Fig. 7-8 Mean-Square Displacement vs. Mass Ratio (ρ) :

$\xi_p = \xi_s = 0.05, \omega_s = 15.561$ rad/sec

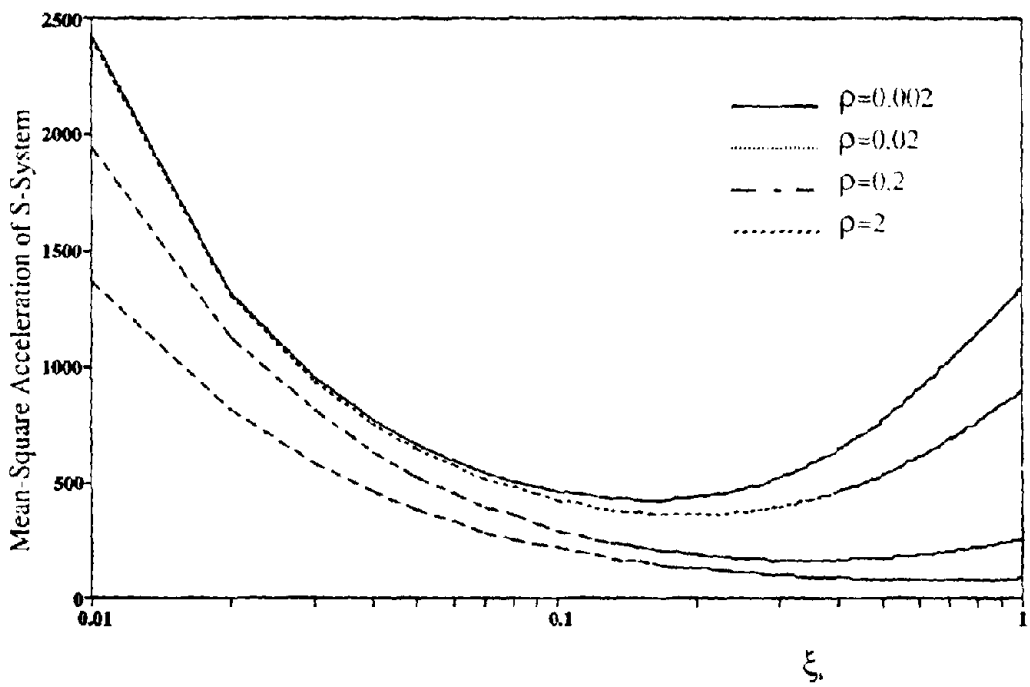

Fig. 7-9(a) Mean-Square Acceleration of S-System at Third Floor vs. ξ_s:

$$\xi_p = 0.01,\ \omega_s/\omega_p = 0.5$$

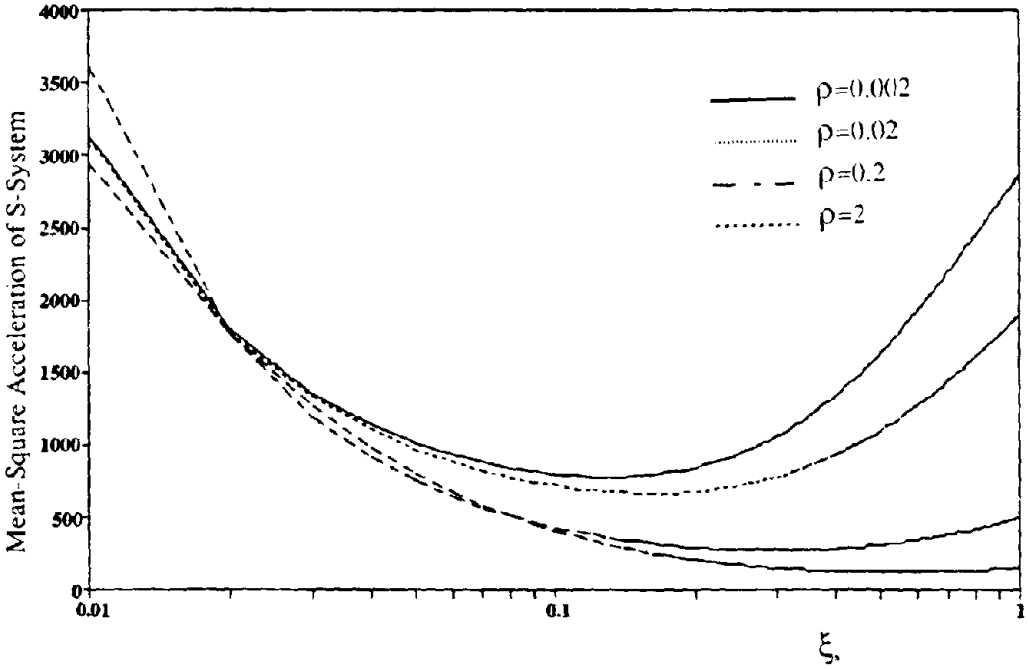

Fig. 7-9(b) Mean-Square Acceleration of S-System at Sixth Floor vs. ξ_s:

$\xi_p = 0.01$, $\omega_s/\omega_{1p} = 0.5$

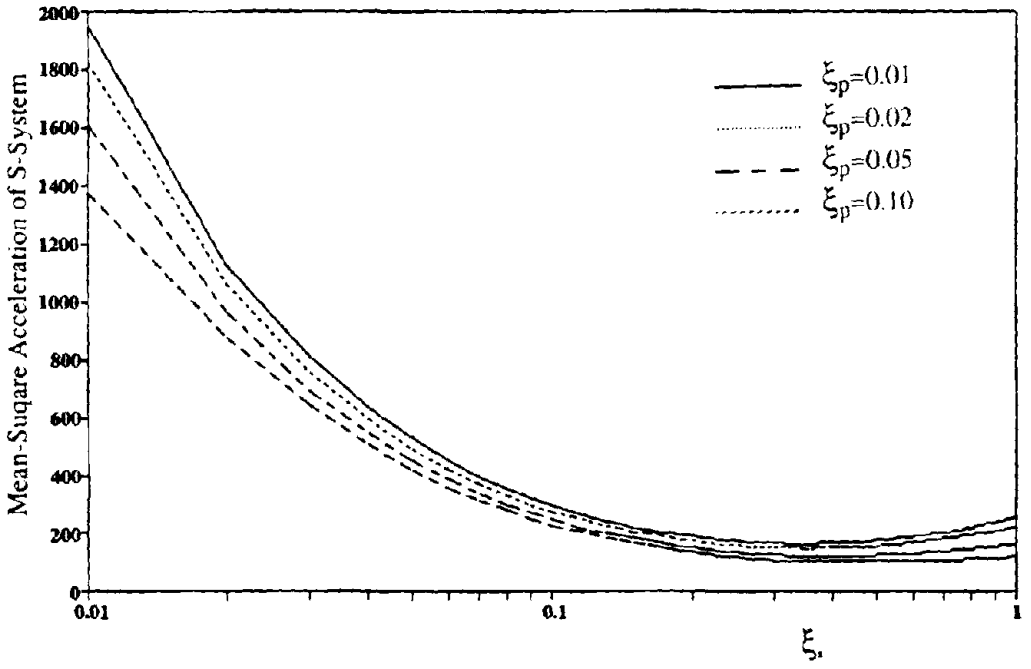

Fig. 7-10(a) Mean-Square Acceleration of S-System at Third Floor vs. ξ_s:

$$\rho = 0.2, \omega_s / \omega_{1p} = 0.5$$

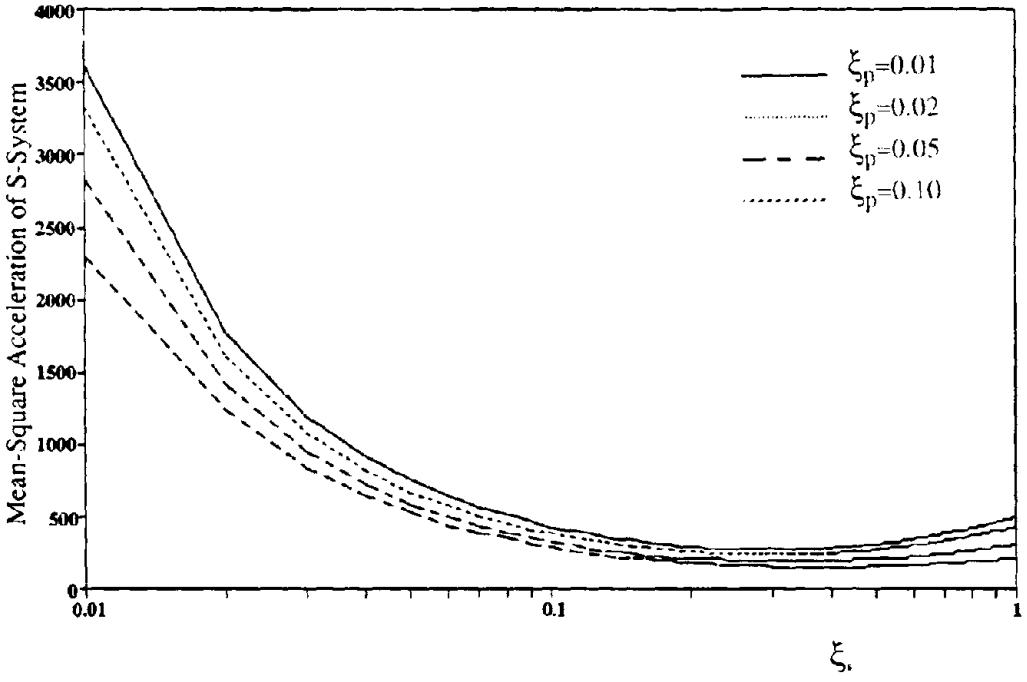

Fig. 7-10(b) Mean-Square Acceleration of S-System at Sixth Floor vs. ξ_s:

$$\rho = 0.2, \omega_s / \omega_{1p} = 0.5$$

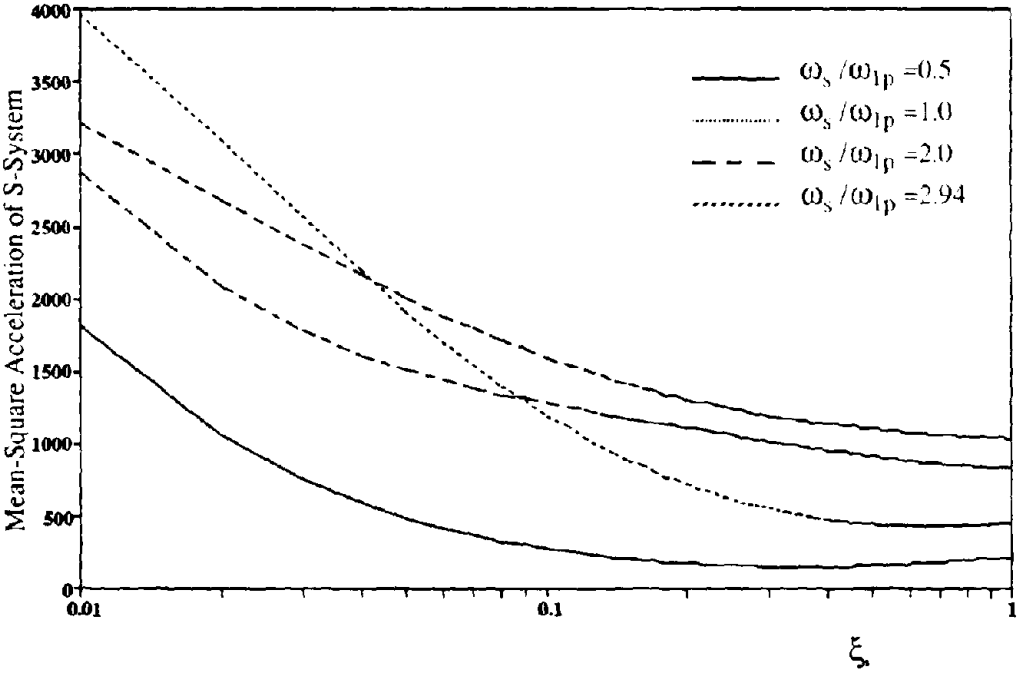

Fig. 7-11(a) Mean-Square Acceleration of S-System at Third Floor vs. ξ_s:

$\rho = 0.2, \xi_p = 0.02$

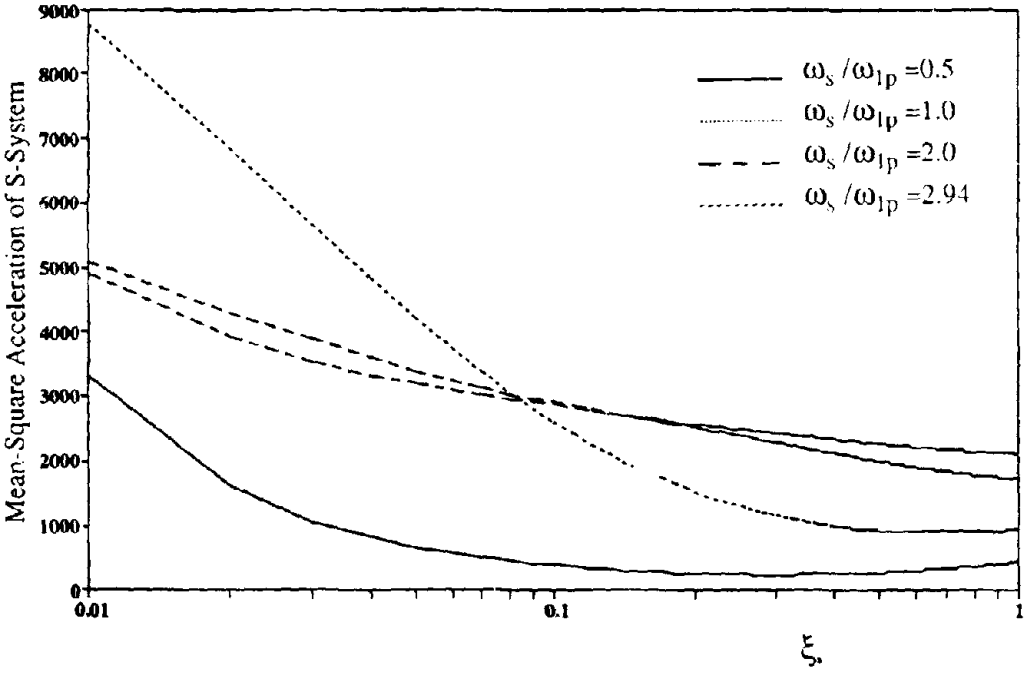

Fig. 7-11(b) Mean-Square Acceleration of S-System at Sixth Floor vs. ξ_s:

$\rho = 0.2, \xi_p = 0.02$

A series of parametric studies on the effect of damping, mass ratio, and frequency ratio on the absolute acceleration response have been accomplished and the results for oscillators attached to the third and sixth floors are presented in Figs. 7-9 - 7-11. All the figures demonstrate that variations of mean-square accelerations of the S-system at two floors with damping of the S-system are generally the same, indicating that contribution from one mode (in the P-system) tuned or nearly tuned with ω_s is significant. In other words, energy is mainly concentrated in one mode of the P-system due to the distribution of oscillators at all building floors. From Figs. 7-9(a, b), one can further observe that, with certain damping (ξ_s), the mean-square acceleration can be minimized as in the case of the simple P-S system discussed in Section 6. A small damping increment of the S-system has more significant influences on the mean-square response than the corresponding damping change in the P-system as demonstrated in Figs. 7-10(a, b). As one can expect, damping in the S-system significantly reduces the acceleration response in the tuned case while the reduction in detuned cases is relatively small as shown in Figs. 7-11(a, b).

7.7.3 Example 3: Effects of Number of DOF and Mass Distribution in a Branch of S-System on Response

The same six-story building in example 2 is employed here. The six oscillators attached to the building, however, are substituted by six 2-DOF branches as shown in Fig. 7-12. When the fundamental frequency designated in the figure varies, the mean-square displacements of the first and top masses of all branches of the S-system are shown in Figs. 7-3(a, b) with mass ratio (ρ) of 0.1 and damping ratios of 0.05 for both the P- and the S- system. It can be seen that response variations of the first and top masses of different branches are consistent. This confirms the results observed in example 2 that energy in the P-system is basically stored in one predominant mode. By comparing Fig. 7-13(b) with Fig. 7-7, one can further see that relative variations of the mean-square displacement with frequency (ω_{1s}) for single- and two- DOF subsystems of each branch are consistent but the magnitudes of the response in Fig. 7-7 are generally less than those in Fig. 7-13(b) due to the distributed mass effect. The distribution of mass tends to reduce the effective modal mass, which in turn increases response of the S-system as demonstrated in Fig. 7-8. A

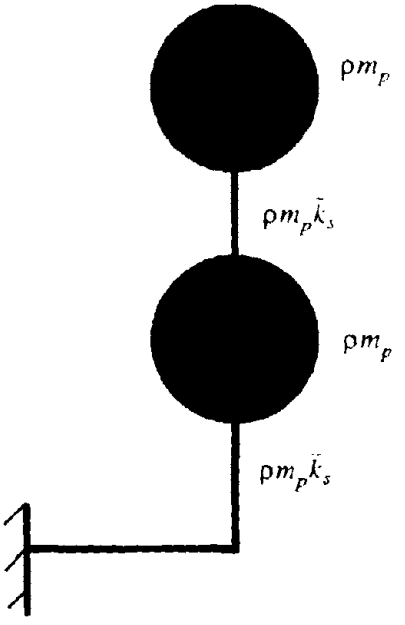

$\bar{k}_s = \frac{2}{3-\sqrt{5}}\omega^2_{1s}$, ω_{1s} is the fundamental frequency of one branch

Fig. 7-12 One Branch of S-System in Example 3

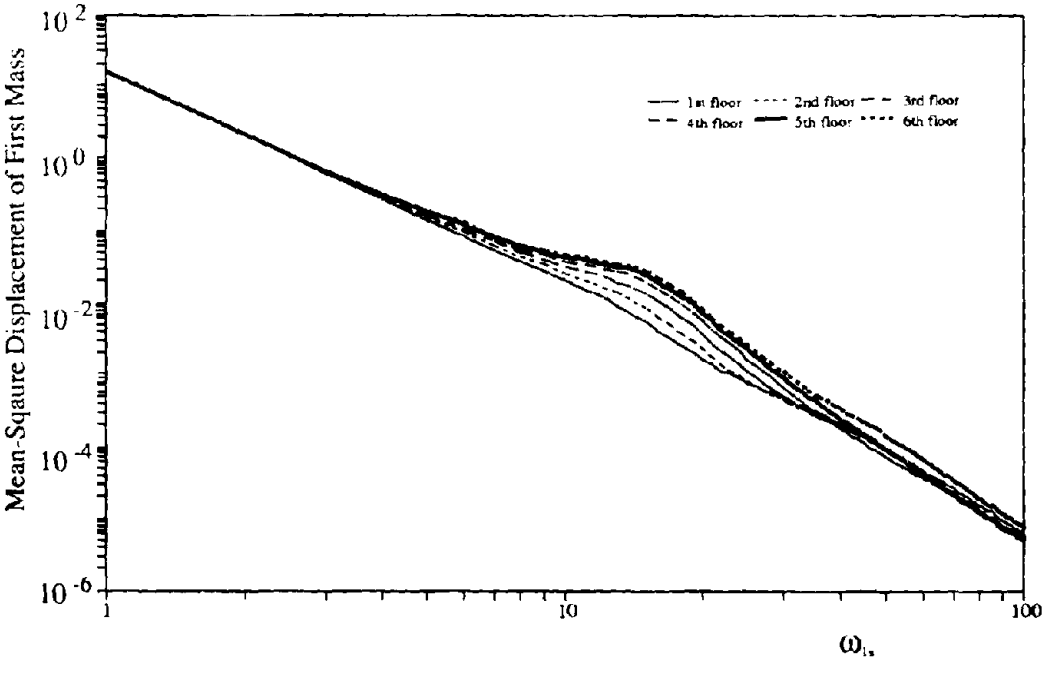

Fig. 7-13(a) Mean-Square Displacement of First Mass vs. ω_{1s}:
$\rho = 0.1, \xi_p = \xi_s = 0.05$

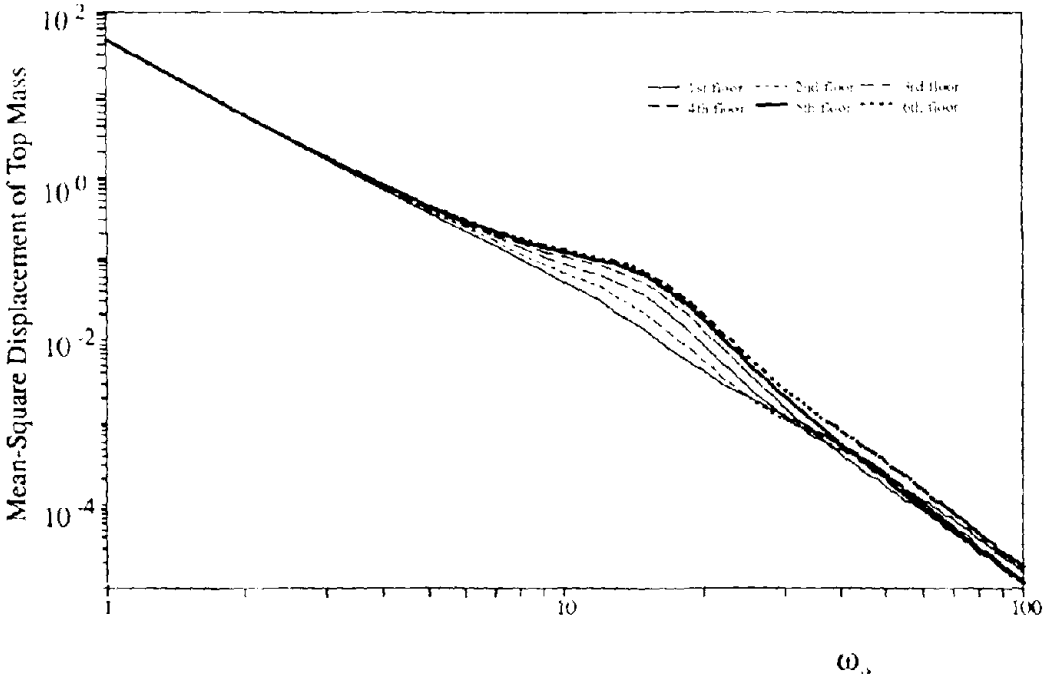

Fig. 7-13(b) Mean-Square Displacement of Top Mass vs. ω_s:

$\rho = 0.1, \xi_p = \xi_s = 0.05$

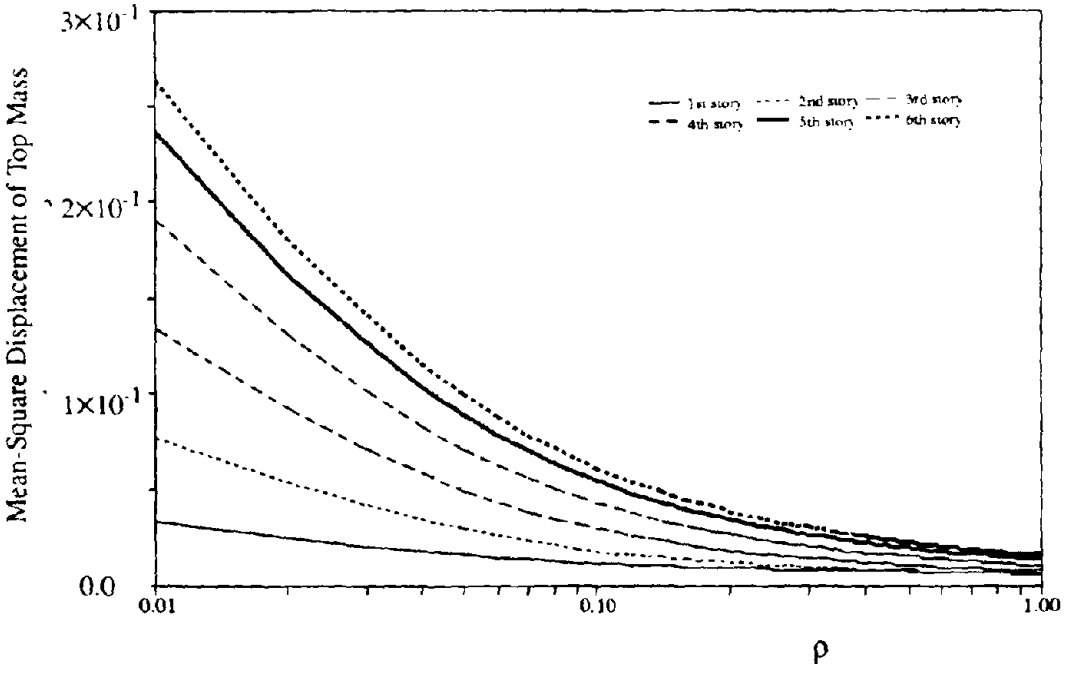

Fig. 7-14 Mean-Square Displacement of Top Mass vs. ρ:

$\xi_p = \xi_s = 0.05, \omega_{1s} = 15.561$ rad/sec

comparison between Fig. 7-14 and Fig. 7-8 further confirms the above analyses. All these results clearly support the statement that a SDOF representation of one uniform branch of the S-system is a good approximation in the complex system under investigation. Based on this observation, the analytical model considered in this section can be reasonably extended to cases with different number of DOF but same fundamental frequency characteristics in each branch of the S-system.

Mean-square displacements of the top mass in each branch of the S-system shown in Fig. 7-1(b) are plotted in Figs. 7-15 and 7-16(a,b) as a function of mass ratio ($\lambda = \overline{m}_{2s}/\overline{m}_{1s}$) between the top and the first masses of the S-system. In the first figure, frequencies of the S-system (ω_{1s} and ω_{2s}) are tuned to the fundamental and second mode frequencies of the P-system alone while, in the remaining figures, they are equal to the first two frequencies of the P-system with the lumped S-system mass, respectively, as given in Table 7-5. The latter case is referred to as nearly tuned case here. For the same mass ratio (λ), there exist two sets of stiffness distributions that generate two identical frequencies of the S-system but different mode vectors. Stiffness constants ($\overline{k}_{1s}$ and $\overline{k}_{2s}$) for these two sets of distribution are also presented in Table 7-5. Figures 7-15 and 7-16(a) show the results for the first set of stiffness distribution and Fig. 7-16(b) for the second set of stiffness distribution. Comparison between Figs. 7-15 and 7-16(a) demonstrates quite different characteristics for the tuned and nearly-tuned cases in the sense that there exists an optimum value of λ which minimizes the mean-square displacements of the S-system in nearly-tuned case. However, for the second set of stiffness distribution, mean-square displacements of the S-system are monotonically decreasing as shown in Fig. 7-16(b). The above analyses indicate that a preliminary design with mass ratio (λ) around 0.7 will generate the minimum response in the S-system corresponding to the first set of stiffness distribution.

7.8 Conclusions

The dynamic response calculation of a class of complex P-S systems defined in this section has been grouped into many subsystems with a small number of DOF so that the closed-form solution of power flow and energy quantities can be obtained under the action of broad-band stochastic

TABLE 7-5: Frequencies of S-System Under Different Mass Distribution

λ	0.1	0.5	0.7	1.0	1.3	1.5	1.6
(1)	(2)	(3)	(4)	(5)	(6)	(7)	(8)
ω_{1s}	16.179	15.895	15.759	15.561	15.370	15.246	15.186
ω_{2s}	47.591	46.756	46.354	45.771	45.210	44.847	44.668
$\bar{k}_{1s}^{(1)}$	291.834	407.959	470.998	576.085	704.985	822.089	906.871
$\bar{k}_{2s}^{(1)}$	203.238	676.939	793.406	880.888	890.719	853.374	812.120
$\bar{k}_{1s}^{(2)}$	2235.62	2030.82	1926.84	1761.78	1575.89	1422.29	1319.70
$\bar{k}_{2s}^{(2)}$	26.5304	135.986	193.940	288.043	398.470	493.253	558.070

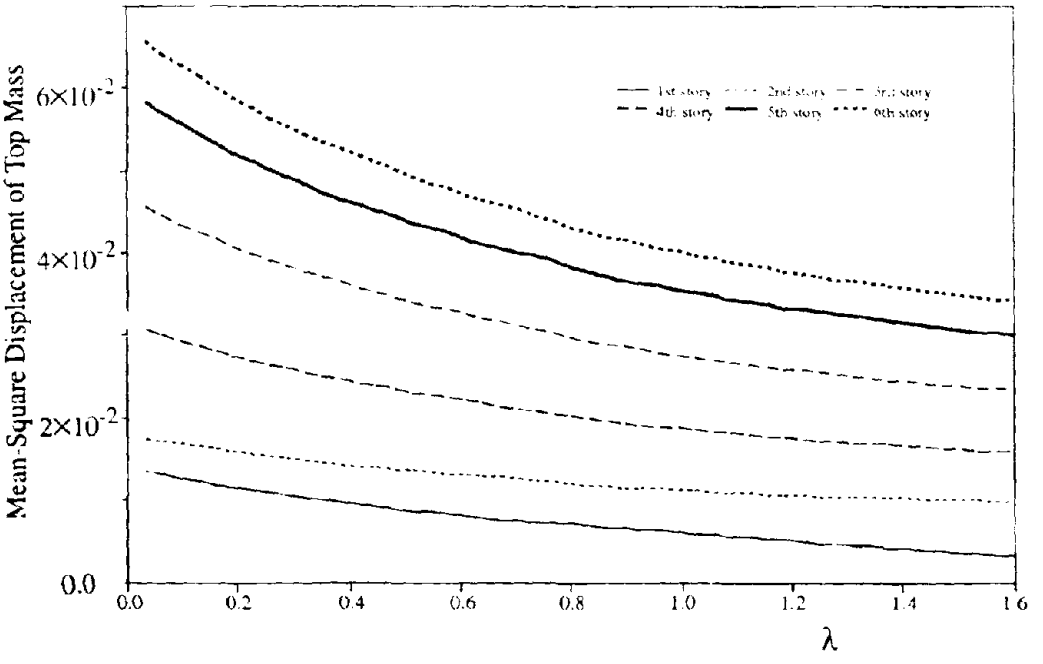

Fig. 7-15 Mean-Square Displacement of Top Mass (Tuned Case) vs. λ:

$\rho = 0.1, \xi_p = \xi_s = 0.05$

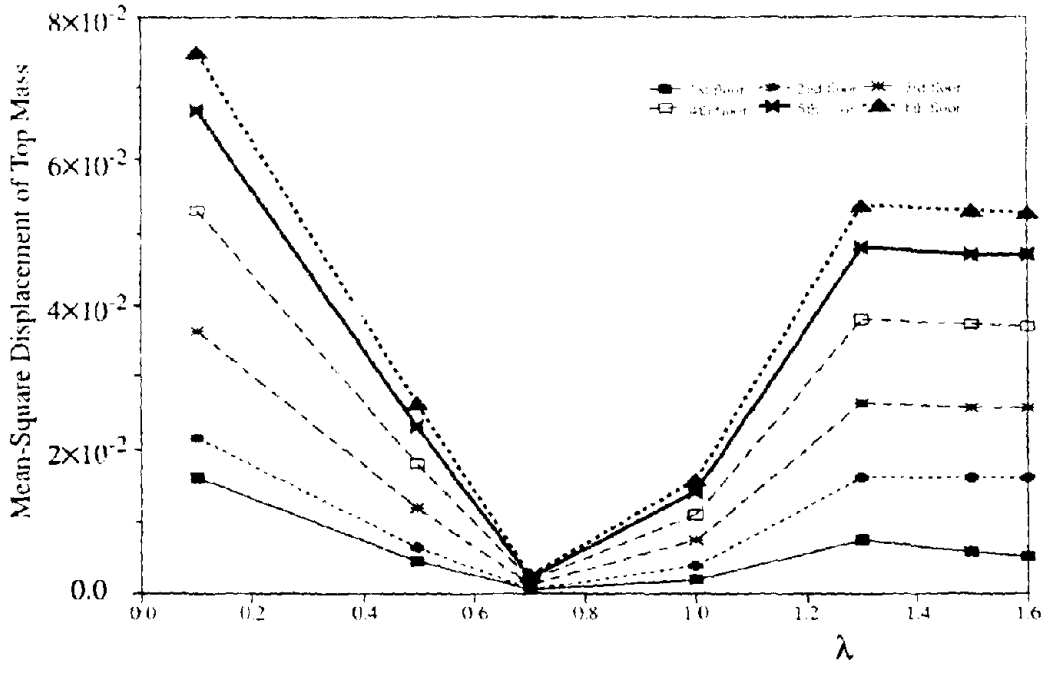

Fig. 7-16(a) Mean-Square Displacement of Top Mass (Nearly Tuned Case) vs.λ:

Stiffness Distribution 1, $\rho = 0.1, \xi_p = \xi_s = 0.05$

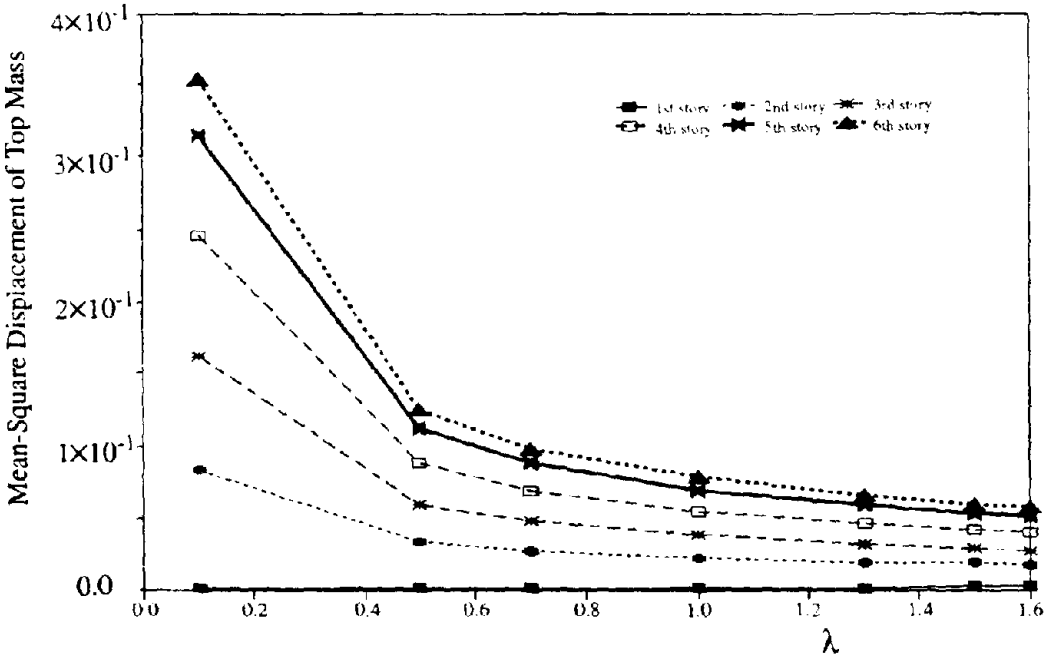

Fig. 7-16(b) Mean-Square Displacement of Top Mass (Nearly Tuned Case) vs. λ:

Stiffness Distribution 2, $\rho = 0.1, \xi_p = \xi_s = 0.05$

forces. Based on the comprehensive studies on the complex system, the following conclusions can be drawn:

(1) Interaction effect between different branches of an S-system is not significant unless they are tuned to the frequencies of the P-system supporting the S-system.

(2) An S system consisting of many uniform MDOF branches can be approximately represented by an S-system consisting of many SDOF branches. The introduction of nonuniform distribution of structural parameters (mass and stiffness) into the S-system can minimize mean-square displacement of the S-system which is nearly tuned to the P-system.

(3) Dynamic response of an S-system such as mean-square acceleration can be minimized by an appropriate selection of its damping characteristics, which has been found in a simple system discussed in Section 6.

(4) Mean-square displacement generally decreases with an increase of frequency of the S-system and mass ratio between S- and P-systems (for constant frequency).

(5) Energy in the S-system is mostly generated by one mode of the P-system whose frequency is close to that of the S-system. For this reason, the energy distribution along different branches basically follows that particular mode shape of the P-system.

SECTION 8

MEAN-SQUARE CONDENSATION METHOD FOR THE DYNAMIC ANALYSIS OF S-SYSTEMS

8.1 Introduction

As surveyed in Section 2, perturbation techniques have been extensively employed to develop modal properties of coupled P-S systems based on their uncoupled properties. It is thus an improvement over traditional uncoupled analyses by taking into account the dynamic interaction effect on the modal properties and dynamic response of the S-system. However, the appropriate application of perturbation theory is based on a good understanding of the relative orders of all the small quantities involved in the P-S system such as mass ratio, tuning parameter, damping ratio, etc., which usually requires expertise evaluations. Any improper identification of these quantities will result in an erroneous conclusion or lead to unstable schemes. For instance, the perturbation scheme may be unstable when the structural damping ratio is of the same order of or less than that of the connection between the P- and S- system but has not been recognized as a small parameter.

A simpler procedure which captures the coupling effect was discussed in [45] based on the statistical energy analysis. This procedure was used in a coupled analysis of simple P-S systems such as one with a SDOF P- and a SDOF S-system with conservative connection. For the general case of non-conservatively coupled systems, a consistent formulation of power flow between these systems as well as energies stored in individual systems has been developed in Section 5. This formulation shows the equivalence of power flow transmitted from a P- to an S-system and energy of the S-system on the one hand, and absolute acceleration of the S-system and relative displacement of the S-system with respect to the P-system on the other. This procedure leads to the exact dynamic response of simple P-S systems as discussed in Section 6 and some special types of complex systems as presented in Section 7. In practice, however, general MDOF models are often necessary which points to the need for extending the basic formula developed for a simple case to more general situations.

In this section, a practical coupled analysis in the modal space is presented for general MDOF P-S systems in which the modal properties of individual P- and S-systems are involved and the MDOF P-system (more than 3-DOF) is substituted by a 3-DOF system, which is then condensed into a 1S-2P model based on energy equivalence of the S-system.

8.2 Basic Formulation

The equations of motion of an arbitrarily combined P-S system as shown in Fig. 8-1(a) can be written as

$$\underline{M}\ddot{\underline{X}}(t) + \underline{C}\dot{\underline{X}}(t) + \underline{K}\underline{X}(t) = \underline{F}(t) \tag{8.1}$$

where

$$\underline{M} = \begin{bmatrix} \underline{M}_p & 0 \\ 0 & \underline{M}_s \end{bmatrix} \tag{8.2}$$

$$\underline{K} = \begin{bmatrix} \underline{K}_{pp} & \underline{K}_{ps} \\ \underline{K}_{sp} & \underline{K}_{ss} \end{bmatrix} \tag{8.3}$$

$$\underline{C} = \begin{bmatrix} \underline{C}_{pp} & \underline{C}_{ps} \\ \underline{C}_{sp} & \underline{C}_{ss} \end{bmatrix} \tag{8.4}$$

In the above, subscripts p and s represent the P- and S-system, respectively; $\underline{M}_p$ and $\underline{M}_s$ are mass matrices of these systems; matrices $\underline{K}_{ij}$ and $\underline{C}_{ij}$ (i,j=p,s) are stiffness and damping matrices between system i and system j, respectively; and $\underline{F}(t)$ and $\underline{X}(t)$ denote the external excitation and displacement vectors in the Newtonian reference frame.

Although Eq. (8.1) describes the motion of the P-S system in a broader sense than Eq. (7.1), they are formally similar. Consequently, in the same fashion as in Section 7, Eq. (8.1) can be transformed into governing equations of motion in the modal space. In order to avoid unnecessary repetition, only the key steps toward this goal are stated in the following.

The secondary mass is considered to be fixed at the attachment points on the P-system to determine its decoupled frequency characteristics while taking into account inertia coupling of the

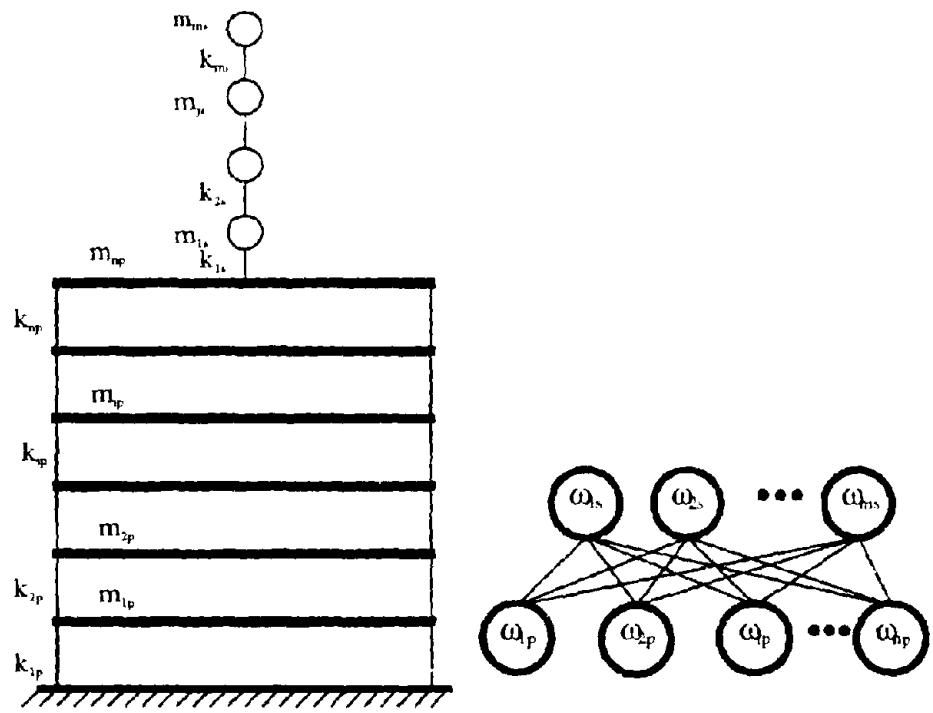

(a) Physical Space (b) Modal Space

Fig. 8–1 Primary and Secondary Systems

P- and S-systems. Thus, the modal properties of the decoupled P- and S-systems can be calculated by solving the following characteristic equations:

$$(-\omega_s^2 \underline{M}_s + \underline{K}_{ss})\,\underline{\Phi}_s = 0 \tag{8.5}$$

$$(-\omega_p^2 \bar{\underline{M}}_p + \bar{\underline{K}}_{pp})\,\underline{\Phi}_p = 0 \tag{8.6}$$

in which the modal vectors $\underline{\Phi}_s$ and $\underline{\Phi}_p$ are normalized to unity modal masses. $\bar{\underline{M}}_p$ and $\bar{\underline{K}}_{pp}$ are effective mass and stiffness matrices associated with the P-system when the effect of the S-system inertia is taken into account; they have the explicit forms

$$\bar{\underline{M}}_p = \underline{M}_p + \underline{T}_1^T \underline{M}_s \underline{T}_1 \tag{8.7}$$

$$\bar{\underline{K}}_{pp} = \underline{K}_{pp} - \underline{K}_{ps} \underline{K}_{ss}^{-1} \underline{K}_{sp} \tag{8.8}$$

where superscript T denotes matrix transpose and $\underline{T}_1$ is a transformation matrix that transforms static displacement of the P-system into that of the S-system. Obviously, $\underline{T}_1$ can be expressed as

$$\underline{T}_1 = -\underline{K}_{ss}^{-1} \underline{K}_{sp} \tag{8.9}$$

The displacement vector $\underline{X}$ can then be decomposed into

$$\underline{X} = \begin{bmatrix} \underline{\Phi}_p & \underline{O} \\ \underline{T}_1 \underline{\Phi}_p & \underline{\Phi}_s \end{bmatrix} \begin{pmatrix} q_p \\ q_s \end{pmatrix} = \underline{\Phi} q \tag{8.10}$$

Upon substituting Eq.(8.10) into Eq.(8.1) and then pre-multiplying $\underline{\Phi}^T$ on both sides, the equations of motion of the P-S system in the modal space take the form

$$\begin{bmatrix} \underline{I}_p & \bar{\underline{M}}_{sp}^T \\ \bar{\underline{M}}_{sp} & \underline{I}_s \end{bmatrix} \begin{pmatrix} \ddot{q}_p \\ \ddot{q}_s \end{pmatrix} + \begin{bmatrix} \underline{\Delta}_p & 0 \\ 0 & \underline{\Delta}_s \end{bmatrix} \begin{pmatrix} \dot{q}_p \\ \dot{q}_s \end{pmatrix} + \begin{bmatrix} \omega_p^2 & 0 \\ 0 & \omega_s^2 \end{bmatrix} \begin{pmatrix} q_p \\ q_s \end{pmatrix} = \begin{pmatrix} \underline{\Phi}_p^T \underline{F}_p \\ 0 \end{pmatrix} \tag{8.11}$$

which corresponds to the P-S system in the modal space as shown in Fig. 8-1(b) when the P-system is the only one directly subjected to excitation $\underline{F}_p$, representing the displacement input as discussed in Section 3. In Eq.(8.11), $\underline{I}_p$ and $\underline{I}_s$ are identity matrices of $n \times n$ and $m \times m$ dimensions, respectively; $\bar{\underline{M}}_{sp} = \underline{\Phi}_s^T \underline{M}_s \underline{T}_1 \underline{\Phi}_p$ is a coupling mass matrix between the P- and S-system; ω_p^2 and ω_s^2 are diagonal stiffness matrices of the P- and S-systems; $\underline{\Delta}_p$ and $\underline{\Delta}_s$ are diagonal

damping matrices whose elements are $\Delta_p = 2\xi_p\omega_p$ and $\Delta_s = 2\xi_s\omega_s$ in which ξ_p and ξ_s are damping ratios of the P- and S-systems, respectively; $\underset{\sim}{q}_p$ and $\underset{\sim}{q}_s$ are displacement vectors in the modal space; and $\underset{\sim}{\Phi}_p$ and $\underset{\sim}{\Phi}_s$ are modal matrices of the P- and S-systems.

In the derivation of the above equations, one assumption is made, i.e., $\underset{\sim}{C}_{pp}\underset{\sim}{T}_1 + \underset{\sim}{C}_{ps} = 0$. This is true only when single attachments of S-systems such as the ones discussed in the preceding sections are considered. For the case of multiple-supported S-systems, this assumption implies that damping of the S-system is in direct proportion to its stiffness.

It is seen from Eq. (8.11) that, due to the introduction of transformation matrix $\underset{\sim}{T}_1$, the coupled P-S system with non-conservative coupling has been transformed into a conservatively-coupled P-S system in the modal space but with mass coupling. Further observation shows that Eq. (8.11) is symmetric in the characteristic parameters of the P- and S-system so that the problem encountered in the dynamic analysis of the P-S system (one attached to another) using the SEA method [109] has been lifted. Statistical energy analysis is now directly applicable to the analysis of dynamic response of the P-S systems [45]. When $n = m = 1$, Eq. (8.11) degenerates into the simple case

$$\ddot{q}_p(t) + \Delta_p\dot{q}_p(t) + \omega_p^2 q_p(t) + m_{sp}\ddot{q}_s(t) = f_p(t) \tag{8.12}$$

$$\ddot{q}_s(t) + \Delta_s\dot{q}_s(t) + \omega_s^2 q_s(t) + m_{sp}\ddot{q}_p(t) = 0 \tag{8.13}$$

The relationship between power flow (P_{ps}) from the P-system to the S-system and the kinetic energies ($E_p^{(k)}$, $E_s^{(k)}$) of the P- and S-systems has been approximately formulated in [53] and modified here to give the exact expression

$$P_{ps} = 2\alpha(E_p^{(k)} - E_s^{(k)}) \tag{8.14}$$

in which the proportional constant α can be expressed as

$$\alpha = \frac{m_{sp}^2\left[\Delta_p\omega_s^4 + \Delta_s\omega_p^4 + \Delta_p\Delta_s(\Delta_p\omega_s^2 + \Delta_s\omega_p^2)\right]}{(1 - m_{sp}^2)\left[(\omega_p^2 - \omega_s^2)^2 + (\Delta_p + \Delta_s)(\Delta_p\omega_s^2 + \Delta_s\omega_p^2)\right]} \tag{8.15}$$

8.3 Energy of P-S System with Closely Spaced Modes

A simpler case in which a MDOF P-S system can be analyzed via statistical energy analysis is one where their modes are closely spaced. In this case, the assumptions made in Section 2.2.2.2 are appropriate and power flow transmitted from the P- to the S-system can be implemented by following the SEA framework discussed in Section 2.2.2.

The energy flow between mode i of the S-system and mode j of the P-system is represented by Eq. (8.14), in which $E_p^{(k)}$ and $E_s^{(k)}$ are respectively substituted by constant mode energies $E_p^{(k)}/n$ and $E_s^{(k)}/m$. When averaged over the ensemble of systems, Eq. (8.14) becomes

$$P_{ps}^{(ji)} = 2 < \alpha > \left(\frac{E_p^{(k)}}{n} - \frac{E_s^{(k)}}{m} \right) \tag{8.16}$$

where $< \alpha >= \pi m_{sp}^2 \omega_c^2 / (2\Delta\omega)$ is the averaged proportional constant over frequencies, with ω_c representing the central frequency over frequency band of the external load.

When all the modes in the P-S system are considered, the total power flow from the P- to the S-system can be expressed by

$$\overline{P}_{ps} = 2nm < \alpha > \left(\frac{E_p^{(k)}}{n} - \frac{E_s^{(k)}}{m} \right) = 4\xi_{ps}\omega_c E_p^{(k)} - 4\xi_{sp}\omega_c E_s^{(k)} \tag{8.17}$$

where $2\xi_{ps} = m < \alpha > /\omega_c$ and $2\xi_{sp} = n < \alpha > /\omega_c$ are the coupling loss factors which can be related to some conventional parameters such as junction impedance.

We may now use Eq. (8.17) to calculate the energies of the P- and S-systems by considering the energy balance equation of each individual system as formulated in Section 2.2.2.3, i.e.,

$$4\xi_s\omega_c E_s^{(k)} + 4\xi_{sp}\omega_c E_s^{(k)} - 4\xi_{ps}\omega_c E_p^{(k)} = 0 \tag{8.18}$$

$$4\xi_p\omega_c E_p^{(k)} + 4\xi_{ps}\omega_c E_p^{(k)} - 4\xi_{sp}\omega_c E_s^{(k)} = P_p^{(in)} \tag{8.19}$$

which give the solutions

$$E_s^{(k)} = \frac{\xi_{ps}}{(\xi_p + \xi_{ps})(\xi_s + \xi_{sp}) - \xi_{sp}\xi_{ps}} \frac{P_p^{(in)}}{4\omega_c} \tag{8.20}$$

$$E_p^{(k)} = \frac{\xi_s + \xi_{sp}}{(\xi_p + \xi_{ps})(\xi_s + \xi_{sp}) - \xi_{sp}\xi_{ps}} \frac{P_p^{(in)}}{4\omega_c} \tag{8.21}$$

where $P_p^{(m)}$ is the input power from the P-system. From Eqs.(8.20) and (8.21), one can easily observe that the kinetic energy of the S-system is always less than that of the P-system when $m=n$.

As one can see, P-S systems with many closely-spaced modes can be readily analyzed. Dynamic properties of the S-system such as its relative displacement or absolute acceleration can be inferred from Eqs. (8.17) and (8.20) as discussed in Section 6.

8.4 Response of P-S System With Sparsely Spaced Modes

A more important case, and more commonly encountered in practice, is one where n and m take intermediate values and the modal frequencies of the P-S system are sparsely distributed. In this case, individual modal contributions to the dynamic response of the S-system are expected to be significant and thus the assumptions made in Section 2.2.2.2 are no longer valid. Hence, statistical energy analysis can not be applied in the strict sense. However, we can still use power flow and energy concepts on an individual modal basis.

Originally, it was intended to develop an approximate relation between power flow transmitted from one mode in the P-system to another in the S-system and modal energies stored in the P- and S- systems. However, it was found that such a relationship is difficult to develop if not impossible due to: (1) All the modal forces acting on the P-system are perfectly correlated; (2) Frequency properties of lower modes are sensitive to the parameter variations so that such a relationship (if exists) could be vulnerable to structural parameter changes. For these reasons, a mean-square condensation procedure has been proposed based on the equivalence of total power flow from the P- to the S- system instead of power flow between two modes from P- and S-systems, respectively.

8.4.1 SDOF S-System and 2-DOF P-System (1S-2P Model)

If we consider the SDOF P-system and SDOF S-system as the simplest case, the next in complexity is one with a SDOF S-system and a 2-DOF P-system. In the procedure proposed in this section, the response behavior of this coupled system is essential for generating knowledge of the dynamic characteristics of general MDOF P-S systems, which is analogous to the representation

of a MDOF system by a 2-DOF model in the traditional analysis of combined systems.

When m and n are set to be one and two, respectively, Eq.(8.11) degenerates into the 1S-2P model represented by Fig. 8-2(a).

$$\ddot{q}_{1p} + \Delta_{1p}\dot{q}_{1p} + \omega_{1p}^2 q_{1p} + m_{1p}\ddot{q}_s = -\Gamma_{1p} f(t) \tag{8.22}$$

$$\ddot{q}_{2p} + \Delta_{2p}\dot{q}_{2p} + \omega_{2p}^2 q_{2p} + m_{2p}\ddot{q}_{2p} = -\Gamma_{2p} f(t) \tag{8.23}$$

$$\ddot{q}_s + \Delta_s \dot{q}_s + \omega_s^2 q_s + m_{1p}\ddot{q}_{1p} + m_{2p}\ddot{q}_{2p} = 0 \tag{8.24}$$

By following the procedure in Section 5, the displacement amplitude under unit-amplitude harmonic load f(t) can be shown to be

$$Q_s = \frac{-H_s\omega^2 (m_{1p}\Gamma_{1p}H_{1p} + m_{2p}\Gamma_{2p}H_{2p})}{1 - H_s\omega^4 (m_{1p}^2 H_{1p} + m_{2p}^2 H_{2p})} F \tag{8.25}$$

in which H_s, H_{1p}, and H_{2p} are transfer functions of the SDOF system with frequencies ω_s, ω_{1p}, and ω_{2p}, respectively.

The mean-square velocity of the S-system (or power flow from the P- to the S- system in this case) can be expressed as

$$E_s = S_f \int_{-\infty}^{\infty} \omega^2 |Q_s(\omega)|^2 d\omega = E_1\Gamma_{1p}^2 + E_2\Gamma_{2p}^2 + 2E_3\Gamma_{1p}\Gamma_{2p} \tag{8.26}$$

in which E_s, E_1 and E_2 are the mean-square velocities (energy parameters) of the S-system, the S-system with $\Gamma_{2p} = 0$ and the S-system with $\Gamma_{1p} = 0$, respectively; E_3 is one-half of the correlated term of the S-system mean-square velocity. Their explicit expressions can be found by referring to Eq.(A.3) and they are

$$E_i = \frac{\pi S_f}{C_0} \cdot \frac{B_0^{(i)}A_1 + B_1^{(i)}A_2 + B_2^{(i)}A_3}{C_1 A_1 - C_3 A_2 + C_5 A_3}, \qquad (i = 1, 2, 3) \tag{8.27}$$

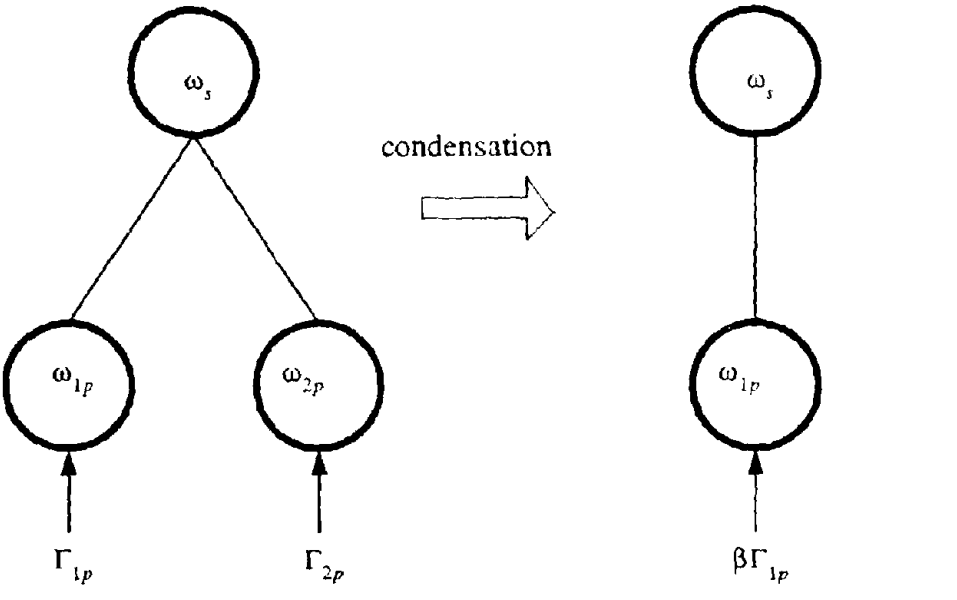

(a) General 1S-2P Model (b) Condensed 1S-1P Model

Fig. 8-2 Condensation Process from 1S-2P Model to 1s-1P Model

in which

$$B_0^{(1)} = m_{1p}^2 , \qquad B_0^{(2)} = m_{2p}^2 , \qquad B_0^{(3)} = m_{1p} m_{2p}$$

$$B_1^{(1)} = m_{1p}^2 (\Delta_{2p}^2 - 2\omega_{2p}^2), \quad B_1^{(2)} = m_{2p}^2 (\Delta_{1p}^2 - 2\omega_{1p}^2), \quad B_1^{(3)} = m_{1p} m_{2p} (\Delta_{1p}\Delta_{2p} - \omega_{1p}^2 - \omega_{2p}^2)$$

$$B_2^{(1)} = m_{1p}^2 \omega_{2p}^4 , \qquad B_2^{(2)} = m_{2p}^2 \omega_{1p}^4 , \qquad B_2^{(3)} = m_{1p} m_{2p} \omega_{1p}^2 \omega_{2p}^2$$

$$A_1 = C_6 (C_2 C_3^2 + C_1^2 C_6 - C_1 C_2 C_5 - C_1 C_3 C_4)$$

$$-C_5 (C_2 C_3 C_4 + C_0 C_4 C_5 + C_1 C_2 C_6 - C_0 C_3 C_6 - C_2^2 C_5 - C_1 C_4^2)$$

$$A_2 = C_0 (C_3^2 C_6 - C_1 C_5 C_6 - C_3 C_4 C_5 + C_2 C_5^2)$$

$$A_3 = C_0 (C_1 C_3 C_6 + C_0 C_5^2 - C_1 C_4 C_5$$

$$C_0 = 1 - m_{1p}^2 - m_{2p}^2$$

$$C_1 = \Delta_s + \Delta_{1p} (1 - m_{2p}^2) + \Delta_{2p} (1 - m_{1p}^2)$$

$$C_2 = \omega_s^2 + \omega_{1p}^2 (1 - m_{2p}^2) + \omega_{2p}^2 (1 - m_{1p}^2) + \Delta_s (\Delta_{1p} + \Delta_{2p}) + \Delta_{1p}\Delta_{2p}$$

$$C_3 = \Delta_s (\omega_{1p}^2 + \omega_{2p}^2 + \Delta_{1p}\Delta_{2p}) + \omega_s^2 (\Delta_{1p} + \Delta_{2p}) + \Delta_{1p}\omega_{2p}^2 + \Delta_{2p}\omega_{1p}^2$$

$$C_4 = \Delta_s (\Delta_{1p}\omega_{2p}^2 + \Delta_{2p}\omega_{1p}^2) + \omega_s^2 (\omega_{1p}^2 + \omega_{2p}^2 + \Delta_{1p}\Delta_{2p}) + \omega_{1p}^2\omega_{2p}^2$$

$$C_5 = \Delta_s \omega_{1p}^2 \omega_{2p}^2 + \omega_s^2 (\Delta_{1p}\omega_{2p}^2 + \Delta_{2p}\omega_{1p}^2)$$

$$C_6 = \omega_s^2 \omega_{1p}^2 \omega_{2p}^2$$

Here, S_f is the power spectral density of the common factor f(t) in the external excitation, which is omitted in Fig. 8-2.

The mean-square velocities E_1 and E_2 as well as energy correlation $E_3/(E_1E_2)^{0.5}$ are shown in Figs.8-3(a, b) as functions of frequency ratios ω_{1p}/ω_s and ω_{2p}/ω_s. It can be observed that E_1 and E_2 generally do not vary appreciably when ω_{1p}/ω_s and ω_{2p}/ω_s deviates from unity. The same

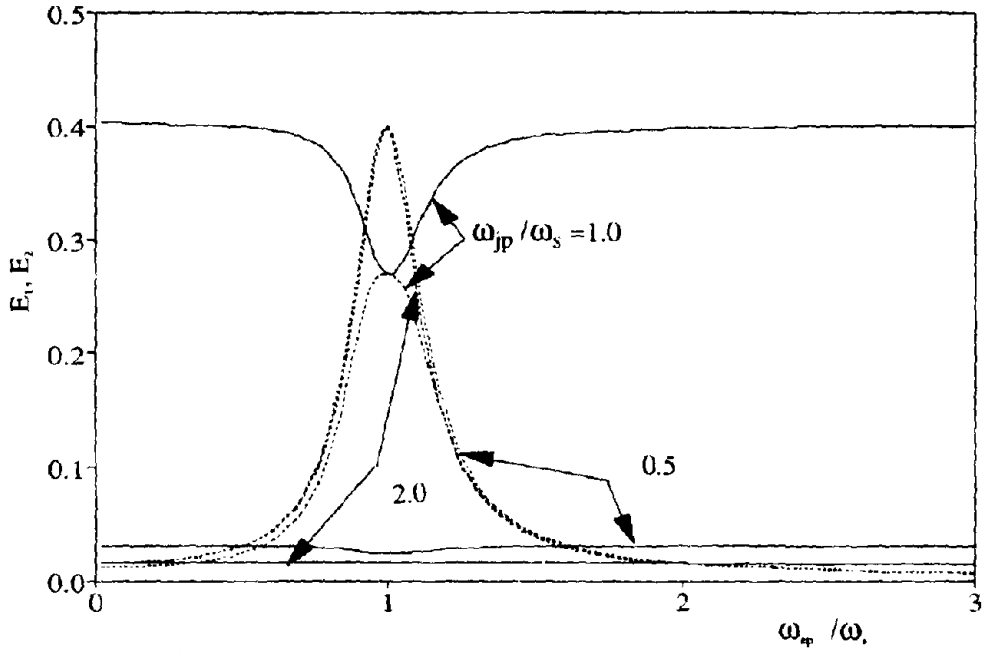

(a) $\xi_s = \xi_{jp} = \xi_{s\varphi} = 0.05$, $m_p = m_\varphi = 0.1$ (— E_1 , --- E_2)

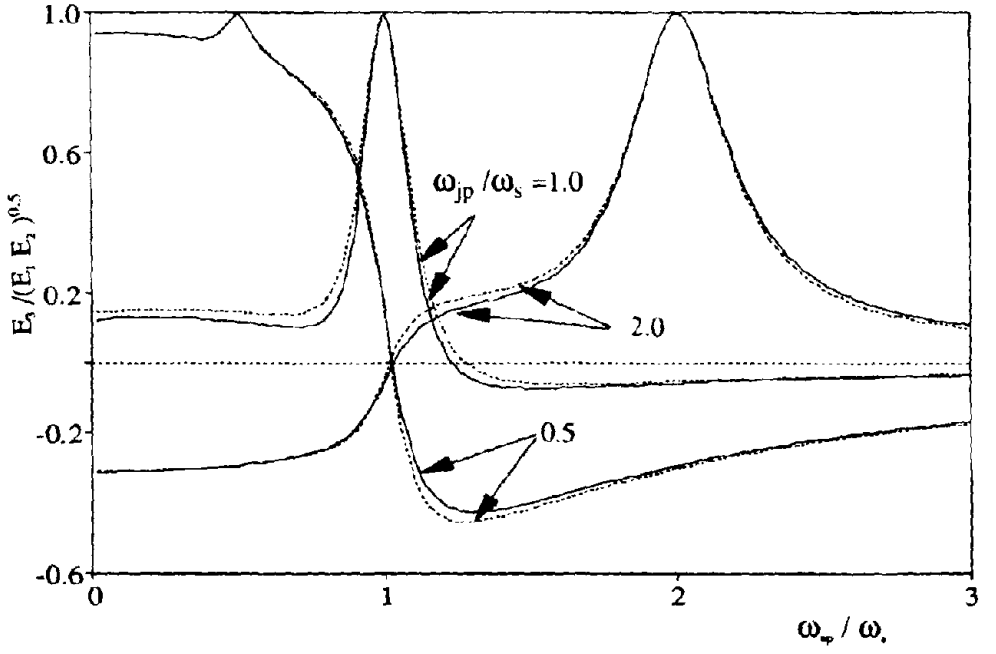

(b) $\xi_s = \xi_p = \xi_{s\varphi} = 0.05$, $m_p = 0.1$ (— $m_\varphi = 0.10$, --- $m_\varphi = 0.05$)

Fig. 8-3 Energy Coefficients and Energy Correlation in 1S-2P Model
$\omega_s = 20$ rad/sec

phenomenon happens to the energy correlation $E_3/(E_1E_2)^{0.5}$ as far as ω_{2p}/ω_s varies outside the range between unity and ω_{1p}/ω_s. These observations imply insensitivity of E_1, E_2 and $E_3/(E_1E_2)^{0.5}$ to the frequency ratio ω_{2p}/ω_s under certain circumstances, which indicates the possibility of condensation of any two modes far away from ω_s. On the other hand, the energy correlation becomes strong when ω_{2p} lies between ω_s and ω_{1p}. This is especially true when ω_{1p} is detuned with ω_s. These observations form the basis of the mean-square condensation method to be developed below. Fig. 8-3(b) also shows that energy correlation does not change significantly when mass coupling m_{2p} varies.

The two modes of the P-system incorporated in the 1S-2P model can be precisely condensed into one mode if some physical parameters such as the mean-square velocity of the S-system are exclusively of interest. In this situation, equivalence of mean-square velocities of the S-system from the 1S-2P model and the 1S-1P model results in an equivalent external force $\beta\Gamma_{1p}f(t)$ (β is a modification factor) as shown in Fig. 8-2(b), whose contribution to the mean-square velocity of the S-system is equivalent to the $\Gamma_{1p}f(t)$ and $\Gamma_{2p}f(t)$ in the 1S-2P model, i.e.,

$$(E_s)_{1S-2P\ model} = (E_s)_{1S-1P\ model} \tag{8.28}$$

For the general case ($n > 2$), it is expected that an MDOF P-system can be condensed into a two-DOF P-system in a similar way. From the power balance equation of the P-S system [13], one can see that kinetic energy of the S-system or power flow from one subsystem to another would be the most important parameter. Together with potential energy, this is also an essential parameter to evaluate the secondary system performance if Gaussian excitation is considered. Based on these observations, the mean-square velocity (or kinetic energy) of the S-system is considered as a major parameter on which the equivalence between the MDOF P-system and the two-DOF P-system is based.

As a rule, two modes of the P-system whose frequencies are farthest from the frequency of the S-system should be condensed into one mode first. However, when the 1S-2P model is used, the dynamic interaction effect of the remaining modes of the P-system on the condensation can not

be taken into account. This means that a solid cut has been made between the two modes of the P-system and the rest, which is not expected to be satisfactory as indicated in the numerical evaluation of the 1S-2P model. In what follows, one more mode of the P-system is added to the 1S-2P model to form a new 1S-3P model as shown in Fig. 8-4(c). The new mode functions as an adjustment element which reflects the energy exchange between the two modes of the P-system in the 1S-2P model and the remaining modes. Whenever one condensation step is being accomplished, three modes of the P-system have been condensed into two modes or the 1S-3P model is transformed into the 1S-2P model. The equivalence condition for these models can be readily established by following Eq. (8.28), i.e.,

$$(E_s)_{1S-3P\ \text{model}} = (E_s)_{1S-2P\ \text{model}} \tag{8.29}$$

8.4.2 The Mean-Square Condensation Method (MSC Method)

Modes of a general P-system are divided into two groups in the MSC method, i.e., predominant and residue groups. The predominant group consists of three consecutive modes of the P-system, the middle mode of which is selected by the following sample criterion:

$$\min_i \left| 1 - \frac{\omega_{ip}^2}{\omega_s^2} \right| \tag{8.30}$$

if the frequency ω_{ip} determined by Eq. (8.30) is neither equal to ω_{1p} nor equal to ω_{np}. Otherwise, the three consecutive modes in the predominant group are chosen as the first three or last three modes of the P-system. All the residue modes of the P-system are condensed into their closest predominant modes.

An immediate question to be posed here is whether the 1S-3P model including three predominant modes of the P-system by neglecting all the residue modes of the P-system is sufficient to represent the total dynamic response of the S-system. Numerical evaluations of a ten-story shear building demonstrate that this treatment is not satisfactory. Thus, methods of

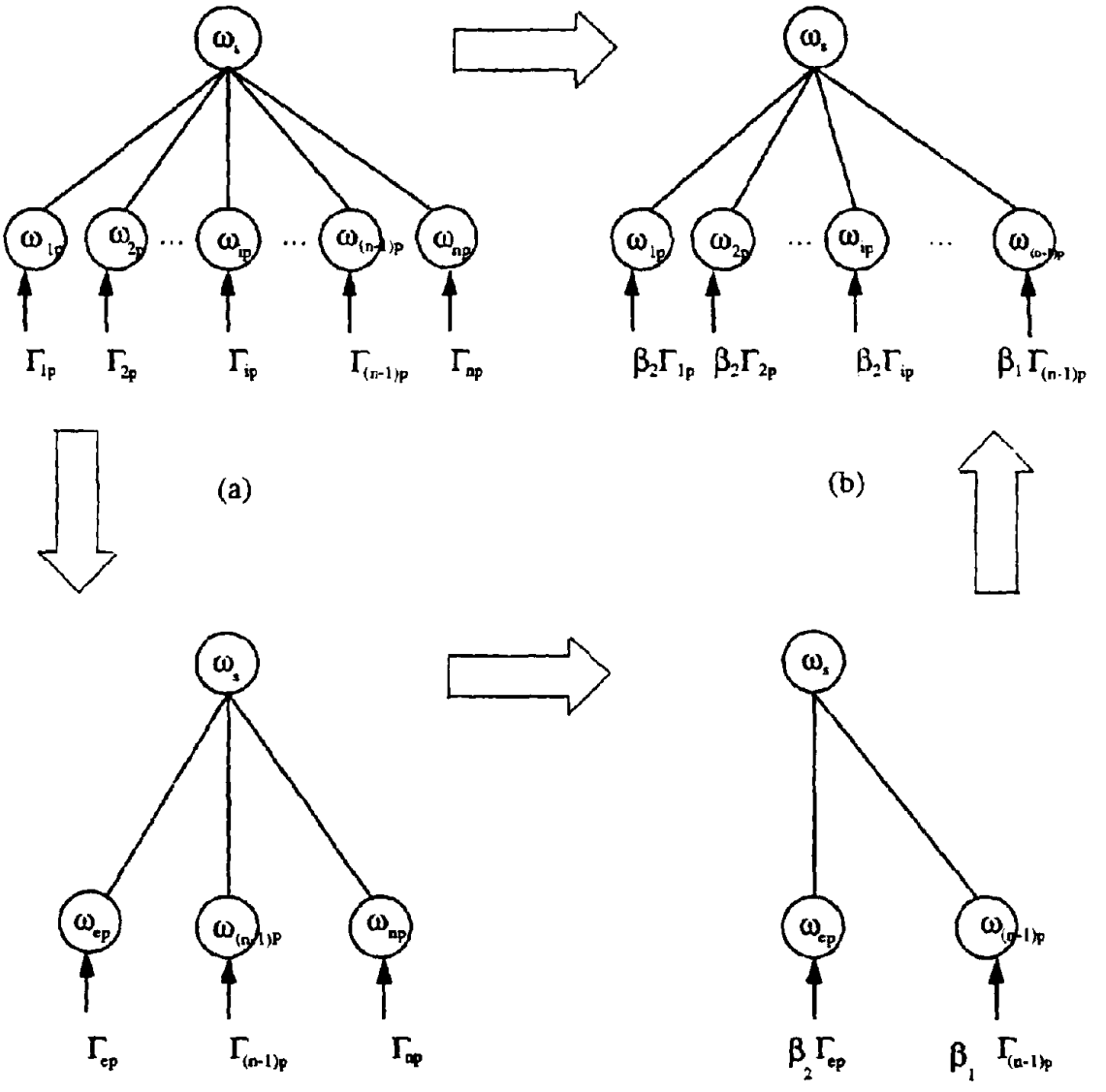

Fig. 8-4 Modal Interaction of P-S System

accounting for the remaining modes are needed and this is accomplished in this section through mean-square condensation.

In order to simplify the illustration of the method, a flexible SDOF S-system with an n-DOF P-system (1S-nP model, $\omega_s \cong \omega_{1p}$) is considered in the following analysis as shown in Fig. 8-4(a). In this case, three predominant modes of the P-system can be easily determined from Eq. (8.30) as the first three modes. Figure 8-4(a) indicates that a one-point input to a physical structure such as an earthquake ground displacement leads to n perfectly correlated inputs to an n-DOF P-system in the modal space. In the next paragraph, only one mode condensation process is illustrated and the remaining residue modes of the P-system can be condensed in the same fashion.

Like the 1S-2P model, we can condense exactly the n-DOF P-system into an $(n-1)$-DOF P-system based on the equivalent mean-square velocity of the S-system. Similarly, the $(n-1)$-DOF of the P-system in Fig. 8-4(b) can finally be condensed into a SDOF P-system. However, this recursive process is impractical because it requires the solution of the 1S-nP model which is of interest here. In the MSC method, every step to condense one DOF of the P-system is executed through a simplified 1S-3P model and its associated 1S-2P model in Figs. 8-4(c) and 8-4(d), respectively. The recursive process stops when only three predominant modes of the P-system determined by Eq. (8.30) are left. All the other quantities of interest such as displacement and acceleration of the S-system can be determined directly from this condensed 1S-3P model. The approximation in this method is uniquely introduced when the first (n-2)-DOF of the P-system is simply substituted by one equivalent mode e (from Fig. 8-4(a) to Fig. 8-4(c)) and the equivalent mode is reversed into $(n-2)$-DOF of the P-system after mode n of the P-system has been condensed (from Fig. 8-4(d) to Fig. 8-4(b)). Here, mode n is the one whose frequency is farthest from ω_s compared to the rest and mode $n-1$ is the next to it. In contrast, mode e is an artificial one whose effect on the response of the S-system is supposed to be approximately equivalent to the substituted $(n-2)$-DOF P-system as far as the modification factor (β_1 and β_2) in the condensed 1S-2P model in Fig. 8-4(c) are concerned. The formulation for calculating artificial frequency ω_{ep} and its associated parameters Δ_{ep}, m_{ep} and Γ_{ep} can be simply implemented as described below.

8.4.3 Determination of Parameters (ω_{ep},Δ_{ep},m_{ep}, Γ_{ep}) Associated with the Artificial Mode

As in Eq. (8.25) for the 1S-2P model, amplitude of S-system in the frequency domain for a general 1S-(n-2)P model can be expressed as

$$Q_s = \frac{-H_s\omega^2 \sum_{i=1}^{n-2} m_{ip}\Gamma_{ip}H_{ip}}{1 - H_s\omega^4 \sum_{i=1}^{n-2} m_{ip}^2 H_{ip}} F \tag{8.31}$$

indicating that amplitude of the S-system for the 1S-(n-2)P model would be identical to that of an artificial 1S-1P model if

$$m_{ep}\Gamma_{ep}H_{ep} = \sum_{i=1}^{n-2} m_{ip}\Gamma_{ip}H_{ip} \tag{8.32}$$

$$m^2_{ep}H_{ep} = \sum_{i=1}^{n-2} m^2_{ip}H_{ip} \tag{8.33}$$

in which m_{ep}, Γ_{ep}, and H_{ep} are mass coupling coefficient, participation factor and transfer function of the artificial mode corresponding to m_{ip}, Γ_{ip}, and H_{ip} of mode i. Unfortunately, the above equations can not be satisfied for all exciting frequencies (ω). In what follows, the artificial parameters m_{ep}, Γ_{ep}, ω_{ep} and Δ_{ep} are divided into two groups: (1) m_{ep} and Γ_{ep} and (2) ω_{ep} and Δ_{ep}. The mass coupling coefficient and participation factor (m_{ep}, Γ_{ep}) are simply selected in such a way that Eqs. (8.32) and (8.33) hold when ω approaches infinity, i.e.,

$$m_{ep} = \sqrt{\sum_{i=1}^{n-2} m_{ip}^2} \tag{8.34}$$

$$\Gamma_{ep} = \sum_{i=1}^{n-2} m_{ip}\Gamma_{ip}/m_{ep} \tag{8.35}$$

while the frequency and damping coefficient (ω_{ep},Δ_{ep}) can be determined based on the least-square principle, i.e.,

$$\int_{-\infty}^{\infty} a_0 \left| m^2_{ep}H_{ep} - \sum_{i=1}^{n-2} m^2_{ip}H_{ip} \right|^2 d\omega + \int_{-\infty}^{\infty} b_0 \left| m_{ep}\Gamma_{ep}H_{ep} - \sum_{i=1}^{n-2} m_{ip}\Gamma_{ip}H_{ip} \right|^2 d\omega \rightarrow minimum \tag{8.36}$$

in which a_0 and b_0 are weighting factors. However, they are implicitly involved in the resulting equations. For the sake of simplicity, the following criteria are employed instead. That is,

$$\int_{-\infty}^{\infty} \sum_{i=1}^{n-2} (m_{ip}\Gamma_{ip})^2 |H_{ip}|^2 d\omega = \int_{-\infty}^{\infty} (m_{ep}\Gamma_{ep})^2 |H_{ep}|^2 d\omega \tag{8.37}$$

$$\int_{-\infty}^{\infty} \omega^2 \sum_{i=1}^{n-2} (m_{ip}\Gamma_{ip})^2 |H_{ip}|^2 d\omega = \int_{-\infty}^{\infty} \omega^2 (m_{ep}\Gamma_{ep})^2 |H_{ep}|^2 d\omega \tag{8.38}$$

Solving Eqs. (8.37) and (8.38) simultaneously gives rise to

$$\omega_{ep} = \sqrt{\sum_{i=1}^{n-2} \frac{(m_{ip}\Gamma_{ip})^2}{\Delta_{ip}} \Big/ \sum_{i=1}^{n-2} \frac{(m_{ip}\Gamma_{ip})^2}{\Delta_{ip}\omega_{ip}^2}} \tag{8.39}$$

$$\Delta_{ep} = \sum_{i=1}^{n-2} (m_{ip}\Gamma_{ip})^2 \Big/ \sum_{i=1}^{n-2} \frac{(m_{ip}\Gamma_{ip})^2}{\Delta_{ip}} \tag{8.40}$$

Numerical calculation for a few weighted-average schemes of ω_{ep}, Δ_{ep}, m_{ep}, Γ_{ep}, independent of ω_s, shows that the mean-square response of the S-system is insensitive to these choices.

8.4.4 Solution Properties

By substituting $\beta_1\Gamma_{(n-1)p}$ and $\beta_2\Gamma_{ep}$ for Γ_{1p} and Γ_{2p} in Eq. (8.26), the analytical procedure to determine the modification factors (β_1 and β_2) in the 1S-2P model in Fig. 8-4(d) can be developed, giving

$$E_1\Gamma_{(n-1)p}^2\beta_1^2 + E_2\Gamma_{ep}^2\beta_2^2 + 2E_3\Gamma_{(n-1)p}\Gamma_{ep}\beta_1\beta_2 = E_s \tag{8.41}$$

in which E_s is the mean-square velocity of the condensing 1S-3P model, i.e., $(E_s)_{1S-3P}$ in Eq. (8.29). For a general system, E_1, E_2 and E_3 are all positive. Furthermore, $(E_3^2 - E_1E_2) < 0$ because $E_s > 0$. From the mathematical point of view, the trajectory that Eq.(8.41) describes is an ellipse in the β_1—β_2 plane. Any point on this ellipse represents one solution of β_1 and β_2, which indicates that the MSC solution exists but is not unique. In order to obtain one unique solution, the condensation process should be imposed on the mode whose frequency is farthest from ω_s. A good selection of β_1 and β_2 might be one by taking β_2 =1.0 when its maximum β_{2b} $(=(E_s E_3/(E_1 E_2 - E_3^2))^{0.5})$

is greater than one and β_2 is set to be $\beta_{2\infty}$ otherwise. For a given β_2, two solutions for β_1 exist, whichever closer to one is the solution. It is worth noting that the closed-form expression of E_e in the 1S-3P model has also been formulated so that the computation of modification factors in each step is surprisingly expedient.

8.4.5 Summary of the MSC Procedure

The MSC procedure for a general 1S-*n*P model can now be summarized as follows:

(1). Find out frequencies (ω_s, $\omega_{1p} < \omega_{2p} < \ , \ldots, \ < \omega_{np}$) of individual S- and P-systems as well as participation factors of the P-system ($\Gamma_{1p}, \Gamma_{2p}, \ldots, \Gamma_{np}$) and mass coupling coefficients ($m_{1p}, m_{2p}, \ldots, m_{np}$).

(2). Select three predominant modes of the P-system based on Eq.(8.30) and let their frequencies be $\omega_{(i-1)p} < \omega_{ip} < \omega_{(i+1)p}$.

(3). Condense all modes of the P-system whose frequencies are larger than $\omega_{(i+1)p}$ into mode $(i+1)$, starting out with mode n as shown in Fig. 8-4 (condensation step I=1). Every circle from Fig. 8-4(a) → Fig. 8-4(c) → Fig. 8-4(d) → Fig. 8-4(b) condenses one mode of the P-system.

(a). Calculate ω_{ep},Δ_{ep},m_{ep} and Γ_{ep} by Eqs. (8.34,8.35,8.39,8.40) for the first *(n-1-1)* modes of the P-system. Together with modes *(n-1)* and *(n+1-1)*, the artificial mode e forms three modes of P-system in the 1S-3P model at this step which is then condensed into its associated 1S-2P model with modification factors β_1 and β_2. The artificial mode e is lastly reversed into the first *(n-1-1)* modes with $\beta_2\Gamma_{kp}$ as a new participation factor for mode k *(k=1,2,..., n-1-1)* and $\beta_1\Gamma_{(n-1)p}$ for mode *(n-1)*. Consequently, the 1S-(n+1-1)P system has been condensed into a 1S-(n-1)P system.

(b). Repeat step (a) with $1+1$ in place of 1 until 1 is equal to $n-i-1$. The original 1S-nP system is then condensed into 1S-(i+1)P system.

(4). Condense all modes of the P-system whose frequencies are smaller than $\omega_{(i-1)p}$ into mode *(i-1)*, starting out with mode 1 (condensation step I=1).

(a). Calculate ω_{ep}, Δ_{ep}, m_{ep} and Γ_{ep} by Eqs. (8.34,8.35,8.39,8.40) for the last *(i-1)* modes of the

condensed P-system. Together with modes I and $I+1$, the artificial mode e forms three modes of the P-system in the 1S-3P model at this step, which is then condensed into its associated 1S-2P model with modification factors β_1 and β_2. The artificial mode e is lastly reversed into the last $(i-1)$ modes with $\beta_2 \Gamma_{kp}$ as a new participation factor for mode k ($k=2+1,3+1,\ldots, i+1$) and $\beta_1 \Gamma_{(I+1)p}$ for mode $(I+1)$. Consequently, the condensed 1S-(i+2-I)P system has been further condensed into a 1S-(i+1-I)P system.

(b). Repeat step (a) with $I+1$ in place of I until I is equal to $i-2$. As a result, the 1S-3P system with three predominant modes of the P-system is established.

(5). Calculate the dynamic response of the S-system and assess its dynamic performance from the condensed 1S-3P system with three predominant modes of the P-system.

8.4.6 Convergence as Mass Ratio (m_s/m_p) Becomes Small

When the mass ratio between the S- and P-systems becomes very small, the following relations hold: (1) ω_s's are kept constant since the stiffness of the S-system are taken to be proportional to the mass of the same system; (2). ω_p's approach $\omega_p^{(0)}$'s which are the frequencies of the P-system without the S-system; (3). $\bar{M}_{sp}$ becomes proportional to the square root of the mass ratio; Γ approaches $\Gamma^{(0)}$ which consists of the participation factors when the S-system vanishes.

As the mass ratio decreases, the effect of the P-modes whose frequencies are far from ω_s usually becomes negligible compared to the remaining modes. The final three P-modes left after the condensation process has been completed contribute almost all the energy to the S-system due to the tuning effect. Numerical experimentation in Fig. 8-5(a) shows that the rate of convergence is good in the tuned case. For the detuned case, however, the converged value may deviate from the exact one as shown in Fig. 8-5(b). This is partially because the energy correlation becomes strong as illustrated in Fig. 8-3(b). In fact, all the parameters such as damping of the P- and S-systems, mass ratio, modal participation factor of the P-system as well as frequency ratio mentioned above will contribute to energy distribution of the S-system. In the detuned situation, the frequency ratio seems no longer to be a major parameter in energy distribution and criterion in

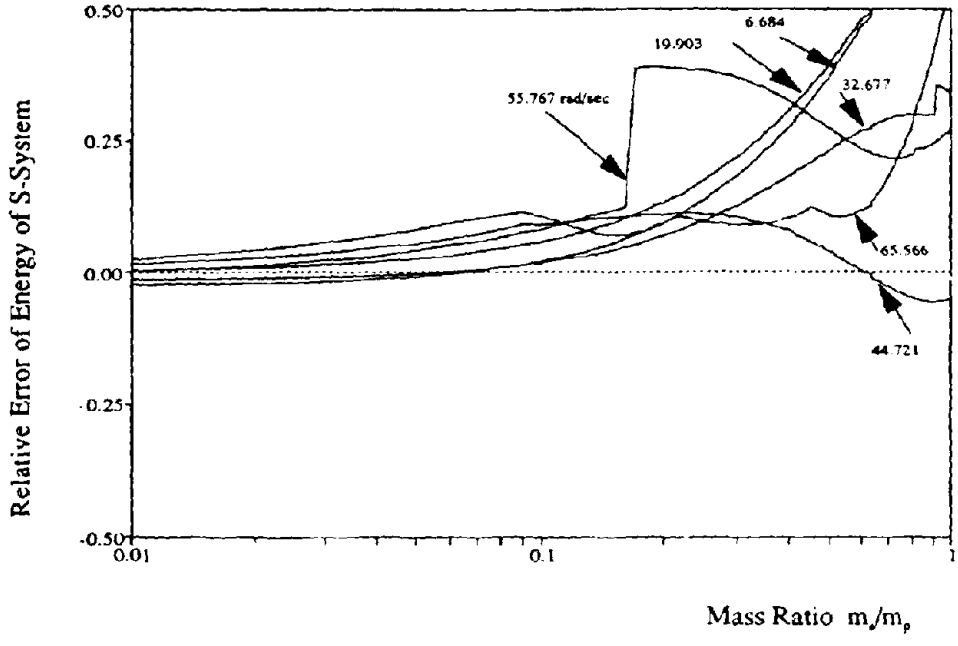

(a) Tuned Case

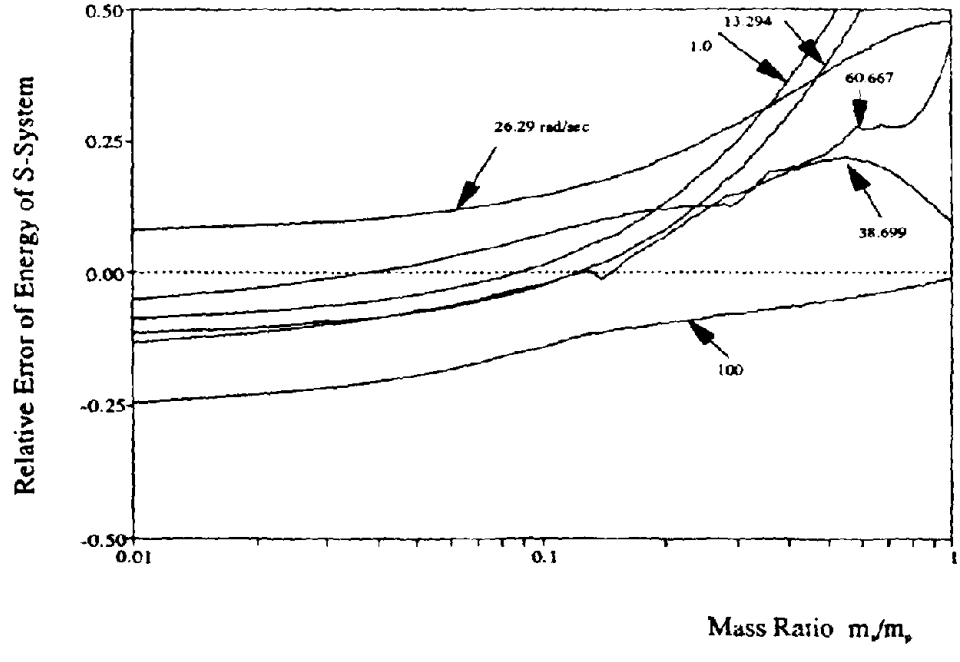

(b) Detuned Case

Fig. 8-5 Convergence of Mean-Square Condensation Method

Eq. (8.30) can not adequately provide three representative modes.

8.5 Numerical Verification

In this section, two illustrative examples are presented and discussed to examine the accuracy and efficiency of the MSC method. While mean-square velocity spectra in the modal space are shown in the following examples, the total response of the MDOF S-system can be combined using any justified rule as summarized in Section 2.1.4.3. The excitation f(t) resulted from the support displacement in the P-system is considered as a broad-band stochastic process with spectral density of 1.0.

8.5.1 Example 1. SDOF S-System and MDOF P-System

A ten-story uniform shear building with mass, stiffness, and modal damping coefficients as shown in Fig. 8-6 is considered. Two attachment positions of the equipment are studied, i.e., one on the 5th-floor and the other on the top floor. In this study, two values of the secondary mass are chosen. They are 925 kg and 46300 kg, which correspond to mass ratios (equipment to floor mass) of 0.53% and 26.4%, respectively. The mean-square velocity spectra of the S-system are presented in Figs. 8-7(a-d). Compared with the integration results (dashed lines in Fig. 8-7), the MSC method predicts very well response spectra of the S-system, especially when the mass ratio is small (Fig. 8-7(a) and Fig. 8-7(c)). In particular, the mean-square velocity corresponding to the tuned case in which the S-system frequency is tuned to one of the frequencies of the P-system is predicted very well. Even when the mass ratio reaches 26.4%, the relative variations of the response spectra of the S-system produced by integration and the MSC method agree well. This is especially important in the preliminary design. The switch of three fundamental modes, when ω_s varies, is responsible for a few discontinuity points in the mean-square spectra. From the 1S-3P model after the condensation process has been done, one can easily calculate other parameters of interest such as relative displacement and absolute acceleration. The mean-square displacement spectra of the S-system is shown in Fig. 8-8, from which one can observe that the accuracy compared to the integration results is better than the mean-square velocity spectra due to the effect of so-called low-pass filter.

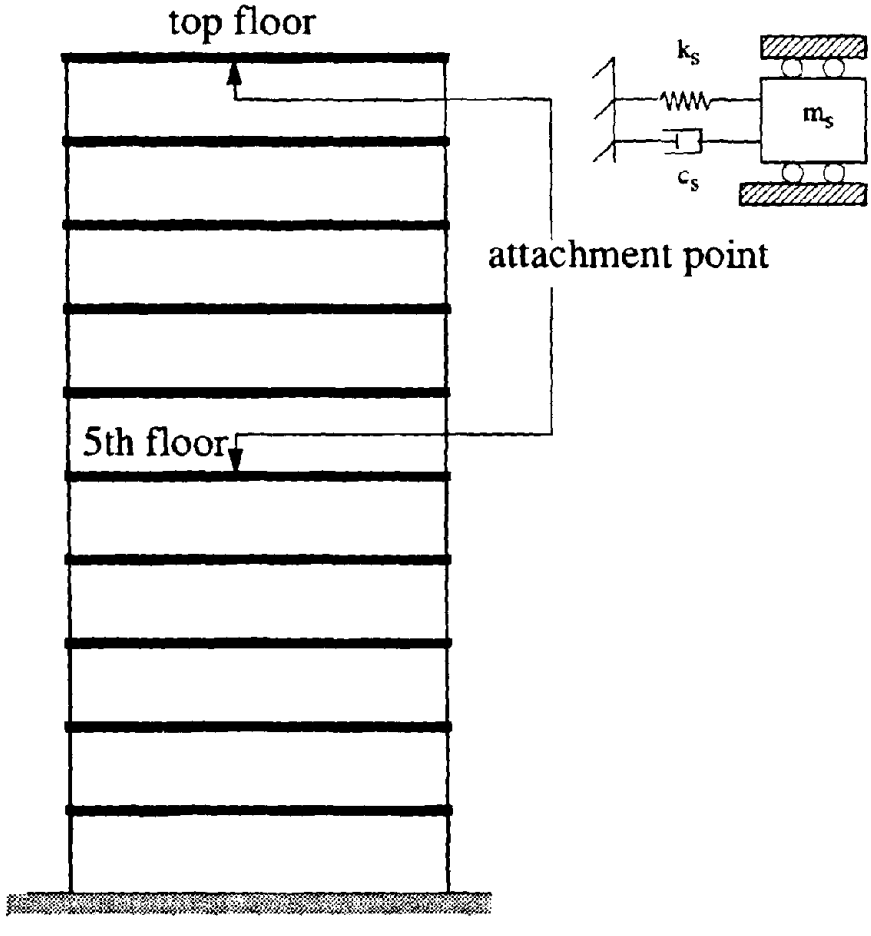

Fig. 8-6 Example Structure and Equipment

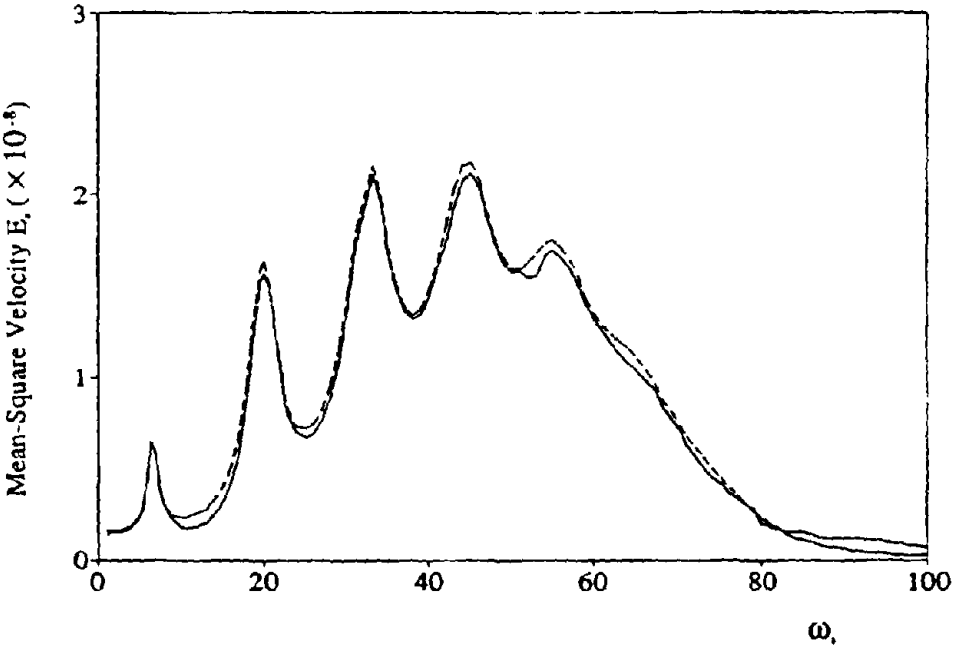

(a) m_s/m_p =0.53%, S-System Attached to Top Floor

Fig. 8-7 Mean-Square Velocity of S-System (— MSC, --- integration)

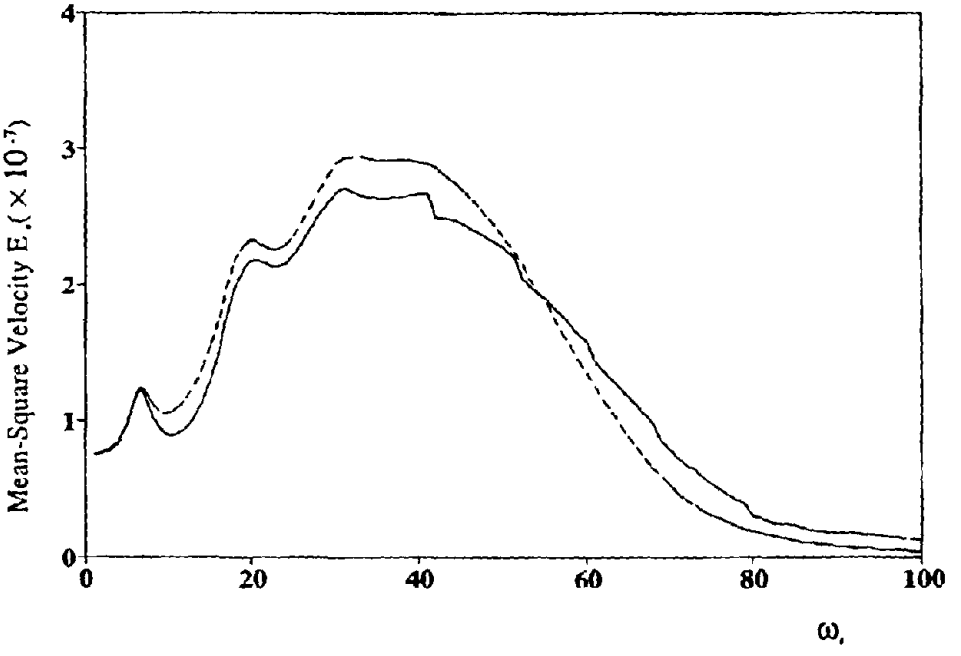

(b) m_s/m_p =26.4%, S-System Attached to Top Floor

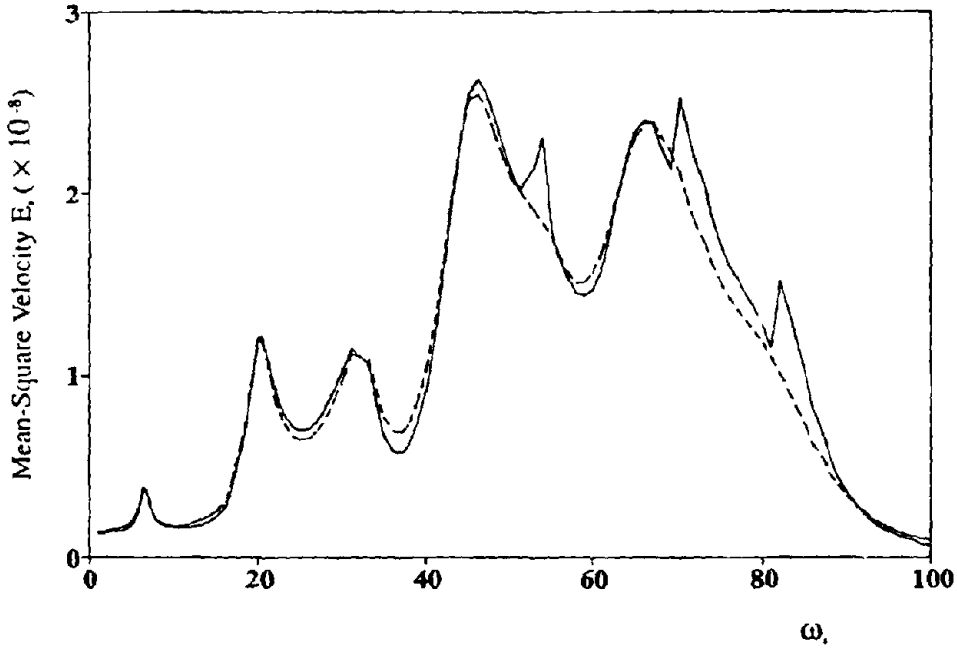

(c) m_s/m_p =0.53%, S-System Attached to 5th Floor

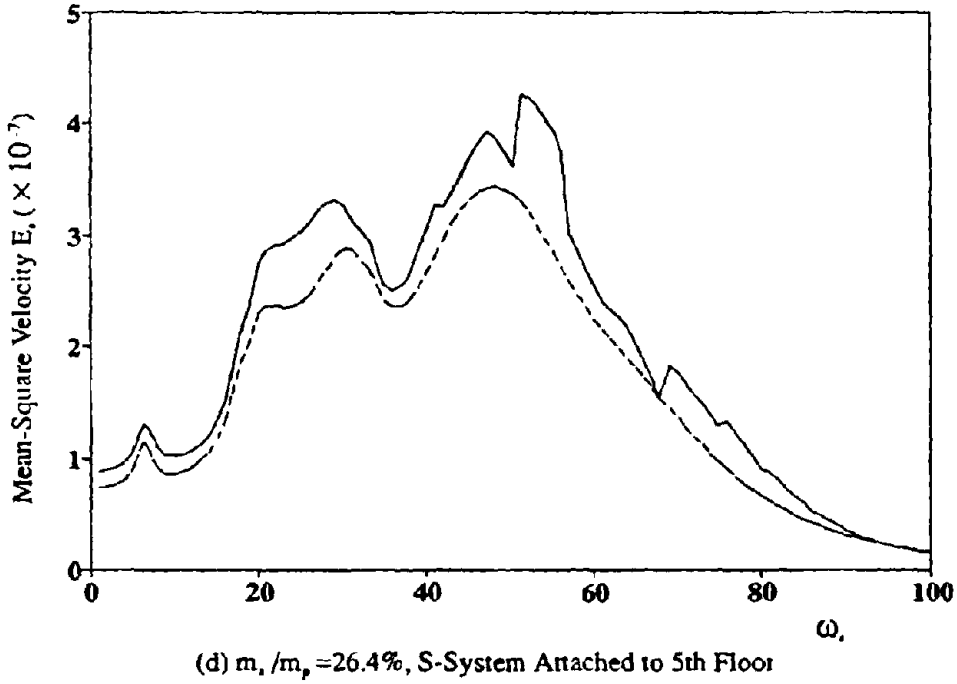

(d) m_s/m_p =26.4%, S-System Attached to 5th Floor

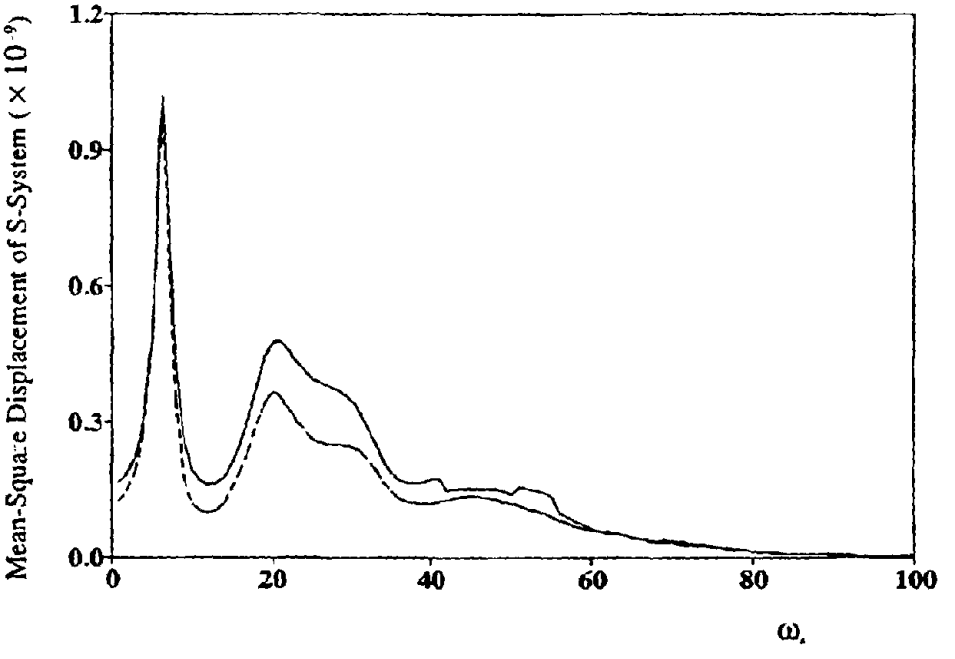

Fig. 8-8 Mean-Square Displacement of S-System (— MSC, --- integration):

m_s / m_r =26.4%, S-System Attached to 5th Floor

By comparing the mean-square velocity spectra shown in Figs. 8-7(a) and 8-7(c), one can observe that the S-system will obtain more energy in the low frequency range for the top-floor configuration than for the 5th-floor configuration. This implies the involvement of more high-order modes of the P-system for the 5th-floor attachment and illustrates the importance of attachment position in the S-system design. For this reason, the mean-square velocity spectra for the top-floor attachment are generally more accurate than the other as demonstrated in Figs. 8-7(a-d).

One of the most attractive features associated with the MSC method is its computational efficiency. The CPU time required to calculate the response of the S-system by the method is a linearly increasing function of the number of DOF of the P-system and independent of ω_s. On the other hand, integration method needs much more time to reduce the relative error of the adjacent two steps when one more DOF of the P-system is introduced. Moreover, the CPU time required is related to the position of ω_s with respect to ω_{pi} (i=1,2,...,n). In this example, the integration method required ten to thirty times of CPU needed to execute the MSC procedure, which is an important factor in practical design.

8.5.2 Example 2. MDOF S-System and MDOF P-System

The technique developed in the preceding section can be easily extended to MDOF S-systems. Conventional static condensation should be carried out to absorb all modes in the S-system except ω_{si} before the technique can be applied. When the P-system is the only one subjected to excitation, the static response of any mode in the S-system, ω_{si} (i=1,2,...,m), is equal to zero.

A six-story building with two secondary masses is considered herein to examine the accuracy of the method regarding to attachment configurations. Each story has the same mass of 1.0 kip s^2/in ($\cong 1.8\times10^5$ kg) and interval stiffness of 5000 kips/in ($\cong 9\times10^8$ N/m) as discussed in Section 7.7.2. Three different connecting configurations are considered in this example. Except for Model B, two secondary masses have the same mass of 0.1kip s^2/in($\cong 1.8\times10^4$ kg) and connecting stiffness k_o. In Model B, two secondary connecting stiffness are taken as k_o and $4k_o$, respectively, to

avoid tuning in the S-system itself. For all three models, five percent of critical damping for both P- and S-system is assumed.

The modal mean-square velocity of the S-system for three different attachment configurations are shown in Figs. 8-9(a-c). It can be seen that the modal responses of the S-system produced by the MSC method and the integration method agree well, especially when the relative response variations are of interest. It can also be observed that the first modal response plays an important role for all three models except for the one with two separate secondary masses in which the second-mode response is about the same as the first-mode response in the low frequency range. This results from the fact that frequency of the second mode in the example is twice that of the first mode which is tuned to the frequencies of the P-system.

8.6 Application in Practical Design

As demonstrated in the preceding section, the method developed herein is quite efficient in calculating the response of S-systems. The previous examples have already shown the potential application in preliminary design about selecting the attachment configuration. The optimum selection of the S-system frequency can be easily made from the mean-square velocity spectrum. Another useful design information pertains to the amount of damping needed to further mitigate vibration of the S-system. Figure 8-10 presents the mean-square velocity versus the damping ratio of the S-system which is attached to the fifth floor of the P-system in the first example. It is observed that no optimum damping ratio exists for the tuned case as discussed in [46]. An efficient damping ratio in this case can be simply chosen as the one with an appropriate trade-off between high sensitivity of response of the S-system and economical considerations.

8.7 Discussions

The mean-square condensation method proposed in this section has been shown to be an efficient way to calculate the dynamic response of S-systems under broad-band excitations. It can be categorized as a coupled analysis of P-S systems while the modal properties of individual subsystems are used so that there is no difficulty in numerical calculation. Unlike the perturbation

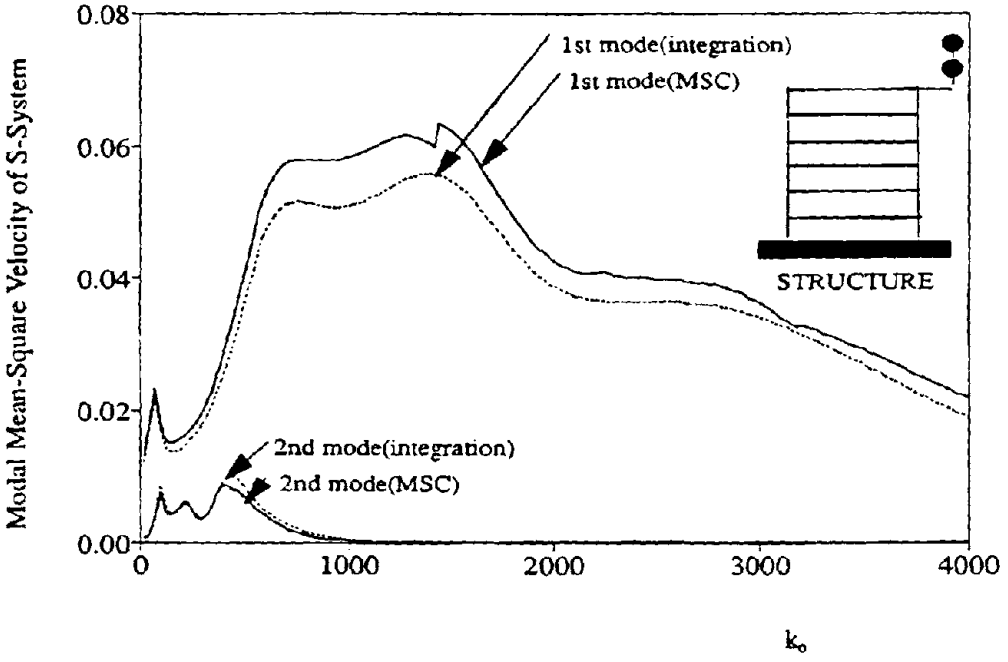

(a) Model A

Fig. 8-9 Modal Mean-Square Velocity of S-System:
(a) Model A: (b) Model B; (c) Model C

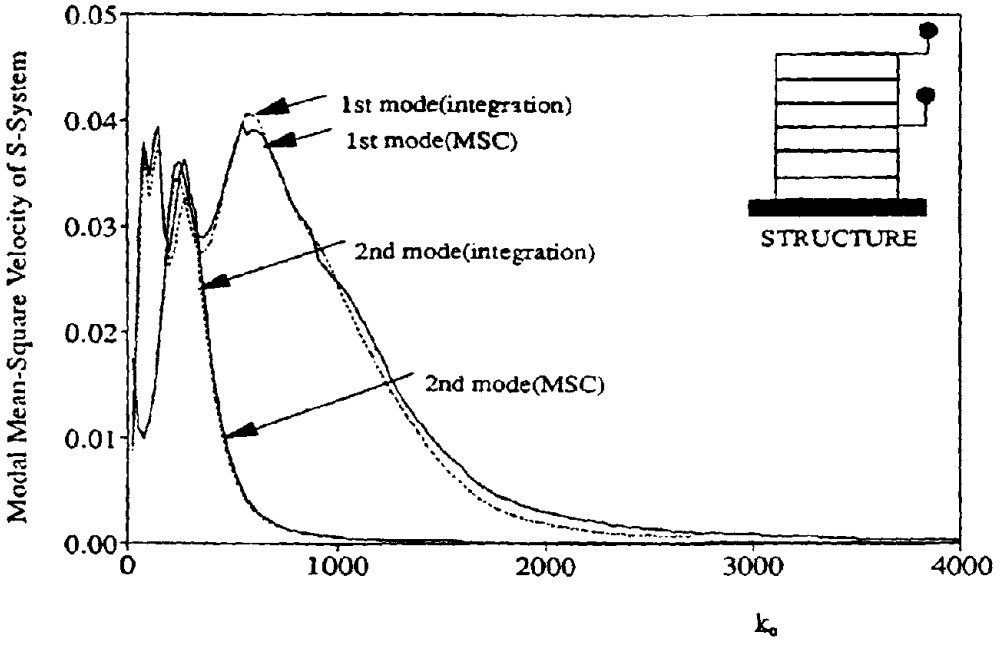
Modal Mean-Square Velocity of S-System
0.05
0.04
0.03
0.02
0.01
0.00
0
1000
2000
3000
4000
k_a
1st mode(integration)
1st mode(MSC)
2nd mode(integration)
2nd mode(MSC)
STRUCTURE

(b) Model B

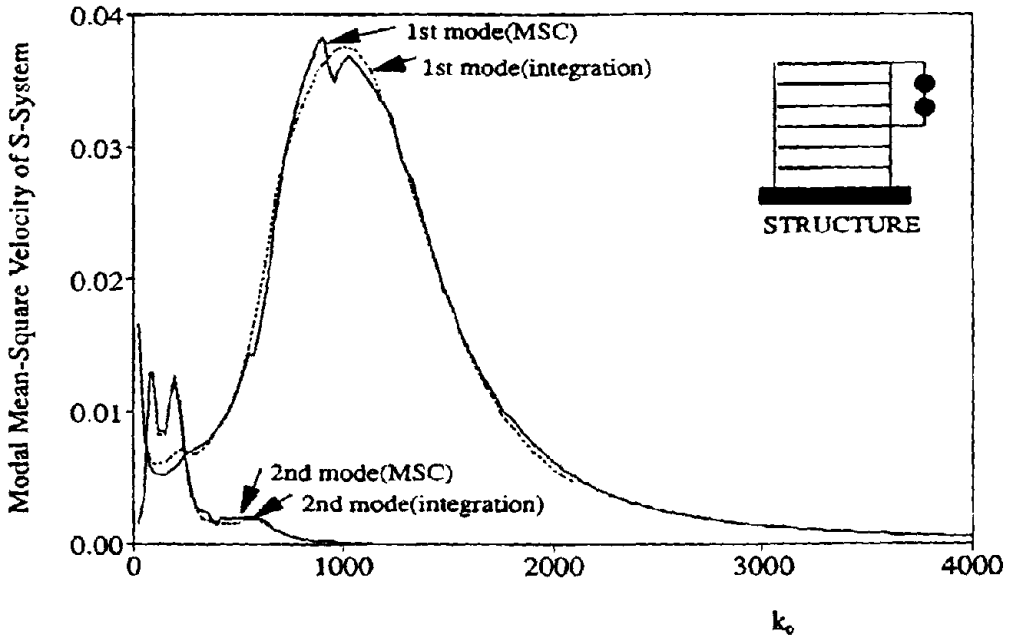
0.04
0.03
0.02
0.01
0.00
0
1000
2000
3000
4000
Modal Mean-Square Velocity of S-System
1st mode(MSC)
1st mode(integration)
2nd mode(MSC)
2nd mode(integration)
STRUCTURE
k_o

(c) Model C

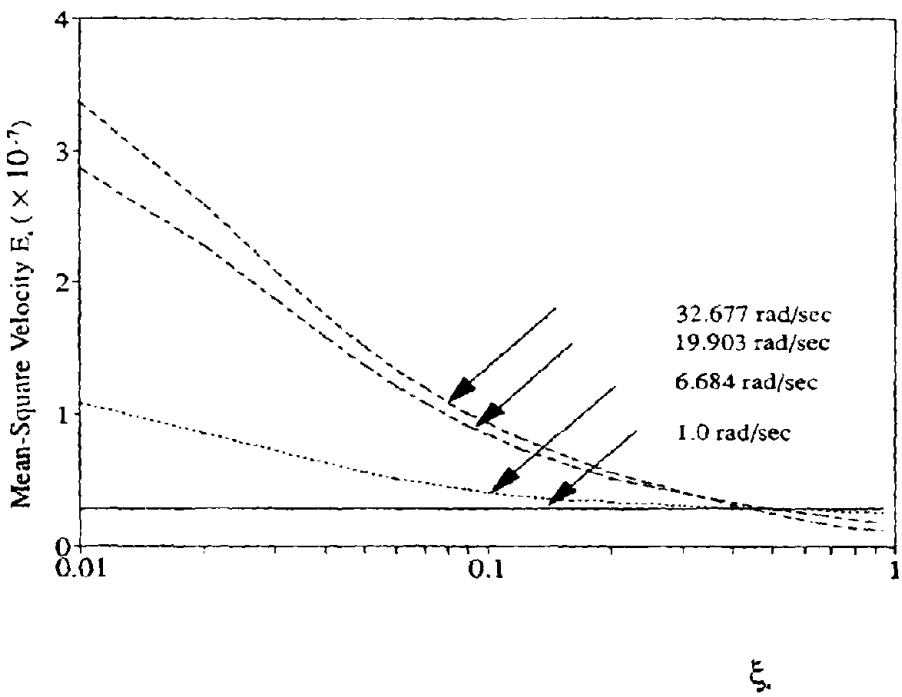

Fig. 8-10 Mean-Square Velocity of S-System :
m_s / m_p =0.1, Damping Ratio of P-System=0.05

scheme, there is no need to divide the general P-S system into tuned and detuned cases here. Furthermore, calculation in the tuned case, of particular interest in most practical designs, is more accurate than that in the detuned case. The frequency characteristics of the combined system is not required to calculate the dynamic response of the S-system. Since all the processes involved in this method are analytical calculations using explicit expressions, the participation of more DOF of the P-system does not significantly increase the calculation and stable solutions can always be obtained for arbitrarily specified P-S configurations and frequency characteristics of the S-system.

Although numerical results in this paper are presented in the form of mean-square displacement and velocity of the S-system when the P-system is subjected to base displacement input, the expectation of maximum response which is more pertinent to practical design can be obtained by multiplying the obtained root-mean-square response by the peak factor. When nonstationarity of seismic loadings has to be considered, the condensation process developed for the case of white noise input can be still effective but the condensed 1S-3P system should be subjected to the nonstationary seismic loading.

For further refinement of this method, the expressions of ω_{φ} ,Δ_{φ} , m_{φ} and Γ_{φ} in Eqs. (8.34,8.35,8.39,8.40) may be related to the frequency of the S-system so that the dynamic interaction effect at this level can be taken into account.

SECTION 9

CONCLUDING REMARKS

9.1 General Remarks on This Study

The work reported in this report is aimed at developing simple yet accurate approaches for the dynamic analysis and design of S-systems. The energy balance principle (SEA for complex systems) is shown to be a good candidate, which is certainly manageable in practical designs. The fundamental principle for all the closed-form formulations developed in this study is to appropriately substitute the energy transfer between two simple systems (typically, SDOF P- and SDOF S-systems) for the calculation of energy flow transmitted from one subsystem to another in a very complex P-S system. Therefore, all the procedures suggested here are basically developed for coupled analyses in which general characteristics listed in Section 2.1.4.1 have been inherently taken into account. Frequency characteristics of individual P- and S-systems are incorporated into the analyses so that the analysis procedure for dynamic response can be simplified and the computational efforts can be considerably reduced for complex systems. Furthermore, the unnecessary error involved in the course of response calculation due to the contaminated frequency characteristics of the coupled P-S system can be totally suppressed.

While statistical energy analysis has been shown to be a powerful technique to analyze the sound-structure interaction effect, it becomes less effective in the analysis of interaction effect between two structures subjected to earthquake loads as the relatively low excitation frequencies in this case generate a few low normal modes of P-S systems that store most of the generated energy. Based on this observation, an approximate approach, namely, the mean-square condensation method, has been developed by incorporating power flow and energy concepts at the level of individual members instead of statistical population. Analytical and numerical verification for the method demonstrates the efficiency and accuracy associated with these simple procedures.

Consequently, they can be used to conduct a performance study in a preliminary design or to qualify an S-system under seismic loads. An important feature about the mean-square condensation method is that calculated responses of an S-system tuned to its supporting system are usually more accurate than those of the detuned system.

Finally, the exact solution for a class of complex P-S systems has been obtained by grouping a general P-S system into many subsystems with small numbers of degree-of-freedom.

9.2 Further Research Directions

9.2.1 Nonstationary and Finite Frequency-Band Inputs

The external loads in this investigation are assumed to be broad-band stochastic processes. In reality, however, earthquakes are nonstationary and of finite frequency-band. The nonstationarity usually suppresses the dynamic response of long period systems [76] whereas the effect of finite frequency-band is much more complicated, depending on the relative variations between the excitation frequencies and system frequencies. These topics, especially the latter, deserve further attention.

9.2.2 Nonlinear Systems

As mentioned in Section 2.1.5, a P-system and/or an S-system may behave inelastically under strong earthquakes. Consideration of these nonlinear behaviors in the response calculation certainly is important in order to develop a practical model for design. In a weak nonlinear situation, equivalent linearization techniques can be used to solve the nonlinear systems by a substituted linear system for which all the formulations derived in this report are applicable. Otherwise, the transfer function procedure applied in the derivation basically fails and new formulations need to be developed in the time domain.

9.2.3 Dynamic Responses of S-System Due to Its Own Disturbance

The performance of rotating S-systems attached to a structure has recently been studied by Singh and Suarez [84]. The speed at which these systems rotate may be very high. Subsequently, these systems themselves generate a few high frequency modes of the coupled P-S system within

small frequency band, a property that fits well with the fundamental assumption in SEA. Therefore, SEA is expected to have promising applications in these cases.

SECTION 10

REFERENCES

1. Amin, M., Hau, W.J., Newmark, N.M. and Kasawara, R.P., 1971. "Earthquake Response of Multiple Connected Light Secondary Systems by Spectrum Methods," *Proc. ASME 1st Congr. Press. Vess. Pip.*, San Francisco, CA.

2. ASCE Working Group on Quantification of Uncertainties, 1986. *Uncertainty and Conservatism in the Seismic Analysis and Design of Nuclear Facilities*, American Society of Civil Engineers, New York, NY.

3. Asfura, A., 1985. "A New Combination Rule for Seismic Analysis of Piping Systems," *Proc. ASME Press. Vess. Pip. Conf.*, New Orleans, LA, PVP-98-3,119-125.

4. Asfura, A. and Der Kiureghian, A., 1986."Floor Response Spectrum Method for Seismic Analysis of Multiply Supported Secondary System," *Earthquake Eng. Struct. Dyn.*, 14(2), 245-265.

5. ASME Boiler and Pressure Vessel Code, 1981. "Rules of Construction of Nuclear Power Plant Components," Division 1, Appendix N, Section III, ANSI/ASME BPV-III-1-A.

6. Aziz, T.S. and Duff, C.G., 1978. "Decoupling Criterion for Seismic Analysis of Nuclear Power Plant Stations," *Proc. ASME Press. Vess. Pip. Conf.*, Montreal, Canada, PVP-29.

7. Aziz, T.S., 1982."Coupling Effects for Secondary System in Nuclear Power Plants," *Proc. ASME Press. Vess. Pip. Conf.*, Orlando, FL.

8. Biggs, J.M. and Roesset, J.M., 1970."Seismic Analysis of Equipment Mounted on a Massive Structure," *Seismic Design of Nuclear Power Plants*, MIT Press, (ed. R.J. Hansen), 319-343.

9. Burdisso, R.A. and Singh, M.P., 1987(a)."Multiply Supported Secondary Systems Part I: Response Spectrum Analysis," *Earthquake Eng. Struct. Dyn.*, 15, 53-72.

10. Burdisso, R.A. and Singh, M.P., 1987(b). "Seismic Analysis of Multiply Supported Secondary Systems with Dynamic Interaction Effects," *Earthquake Eng. Struct. Dyn.*, 15, 1005-1022.

11. Chakravorty, M.K. and Vanmarke, E.H., 1973. "Probabilistic Analysis of Light Equipment within Buildings," *Proc. 5th WCEE*, Rome, Italy, II.

12. Chen, Genda and Soong, T.T., 1991. "Power Flow and Energy Balance Between Nonconservatively Coupled Oscillators," *J. Vib. Acoust.*, ASME, 113(4), 448-454.

13. Chen, Genda and Soong, T.T., 1992. "Power Flow and Energy in Primary-Secondary Systems," *J. Eng. Mech.*, ASCE, 118(5), 1046-1051.

14. Chen, Y.Q. and Soong, T.T., 1988. "State-of-the-Art Review: Seismic Response of Secondary System," *Eng. Struct.*, 10, 218-228.

15. Clough, R.W. and Penzien, J., 1975. *Dynamics of Structures*, McGraw-Hill, Inc., NY.

16. Crandall, S.H. and Mark, W.D., 1963. *Random Vibration in Mechanical Systems*, Academic Press, Inc., NY.

17. Der Kiureghian, A., Asfura, A., Sackman, J.L. and Kelly J.M., 1983. "Seismic Response of Multiple Supported Piping Systems," *Proc. 7th Int. Conf. on SMiRT*, Chicago, IL.

18. Der Kiureghian, A., Sackman, J.L. and Nour-Omid, B., 1983. "Dynamic Analysis of Light Equipment in Structure: Response to Stochastic input," *J. Eng. Mech.*, ASCE, 109(1), 90-110.

19. Dowell, E.H. and Kubota, Y., 1985. "Asymptotic Modal Analysis and Statistical Energy Analysis of Dynamical Systems," *J. Apl. Mech.*, ASME, 52-949-957.

20. Eichler, E., 1963. "Thermal Circuit Approach to Vibrations in Coupled Systems and the Noise Reduction of a Rectangular Box," *J. Acoust. Soc. Am.*, 37(6), 995-1007.

21. Eichler, E., 1964. "Plate-Edge Admittances," *J. Acoust. Soc. Am.*, 36(2), 344-348.

22. Fahy, F.J. and Yao, D.Y., 1987. "Power Flow Between Nonconservatively Coupled Oscillators," *J. Sound Vib.*, 112, 1-11.

23. Geraetes, L.H., 1985. "Use of Full ZPA Method for the Seismic Response from Rigid Modes," *Proc. ASME Press. Vess. Pip. Conf.*, New Orleans, LA, PVP-98-3, 61-67.

24. Gou, P.F., Karim-Panahi, K. and Lange, C.H., 1983. "Secondary Dynamic System Response to Loads with High Frequency Content," *Proc. ASME 4th Congr. Press. Vess. Pip.*, Portland, Oregon, PVP-73, 61-70.

25. Gupta, A.K. and Cordero, K., 1981. "Combination of Modal Responses," *Proc. 6th Int. Conf. on SMiRT*, Paris, France, K7/5.

26. Gupta, A.K. and Tembulkar, J.M., 1984(a). "Dynamic Decoupling of Secondary Systems," *Nucl. Eng. Des.*, 81, 359-373.

27. Gupta, A.K. and Tembulkar, J.M., 1984(b). "Dynamic Decoupling of Multiple Connected MDOF Secondary System," *Nucl. Eng. Des.*, 81, 375-383.

28. Gupta, A.K. and Jaw, J.W., 1986. "Response Spectrum Method for Non-Classically Damped systems," *Nucl. Eng. Des.*, 91, 161-169.

29. Hadjian, A.H., 1977. "On the Decoupling of Secondary Systems for Seismic Analysis," *Proc. 6th WCEE*, New Delhi, India, III, 3286-3291.

30. Hadjian, A.H., 1981. "Seismic Response of Structures by the Response Spectrum Method," *Nucl. Eng. Des.*, 66, 179-201.

31. Hadjian, A.H. and Ellison, B., 1984. "Decoupling of Secondary Systems for Seismic Analysis," *Proc. ASME Press. Vess. Pip. Conf.*, San Antonio, TX.

32. Heckl, M., 1962. "Vibrations of Point Driven Cylindrical Shells," *J. Acoust. Soc. Am.*, 34(10), 1553-1557.

33. Hemried, A.G. and Jeng, H., 1988. "Dynamic Response of Multiple Connected MDOF Secondary Systems," *Proc. ASME Press. Vess. Pip. Conf.*, Pittsburgh, PA, 1-7.

34. Igusa, T. and Der Kiureghian, A., 1985(a). "Dynamic Characterization of Two-Degree-of-Freedom Equipment-Structure System," *J. Eng. Mech.*, ASCE, 111(1), 1-19.

35. Igusa, T. and Der Kiureghian, A., 1985(b). "Dynamic Response of Multiple Supported Secondary System," *J. Eng. Mech.*, ASCE, 111(1), 20-41.

36. Igusa, T. and Der Kiureghian, A., 1985(c). "Generation of Floor Response Spectra Including Oscillator-Structure Interaction," *Earthquake Eng. Struct. Dyn.*, 13, 661-676.

37. Igusa, T. and Der Kiureghian, A., 1988. "Interaction in Primary-Secondary Systems," *Proc. ASME Press. Vess. Pip. Conf.*, Pittsburgh, PA, 45-50.

38. Igusa, T., 1990. "Response Characteristics of Inelastic 2-DOF Primary-Secondary System," *J. Eng. Mech.*, ASCE, 116(5), 1160-1174.

39. Kapur, K.K. and Shao, L.C., 1973. "Generation of Seismic Floor Response Spectra for Equipment Design," *Proc. Specialty Conf. on Structural Design of Nuclear Power Plant Facilities*, ASCE, Chicago, IL.

40. Kamopp, D., 1967. "Power Balance Method for Nonlinear Random Vibration," *J. Appl. Mech.*, ASME, 212-214.

41. Kelly, J.M. and Tsai, H., 1985."Seismic Response of Light Equipment in Base-Isolated Structures," *Earthquake Eng. Struct. Dyn.*, 13, 711-732.

42. Keswick, R.R. and Norton, M.P., 1987. "Coupling Damping Estimates of Non-conservatively Coupled Cylindrical Shells," *Statistical Energy Analysis* (Ed by Hsu, K.H., Nesfske, D.J. and Akay, A.), NCA-Vol.3, ASME Winter Meeting, Boston, MA, 19-24.

43. Kubota, Y., Dionne, H.D. and Dowell, E.H., 1988. "Asymptotic Modal Analysis and Statistical Energy Analysis of an Acoustic Cavity," *J. Vib. Acoust. Stress Reliab. Des.*, 110, 371-377.

44. Lai, M.L., 1988. "Modelling of Transient Vibrations With Statistical Energy Analysis Techniques," *Ph.D Dissertation*, Dept. of Mechanical and Aerospace Engineering, State University of New York at Buffalo, Buffalo, NY.

45. Lai, M.L. and Soong, T.T., 1990. "Statistical Energy Analysis of Primary-Secondary Structural Systems, " *J. Eng. Mech.*, ASCE, 116, 2400-2413.

46. Lai, M.L. and Soong, T.T., 1991. "Seismic Design Considerations for Secondary Structural Systems," *J. Struct. Eng.*, ASCE, 117(2), 459-472.

47. Lee, M.C. and Penzien, J., 1980."Stochastic Seismic Analysis of Nuclear Power Plants and Piping Systems Subjected to Multiple Excitations," *Report. UCB/EERC-80/19*, University of California, Berkerly, CA.

48. Lin, C.W. and Liu, T.H., 1975."A Discussion of Coupling and Resonance Effects for Integrated Systems Consisting of Subsystems," *Proc. Extreme Load Conditions and Limit Analysis Procedures for Structural Reactor Safeguards and Containment Structures*, Berlin, Germany, Paper U3/3.

49. Lin, C.W. and Esselman, T.C., 1983. "Piping Dynamic Analysis with Subsystem/System Interaction," *Proc. ASME 4th Congr. Press. Vess. Pip.*, Portland, Oregon, PVP-73, 1-20.

50. Lin, J. and Mahin, S., 1985."Seismic Response of Light Subsystems on Inelastic Structures," *J. Struct. Eng.*, ASCE, 111(2), 400-417.

51. Luft, R.W., 1979. "Optimal Tuned Mass Dampers for Buildings," *J. Struct. Div.*, ASCE, 105, 2766-2772.

52. Lyon, R.H. and Eichler, E., 1964. "Random Vibration of Connected Structures," *J. Acoust. Soc. Am.*, 36(7), 1344-1354.

53. Lyon, R.H. and Maidanik, G., 1961. "Power Flow Between Linearly Coupled Oscillators," *J Acoust. Soc. Am.*, 34(5), 623-639.

54. Lyon, R.H. and Scharton, T.D., 1965. "Vibrational Energy Transmission in Three Element Structure," *J. Acoust. Soc. Am.*, 38(2), 253-261.

55. Lyon, R.H., 1975. *Statistical Energy Analysis of Dynamical Systems: Theory and Applications*, MIT Press, Cambridge, MA.

56. McCue, G.M. and Kost, G., 1976. "The Interaction of Building Components During Earthquakes," *U.S. Department of Commerce*, PB-258 326.

57. McNamara, R.J., 1977. "Tuned Mass Dampers for Buildings," *J. Struct. Div.*, ASCE, 103, 1785-1798.

58. Nakhata, T., Newmark, N.M. and Hall, W.J., 1973."Approximate Dynamic Response of Light Secondary Systems," *Struct. Research Series Report No. 396,* Civil Engineering Studies, University of Illinois, Urbana, Ill.

59. Newland, D.E., 1966. "Calculation of Power Flow Between Coupled Oscillators," *J. Sound Vib.*, 3(3), 262-276.

60. Newmark, N.M., 1972. "Earthquake Response Analysis of Reactor Structures," *Nucl. Eng. Des.*, 20(2), 303-322.

61. Penzien, J. and Chopra, A.K., 1965."Earthquake Response of Appendage on a Multistory Building," *Proc. 3rd WCEE*, New Zealand, II, 476-486.

62. Peters, K.A., Schmitz, D. and Wagner, U., 1977. "Determination of Floor Response Spectra on the Basis of the Response Spectrum Method," *Nucl. Eng. Des.*, 44, 255-262.

63. Porush, A.R., 1990. "An Overview of the Current Building Code Seismic Requirements for Nonstructural Elements," *ATC-29 Seminar: Seismic Design and Performance of Equipment and Nonstructural Elements in Building and Industrial Structures*, Irvine, CA.

64. Powell, G.H., 1979. "Missing Mass Correction in Modal Analysis of Piping Systems," *Proc. 5th Int. Conf. on SMiRT*, Berlin, Germany, K10/3, 1-7.

65. Powell, R.E. and Quartararo, L.R., 1987. "Statistical Energy Analysis of Transient Vibration," *Statistical Energy Analysis* (Ed. by Hsu, K.H., Nefske, D.J. and Akay, A.), NCA-Vol. 3, ASME Winter Meeting, Boston, MA, 3-7.

66. Remington, P.J. and Manning, J.E., 1975. "Comparison of Statistical Energy Analysis Power Flow Predictions with an "Exact" Calculation," *J. Acoust. Soc. Am.*, 57(2), 374-379.

67. RTD Standard F9-2T, 1974. *Seismic Requirements for Design of Nuclear Power Plants and Test Facilities.*

68. Ruzicka, G.C. and Robinson, A.R., 1980. "Dynamic Response of Tuned Secondary Systems," Report *UILU-ENG-80-2020*, University of Illinois, Urbana, IL.

69. Sackaman, J.L. and Kelly, J.M., 1979. "Seismic Analysis of Internal Equipment and Components in Structures," *J. Eng. Struct.*, ASCE, 1(4), 179-190.

70. Sackman, J.L., Der Kiureghian, A. and Nour-Omid, B., 1983. "Dynamic Analysis of Light Equipment in Structures: Modal Properties of the Combined Systems," *J. Eng. Mech.*, ASCE, 109, 73-89.

71. Scanlan, R.H. and Sachs, K., 1974. "Earthquake Time History and Response Spectra," *J. Eng. Mech.*, ASCE, 100(4), 635-655.

72. Scharton, T.D. and Lyon, R.H., 1968. "Power Flow and Energy Sharing in Random Vibration," *J. Acoust. Soc. Am.*, 43(6), 1332-1343.

73. Shaw, D.E., 1975. "Seismic Structural Response Analysis for Multiple Support Excitation," *Proc. 3rd Int. Conf. on SMiRT*, London, England, K5/2.

74. Singh, A.K. and Ang, A.H.S., 1974. "Stochastic Prediction of Maximum Seismic Response of Light Secondary System," *Nucl. Eng. Des.*, 29(2), 218-230.

75. Singh, M.P., 1975. "Generation of Seismic Floor Spectra," *J. Eng. Mech.*, ASCE, 101(5), 593-607.

76. Singh, M.P., 1980. "Seismic Design Input for Secondary Structures," *J. Struct. Div.*, ASCE, 106(2), 505-517.

77. Singh, M.P. and Mehta, K.B., 1983. "Seismic Design Response by an Alternative SRSS Rule," *Earthquake Eng. Struct. Dyn.*, 11(6), 771-783.

78. Singh, M.P. and Sharma, A.M., 1985. "Seismic Floor Spectra by Mode Acceleration Approach," *J. Eng. Mech.*, ASCE, 111(11), 1402-1419.

79. Singh, M.P. and Suarez, L.E., 1986. "A Perturbation Analysis of the Eigenproperties of Equipment-Structure System," *Nucl. Eng. Des.*, 97(2), 167-185.

80. Singh, M.P. and Burdisso, R.A., 1987. "Multiple Supported Secondary Systems Part II: Seismic Inputs," *Earthquake Eng. Struct. Dyn.*, 15(1), 73-90.

81. Singh, M.P. and Suarez, L.E., 1987. "Seismic Response Analysis of Structure-Equipment System with Non-Classical Damping Effects," *Earthquake Eng. Struct. Dyn.*, 15(7), 871-888.

82. Singh, M.P., 1988. "Seismic Design of Secondary Systems," *Probabilistic Engineering Mechanics*, 3(3), 151-158.

83. Singh, M.P., 1990. "An Overview of Techniques for Analysis of Non-Structural Components," *ATC-29 Seminar: Seismic Design and Performance of Equipment and Nonstructural Elements in Building and Industrial Structures*, Irving, CA.

84. Singh, M.P. and Suarez, L.E., 1990. "Seismic Design of Rotating Systems," *ATC-29 Seminar: Seismic Design and Performance of Equipment and Nonstructural Elements in Building and Industrial Structures*, Irvine, CA.

85. Smeby, W. and Der Kiureghian, A., 1985. "Modal Combination Rules for Multicomponent Earthquake Excitation," *Earthquake Eng. Struct. Dyn.*, 13(1), 1-12.

86. Smith, P.W. Jr., 1962. "Response and Radiation of Structural Modes Excited by Sound," *J. Acoust. Soc. Am.*, 34(5), 640-647.

87. Soong, T.T., 1989. "Stochastic Structural Dynamics: Research vs. Practice," *Structural Safety*, 6, 129-134.

88. Soong, T.T., Chen, Genda, Wu, Z., Zhang, R-H and Grigoriu, M., 1993. "Assessment of the 1991 NEHRP Provisions for Nonstructural Components and Recommended Revisions," *Report NCEER-93-0003, National Center for Earthquake Engineering Research*, Buffalo, NY.

89. Suarez, L.E. and Singh, M.P., 1986. "Mode Synthesis Approach for the Analysis of Secondary Systems," *Report VPI-E-86-8*, Virginia Polytechnic Institute & State University, Blacksburg, VA.

90. Suarez, L.E. and Singh, M.P, 1988."An Exact Component Mode Synthesis Approach," *Earthquake Eng. Struct. Dyn.*,16(2), 293-310.

91. Sun, J.C., Lalor, N. and Richards, E.J., 1987. "Power Flow and Energy Balance of Nonconservatively Coupled Structures, I: Theory," *J. Sound Vib.*, 112, 321-330.

92. Sun, J.C., Chow, L.C., Lalor, N. and Richards, E.J., 1987. "Power Flow and Energy Balance of Nonconservatively Coupled Structures, II: Experimental Verification of Theory, " *J. Sound Vib.*, 112, 331-343.

93. Sun, J.C. and Ming, R.S., 1988. "Distributive Relationships of Dissipative Energy by Coupling Damping in Nonconservatively Coupled Structure, " *Proc. Inter-Noise 88*, France, 323-326.

94. Toro, G.R.and Mcguire, R.K., 1989."Linear and Nonlinear Response of Structures and Equipment to California and Eastern United States Earthquake," *Electric Power Research Institute*, NP-5566.

95. Tsai, N.C., 1988."Non-Classical Damping in Dynamic Analysis of Base-Isolated Structures with Internal Equipment," *Earthquake Eng. Struct. Dyn.*,16, 29-43.

96. UBC, 1991. *Uniform Building Code*, International Conference of Building Officials, Whittier, California.

97. Ungar, E.E., 1967. "Statistical Energy Analysis of Vibrating Systems, " *J. Eng. Ind.*, ASME, 626-632.

98. U.S. Nuclear Regulatory Commision, 1975. "Standard Review Plan," NUREG-75/087.

99. U.S. Nuclear Regulatory Commision, 1976. "Combination of Modes and Spatial Components in Seismic Response Analysis," *Regulatory Guide* 1.92.

100. U.S. Nuclear Regulatory Commision, 1978. "Regulatory Guide," Revision 1.122.

101. U.S. Nuclear Regulatory Commision, 1980. "Structural Building Response Review," *NUREG/CR-1423*, I-II.

102. U.S. Nuclear Regulatory Commision, 1981. "Subsystem Response Review," NUREG/CR-1700.

103. Vanmarke, E.H., 1977."A Simplified Procedure for Predicting Amplified Response Spectra and Equipment Response," *Proc. 6th WCEE*, III, New Delhi, India.

104. Vashi, K.M.,1975."Seismic Spectral Analysis of Structural Systems Subjected to Nonuniform Excitation at Supports," *Proc. 2nd ASCE Specialty Conf.*, New Orleans, LA,1-A, 188-811.

105. Villaverde, R. and Newmark, N.M., 1980. "Seismic Response of Light Attachments to Buildings," *Structural Research Series No. 469*, University of Illinois, Urbana, Illinois.

106. Wang, Y.K., Subudhi, M. and Bezler, P., 1981."Comparison Study of Time History and Response Spectrum Response for Multiply Supported Piping Systems," *Proc. 7th Int. Conf. on SMiRT*, Chicago, IL, K7/5, 477-483.

107. Warburton, G.B. and Soni, S.R., 1977. "Errors in Response Calculation of Non-Classically Damped Structural Dynamics," *Earthquake Eng. Struct. Dyn.*, 5, 363-375.

108. Wilson, E.L., Der Kiureghian, A. and Bayo, E.P., 1981."A Replacement for the SRSS Method in Seismic Analysis," *Earthquake Eng. Struct. Dyn.*, 9, 187-194.

109. Woodhouse, J., 1981. "Approach to the Background of Statistical Energy Analysis Applied to Structural Vibration," *J. Acoust. Soc. Am.*, 69(6), 1695-1709.

110. Yang, J.N., Sarkani, S. and Long, F.X., 1988."Modal Analysis of Non-Classically Damped Structure Systems Using Canonical Transformations," *Report NCEER-88-0014, National Center for Earthquake Engineering Research*, Buffalo, NY.

111. Zeman, J.L. and Bogdanoff, J.L., 1969. "A Comment on Complex Structural Response to Random Vibrations," *AIAA J.*, 7(7), 1225-1231.

112. Zeman, J.L. and Bogdanoff, J.L., 1971(a). "Letter to the Editor, " *Shock Vib. Digest*, 3(1), 2.

111. Zeman, J.L. and Bogdanoff, J.L., 1971(b). "Statistical Approach to Complex Random Vibration, " *J. Acoust. Soc. Am.*, 50(3), Part 2, 1019-1027.

114. Zhang, R.H. and Soong, T.T. , 1992. "Design and Optimal Placement of Viscoelastic Dampers for Structural Applications," *J. Struct. Eng.*, ASCE, 118(5), 1375-1392.

Appendix A

INTEGRATION FORMULAS

In this appendix, definite integrations of a class of functions have been carried out and listed below. All the roots of $h_i(\omega)$ $(i = 2, 4, 6, 8)$ are assumed in the upper plane.

When $g_2(\omega) = B_0\omega^2 + B_1$ *and* $h_2(\omega) = -C_0\omega^2 + C_1 j\omega + C_2$

$$\int_{-\infty}^{\infty} \frac{g_2(\omega)}{|h_2(\omega)|^2} d\omega = \frac{\pi(B_0C_2 + B_1C_0)}{C_0C_1C_2} \tag{A. 1}$$

When $g_4(\omega) = B_0\omega^6 + B_1\omega^4 + B_2\omega^2 + B_3$

$h_4(\omega) = C_0\omega^4 - C_1 j\omega^3 - C_2\omega^2 + C_3 j\omega + C_4$

$$\int_{-\infty}^{\infty} \frac{g_4(\omega)}{|h_4(\omega)|^2} d\omega = \frac{\pi[B_0(C_1C_4 - C_2C_3) - B_1C_0C_3 - B_2C_0C_1 + B_3C_0(C_0C_3 - C_1C_2)/C_4]}{C_0(C_0C_3^2 + C_1^2C_4 - C_1C_2C_3)} \tag{A. 2}$$

When $g_6(\omega) = B_0\omega^{10} + B_1\omega^8 + B_2\omega^6 + B_3\omega^4 + B_4\omega^2 + B_5$

$h_6(\omega) = -C_0\omega^6 + C_1 j\omega^5 + C_2\omega^4 - C_3 j\omega^3 - C_4\omega^2 + C_5 j\omega + C_6$

$$\int_{-\infty}^{\infty} \frac{g_6(\omega)}{|h_6(\omega)|^2} d\omega = \frac{\pi(B_0A_1 + B_1A_2 + B_2A_3 + B_3A_4 + B_4A_5 + B_5A_6)}{C_0(C_1A_1 - C_3A_2 + C_5A_3)} \tag{A. 3}$$

in which

$$A_1 = C_6^2(C_2C_3^2 + C_1^2C_6 - C_1C_2C_5 - C_1C_3C_4) - C_5C_6(C_2C_3C_4 + C_0C_4C_5 + C_1C_2C_6 - C_0C_3C_6 - C_2^2C_5 - C_1C_4^2)$$

$$A_2 = C_0C_6(C_3^2C_6 - C_1C_5C_6 - C_3C_4C_5 + C_2C_5^2)$$

$$A_3 = C_0C_6(C_0C_5^2 + C_1C_3C_6 - C_1C_4C_5)$$

$$A_4 = C_0C_6(C_0C_3C_5 + C_1^2C_6 - C_1C_2C_5)$$

$$A_5 = C_0C_6(C_0C_3^2 - C_0C_1C_5 + C_1^2C_4 - C_1C_2C_3)$$

$$A_6 = C_0^2(C_0C_5^2 + C_3^2C_4 - C_1C_4C_5 - C_2C_3C_5)$$

$$-C_0C_1(C_0C_4C_5 + C_1C_2C_6 + C_2C_3C_4 - C_0C_3C_6 - C_2^2C_5 - C_1C_4^2)$$

When $g_8(\omega) = B_0\omega^{14} + B_1\omega^{12} + B_2\omega^{10} + B_3\omega^8 + B_4\omega^6 + B_5\omega^4 + B_6\omega^2 + B_7$

$$h_8(\omega) = C_0\omega^8 - C_1j\omega^7 - C_2\omega^6 + C_3j\omega^5 + C_4\omega^4 - C_5j\omega^3 - C_6\omega^2 + C_7j\omega + C_8$$

$$\int_{-\infty}^{\infty} \frac{g_8(\omega)}{|h_8(\omega)|^2} d\omega = \frac{\pi(B_0A_1 + B_1A_2 + B_2A_3 + B_3A_4 + B_4A_5 + B_5A_6 + B_6A_7 + B_7A_8)}{C_0(C_1A_1 - C_3A_2 + C_5A_3 - C_7A_4)} \quad \text{(A. 4)}$$

in which

$$A_1 = (C_6C_7 - C_5C_8)D_1 - C_7^2D_2 + C_7C_8D_3 + C_7C_8D_{14} - C_8^2D_{15}$$

$$A_2 = C_1C_7D_{16} - C_1C_8D_7 - C_0C_7D_{17} + C_0C_8D_9$$

$$A_3 = C_1C_7D_{18} - C_1C_8D_{19} - C_0C_7D_{20} + C_0C_8D_{21}$$

$$A_4 = C_1C_7D_{22} - C_1C_8D_{23} - C_0C_7D_{24} + C_0C_8D_{25}$$

$$A_5 = C_1C_7D_{26} - C_1C_8D_{27} - C_0C_7D_3 + C_0C_8D_{15}$$

$$A_6 = C_1C_2D_1 - C_1^2D_4 + C_0C_1D_7 - C_0C_3D_1 + C_0C_1D_{28} - C_0^2D_9$$

$$A_7 = [(C_1C_2 - C_0C_3)(C_6D_1 - C_7D_2 + C_8D_3) - C_1^2(C_6D_4 - C_7D_5 + C_8D_6)$$
$$+ C_0C_1(C_6D_7 - C_7D_8 + C_6D_{28} - C_7D_{29} + C_8D_{30}) - C_0^2(C_6D_9 - C_7D_{31})]/C_8$$

$$D_1 = C_3C_4C_5 + C_1C_5C_6 + C_2C_3C_7 - C_1C_4C_7 - C_3^2C_6 - C_2C_5^2$$

$$D_2 = C_3C_4^2 + C_2^2C_7 + C_0C_5C_6 - C_0C_4C_7 - C_2C_3C_6 - C_2C_4C_5$$

$$D_3 = C_3^2C_4 + C_0C_5^2 + C_1C_2C_7 - C_0C_3C_7 - C_2C_3C_5 - C_1C_4C_5$$

$$D_4 = C_4^2C_5 + C_1C_6^2 + C_2C_3C_8 - C_1C_4C_8 - C_3C_4C_6 - C_2C_5C_6$$

$$D_5 = C_4^3 + C_0C_6^2 + C_2^2C_8 - C_0C_4C_8 - 2C_2C_4C_6$$

$$D_6 = C_3C_4^2 + C_1C_2C_8 + C_0C_5C_6 - C_0C_3C_8 - C_2C_4C_5 - C_1C_4C_6$$

$$D_7 = C_4C_5^2 + C_1C_6C_7 + C_3^2C_8 - C_1C_5C_8 - C_3C_4C_7 - C_3C_5C_6$$

$$D_8 = C_4^2C_5 + C_2C_3C_8 + C_0C_6C_7 - C_0C_5C_8 - C_2C_4C_7 - C_3C_4C_6$$

$$D_9 = C_5^3 + C_1C_7^2 - 2C_3C_5C_7$$

$$D_{10} = C_5^2C_6 + C_1C_7C_8 - C_3C_5C_8 - C_4C_5C_7$$

$$D_{11} = C_5^2C_6 + C_1C_7C_8 - C_3C_6C_7 - C_3C_5C_8$$

$$D_{12} = C_1C_8^2 - C_3C_6C_8 + C_5C_6^2 - C_4C_5C_8$$

$$D_{13} = C_3C_4C_5 + C_1C_3C_8 - C_1C_4C_7 - C_3^2C_6$$

$$D_{14} = C_3^2C_4 + C_1C_2C_7 - C_1C_3C_6 - C_2C_3C_5$$

$$D_{15} = C_3^3 + C_1^2C_7 - 2C_1C_3C_5$$

$$D_{16} = C_4C_5C_6 + C_2C_6C_7 + C_3C_4C_8 - C_2C_5C_8 - C_4^2C_7 - C_3C_6^2$$

$$D_{17} = C_5^2C_6 + C_2C_7^2 - C_4C_5C_7 - C_3C_6C_7$$

$$D_{18} = C_2C_5C_6 + C_0C_6C_7 + C_1C_4C_8 - C_0C_5C_8 - C_2C_4C_7 - C_1C_6^2$$

$$D_{19} = C_2C_5^2 + C_1C_3C_8 - C_2C_3C_7 - C_1C_5C_6$$

$$D_{20} = C_3C_5C_6 + C_0C_7^2 - C_3C_4C_7 - C_1C_6C_7$$

$$D_{21} = C_3C_5^2 - C_3^2C_7 - C_1C_5C_7$$

$$D_{22} = C_2C_3C_6 + C_0C_4C_7 + C_1C_2C_8 - C_0C_3C_8 - C_2^2C_7 - C_1C_4C_6$$

$$D_{23} = C_2C_3C_5 + C_1^2C_8 - C_1C_2C_7 - C_1C_4C_5$$

$$D_{24} = C_3^2C_6 + C_0C_5C_7 - C_2C_3C_7 - C_1C_5C_6$$

$$D_{25} = C_3^2C_5 - C_1C_3C_7 - C_1C_5^2$$

$$D_{26} = C_2C_3C_4 + C_1C_2C_6 + C_0C_4C_5 - C_0C_3C_6 - C_2^2C_5 - C_1C_4^2$$

$$D_{27} = C_2C_3^2 + C_1^2C_6 - C_1C_2C_5 - C_1C_3C_4$$

$$D_{28} = C_4C_5^2 + C_1C_6C_7 - C_3C_5C_6 - C_2C_5C_7$$

$$D_{29} = C_4^2C_5 + C_0C_6C_7 - C_2C_5C_6 - C_2C_4C_7$$

$$D_{30} = C_3C_4C_5 + C_0C_5C_7 - C_2C_5^2 - C_1C_4C_7$$

$$D_{31} = C_4C_5^2 + C_0C_7^2 - C_2C_5C_7 - C_3C_4C_7$$

NATIONAL CENTER FOR EARTHQUAKE ENGINEERING RESEARCH
LIST OF TECHNICAL REPORTS

The National Center for Earthquake Engineering Research (NCEER) publishes technical reports on a variety of subjects related to earthquake engineering written by authors funded through NCEER. These reports are available from both NCEER's Publications Department and the National Technical Information Service (NTIS). Requests for reports should be directed to the Publications Department, National Center for Earthquake Engineering Research, State University of New York at Buffalo, Red Jacket Quadrangle, Buffalo, New York 14261. Reports can also be requested through NTIS, 5285 Port Royal Road, Springfield, Virginia 22161. NTIS accession numbers are shown in parenthesis, if available.

NCEER-87-0001 "First-Year Program in Research, Education and Technology Transfer," 3/5/87, (PB88-134275).

NCEER-87-0002 "Experimental Evaluation of Instantaneous Optimal Algorithms for Structural Control," by R.C. Lin, T.T. Soong and A.M. Reinhorn, 4/20/87, (PB88-134341).

NCEER-87-0003 "Experimentation Using the Earthquake Simulation Facilities at University at Buffalo," by A.M. Reinhorn and R.L. Ketter, to be published.

NCEER-87-0004 "The System Characteristics and Performance of a Shaking Table," by J.S. Hwang, K.C. Chang and G.C. Lee, 6/1/87, (PB88-134259). This report is available only through NTIS (see address given above).

NCEER-87-0005 "A Finite Element Formulation for Nonlinear Viscoplastic Material Using a Q Model," by O. Gyebi and G. Dasgupta, 11/2/87, (PB88-213764).

NCEER-87-0006 "Symbolic Manipulation Program (SMP) - Algebraic Codes for Two and Three Dimensional Finite Element Formulations," by X. Lee and G. Dasgupta, 11/9/87, (PB88-218522).

NCEER-87-0007 "Instantaneous Optimal Control Laws for Tall Buildings Under Seismic Excitations," by J.N. Yang, A. Akbarpour and P. Ghaemmaghami, 6/10/87, (PB88-134333). This report is only available through NTIS (see address given above).

NCEER-87-0008 "IDARC: Inelastic Damage Analysis of Reinforced Concrete Frame - Shear-Wall Structures," by Y.J. Park, A.M. Reinhorn and S.K. Kunnath, 7/20/87, (PB88-134325).

NCEER-87-0009 "Liquefaction Potential for New York State: A Preliminary Report on Sites in Manhattan and Buffalo," by M. Budhu, V. Vijayakumar, R.F. Giese and L. Baumgras, 8/31/87, (PB88-163704). This report is available only through NTIS (see address given above).

NCEER-87-0010 "Vertical and Torsional Vibration of Foundations in Inhomogeneous Media," by A.S. Veletsos and K.W. Dotson, 6/1/87, (PB88-134291).

NCEER-87-0011 "Seismic Probabilistic Risk Assessment and Seismic Margins Studies for Nuclear Power Plants," by Howard H.M. Hwang, 6/15/87, (PB88-134267).

NCEER-87-0012 "Parametric Studies of Frequency Response of Secondary Systems Under Ground-Acceleration Excitations," by Y. Yong and Y.K. Lin, 6/10/87, (PB88-134309).

NCEER-87-0013 "Frequency Response of Secondary Systems Under Seismic Excitation," by J.A. HoLung, J. Cai and Y.K. Lin, 7/31/87, (PB88-134317).

NCEER-87-0014 "Modelling Earthquake Ground Motions in Seismically Active Regions Using Parametric Time Series Methods," by G.W. Ellis and A.S. Cakmak, 8/25/87, (PB88-134283).

NCEER-87-0015 "Detection and Assessment of Seismic Structural Damage," by E. DiPasquale and A.S. Cakmak, 8/25/87, (PB88-163712).

NCEER-87-0016 "Pipeline Experiment at Parkfield, California," by J. Isenberg and E. Richardson, 9/15/87, (PB88-163720). This report is available only through NTIS (see address given above).

NCEER-87-0017 "Digital Simulation of Seismic Ground Motion," by M. Shinozuka, G. Deodatis and T. Harada, 8/31/87, (PB88-155197). This report is available only through NTIS (see address given above).

NCEER-87-0018 "Practical Considerations for Structural Control: System Uncertainty, System Time Delay and Truncation of Small Control Forces," J.N. Yang and A. Akbarpour, 8/10/87, (PB88-163738).

NCEER-87-0019 "Modal Analysis of Nonclassically Damped Structural Systems Using Canonical Transformation," by J.N. Yang, S. Sarkani and F.X. Long, 9/27/87, (PB88-187851).

NCEER-87-0020 "A Nonstationary Solution in Random Vibration Theory," by J.R. Red-Horse and P.D. Spanos, 11/3/87, (PB88-163746).

NCEER-87-0021 "Horizontal Impedances for Radially Inhomogeneous Viscoelastic Soil Layers," by A.S. Veletsos and K.W. Dotson, 10/15/87, (PB88-150859).

NCEER-87-0022 "Seismic Damage Assessment of Reinforced Concrete Members," by Y.S. Chung, C. Meyer and M. Shinozuka, 10/9/87, (PB88-150867). This report is available only through NTIS (see address given above).

NCEER-87-0023 "Active Structural Control in Civil Engineering," by T.T. Soong, 11/11/87, (PB88-187778).

NCEER-87-0024 "Vertical and Torsional Impedances for Radially Inhomogeneous Viscoelastic Soil Layers," by K.W. Dotson and A.S. Veletsos, 12/87, (PB88-187786).

NCEER-87-0025 "Proceedings from the Symposium on Seismic Hazards, Ground Motions, Soil-Liquefaction and Engineering Practice in Eastern North America," October 20-22, 1987, edited by K.H. Jacob, 12/87, (PB88-188115).

NCEER-87-0026 "Report on the Whittier-Narrows, California, Earthquake of October 1, 1987," by J. Pantelic and A. Reinhorn, 11/87, (PB88-187752). This report is available only through NTIS (see address given above).

NCEER-87-0027 "Design of a Modular Program for Transient Nonlinear Analysis of Large 3-D Building Structures," by S. Srivastav and J.F. Abel, 12/30/87, (PB88-187950).

NCEER-87-0028 "Second-Year Program in Research, Education and Technology Transfer," 3/8/88, (PB88-219480).

NCEER-88-0001 "Workshop on Seismic Computer Analysis and Design of Buildings With Interactive Graphics," by W. McGuire, J.F. Abel and C.H. Conley, 1/18/88, (PB88-187760).

NCEER-88-0002 "Optimal Control of Nonlinear Flexible Structures," by J.N. Yang, F.X. Long and D. Wong, 1/22/88, (PB88-213772).

NCEER-88-0003 "Substructuring Techniques in the Time Domain for Primary-Secondary Structural Systems," by G.D. Manolis and G. Juhn, 2/10/88, (PB88-213780).

NCEER-88-0004 "Iterative Seismic Analysis of Primary-Secondary Systems," by A. Singhal, L.D. Lutes and P.D. Spanos, 2/23/88, (PB88-213798).

NCEER-88-0005 "Stochastic Finite Element Expansion for Random Media," by P.D. Spanos and R. Ghanem, 3/14/88, (PB88-213806).

NCEER-88-0006 "Combining Structural Optimization and Structural Control," by F.Y. Cheng and C.P. Pantelides, 1/10/88, (PB88-213814).

NCEER-88-0007 "Seismic Performance Assessment of Code-Designed Structures," by H.H-M. Hwang, J-W. Jaw and H-J. Shau, 3/20/88, (PB88-219423).

NCEER-88-0008 "Reliability Analysis of Code-Designed Structures Under Natural Hazards," by H.H-M. Hwang, H. Ushiba and M. Shinozuka, 2/29/88, (PB88-229471).

NCEER-88-0009 "Seismic Fragility Analysis of Shear Wall Structures," by J-W Jaw and H.H-M. Hwang, 4/30/88, (PB89-102867).

NCEER-88-0010 "Base Isolation of a Multi-Story Building Under a Harmonic Ground Motion - A Comparison of Performances of Various Systems," by F-G Fan, G. Ahmadi and I.G. Tadjbakhsh, 5/18/88, (PB89 122238)

NCEER-88-0011 "Seismic Floor Response Spectra for a Combined System by Green's Functions," by F.M. Lavelle, L.A. Bergman and P.D. Spanos, 5/1/88, (PB89-102875).

NCEER-88-0012 "A New Solution Technique for Randomly Excited Hysteretic Structures," by G.Q. Cai and Y.K. Lin, 5/16/88, (PB89-102883).

NCEER-88-0013 "A Study of Radiation Damping and Soil-Structure Interaction Effects in the Centrifuge," by K. Weissman, supervised by J.H. Prevost, 5/24/88, (PB89-144703).

NCEER-88-0014 "Parameter Identification and Implementation of a Kinematic Plasticity Model for Frictional Soils," by J.H. Prevost and D.V. Griffiths, to be published.

NCEER-88-0015 "Two- and Three- Dimensional Dynamic Finite Element Analyses of the Long Valley Dam," by D.V. Griffiths and J.H. Prevost, 6/17/88, (PB89-144711).

NCEER-88-0016 "Damage Assessment of Reinforced Concrete Structures in Eastern United States," by A.M. Reinhorn, M.J. Seidel, S.K. Kunnath and Y.J. Park, 6/15/88, (PB89-122220).

NCEER-88-0017 "Dynamic Compliance of Vertically Loaded Strip Foundations in Multilayered Viscoelastic Soils," by S. Ahmad and A.S.M. Israil, 6/17/88, (PB89-102891).

NCEER-88-0018 "An Experimental Study of Seismic Structural Response With Added Viscoelastic Dampers," by R.C. Lin, Z. Liang, T.T. Soong and R.H. Zhang, 6/30/88, (PB89-122212). This report is available only through NTIS (see address given above).

NCEER-88-0019 "Experimental Investigation of Primary - Secondary System Interaction," by G.D. Manolis, G. Juhn and A.M. Reinhorn, 5/27/88, (PB89-122204).

NCEER-88-0020 "A Response Spectrum Approach For Analysis of Nonclassically Damped Structures," by J.N. Yang, S. Sarkani and F.X. Long, 4/22/88, (PB89-102909).

NCEER-88-0021 "Seismic Interaction of Structures and Soils: Stochastic Approach," by A.S. Veletsos and A.M. Prasad, 7/21/88, (PB89-122196).

NCEER-88-0022 "Identification of the Serviceability Limit State and Detection of Seismic Structural Damage," by E. DiPasquale and A.S. Cakmak, 6/15/88, (PB89-122188). This report is available only through NTIS (see address given above).

NCEER-88-0023 "Multi-Hazard Risk Analysis: Case of a Simple Offshore Structure," by B.K. Bhartia and E.H. Vanmarcke, 7/21/88, (PB89-145213).

NCEER-88-0024 "Automated Seismic Design of Reinforced Concrete Buildings," by Y.S. Chung, C. Meyer and M. Shinozuka, 7/5/88, (PB89-122170). This report is available only through NTIS (see address given above).

NCEER-88-0025 "Experimental Study of Active Control of MDOF Structures Under Seismic Excitations," by L.L. Chung, R.C. Lin, T.T. Soong and A.M. Reinhorn, 7/10/88, (PB89-122600).

NCEER-88-0026 "Earthquake Simulation Tests of a Low-Rise Metal Structure," by J.S. Hwang, K.C. Chang, G.C. Lee and R.L. Ketter, 8/1/88, (PB89-102917).

NCEER-88-0027 "Systems Study of Urban Response and Reconstruction Due to Catastrophic Earthquakes," by F. Kozin and H.K. Zhou, 9/22/88, (PB90-162348).

NCEER-88-0028 "Seismic Fragility Analysis of Plane Frame Structures," by H.H-M. Hwang and Y.K. Low, 7/31/88, (PB89-131445).

NCEER-88-0029 "Response Analysis of Stochastic Structures," by A. Kardara, C. Bucher and M. Shinozuka, 9/22/88, (PB89-174429).

NCEER-88-0030 "Nonnormal Accelerations Due to Yielding in a Primary Structure," by D.C.K. Chen and L.D. Lutes, 9/19/88, (PB89-131437).

NCEER-88-0031 "Design Approaches for Soil-Structure Interaction," by A.S. Veletsos, A.M. Prasad and Y. Tang, 12/30/88, (PB89-174437). This report is available only through NTIS (see address given above).

NCEER-88-0032 "A Re-evaluation of Design Spectra for Seismic Damage Control," by C.J. Turkstra and A.G. Tallin, 11/7/88, (PB89-145221).

NCEER-88-0033 "The Behavior and Design of Noncontact Lap Splices Subjected to Repeated Inelastic Tensile Loading," by V.E. Sagan, P. Gergely and R.N. White, 12/8/88, (PB89-163737).

NCEER-88-0034 "Seismic Response of Pile Foundations," by S.M. Mamoon, P.K. Banerjee and S. Ahmad, 11/1/88, (PB89-145239).

NCEER-88-0035 "Modeling of R/C Building Structures With Flexible Floor Diaphragms (IDARC2)," by A.M. Reinhorn, S.K. Kunnath and N. Panahshahi, 9/7/88, (PB89-207153).

NCEER-88-0036 "Solution of the Dam-Reservoir Interaction Problem Using a Combination of FEM, BEM with Particular Integrals, Modal Analysis, and Substructuring," by C-S. Tsai, G.C. Lee and R.L. Ketter, 12/31/88, (PB89-207146).

NCEER-88-0037 "Optimal Placement of Actuators for Structural Control," by F.Y. Cheng and C.P. Pantelides, 8/15/88, (PB89-162846).

NCEER-88-0038 "Teflon Bearings in Aseismic Base Isolation: Experimental Studies and Mathematical Modeling," by A. Mokha, M.C. Constantinou and A.M. Reinhorn, 12/5/88, (PB89-218457). This report is available only through NTIS (see address given above).

NCEER-88-0039 "Seismic Behavior of Flat Slab High-Rise Buildings in the New York City Area," by P. Weidlinger and M. Ettouney, 10/15/88, (PB90-145681).

NCEER-88-0040 "Evaluation of the Earthquake Resistance of Existing Buildings in New York City," by P. Weidlinger and M. Ettouney, 10/15/88, to be published.

NCEER-88-0041 "Small-Scale Modeling Techniques for Reinforced Concrete Structures Subjected to Seismic Loads," by W. Kim, A. El-Attar and R.N. White, 11/22/88, (PB89-189625).

NCEER-88-0042 "Modeling Strong Ground Motion from Multiple Event Earthquakes," by G.W. Ellis and A.S. Cakmak, 10/15/88, (PB89-174445).

NCEER-88-0043 "Nonstationary Models of Seismic Ground Acceleration," by M. Grigoriu, S.E. Ruiz and E. Rosenblueth, 7/15/88, (PB89-189617).

NCEER-88-0044 "SARCF User's Guide: Seismic Analysis of Reinforced Concrete Frames," by Y.S. Chung, C. Meyer and M. Shinozuka, 11/9/88, (PB89-174452).

NCEER-88-0045 "First Expert Panel Meeting on Disaster Research and Planning," edited by J. Pantelic and J. Stoyle, 9/15/88, (PB89-174460).

NCEER-88-0046 "Preliminary Studies of the Effect of Degrading Infill Walls on the Nonlinear Seismic Response of Steel Frames," by C.Z. Chrysostomou, P. Gergely and J.F. Abel, 12/19/88, (PB89-208383).

NCEER-88-0047 "Reinforced Concrete Frame Component Testing Facility - Design, Construction, Instrumentation and Operation," by S.P. Pessiki, C. Conley, T. Bond, P. Gergely and R.N. White, 12/16/88, (PB89-174478).

NCEER-89-0001 "Effects of Protective Cushion and Soil Compliancy on the Response of Equipment Within a Seismically Excited Building," by J.A. HoLung, 2/16/89, (PB89-207179).

NCEER-89-0002 "Statistical Evaluation of Response Modification Factors for Reinforced Concrete Structures," by H.H-M. Hwang and J-W. Jaw, 2/17/89, (PB89-207187).

NCEER-89-0003 "Hysteretic Columns Under Random Excitation," by G-Q. Cai and Y.K. Lin, 1/9/89, (PB89-196513).

NCEER-89-0004 "Experimental Study of 'Elephant Foot Bulge' Instability of Thin-Walled Metal Tanks," by Z-H. Jia and R.L. Ketter, 2/22/89, (PB89-207195).

NCEER-89-0005 "Experiment on Performance of Buried Pipelines Across San Andreas Fault," by J. Isenberg, E. Richardson and T.D. O'Rourke, 3/10/89, (PB89-218440). This report is available only through NTIS (see address given above).

NCEER-89-0006 "A Knowledge-Based Approach to Structural Design of Earthquake-Resistant Buildings," by M. Subramani, P. Gergely, C.H. Conley, J.F. Abel and A.H. Zaghw, 1/15/89, (PB89-218465).

NCEER-89-0007 "Liquefaction Hazards and Their Effects on Buried Pipelines," by T.D. O'Rourke and P.A. Lane, 2/1/89, (PB89-218481).

NCEER-89-0008 "Fundamentals of System Identification in Structural Dynamics," by H. Imai, C-B. Yun, O. Maruyama and M. Shinozuka, 1/26/89, (PB89-207211).

NCEER-89-0009 "Effects of the 1985 Michoacan Earthquake on Water Systems and Other Buried Lifelines in Mexico," by A.G. Ayala and M.J. O'Rourke, 3/8/89, (PB89-207229).

NCEER-89-R010 "NCEER Bibliography of Earthquake Education Materials," by K.E.K. Ross, Second Revision, 9/1/89, (PB90-125352).

NCEER-89-0011 "Inelastic Three-Dimensional Response Analysis of Reinforced Concrete Building Structures (IDARC-3D), Part I - Modeling," by S.K. Kunnath and A.M. Reinhorn, 4/17/89, (PB90-114612).

NCEER-89-0012 "Recommended Modifications to ATC-14," by C.D. Poland and J.O. Malley, 4/12/89, (PB90-108648).

NCEER-89-0013 "Repair and Strengthening of Beam-to-Column Connections Subjected to Earthquake Loading," by M. Corazao and A.J. Durrani, 2/28/89, (PB90-109885).

NCEER-89-0014 "Program EXKAL2 for Identification of Structural Dynamic Systems," by O. Maruyama, C-B. Yun, M. Hoshiya and M. Shinozuka, 5/19/89, (PB90-109877).

NCEER-89-0015 "Response of Frames With Bolted Semi-Rigid Connections, Part I - Experimental Study and Analytical Predictions," by P.J. DiCorso, A.M. Reinhorn, J.R. Dickerson, J.B. Radziminski and W.L. Harper, 6/1/89, to be published.

NCEER-89-0016 "ARMA Monte Carlo Simulation in Probabilistic Structural Analysis," by P.D. Spanos and M.P. Mignolet, 7/10/89, (PB90-109893)

NCEER-89-P017 "Preliminary Proceedings from the Conference on Disaster Preparedness - The Place of Earthquake Education in Our Schools," Edited by K.E.K. Ross, 6/23/89, (PB90-108606).

NCEER-89-0017 "Proceedings from the Conference on Disaster Preparedness - The Place of Earthquake Education in Our Schools," Edited by K.E.K. Ross, 12/31/89, (PB90-207895). This report is available only through NTIS (see address given above).

NCEER-89-0018 "Multidimensional Models of Hysteretic Material Behavior for Vibration Analysis of Shape Memory Energy Absorbing Devices, by E.J. Graesser and F.A. Cozzarelli, 6/7/89, (PB90-164146).

NCEER-89-0019 "Nonlinear Dynamic Analysis of Three-Dimensional Base Isolated Structures (3D-BASIS)," by S. Nagarajaiah, A.M. Reinhorn and M.C. Constantinou, 8/3/89, (PB90-161936). This report is available only through NTIS (see address given above).

NCEER-89-0020 "Structural Control Considering Time-Rate of Control Forces and Control Rate Constraints," by F.Y. Cheng and C.P. Pantelides, 8/3/89, (PB90-120445).

NCEER-89-0021 "Subsurface Conditions of Memphis and Shelby County," by K.W. Ng, T-S. Chang and H-H.M. Hwang, 7/26/89, (PB90-120437).

NCEER-89-0022 "Seismic Wave Propagation Effects on Straight Jointed Buried Pipelines," by K. Elhmadi and M.J. O'Rourke, 8/24/89, (PB90-162322).

NCEER-89-0023 "Workshop on Serviceability Analysis of Water Delivery Systems," edited by M. Grigoriu, 3/6/89, (PB90-127424).

NCEER-89-0024 "Shaking Table Study of a 1/5 Scale Steel Frame Composed of Tapered Members," by K.C. Chang, J.S. Hwang and G.C. Lee, 9/18/89, (PB90-160169).

NCEER-89-0025 "DYNA1D: A Computer Program for Nonlinear Seismic Site Response Analysis - Technical Documentation," by Jean H. Prevost, 9/14/89, (PB90-161944). This report is available only through NTIS (see address given above).

NCEER-89-0026 "1:4 Scale Model Studies of Active Tendon Systems and Active Mass Dampers for Aseismic Protection," by A.M. Reinhorn, T.T. Soong, R.C. Lin, Y.P. Yang, Y. Fukao, H. Abe and M. Nakai, 9/15/89, (PB90-173246).

NCEER-89-0027 "Scattering of Waves by Inclusions in a Nonhomogeneous Elastic Half Space Solved by Boundary Element Methods," by P.K. Hadley, A. Askar and A.S. Cakmak, 6/15/89, (PB90-145699).

NCEER-89-0028 "Statistical Evaluation of Deflection Amplification Factors for Reinforced Concrete Structures," by H.H.M. Hwang, J-W. Jaw and A.L. Ch'ng, 8/31/89, (PB90-164633).

NCEER-89-0029 "Bedrock Accelerations in Memphis Area Due to Large New Madrid Earthquakes," by H.H.M. Hwang, C.H.S. Chen and G. Yu, 11/7/89, (PB90-162330).

NCEER-89-0030 "Seismic Behavior and Response Sensitivity of Secondary Structural Systems," by Y.Q. Chen and T.T. Soong, 10/23/89, (PB90-164658).

NCEER-89-0031 "Random Vibration and Reliability Analysis of Primary-Secondary Structural Systems," by Y. Ibrahim, M. Grigoriu and T.T. Soong, 11/10/89, (PB90-161951).

NCEER-89-0032 "Proceedings from the Second U.S. - Japan Workshop on Liquefaction, Large Ground Deformation and Their Effects on Lifelines, September 26-29, 1989," Edited by T.D. O'Rourke and M. Hamada, 12/1/89, (PB90-209388).

NCEER-89-0033 "Deterministic Model for Seismic Damage Evaluation of Reinforced Concrete Structures," by J.M. Bracci, A.M. Reinhorn, J.B. Mander and S.K. Kunnath, 9/27/89.

NCEER-89-0034 "On the Relation Between Local and Global Damage Indices," by E. DiPasquale and A.S. Cakmak, 8/15/89, (PB90-173865).

NCEER-89-0035 "Cyclic Undrained Behavior of Nonplastic and Low Plasticity Silts," by A.J. Walker and H.E. Stewart, 7/26/89, (PB90-183518).

NCEER-89-0036 "Liquefaction Potential of Surficial Deposits in the City of Buffalo, New York," by M. Budhu, R. Giese and L. Baumgrass, 1/17/89, (PB90-208455).

NCEER-89-0037 "A Deterministic Assessment of Effects of Ground Motion Incoherence," by A.S. Veletsos and Y. Tang, 7/15/89, (PB90-164294).

NCEER-89-0038 "Workshop on Ground Motion Parameters for Seismic Hazard Mapping," July 17-18, 1989, edited by R.V. Whitman, 12/1/89, (PB90-173923).

NCEER-89-0039 "Seismic Effects on Elevated Transit Lines of the New York City Transit Authority," by C.J. Costantino, C.A. Miller and E. Heymsfield, 12/26/89, (PB90-207887).

NCEER-89-0040 "Centrifugal Modeling of Dynamic Soil-Structure Interaction," by K. Weissman, Supervised by J.H. Prevost, 5/10/89, (PB90-207879).

NCEER-89-0041 "Linearized Identification of Buildings With Cores for Seismic Vulnerability Assessment," by I-K. Ho and A.E. Aktan, 11/1/89, (PB90-251943).

NCEER-90-0001 "Geotechnical and Lifeline Aspects of the October 17, 1989 Loma Prieta Earthquake in San Francisco," by T.D. O'Rourke, H.E. Stewart, F.T. Blackburn and T.S. Dickerman, 1/90, (PB90-208596).

NCEER-90-0002 "Nonnormal Secondary Response Due to Yielding in a Primary Structure," by D.C.K. Chen and L.D. Lutes, 2/28/90, (PB90-251976).

NCEER-90-0003 "Earthquake Education Materials for Grades K-12," by K.E.K. Ross, 4/16/90, (PB91-251984).

NCEER-90-0004 "Catalog of Strong Motion Stations in Eastern North America," by R.W. Busby, 4/3/90, (PB90-251984).

NCEER-90-0005 "NCEER Strong-Motion Data Base: A User Manual for the GeoBase Release (Version 1.0 for the Sun3)," by P. Friberg and K. Jacob, 3/31/90 (PB90-258062).

NCEER-90-0006 "Seismic Hazard Along a Crude Oil Pipeline in the Event of an 1811-1812 Type New Madrid Earthquake," by H.H.M. Hwang and C-H.S. Chen, 4/16/90(PB90-258054).

NCEER-90-0007 "Site-Specific Response Spectra for Memphis Sheahan Pumping Station," by H.H.M. Hwang and C.S. Lee, 5/15/90, (PB91-108811).

NCEER-90-0008 "Pilot Study on Seismic Vulnerability of Crude Oil Transmission Systems," by T. Ariman, R. Dobry, M. Grigoriu, F. Kozin, M. O'Rourke, T. O'Rourke and M. Shinozuka, 5/25/90, (PB91-108837).

NCEER-90-0009 "A Program to Generate Site Dependent Time Histories: EQGEN," by G.W. Ellis, M. Srinivasan and A.S. Cakmak, 1/30/90, (PB91-108829).

NCEER-90-0010 "Active Isolation for Seismic Protection of Operating Rooms," by M.E. Talbott, Supervised by M. Shinozuka, 6/8/9, (PB91-110205).

NCEER-90-0011 "Program LINEARID for Identification of Linear Structural Dynamic Systems," by C-B. Yun and M. Shinozuka, 6/25/90, (PB91-110312).

NCEER-90-0012 "Two-Dimensional Two-Phase Elasto-Plastic Seismic Response of Earth Dams," by A.N. Yiagos, Supervised by J.H. Prevost, 6/20/90, (PB91-110197).

NCEER-90-0013 "Secondary Systems in Base-Isolated Structures: Experimental Investigation, Stochastic Response and Stochastic Sensitivity," by G.D. Manolis, G. Juhn, M.C. Constantinou and A.M. Reinhorn, 7/1/90, (PB91-110320).

NCEER-90-0014 "Seismic Behavior of Lightly-Reinforced Concrete Column and Beam-Column Joint Details," by S.P. Pessiki, C.H. Conley, P. Gergely and R.N. White, 8/22/90, (PB91-108795).

NCEER-90-0015 "Two Hybrid Control Systems for Building Structures Under Strong Earthquakes," by J.N. Yang and A. Danielians, 6/29/90, (PB91-125393).

NCEER-90-0016 "Instantaneous Optimal Control with Acceleration and Velocity Feedback," by J.N. Yang and Z. Li, 6/29/90, (PB91-125401).

NCEER-90-0017 "Reconnaissance Report on the Northern Iran Earthquake of June 21, 1990," by M. Mehrain, 10/4/90, (PB91-125377).

NCEER-90-0018 "Evaluation of Liquefaction Potential in Memphis and Shelby County," by T.S. Chang, P.S. Tang, C.S. Lee and H. Hwang, 8/10/90, (PB91-125427).

NCEER-90-0019 "Experimental and Analytical Study of a Combined Sliding Disc Bearing and Helical Steel Spring Isolation System," by M.C. Constantinou, A.S. Mokha and A.M. Reinhorn, 10/4/90, (PB91-125385).

NCEER-90-0020 "Experimental Study and Analytical Prediction of Earthquake Response of a Sliding Isolation System with a Spherical Surface," by A.S. Mokha, M.C. Constantinou and A.M. Reinhorn, 10/11/90, (PB91-125419).

NCEER-90-0021 "Dynamic Interaction Factors for Floating Pile Groups," by G. Gazetas, K. Fan, A. Kaynia and E. Kausel, 9/10/90, (PB91-170381).

NCEER-90-0022 "Evaluation of Seismic Damage Indices for Reinforced Concrete Structures," by S. Rodriguez-Gomez and A.S. Cakmak, 9/30/90, PB91-171322).

NCEER-90-0023 "Study of Site Response at a Selected Memphis Site," by H. Desai, S. Ahmad, E.S. Gazetas and M.R. Oh, 10/11/90, (PB91-196857).

NCEER-90-0024 "A User's Guide to Strongmo: Version 1.0 of NCEER's Strong-Motion Data Access Tool for PCs and Terminals," by P.A. Friberg and C.A.T. Susch, 11/15/90, (PB91-171272).

NCEER-90-0025 "A Three-Dimensional Analytical Study of Spatial Variability of Seismic Ground Motions," by L-L. Hong and A.H.-S. Ang, 10/30/90, (PB91-170399).

NCEER-90-0026 "MUMOID User's Guide - A Program for the Identification of Modal Parameters," by S. Rodriguez-Gomez and E. DiPasquale, 9/30/90, (PB91-171298).

NCEER 90-0027 "SARCF-II User's Guide - Seismic Analysis of Reinforced Concrete Frames," by S. Rodriguez-Gomez, Y.S. Chung and C. Meyer, 9/30/90, (PB91-171280).

NCEER-90-0028 "Viscous Dampers: Testing, Modeling and Application in Vibration and Seismic Isolation," by N. Makris and M.C. Constantinou, 12/20/90 (PB91-190561).

NCEER-90-0029 "Soil Effects on Earthquake Ground Motions in the Memphis Area," by H. Hwang, C.S. Lee, K.W. Ng and T.S. Chang, 8/2/90, (PB91-190751).

NCEER-91-0001 "Proceedings from the Third Japan-U.S. Workshop on Earthquake Resistant Design of Lifeline Facilities and Countermeasures for Soil Liquefaction, December 17-19, 1990," edited by T.D. O'Rourke and M. Hamada, 2/1/91, (PB91-179259).

NCEER-91-0002 "Physical Space Solutions of Non-Proportionally Damped Systems," by M. Tong, Z. Liang and G.C. Lee, 1/15/91, (PB91-179242).

NCEER-91-0003 "Seismic Response of Single Piles and Pile Groups," by K. Fan and G. Gazetas, 1/10/91, (PB92-174994).

NCEER-91-0004 "Damping of Structures: Part 1 - Theory of Complex Damping," by Z. Liang and G. Lee, 10/10/91, (PB92-197235).

NCEER-91-0005 "3D-BASIS - Nonlinear Dynamic Analysis of Three Dimensional Base Isolated Structures: Part II," by S. Nagarajaiah, A.M. Reinhorn and M.C. Constantinou, 2/28/91, (PB91-190553).

NCEER-91-0006 "A Multidimensional Hysteretic Model for Plasticity Deforming Metals in Energy Absorbing Devices," by E.J. Graesser and F.A. Cozzarelli, 4/9/91, (PB92-108364).

NCEER-91-0007 "A Framework for Customizable Knowledge-Based Expert Systems with an Application to a KBES for Evaluating the Seismic Resistance of Existing Buildings," by E.G. Ibarra-Anaya and S.J. Fenves, 4/9/91, (PB91-210930).

NCEER-91-0008 "Nonlinear Analysis of Steel Frames with Semi-Rigid Connections Using the Capacity Spectrum Method," by G.G. Deierlein, S-H. Hsieh, Y-J. Shen and J.F. Abel, 7/2/91, (PB92-113828).

NCEER-91-0009 "Earthquake Education Materials for Grades K-12," by K.E.K. Ross, 4/30/91, (PB91-212142).

NCEER-91-0010 "Phase Wave Velocities and Displacement Phase Differences in a Harmonically Oscillating Pile," by N. Makris and G. Gazetas, 7/8/91, (PB92-108356).

NCEER-91-0011 "Dynamic Characteristics of a Full-Size Five-Story Steel Structure and a 2/5 Scale Model," by K.C. Chang, G.C. Yao, G.C. Lee, D.S. Hao and Y.C. Yeh," 7/2/91, (PB93-116648).

NCEER-91-0012 "Seismic Response of a 2/5 Scale Steel Structure with Added Viscoelastic Dampers," by K.C. Chang, T.T. Soong, S-T. Oh and M.L. Lai, 5/17/91, (PB92-110816).

NCEER-91-0013 "Earthquake Response of Retaining Walls; Full-Scale Testing and Computational Modeling," by S. Alampalli and A-W.M. Elgamal, 6/20/91, to be published.

NCEER-91-0014 "3D-BASIS-M: Nonlinear Dynamic Analysis of Multiple Building Base Isolated Structures," by P.C. Tsopelas, S. Nagarajaiah, M.C. Constantinou and A.M. Reinhorn, 5/28/91, (PB92-113885).

NCEER-91-0015 "Evaluation of SEAOC Design Requirements for Sliding Isolated Structures," by D. Theodossiou and M.C. Constantinou, 6/10/91, (PB92-114602).

NCEER-91-0016 "Closed-Loop Modal Testing of a 27-Story Reinforced Concrete Flat Plate-Core Building," by H.R. Somaprasad, T. Toksoy, H. Yoshiyuki and A.E. Aktan, 7/15/91, (PB92-129980)

NCEER-91-0017 "Shake Table Test of a 1/6 Scale Two-Story Lightly Reinforced Concrete Building," by A.G. El-Attar, R.N. White and P. Gergely, 2/28/91, (PB92-222447).

NCEER-91-0018 "Shake Table Test of a 1/8 Scale Three-Story Lightly Reinforced Concrete Building," by A.G. El-Attar, R.N. White and P. Gergely, 2/28/91, (PB93-116630).

NCEER-91-0019 "Transfer Functions for Rigid Rectangular Foundations," by A.S. Veletsos, A.M. Prasad and W.H. Wu, 7/31/91.

NCEER-91-0020 "Hybrid Control of Seismic-Excited Nonlinear and Inelastic Structural Systems," by J.N. Yang, Z. Li and A. Danielians, 8/1/91, (PB92-143171).

NCEER-91-0021 "The NCEER-91 Earthquake Catalog: Improved Intensity-Based Magnitudes and Recurrence Relations for U.S. Earthquakes East of New Madrid," by L. Seeber and J.G. Armbruster, 8/28/91, (PB92-176742).

NCEER-91-0022 "Proceedings from the Implementation of Earthquake Planning and Education in Schools: The Need for Change - The Roles of the Changemakers," by K.E.K. Ross and F. Winslow, 7/23/91, (PB92-129998).

NCEER-91-0023 "A Study of Reliability-Based Criteria for Seismic Design of Reinforced Concrete Frame Buildings," by H.H.M. Hwang and H-M. Hsu, 8/10/91, (PB92-140235).

NCEER-91-0024 "Experimental Verification of a Number of Structural System Identification Algorithms," by R.G. Ghanem, H. Gavin and M. Shinozuka, 9/18/91, (PB92-176577).

NCEER-91-0025 "Probabilistic Evaluation of Liquefaction Potential," by H.H.M. Hwang and C.S. Lee," 11/25/91, (PB92-143429).

NCEER-91-0026 "Instantaneous Optimal Control for Linear, Nonlinear and Hysteretic Structures - Stable Controllers," by J.N. Yang and Z. Li, 11/15/91, (PB92-163807).

NCEER-91-0027 "Experimental and Theoretical Study of a Sliding Isolation System for Bridges," by M.C. Constantinou, A. Kartoum, A.M. Reinhorn and P. Bradford, 11/15/91, (PB92-176973).

NCEER-92-0001 "Case Studies of Liquefaction and Lifeline Performance During Past Earthquakes, Volume 1: Japanese Case Studies," Edited by M. Hamada and T. O'Rourke, 2/17/92, (PB92-197243).

NCEER-92-0002 "Case Studies of Liquefaction and Lifeline Performance During Past Earthquakes, Volume 2: United States Case Studies," Edited by T. O'Rourke and M. Hamada, 2/17/92, (PB92-197250).

NCEER-92-0003 "Issues in Earthquake Education," Edited by K. Ross, 2/3/92, (PB92-222389).

NCEER-92-0004 "Proceedings from the First U.S. - Japan Workshop on Earthquake Protective Systems for Bridges," Edited by I.G. Buckle, 2/4/92.

NCEER-92-0005 "Seismic Ground Motion from a Haskell-Type Source in a Multiple-Layered Half-Space," A.P. Theoharis, G. Deodatis and M. Shinozuka, 1/2/92, to be published.

NCEER-92-0006 "Proceedings from the Site Effects Workshop," Edited by R. Whitman, 2/29/92, (PB92-197201).

NCEER-92-0007 "Engineering Evaluation of Permanent Ground Deformations Due to Seismically-Induced Liquefaction," by M.H. Baziar, R. Dobry and A-W.M. Elgamal, 3/24/92, (PB92-222421).

NCEER-92-0008 "A Procedure for the Seismic Evaluation of Buildings in the Central and Eastern United States," by C.D. Poland and J.O. Malley, 4/2/92, (PB92-222439).

NCEER-92-0009 "Experimental and Analytical Study of a Hybrid Isolation System Using Friction Controllable Sliding Bearings," by M.Q. Feng, S. Fujii and M. Shinozuka, 5/15/92, (PB93-150282).

NCEER-92-0010 "Seismic Resistance of Slab-Column Connections in Existing Non-Ductile Flat-Plate Buildings," by A.J. Durrani and Y. Du, 5/18/92.

NCEER-92-0011 "The Hysteretic and Dynamic Behavior of Brick Masonry Walls Upgraded by Ferrocement Coatings Under Cyclic Loading and Strong Simulated Ground Motion," by H. Lee and S.P. Prawel, 5/11/92, to be published.

NCEER-92-0012 "Study of Wire Rope Systems for Seismic Protection of Equipment in Buildings," by G.F. Demetriades, M.C. Constantinou and A.M. Reinhorn, 5/20/92.

NCEER-92-0013 "Shape Memory Structural Dampers: Material Properties, Design and Seismic Testing," by P.R. Witting and F.A. Cozzarelli, 5/26/92.

NCEER-92-0014 "Longitudinal Permanent Ground Deformation Effects on Buried Continuous Pipelines," by M.J. O'Rourke, and C. Nordberg, 6/15/92.

NCEER-92-0015 "A Simulation Method for Stationary Gaussian Random Functions Based on the Sampling Theorem," by M. Grigoriu and S. Balopoulou, 6/11/92, (PB93-127496).

NCEER-92-0016 "Gravity-Load-Designed Reinforced Concrete Buildings: Seismic Evaluation of Existing Construction and Detailing Strategies for Improved Seismic Resistance," by G.W. Hoffmann, S.K. Kunnath, A.M. Reinhorn and J.B. Mander, 7/15/92.

NCEER-92-0017 "Observations on Water System and Pipeline Performance in the Limón Area of Costa Rica Due to the April 22, 1991 Earthquake," by M. O'Rourke and D. Ballantyne, 6/30/92, (PB93-126811).

NCEER-92-0018 "Fourth Edition of Earthquake Education Materials for Grades K-12," Edited by K.E.K. Ross, 8/10/92.

NCEER-92-0019 "Proceedings from the Fourth Japan-U.S. Workshop on Earthquake Resistant Design of Lifeline Facilities and Countermeasures for Soil Liquefaction," Edited by M. Hamada and T.D. O'Rourke, 8/12/92, (PB93-163939).

NCEER-92-0020 "Active Bracing System: A Full Scale Implementation of Active Control," by A.M. Reinhorn, T.T. Soong, R.C. Lin, M.A. Riley, Y.P. Wang, S. Aizawa and M. Higashino, 8/14/92, (PB93-127512).

NCEER-92-0021 "Empirical Analysis of Horizontal Ground Displacement Generated by Liquefaction-Induced Lateral Spreads," by S.F. Bartlett and T.L. Youd, 8/17/92, (PB93-188241).

NCEER-92-0022 "IDARC Version 3.0: Inelastic Damage Analysis of Reinforced Concrete Structures," by S.K. Kunnath, A.M. Reinhorn and R.F. Lobo, 8/31/92, (PB93-227502, A07, MF-A02).

NCEER-92-0023 "A Semi-Empirical Analysis of Strong-Motion Peaks in Terms of Seismic Source, Propagation Path and Local Site Conditions, by M. Kamiyama, M.J. O'Rourke and R. Flores-Berrones, 9/9/92, (PB93-150266).

NCEER-92-0024 "Seismic Behavior of Reinforced Concrete Frame Structures with Nonductile Details, Part I: Summary of Experimental Findings of Full Scale Beam-Column Joint Tests," by A. Beres, R.N. White and P. Gergely, 9/30/92, (PB93-227783, A05, MF-A01).

NCEER-92-0025 "Experimental Results of Repaired and Retrofitted Beam-Column Joint Tests in Lightly Reinforced Concrete Frame Buildings," by A. Beres, S. El-Borgi, R.N. White and P. Gergely, 10/29/92, (PB93-227791, A05, MF-A01).

NCEER-92-0026 "A Generalization of Optimal Control Theory: Linear and Nonlinear Structures," by J.N. Yang, Z. Li and S. Vongchavalitkul, 11/2/92, (PB93-188621).

NCEER-92-0027 "Seismic Resistance of Reinforced Concrete Frame Structures Designed Only for Gravity Loads: Part I - Design and Properties of a One-Third Scale Model Structure," by J.M. Bracci, A.M. Reinhorn and J.B. Mander, 12/1/92.

NCEER-92-0028 "Seismic Resistance of Reinforced Concrete Frame Structures Designed Only for Gravity Loads: Part II - Experimental Performance of Subassemblages," by L.E. Aycardi, J.B. Mander and A.M. Reinhorn, 12/1/92.

NCEER-92-0029 "Seismic Resistance of Reinforced Concrete Frame Structures Designed Only for Gravity Loads: Part III - Experimental Performance and Analytical Study of a Structural Model," by J.M. Bracci, A.M. Reinhorn and J.B. Mander, 12/1/92, (PB93-227528, A09, MF-A01).

NCEER-92-0030 "Evaluation of Seismic Retrofit of Reinforced Concrete Frame Structures: Part I - Experimental Performance of Retrofitted Subassemblages," by D. Choudhuri, J.B. Mander and A.M. Reinhorn, 12/8/92.

NCEER-92-0031 "Evaluation of Seismic Retrofit of Reinforced Concrete Frame Structures: Part II - Experimental Performance and Analytical Study of a Retrofitted Structural Model," by J.M. Bracci, A.M. Reinhorn and J.B. Mander, 12/8/92.

NCEER-92-0032 "Experimental and Analytical Investigation of Seismic Response of Structures with Supplemental Fluid Viscous Dampers," by M.C. Constantinou and M.D. Symans, 12/21/92, (PB93-191435).

NCEER-92-0033 "Reconnaissance Report on the Cairo, Egypt Earthquake of October 12, 1992," by M. Khater, 12/23/92, (PB93-188621).

NCEER-92-0034 "Low-Level Dynamic Characteristics of Four Tall Flat-Plate Buildings in New York City," by H. Gavin, S. Yuan, J. Grossman, E. Pekelis and K. Jacob, 12/28/92, (PB93-188217).

NCEER-93-0001 "An Experimental Study on the Seismic Performance of Brick-Infilled Steel Frames With and Without Retrofit," by J.B. Mander, B. Nair, K. Wojtkowski and J. Ma, 1/29/93, (PB93-227510, A07, MF-A02).

NCEER-93-0002 "Social Accounting for Disaster Preparedness and Recovery Planning," by S. Cole, E. Pantoja and V. Razak, 2/22/93, to be published.

NCEER-93-0003 "Assessment of 1991 NEHRP Provisions for Nonstructural Components and Recommended Revisions," by T.T. Soong, G. Chen, Z. Wu, R-H. Zhang and M. Grigoriu, 3/1/93, (PB93-188639).

NCEER-93-0004 "Evaluation of Static and Response Spectrum Analysis Procedures of SEAOC/UBC for Seismic Isolated Structures," by C.W. Winters and M.C. Constantinou, 3/23/93, (PB93-198299).

NCEER-93-0005 "Earthquakes in the Northeast - Are We Ignoring the Hazard? A Workshop on Earthquake Science and Safety for Educators," edited by K.E.K. Ross, 4/2/93.

NCEER-93-0006 "Inelastic Response of Reinforced Concrete Structures with Viscoelastic Braces," by R.F. Lobo, J.M. Bracci, K.L. Shen, A.M. Reinhorn and T.T. Soong, 4/5/93, (PB93-227486, A05, MF-A02).

NCEER-93-0007 "Seismic Testing of Installation Methods for Computers and Data Processing Equipment," by K. Kosar, T.T. Soong, K.L. Shen, J.A. HoLung and Y.K. Lin, 4/12/93, (PB93-198299).

NCEER-93-0008 "Retrofit of Reinforced Concrete Frames Using Added Dampers," by A. Reinhorn, M. Constantinou and C. Li, to be published.

NCEER-93-0009 "Seismic Applications of Viscoelastic Dampers to Steel Frame Structures," by K.C. Chang and T.T. Soong, to be published.

NCEER-93-0010 "Seismic Performance of Shear-Critical Reinforced Concrete Bridge Piers," by J.B. Mander, S.M. Waheed, M.T.A. Chaudhary and S.S. Chen, 5/12/93, (PB93-227494, A08, MF-A02).

NCEER-93-0011 "3D-BASIS-TABS: Computer Program for Nonlinear Dynamic Analysis of Three Dimensional Base Isolated Structures," by S. Nagarajaiah, C. Li, A.M. Reinhorn and M.C. Constantinou, 8/2/93.

NCEER-93-0012 "Effects of Hydrocarbon Spills from an Oil Pipeline Break on Ground Water," by O.J. Helweg and H.H.M. Hwang, 8/3/93.

NCEER-93-0013 "Simplified Procedures for Seismic Design of Nonstructural Components and Assessment of Current Code Provisions," by M.P. Singh, L.E. Suarez, E.E. Matheu and G.O. Maldonado, 8/4/93.

NCEER-93-0014 "An Energy Approach to Seismic Analysis and Design of Secondary Systems," by G. Chen and T.T. Soong, 8/6/93.